ADSORPTIVE EVALUATION OF NANOPARTICLES LOADED CARBON DERIVED FROM USED TIRES

BY

DANMALIKI GADDAFI IBRAHIM

A Thesis Presented to the

DEANSHIP OF GRADUATE STUDIES

KING FAHD UNIVERSITY OF PETROLEUM & MINERALS

DHAHRAN, SAUDI ARABIA

In Partial Fulfillment of the
Requirements for the Degree of

MASTER OF SCIENCE

In

ENVIRONMENTAL SCIENCE

MAY, 2015

KING FAHD UNIVERSITY OF PETROLEUM & MINERALS

DHAHRAN- 31261, SAUDI ARABIA

DEANSHIP OF GRADUATE STUDIES

This thesis, written by **DANMALIKI GADDAFI IBRAHIM** under the direction of his thesis advisor and approved by his thesis committee, has been presented and accepted by the Dean of Graduate Studies, in partial fulfillment of the requirements for the degree of

MASTER OF SCIENCE IN ENVIRONMENTAL SCIENCE

Dr. Tawfik A. Saleh
(Advisor)

Dr. Abdulaziz M. Al-Shaibani

Department Chairman

Dr. Abulkibash Abdullah
(Member)

Dr. Salam A. Zummo
Dean of Graduate Studies

Dr. Mohammad Abu Jafar Mazumder

(Member)

2/6/15

Date

DEDICATION

I have dedicated this work to my late mother, Hajiya Sadiya Abdullahi. Your love, words and memories are still vivid in my mind and you will forever remain in my heart. May we meet in Aljannatul Firdaus.

ACKNOWLEDGMENTS

I would like to thank Allah, the lord of the universe and the inventor of forms who gave me the wisdom, strength, ability and health to accomplish this work in detailed fashion. I would like to thank my parents for their life long support in the pursuit of my carrier goals, their support has helped me accomplish so many things in life.

I acknowledge the support of King Fahd University of Petroleum and Minerals for given me the opportunity to pursue my masters as full-time student, my deep and sincere thanks go to my thesis advisor in person of Dr. Tawfik A. Saleh for his guidance, encouragement and the experience he shared along with me both in academics and otherwise. I remain indebted to your words of advice. I would also like to thank my committee members viz: Dr. Abulkibash Abdullah and Dr. Mazumder MA Jafar for their invaluable suggestions and contributions to this research work.

My thanks are to Dr. Bassam S. Tawabini for serving as my academic advisor throughout my stay in KFUPM. I remain indebted to your words of courage and advice and the opportunity you have given us to mingle with Saudi community through community services and environmental awareness campaigns.

I would also register my thanks to Usmanu Danfodiyo University Sokoto for supporting me to pursue my Master's degree in KFUPM. I also appreciate the help of my teacher, colleague and friend in person of Dr. Ahmad Galadima for your immense help and support. Finally, I would thank the entire staff of chemistry department and environmental science program in particular Mr. Darwin, Mr. Hateem, Mr Naeem and some of my colleagues in particular Mr. Auwal Muhammad Musa, Shuaib Damola Taye, Omobayo Adio Salawu,

Malam Bashir Jelani for extending their hands at the times of need. I am really grateful for all the help you rendered. Thank you

TABLE OF CONTENTS

LIST OF TABLES

LIST OF FIGURES

LIST OF ABBREVIATIONS

AC:	Activated Carbon
BT:	Benzothiophene:
DBT:	Dibenzothiophene
DMDBT:	4, 6 Dimethyldibenzothiophene:
ADS:	Adsorptive desulfurization
ILD:	Ionic Liquids Desulfurization
ELTs:	End of life Tires
WRTs:	Waste Rubber Tires
FTIR:	Fourier Transform Infrared Spectroscopy
XRD:	X-ray Diffraction
SEM:	Scanning Electron Microscope
EDX:	Energy Dispersive Spectroscope
TGA:	Thermogravimetric Analysis

ABSTRACT

Full Name : Danmaliki Gaddafi Ibrahim

Thesis Title : Adsorptive Evaluation Of Nanoparticles Loaded Carbon Derived From Used Tires

Major Field : Environmental Science

Date of Degree : May, 2015

The disposal of waste tires represents a major environmental issue throughout the world. The aim of this thesis was to prepare activated carbon (AC) from waste rubber tires. The AC was then treated with NaOH and HNO_3 for enhancement of active sites. The synthesized AC was used as a support for loading Ni, Ce, and Fe nanoparticles and in combination of these metals. Raw, treated and loaded carbon samples were then characterized by BET surface area analyzer, surface pH, Boehm's titration experiment, FT-IR, XRD, and SEM/EDX spectrophotometers. The optimum carbonization temperature and time for the production of better yield carbon black were 500°C for 5 h and the optimum activation temperature for enhancement of porosity was 900°C. The synthesized materials were then tested for their efficiency in adsorptive desulfurization of thiophene (T), benzothiophene (BT) and dibenzothiophene (DBT) in line with the roadmap to achieve 10 ppm sulfur concentration in fuels. The regeneration abilities of the synthesized adsorbents were investigated. AC treated with HNO_3 yielded carbons with higher surface area and better adsorptive properties. The amount of refractory sulfur compounds adsorbed followed the order DBT > BT > T. Synthesized AC loaded with metals showed significant improvement in the adsorption of the refractory sulfur compounds. Nickel loaded on AC (AC/Ni) and cerium in combination with iron loaded on AC (AC/CeO_2/Fe) showed the best performance.

ARABIC ABSTRACT

ملخص الرسالة

الاسم الكامل: القذافي إبراهيم

عنوان الرسالة: تقييم كفاءة الادمصاص للمواد النانوية المحملة على سطح الكربون المحضر من الإطارات

التخصص: العلوم البيئية

تاريخ الدرجة العلمية: مايو 2015

التخلص من نفايات الإطارات يمثل مشكلة بيئية رئيسية في جميع أنحاء العالم. في هذه الدراسة تم تحضير الكربون الفعال من الإطارات المستخدمة. تم معالجة الكربون المحضر بهيدروكسيد الصوديوم او بحمض النيتريك تحت ظروف حرارية مختلفة بغرض تعزيز الكفاءة. ومن ثم تم استخدام الكربون الناتج كداعم لأنواع مختلفة من المواد النانوية مثل المنغنيز والحديد والنيكل وغيرها. تم توصيف المواد المحضرة باستخدام أجهزة توصيف مختلفة مثل تحليل مساحة السطح ودرجة حموضة السطح، وتجربة بوهم للمعايرة ومطيافية المسح الالكتروني ومطيافية الانتقالات الالكترونية ومطيافية الذرة وتشتت اشعة اكس وجهاز مطيافية الاشعة تحت الحمراء وغيرها. تم ايضاً اختبار المواد المحضرة في إزالة مركبات الكبريت مثل الثيوفين وبنزو ثيوفين وثنائي بنزو ثيوفين لتحقيق كفاءة إزالة للكبريت عالية. تم دراسة تأثير متغيرات عملية متعددة مثل التراكيز الابتدائية وكمية المواد المستخدمة وزمن التعريض على معدل الادمصاص وغيرها من العوامل التجريبية وذلك لاختيار أفضل الظروف. وكانت درجة حرارة الكربنة المثلى والوقت لإنتاج أفضل عائد من مادة الكربون خمسمائة درجة مئوية لمدة خمس ساعات وكانت درجة الحرارة المثلى لتفعيل وتعزيز المسامية تسعمائة درجة مئوية. ترتيب المركبات بالنسبة لكفاءة الازالة كانت ثنائي بنزو ثيوفين > بنزو ثيوفين > الثيوفين. أظهرت المركبات النانوية على سطح الكربون كفاءة أفضل من الكربون فقط مع إعادة استخدمها. أظهر النيكل كفاءة أفضل من السيريوم ثم الحديد.

CHAPTER 1

INTRODUCTION

Every aspect of land transportation involves the utilization of rubber tires. The global production of rubber tires is around 1 billion and 4 billion end-of-life tires are currently in landfills (WBCSD 2008). These materials are non-biodegradable and they cause significant environmental and land management impacts. However, despite their recalcitrant nature, they still have other useful applications in the production of fuel and valuable materials such as AC for industrial purpose. The present study aim to utilize active carbon synthesized from end of life tires (ELTs) for ADS. Studies on the utilization of this form of adsorbent focus on the removal of dyes, pesticides and heavy metals from waste water (Tawfik *e*t *a*l., 2013, 2014).

Fossil fuels are the main source of energy worldwide; crude oil, which occurs naturally and comprises of several organic components (such as diesel, gasoline, jet fuels, kerosene etc.), serves as the major source of energy in the world. Crude oils are usually classified based on density and the sulfur content. The lighter the crude oil the better its value and the lower the sulfur content in crude oil the better its profitability. American Petroleum institute gravity (API) and sulfur content are the major factors that determines the value of crude oil worldwide. Depending on the type of crude oil the sulfur content varies from (< 0.1% - > 5%). The level of sulfur in the global supply of crude oil is depicted in Table 1.1 (Vimal 2012).

Table 1.1: Sulfur levels in the global crude oil supplies

Region	Crude oil gravity (API)	Sulfur weight (%, 2010)	Production (tpd)
Alaska	28.34	0.99	1645
Canada	32	1.62	2500
California	18.73	2.6	951
Rest of USA	36.93	0.88	2470
Africa	32.64	0.18	6100
Europe	33.7	1.1	15530
Latin America	27.1	1.82	9850
Middle East	34.35	1.71	35760
Far East	37.3	1.1	15530
World Average	32.81	1.27	83450

tpd = tons/day

Saudi Arabia is the largest producer and exporter of total petroleum products in 2010 and it is the largest consumer of petroleum products in Middle East. Saudi crude oils are classified based on their gravity into: Arabian Supper Light (ASL), Arabian Extra Light (AEL), Arabian Light (AL), Arabian Medium (AM) and Arabian Heavy (AH). The higher the API gravity and the lower the sulfur content determines the value of the crude oil (Omer *et a*l., 2009). Table 1.2 outlines the classification and properties of the Arabian crude oil.

Table 1.2: Arabian crude oil classification and properties

Property	ASL	AEL	AL	AM	AH
Gravity	51.4	39.5	33	31.1	27.6
Sulfur (wt. %)	0.05	1.07	1.83	2.42	2.94
Nitrogen ppm w	70	446	1064	1417	1651
Nickel + Vanadium ppm w	< 0.1	2.9	21	34	67

wt% is percent by weight while ppm w is parts per million by weight

The hetero-element found in crude oil include: nickel, vanadium, nitrogen, sulfur etc. Sulfur is the main important hetero-element found in crude oil and has the most significant effect on refining. It poisons catalyst, corrode refining equipment, and combustion of the products of sulfur by automobiles impair the emission control technology designed to meet nitrogen oxides (NOx) and particulates emission standards which leads to environmental pollution. It contributes to the deterioration of air quality and affects public health and the ecosystem. The maximum allowable sulfur content in highway diesel fuel is 15 ppmw in 2006 in the US and will be less than 10 ppmw by 2017. Sulfur compounds found in crude oil are divided into aliphatic (mercaptans, sulfides, disulfides) and aromatic refractory group (thiophenes derivatives). The major classes of sulfur compounds found in fuel are summarized in Table 1.3 (Song *e*t *a*l., 2003)

Table 1.3: Classes of sulfur compounds found in crude oil

Sulfur Compounds	Chemical Structure
Thiols	R-SH
Sulfides	R-S-R
Disulfides	R-S-S-R
Thiophenes	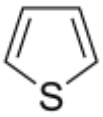
Benzothiophene (BT)	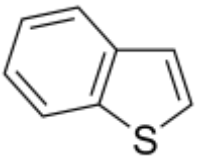
Dibenzothiophene (DBT)	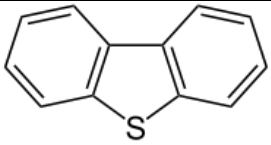

The methods in use for the removal of sulfur compounds in fuels are either pre-combustion techniques or the post combustion techniques. The pre-combustion techniques are the best methods and they involve the decomposition of sulfur compounds, removal of the compounds without decomposition and finally separation of the compounds followed by decomposition (Babich *e*t *a*l., 2003). The conventional method used by refineries for the removal of sulfur from fuel is hydrodesulphurization (HDS) (Bej 2004). It is efficient in the removal of most aliphatic sulfur compounds from fuels e.g. thiols. However, it is not

efficient in the removal of aromatic refractory sulfur compounds e.g. thiophene derivatives (DBT and 4, 6 dimethyl dibenzothiophene (DMDBT)) which are the least reactive and pose more serious danger to the environment. In addition it requires high temperature, pressure and high dosage of catalyst before achieving the desired objective which is uneconomical (Farhat *e*t *a*l., 2006).

Other methods of desulfurization in use to provide solutions to the problems of HDS include: Oxidative desulfurization (ODS), ionic liquids desulfurization (ILD) (Prashant *e*t *a*l., 2010), bio-desulfurization and ADS (Farhat *e*t *a*l., 2006; Guoxian *e*t *a*l., 2005; Soleimani *e*t *a*l 2007; Isam *e*t *a*l., 2013; Celia *e*t *a*l., 2010). Most of these methods utilize catalyst to speed up the rate of sulfur removal and they are considered viable alternatives in desulfurization. In ODS, all refractory sulfur compounds are oxidized by oxidants (such as H_2O_2, H_2SO_4, tBuOOH, O_3 and NO_2) to less harmful polar derivatives (sulfoxides and sulfones) that can be easily isolated by adsorption or extraction at room temperature and pressure. Most petroleum refineries use solvent extraction to extract the sulfur compounds from fuels thereby recovering the solvent by distillation (Babich *e*t *a*l., 2003). The major disadvantages of ODS are: one, in appropriate oxidant may cause unwanted side reactions with other components in the fuel that are of interest and second, solvent selection is critical because undesirable solvents may extract other components of the fuel that will affect overall quality of the product. The use of IL in extractive and oxidative-extractive desulfurization started in 2001 (Bösmann *e*t *a*l., 2001) and it has become an area of interesting research since then. IL are organic salts composed of anions and cations and they have low melting temperature. They are nonvolatile, nonflammable, chemically and thermally stable and they are easily regenerated due to their negligible vapor pressure.

Different types of anions and cations have been used in this process such as: $[BF_4]^-$, $[PF_6]^-$, alkylsulfates, thiocyanate or bis(trifluoromethylsulfonyl)imide, acetate, dialkylphosphate, alkylpyridinium, pyridinium, imidazolium, pyrrolidinium etc. Varying degrees of affinity and selectivity to sulfur compounds by different ionic IL have been noticed. Cost, lack of thermodynamic data, regeneration of the IL, effect of the liquids to other fuel constituents and corrosion related problems are the major drawbacks of this technology. (Zhang *et al*., 2004; Eber *et al*., 2004; Mochizuki *et al*., 2008; Cheruku *et al*., 2012; Holbrey *et al*., 2008; Borja *et al*., 2014). Biodesulfurization serves as an alternative to HDS due to its specificity, selectivity to sulfur compounds and mild operating conditions. In BDS, microbial species are used to consume sulfur compounds in fuels as their main energy source. They may either oxidize or reduce the sulfur compounds to sulfate or hydrogen sulfide respectively. Oxidizing the sulfur compounds is the most desirable pathway due to the fact that there will be no further treatment unlike the reduction pathway that requires further treatment of hydrogen sulfide through Clauss process to elemental sulfur. Various strains of microbes have been studied to increase desulfurization activity such as: Rhodocuccus, desulfovibrio desulfuricans, Arthrobacter, Brevibacterium Pseudomonas, and Gordona spp. Slow reaction rate, cost and inability to recover biocatalyst, isolation of the microbial specie after the reaction, emulsion formation, and complex reactor design are the major problems limiting the commercialization of this technology (Vimal 2012).

The use of nanomaterials and nanocomposites as adsorbents in ADS will be the main aim of this thesis. Variety of adsorbents are currently used in desulfurization for the selective removal of sulfur from petroleum products. It has advantages over other methods of

desulfurization because of mild operating conditions, less expensive and does not have scaling or corrosion problems. It has ease of application, and some of the adsorbents have efficient sulfur removal and excellent regenerative ability (Kostas *e*t *a*l., 2014). The known adsorbent materials in use are: nickel based sorbents, zeolites based sorbents, alumina based sorbents, silica, AC, metal oxides, metal sulfide and reduced metals based sorbents (Ma *e*t *a*l., 2003; Fukunaga *e*t *a*l., 2003; Vinay *e*t *a*l., 2006; Hernandez *e*t *a*l., 2010). Current area of research in ADS focuses on the development of cost effective, efficient and reliable adsorbent materials that will have high sorption capacity and selectivity to reduce the sulfur content of fuel to minimal concentrations and to be easily regenerated to minimize disposal impacts.

1.1 Environmental concerns

The increased utilization of fossil fuels and subsequent industrialization in most part of the world has led to a remarkable increase in the atmospheric sulfur compounds concentrations (Leh *e*t *a*l., 1973). Pollution released by the use of petroleum based fuels contributes immensely to the deterioration of air quality despite regulatory and technological advances in place (USEPA 2000). SOx, NOx, and particulate matter are constantly emitted to the environment which affects public health, ecosystem and general wellbeing of the people living mostly in urban areas. Sulfur dioxide which is the immediate sulfur compound found in the lower atmosphere after combustion of fuels has a major role to play in the formation of acid rain, smog formation, and particulate aerosols. Each of these formations affects the healthy living of animals, plants, soils, water and the general ecosystem (Mathieu *e*t *a*l., 2012).

The four-day event of "London smog" that took place in December 1952 claimed the life of over 4000 people is a noticeable example of the dangers of sulfur compounds in the atmosphere. A similar tragedy happened in London in 1957 with a recorded casualty of over 700 lives. The lower the sulfur content in a fuel the better its quality and marketability (Song 2003). The purpose of this thesis is to provide cheap and reliable nanomaterials that will help in reducing the amount of sulfur released from hydrocarbon based fuels into the environment.

There are evidences of substantial the increase of sulfur compounds over the past few decades in our immediate environment (Georgii 1970). These compounds are the major contaminants found in hydrocarbon fuels (Shahadat *e*t *a*l., 2013) and they are equally reactive (Leh *e*t *a*l., 1973). Sulfur compounds released mainly from burning of fossil fuels results in breathing impairment, respiratory illnesses, alterations in lung defenses, and aggravation of existing cardiovascular disease. These compounds equally have grievous consequences to asthmatic patients.

1.2 Regulations on sulfur emission

Many countries have laws for regulating the emission of sulfur from fuels e.g. In the US, USEPA enacted a law known as ultra-low sulfur diesel (ULSD) since 2006 for maintaining the sulfur content in diesel at 15ppm from the previous 500ppm law (low sulfur diesel) (USEPA 2006). Diesel engines since then were produced with devices that minimize the emissions of sulfur to the environment. This had the immediate health benefit to the population and the environment. The expected results from the enactment of the law were that: 8300 premature deaths, 23100 cases of bronchitis, and 360,000 asthma attacks are expected to be prevented annually. In addition, 7100 hospital visits, 2400 emergency visits

of asthmatic patients and 1.5 million days of productivity loss will be avoided (USEPA 2006).

USEPA has a tier 3 motor vehicle and fuel standard approach to reduce the sulfur content in gasoline. It is an upgrade version of the tier 2 approach and it is one of the most effective air quality control measures in place (USEPA 2014a). This rule is expected to be enacted by 2017 and it will consider both the vehicle and the fuel as an integrated system; the expected sulfur level will be 10ppm on annual average. Japan, Europe, Canada and South Korea have already achieved the tier 3 limits of sulfur in gasoline (Dasgupta *e*t *a*l 2013). Lower sulfur gasoline will aid in the development of better technologies that will further improve fuel economy, reduce greenhouse gas effect and improve public health (USEPA 2014b). It is projected that by 2030, tier 3 will annually prevent: close to 2000 premature death, over 2000 hospital visits and asthma related cases, and almost 1.5 million days of productivity loss (USEPA 2014a). Therefore, it is required to reduce the sulfur content in the fuel itself during the refining process to protect the environment. Table 1.4 outlines the regulations enacted in various countries and their projections to the future.

Table 1.4: Maximum allowable sulfur limits in ppm

	Year	
Region	**2015**	**2025**
US/Canada	15	10
Europe	10	10
Japan	10	10
South Korea	10	10
Middle East	350	175

1.3 Statement of the problem

More than 1 billion ELTs are generated every year; 4 billion end-of-life tires are currently in landfills, disposing this material that pose serious environmental impact in an environmentally friendly way should be the main aim of waste managers (WBCSD 2008). So many initiatives have been launched to address the disposal issue of ELTs across the globe. These initiatives believe that ELTs should have useful applications in providing fuel for energy generation and secondary raw materials for the production of other products. Luckily enough, these initiatives are supported by government agencies and the rubber industry. However, despite the initiatives in place, there is no effective management system that will curtail the impact as the production of tyres across the globe is always on a rise which is why the final depository always ends up in a landfill (WBCSD 2008).

The increased utilization of fossil fuels and subsequent industrialization in most part of the world has led to a remarkable increase in the atmospheric sulfur compounds concentrations [Leh *e*t *a*l., 1973]. Pollution released by the use of petroleum based fuels contributes

immensely to the deterioration of air quality despite regulatory and technological advances in place [USEPA 2000]. SOx, NOx, and particulate matter are constantly emitted to the environment which affects public health, ecosystem and general wellbeing of the people living mostly in urban areas. Sulfur dioxide which is the immediate sulfur compound found in the lower atmosphere after combustion of fuels has a major role to play in the formation of acid rain, smog formation, and particulate aerosols. Each of these formations affects the healthy living of animals, plants, soils, water and the general ecosystem. Billions of dollars are invested in: first, the refining industries to lower the level of sulphur to improve fuel quality in the market, second environmental cost incurred to economy on cleaning up the environment and health impacts.

1.4 Significance of the study

This study is significant in response to the management of ELTs disposal in different part of the globe. ELTs can be used in place of virgin materials which will reduce depletion of resources and environmental damage. AC will be produced to replace the commercially expensive adsorbent currently in use. This study is equally important in line with the roadmap that Saudi Arabia has adopted from Europe for zero levels of sulphur in diesel and gasoline from 2013 to 2016. The levels of sulphur in the fuels of Saudi Arabia is around 10,000ppm which is reduced to around 500pm in the current desulfurization capacity, some of the companies that the kingdom has set to meet up with the mission of 10ppm sulphur levels are: Riyadh Refinery Clean Transportation Fuel project, Ras Tanura Refinery Clean Fuels and Aromatics project, Saudi Aramco Mobil Refinery Co. Clean Fuels project and PetroRabigh Clean Fuels project. The two other goals in line with the roadmap are to protect the environment and public health, maintenance of global position in exporting fuel.

CHAPTER 2

LITERATURE REVIEW

2.1 Adsorbent Materials

Adsorbent materials are generally classified into organic sources (carbons, polymers and biomass) and inorganic (aluminas, silicas and zeolites). Some of the main required properties of these adsorbent materials are outlined as:

The material should be thermally and mechanically stable.

It should be highly porous with balance between micro and macro-pores.

It should have high surface area.

It should have high affinity for the adsorbate.

It should be cheap and be easily regenerated.

The adsorptive capacity of any adsorbent material depends on the number of pores in the internal area relative to the number of pores on the outer surface. The internal area is much higher than the outer surface area which is the major reason why adsorbent materials adsorb large quantity of the adsorbate. These materials are further classified based on their pore sizes which determines which material they can adsorb into three classes viz:

Micro porous adsorbents (between 2A° to 20A°)

Meso porous adsorbents (between 20 A° to 500 A°)

Macro porous adsorbents (>500 A°)

A° = Angstrom which is equivalent to 10-10 meters = 0.1 nm

2.1.1 Activated carbon

AC is a special class of organic adsorbent that is armophorous and possess microcrystalline structure with large surface area and high porosity. Its pores are dispersed having different sizes and shapes. It is sometimes referred to as activated coal or active charcoal; it is produced from carbon-rich parent materials e.g. charcoal, biochar, wood, peat, sewage sludge, animal bones, hair etc. that are subjected to physical or chemical activation.

The physical production of AC involves two processes viz: carbonization of the parent material and activation of the material formed. The chemical methods of producing AC involves treatment of the parent material with acid, base or salt followed by contact with controlled atmosphere to aid in the activation process. It requires less amount of heat compared to the physical process of producing AC.

Carbonization

In carbonization, the parent materials are subjected to pyrolysis at a temperature $\leq 800°C$ under controlled conditions of atmosphere and heat. At this stage, all elemental composition of the parent material used will be decomposed leaving behind only the aggregates of carbon that are randomly linked together forming residual pores which are used for adsorption. AC is widely known for its monumental adsorptive capacity; a gram of AC contains an area of around $500m^2$ while a pound of AC contains an area equal to six football pitches.

Activation

The material formed after pyrolysis will be further modified, enhanced and developed to form great number of pores for tremendous applications using temperature between 800°C-900°C and a controlled atmosphere. This will improve the surface area of the AC produced depending on the parent material. The activated material that will be produced after this process will have the potential to bind with different elements. Table 2.1 outlines the properties of AC derived from different parent materials

Table 2. 1: Comparison of the properties of activated carbon derived from different parent materials

Reference	Raw Material	Activation method	Activation tool	Temperature	Time(mins)	BET surface area (m^2 g^{-1})
Toles *et al*., 2000	Almond Shale	Physical	High Temperature furnace	800°C	120	484
Billy *et al*., 2013	Corn husk and Sugar cane bagasse	Physical	Laboratory tube furnace	800°C	40	256
Khezami *et al*., 2007	Firewood	Physical	Stainless steel vertical reactor	750°C	180	587
Asadullah *et al*., 2007	Jute Stick Char	Physical	Stainless steel horizontal reactor	750°C	60	724
Bouchelta *et al*., 2008	Date Stone	Physical	Tubular furnace	700°C	60	322
Demiral *et al*., 2011	Olive bagasse	Physical	Vertical tube furnace	750°C	30	523
Yang *et al*., 2010	Coconut shell	Physical	Microwave tubular furnace	900°C	210	2288
Olivares- Marín *et al*., 2012	Cherry stones	Physical	Horizontal tubular furnace	550°C	120	479

AC is divided into three classes based on their sizes viz: powdered AC, granular AC and extruded AC. ACshows little selectivity in the adsorption of molecules of different sizes which is why it is sometimes impregnated or coated to desired material or molecular sieves for selective adsorption of persistent pollutants, air seperation and clean-up of off gasses in nuclear facilities. The modification of AC to molecular sieves allows the development of effective micropore diameter for enhanced applications. It is widely used in purification of water, waste water and sewage and air; clean-up of oil spill, in groundwater remediation, widely used as a catalyst and in medical applications like treatment of poisoning, food and pharmaceutical industries etc.

2.2 Recycling of WRTs for AC Production

Every aspect of land transportation involves the utilization of rubber tires which is why its production is soaring globally. Tires are made up of copolymer of long chain polymers including styrene, isoprene and butadiene that are connected to each other and other inorganic constituents by the addition of sulfur (vulcanization). There are several methods in use for the management of WRTs which include retreating, shredding, recycling and many others. Recycling as a management tool is most widely accepted method but it is expensive however, there are alternative methods such as pyrolysis and gasification in place for the production of useful products from WRTs.

There are many methods to recycle WRTs which are sub-divided into two categories. The first category involves physical methods of grinding the waste mechanically into smaller pieces to produce fine particles without altering chemical composition while the second category uses mechanochemical means to breakdown the three-dimensional network with the aid of different forms of energy. Thermal, mechanical, biological, chemical, ultrasonic

and microwave treatments are used to convert the waste insoluble thermoset into a reprocessable elastomer (De *e*t *a*l., 2005). The best method suitable for tire recycling is pyrolysis (Kaminsky *e*t *a*l., 1995), pyrolysis is the thermal decomposition of rubbers in a closed system for the production of oil (which consist of non- aromatics, aromatics, oxygen, nitrogen and sulfur containing compounds) gases (H_2S, Carbon oxides, hydrocarbons and hydrogen) for reuse in petrochemical industries and solid remains such as carbon black for use as filler materials. The gases produced are purified using appliances such as wet and spray-dry scrubbers.

There is a significant progress in the pyrolysis technology of waste rubber tire, however, despite the progress, pyrolysis is done on a limited scale due to the absence of market for the derived products. The product yield based on pyrolysis is dependent on temperature and pressure employed during the production and the residence time which determines particle size to be produced. Pyrolysis gas and oil yield are known to increase with temperature but the yield is affected by extreme temperatures. Temperatures between 400°C-800°C are known to be optimum for char production, lower pressure reduces the energy requirement and enhances the liquid and char yields (Martinez *e*t *a*l., 2013; Antoniou *e*t *a*l., 2014)

Researchers in recent years have focused more in the recycling and reuse of WRTs among the initiative is the derivation of AC after pyrolysis for various adsorption studies. AC from waste rubber tire have the ability of adsorbing different compounds however its adsorption capacity is relatively low compared with other adsorbent materials in use. There are various methods of improving the adsorption capacity of the fine powdered particles. AC from waste rubber tire was synthesized by pyrolysis at 500°C-700°C and later treated with

activating agents such as zinc chloride and potassium hydroxide in a study conducted by (Nunes *e*t *a*l., 2011). The adsorbent showed a mesoporous structure containing sulfur and zinc and it showed the possibility of waste water treatment.

The work conducted by (Zabaniotou *e*t *a*l., 2014) derived AC from WRTs by pyrolysis at 800°C in a fixed bed reactor and physical method of activation using CO_2 for the removal of pesticide(bromopropylate) by adsorption from aqueous solution. The surface area of the AC was found to reach 432 m^2 g^{-1} and nearly 100% of the pesticide was removed in just 60mins of the experiment. The study of (Edward *e*t *a*l., 2010) derived AC from ELTs by carbonization for the effective removal of dyes from effluents. It was observed that temperatures above 770K resulted in lower yield adsorbent.

WRTs were pyrolyzed in nitrogen atmospheres at various temperatures for char production (Manchon-Vizuete *e*t *a*l., 2005). The char was activated by oxygenation at different temperatures and were used for the removal of mercury from aqueous solutions. The study concluded that the optimum temperature for pyrolysis in nitrogen atmospheres is 550◦C. The study of (Abdulaziz *e*t *a*l., 2013) used spectroscopic and computational studies to examine the chemistry of cadmium adsorption by activated from WRTs in aqueous solutions. The adsorption process was found to be fast and equilibrium was achieved after 60mins of interaction. Finally, binding energy of cadmium to carbonyl groups was found to be higher than other functional groups present.

The study conducted by (Vinod *e*t *a*l., 2012) synthesized AC from ELT by physical activation and used it as an adsorbent for the removal of nickel and lead ions from aqueous solutions. The adsorbent was found to have more affinity to the lead ions (96% removal)

and the adsorption process was believed to start from initial surface adsorption followed by intra-particle diffusion. The regeneration ability of the adsorbent was also tested and they believed it may be a substitute to the expensive commercial AC currently in use for pollution clean-up. (Vinod *e*t *a*l., 2014) synthesized different brands of AC from WRTs by microwave assisted chemical treatment and physical heating for the adsorption of phenolic compounds.

Granular particles of tire were carbonized and pyrolyzed by heating at 773K and 1223K respectively in nitrogen atmosphere for the production of active carbon in a study conducted by (Edward *e*t *a*l., 2010). The product produced was activated by carbon di oxide in nitrogen atmosphere and later subjected to acid treatment. The synthesized adsorbent was used in the removal of dyes from waste water and it had a higher surface area and better yield. A study conducted by (Quek *e*t *a*l., 2009) synthesized AC possessing high surface area (414 m^2/g) without pyrolysis in a one-step cost effective approach. The study used thermochemical degradation of granular tires in a carbon di oxide environment. Table 2.2 outlines some selected literatures on the production of AC from ELTs.

Table 2.2 Selected literature on the production of activated carbon from end of life tires

Reference	Pyrolysis		Activation			BET (m^2/g)
	Temperature (°C)	*Residence time*	*Temperature (°C)*	*Residence time*	*Activaing Agent*	
Aranda *et al*., 2012	600	4 mins	850	2 h	Steam	528
Min *et al*., 2006	700	30 mins	900	4 h	CO_2	732
Gonzalez *et al*., 2006	800	1 h	900	2 h	Steam	1317
Gonzalez *et al*., 2007	800	1 h	850	3 h	CO_2	496
Mui *et al*., 2011	500	2 h	950	8 h	CO_2	787
Gupta *et al*., 2011	500	5 h	900	2 h	KOH	981
Vinod *et al*., 2012	500	5 h	900	2 h	CO_2	562
Zabaniotou *et al*., 2004	800	45 mins	950	2.4 h	Steam	472
Gupta *et al*., 2012	500	5 h	900	2 h	HNO_3	397
Nagakagawa *et al*., 2004	500	1 h	850	90 mins	Steam	1000
Ariyadejwanich *et al*., 2003	500	1 h	850	3 h	Steam	1177
Stavropoulos *et al*., 2005	800	1 h	800	2 h	KOH	758
Choi *et al*., 2014	500	2 h	950	3 h	CO_2	437
Shah *et al*., 2006	450	2 h	900	2 h	limited air	940

2.3 Companies involved in tire recycling in Saudi Arabia

Riyada Jeddah, Ali Plastic Recycled Company, Pure Recycling, Sabk International, Amud Trading, Almanat Trading, Al Madeeni Est, Tadaruk Global Corporation, East Grant Trading Services, NAC.Jeddah, Deal Makers Trading, and TCI Arabia etc.

2.4 Principles of adsorption

Adsorption is defined as the increase in the density of a fluid within the vicinity of an interface. Adsorption occur when a solid surface is exposed to a liquid or a gas, the gases and liquids tend to adhere to the unoccupied spaces in solid particles due to the presence of unsaturated molecular forces within a solid material. The principle of adsorption is based on the removal of certain substances called adsorbate (liquid or gas) by an adsorbent (solid material). It can further be defined as the adherence of substances to solid materials. Nearly all substances may have trace capability for adsorption but depending on some favorable characteristics like surface area, active sites, pore size and volume, some materials are far better than others in the way and manner they adsorb particles.

Adsorption involves two types of forces viz: physical forces which may include dispersive forces, polarization forces, or dipole and chemical forces due to the interaction of electrons between solid particles and the atoms of liquids or vapor phase (Roop *e*t *a*l., 2005). Three principal forces responsible for adsorption which include: van der Waal's forces, chemical affinity and electrostatic attraction. There are two different types of adsorption mainly Physiosorption which is reversible and chemiosorption that is irreversible (Zeki 2013). The adsorption process is primarily studied based on certain types of equations and models. The most widely used equations are: Freundlich which is based on empirical equations that describe the adsorption characteristics on heterogeneous surface (Freundlich 1906),

Langmuir equation which is based on monolayer adsorption process on energetically homogeneous surface (Langmuir 1918) and Brunauer-Emmett-Teller (BET) equation which is mostly used in gas phase adsorption and it is based on statistical analysis of adsorption sites occupied during a multi-layer adsorption of gasses (Brunauer *et al*., 1938).

2.5 Types of adsorptive desulfurization

There are different forms of ADS which will be discussed in this section. These include: reactive adsorption, polar adsorption, selective adsorption, integrated adsorption, π-complexation. The schematic of different forms of desulfurization is given in Figure 2.1.

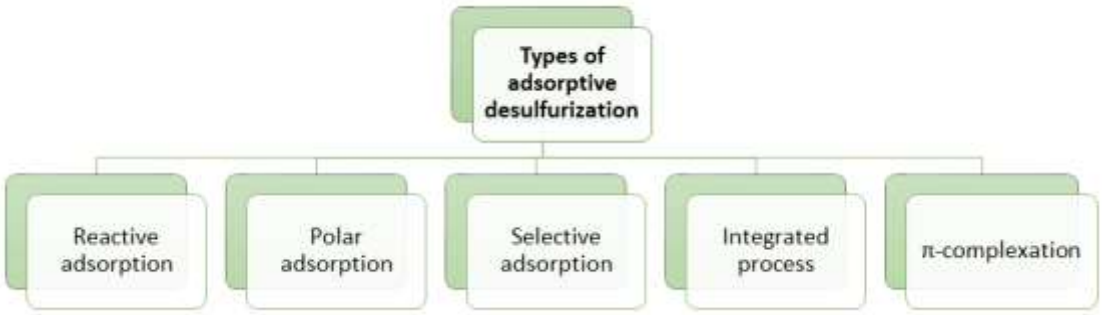

Figure 2.1*:* Types of adsorptive desulfurization

2.5.1 Reactive adsorption

Reactive adsorption is a form of ADS whereby the sulfur compounds in fuel are removed by chemical interaction between the fuel and the sorbent material. The reaction involves removal or transfer of the sulfur compounds from the fuel followed by attachment of the compounds to the sorbent material which will allow the sulfur free fuel to be collected in the main stream. The process uses metal-based sorbent for sulfur removal to form metal sulfide. The sorbent material can be regenerated by disposing off the sulfur compounds in the form of SO_2, H_2S, or elemental sulfur depending on the method employed. Reactive adsorption can be carried out at ambient conditions, at elevated temperatures and with the

aid of hydrogen at elevated temperatures. The efficiency of reactive adsorption depends on the adsorption capacity of the sorbent material, its affinity to the sulfur compounds, its thermal and mechanical stability and its ability to be regenerated. The overall mechanism of the process is outlined in Figure 2.2.

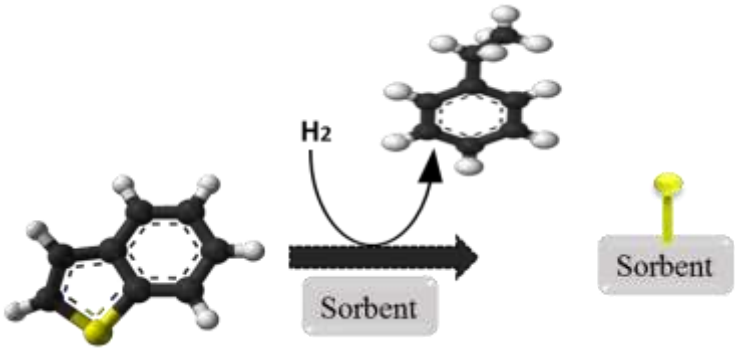

Figure 2 2: Reactive adsorption of BT on sorbent material in the presence of hydrogen

This process is widely used in the US as the S Zorb process developed by Philips Petroleum for efficient desulfurization at higher temperatures of between 340 -410°C and lower pressure of H_2 between 2-20 bars. Reactive ADS combines the advantages of both the catalytic HDS and adsorption desulfurization and thus highly efficient for deep desulfurization. Research Triangle Institute (RTI) has developed a technology called TReND based on reactive adsorption desulfurization that utilizes metal oxides as sorbents materials to effectively remove sulfur compounds from fuels in the presence of hydrogen at a temperature of 426-535°C. Mercaptans are completely removed from fuels in this process in the absence of hydrogen but thiophenes requires considerable amount of hydrogen for its successful removal (Turk *e*t *a*l., 2001). Reactive adsorption can be aided with hydrogen at elevated temperatures using selective adsorbents. ZnO has been reported and industrially applied as a promising adsorbent for desulfurization processes. Addition of hydrogen in the process helps in the complete removal of thiophene in fuel.

2.5.2 Polar adsorption

Polar adsorption (IRVAD process) is a less expensive method of providing low sulfur gasoline and it was developed and commercialized by Black and Veatch Pritchard and Alcoa Industrial chemicals to address even low concentrations of sulfur compounds in fuels. Activated alumina in particular Alcoa Selexsorb is widely used as the sorbent material for the removal of polar compounds. The adsorption process is performed in a counter-current moving bed with alumina adsorbent in contact with liquid hydrocarbon in a multi stage adsorber. The adsorbent is normally regenerated using hydrogen at various temperatures due to its heat capacity, thermal conductivity and its availability. The regenerated adsorbent is then recycled for another round of the reaction. The process operates at lower pressures and does not consume high amount of hydrogen. The mechanism is based on the polarity of sulfur in gasoline and it is known to reduce sulfur from fuels to as low as 0.5ppmw.

2.5.3 Selective adsorption for removal of sulfur compounds (SARS)

The idea behind SARS is to remove sulfur compounds from fuels which constitute only less than 1% of the fuels at ambient conditions without hydrogen and to leave behind the remaining hydrocarbon contents of fuels which can be used as ultra-low sulfur fuels. This process was first demonstrated by Pennsylvania state university (Song *e*t *a*l., 2003) and if fully developed can be used in refinery operations and other mobile/stationary applications. The prime goal of SARS is to design appropriate adsorbents with surface sites having high affinity for sulfur compounds in the presence of aromatics. The adsorbents need to be effective, selective and apt for sulfur removal. Nickel based sorbents and air regenerable metal oxide based sorbents are the most common adsorbent materials used in this process. The basis for the SARS technology is that there is site specific interaction between sulfur

and metal species that is possible with selected organometallic complexes. The likely adsorption configurations of thiophenic compounds on adsorbents used in SARS process can be explained from the known coordination geometries that thiophene exerted upon contact with organometallic complexes. Examples of coordination geometries are given in Figure 2.3. It is a known fact that both thiophenic sulfur compounds and non-sulfur aromatic compounds in fuels can interact with metal species by pi-electrons which is why the likely coordinating geometries that will best explain the interaction of sulfur atom of the thiophenic compounds with the adsorbent used in SARS are: η^1S (sulfur atom of thiophenes and a metal relation) and S-μ^3 (sulfur atom of thiophenes and two metal species).

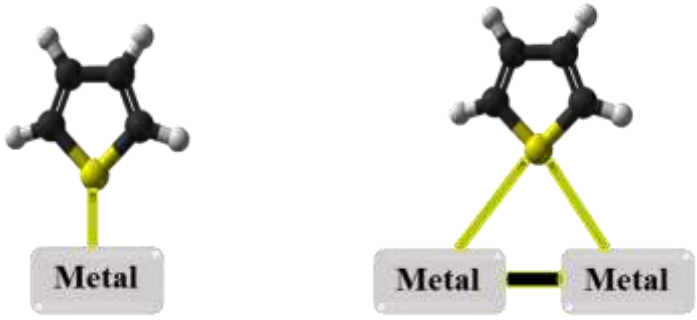

Figure 2.3*:* Coordination geometries of thiophene in organometallic complexes.

2.5.4 Integrated process adsorption

This is a recent technology that combines selective adsorption with HDS technology using highly efficient catalysts for effective removal of sulfur compounds from fuels. It will confer added advantages like reduction in cost, better efficiency, faster desulfurization rates and reduction in reactor volumes than using single processes alone. The schematic diagram for the technology is outlined elsewhere by (Chunshan *et a*l., 2003).

2.5.5 ADS by π-complexation

Adsorption by chemical complexation (π-complexation) has been reported by Yang group of researchers (Yang *e*t *a*l., 2001; Arturo *e*t *a*l., 2004; Yuesong *e*t *a*l., 2012). Cations such as Na^{+}, Zn^{2+}, Ni^{2+}, Cu^{+}, Ag^{+}, Fe^{2+}, Ce^{4+} are used mostly on zeolites due to its larger pores and pore volumes to adsorb large quantities of thiophene, BT and DBT from diesel, gasoline and jet fuels by forming π-complexes between the metals and the compounds of interest. The cations form σ-bonds with free s-orbitals and the d-orbitals will back-donate electron density to the antibonding π-orbitals in the sulfur containing ring of thiophenes. Bonds formed due to this interaction are stronger and yet easily broken by alternating the temperature or pressure which enhances the capacity and selectivity to sulfur compounds. ADS by π-complexation yields better results compared to the normal vanderwaals interactions occurring in adsorption studies. Aside from desulfurization, different sorbents have been developed based on this mechanism for aliphatic, olefins and aromatics separation (Takahashi *e*t *a*l., 2001). The mechanism is shown in Figure 2.4.

Figure 2.4*:* ADS of DBT by π-complexation

2.6 Synthesis of nanomaterials

A nanomaterial is a broad name given to all types of materials found at the nanoscale; it is a material that has a unit size between the ranges of 1-100nm. They can be naturally occurring or chemically/mechanically synthesized with zero dimension (0-D), one dimension (1-D), two dimensions (2-D) or three dimensions (3-D). They have a wide range of both structural and non-structural industrial applications due to their sizes, shapes, chemistry and high surface area. They are applied in most industrial applications to improve performance because their surface properties far exceed their bulk properties. Nano-materials such as alumina, zirconia, silica, and AC have been the subject of research recently due to their promise in adsorption desulfurization. Adsorbents are generally classified into organic sources and inorganic sources. Adsorption on commercial and industrial scale depends solely on the type, quantity, economic cost and effectiveness of adsorbent material. This is why studies on adsorption studies currently focus on the development of better adsorbent materials for large scale industrial applications. Most materials used as adsorbents are relatively porous and have a wide surface area with pore diameter of tens of angstroms.

The most widely used adsorbents are: AC, silica gel, zeolites, molecular sieve carbon, activated alumina, polymers and nanocomposites. Each of these materials has distinct physical and chemical characteristics such as pore sizes and structure, porosity and nature of the adsorbing surface that are different from other materials. The materials that can be used as adsorbent should be thermally and mechanically stable, highly porous with balance between micro and macro-pores with high surface area, high affinity for the adsorbate and should be cheap and be easily regenerated.

The adsorptive capacity of any adsorbent material depends on the number of pores in the internal area relative to the number of pores on the outer surface. The internal area is much higher than the outer surface area which is the major reason why adsorbent materials adsorb large quantity of the adsorbate. These materials are further classified based on their pore sizes which determines which material they can adsorb into three classes viz: Micro porous adsorbents (between 2A° to 20A°), Meso porous adsorbents (between 20 A° to 500 A°) and Macro porous adsorbents (>500 A°). Where A° = Angstrom which is equivalent to 10-10 meters = 0.1 nm. Adsorption capacity or otherwise adsorption isotherm depends upon temperature and vapor pressure which help us to classify different forms of adsorbent. Adsorption isotherms are classified into six different classes (Sing 1982). The graphical illustration of the isotherms is shown in Figure 2.5.

- Type one Isotherms: They consist mostly of micro porous adsorbents. E.g. Silica gel and most carbons fall in this category

- Type two Isotherms: They consist of non-porous surfaces and macro porous adsorbents. E.g. Graphitized carbon and some hardened powders of silica.

- Type three Isotherms: They consist of non-porous and macro porous solids. E.g. synthetic polymers used as adsorbent materials

- Type four Isotherms: This class exhibit special attribute of hysteresis which means capillary condensation showed by the mesoporous adsorbents. E.g. Low density silica gel

- Type five Isotherms: This class exhibit hysteresis as well but they show similar characteristics to Type three isotherms.

• Type six isotherms: This isotherm share similar characteristics to type two isotherms but however, the adsorbent belonging to this class adsorb in a multilayered passion.

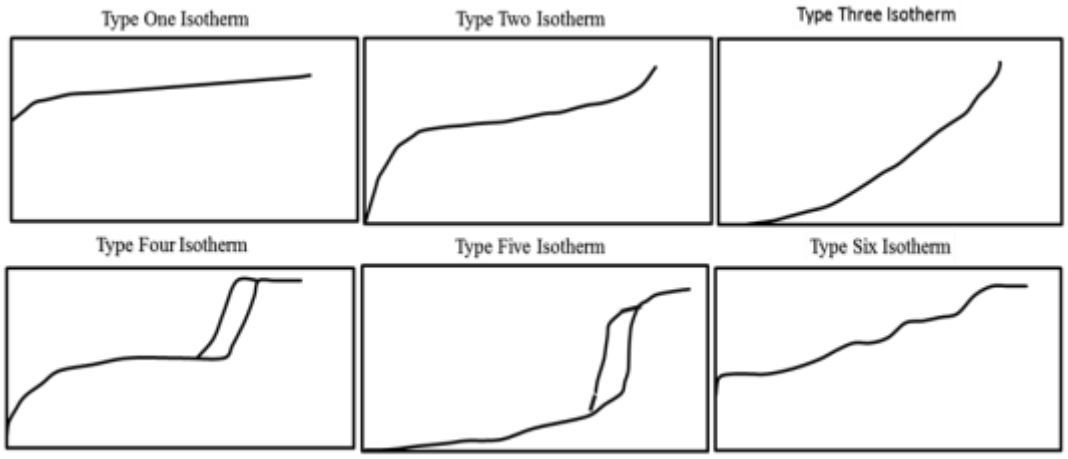

Figure 2.5*:* Graphical illustration of different isotherms models

2.6.1 Synthesis of nanomaterials

Nanomaterials are synthesized using two different approaches viz; bottom-up approach and top-down approach. In the bottom-up approach, the nanoparticles are first obtained at the atomic level and later integrated into the desired material e.g. is the formation of nanoparticle from colloidal dispersion or the formation of powders from sol-gel method followed by a later stage of integration. The top-down approach starts with a bulk material at the macroscopic level followed by trimming of the material to the desired nanoparticles e.g. etching and ball milling. Schematic illustrations of the synthesis methods are provided in Figure 2.6 (a & b).

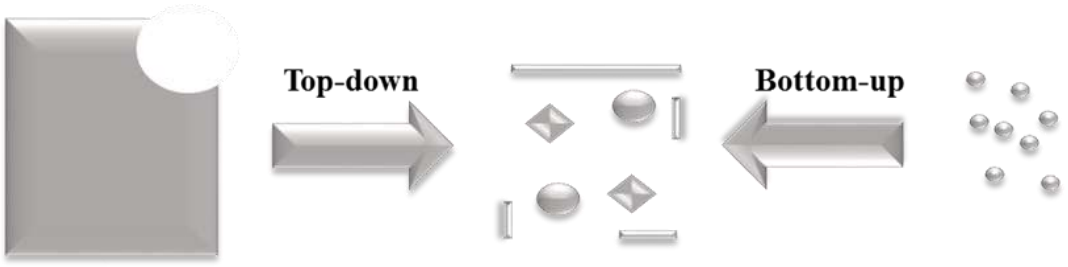

Figure 2.6 a: Synthesis of Nanomaterial

The general outline for the production of nanomaterials involves three different process; grinding, wet chemical processes otherwise called liquid phase processes and lastly the gas phase processes of producing nanomaterials. These processes are outlined below:

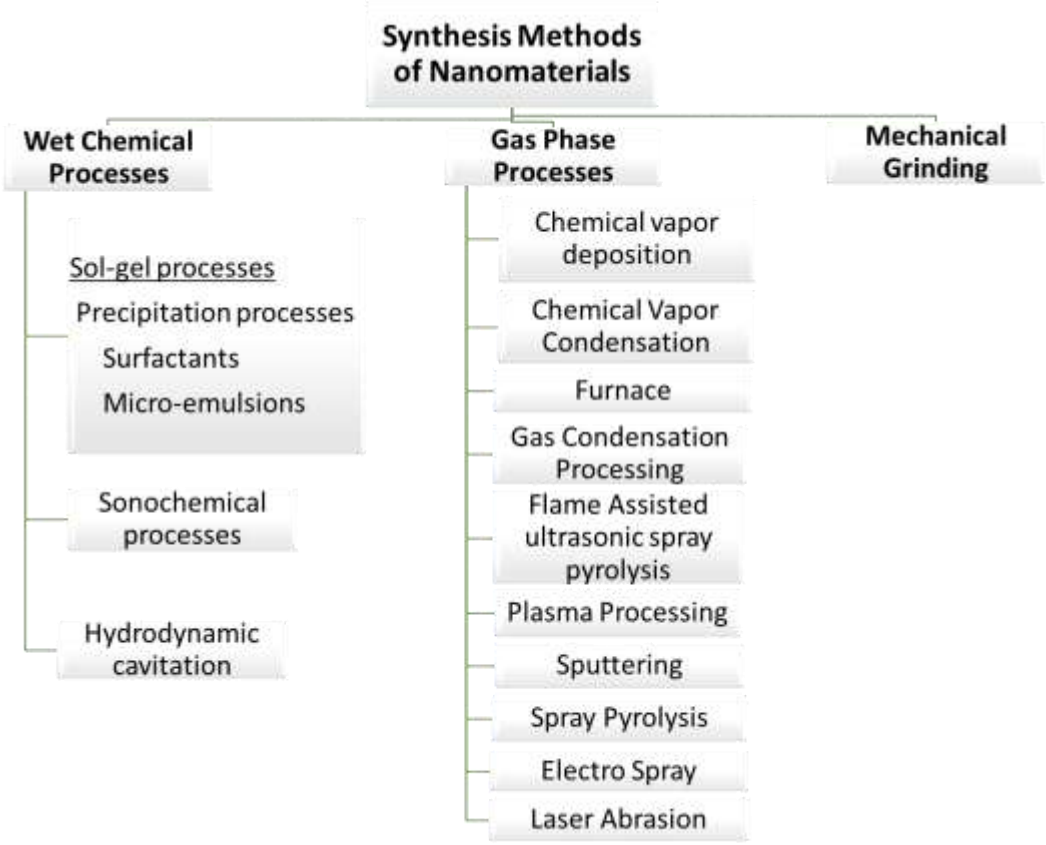

Figure 2.6 b: Synthesis routes of nanomaterials

2.6.2 Synthesis of nanocomposites

Nanocomposites are special classes of materials formed by combining two phases of different materials and they tend to retain the properties of each material used in their formation. A matrix (filler and resin) and a reinforcement (mostly fibers) are required for the formation of a composite. Properties of composites depends on the properties of each material, their relative amounts and overall geometry. In essence, nanocomposites are materials having one or more of their phases in the nanoscale size embedded in a polymer matrix, ceramic matrix or metal matrix. They have nanoparticle properties, high thermal and mechanical stability, multifunctional capabilities, chemical functionalization and huge interphase zone. The combination confer added advantage to them which is why they are currently utilized in various fields of science and technology. They are widely used in catalysis, nanosensors and nanoprobes production, sorption process, chemical and biological applications, fuel cells, non-linear optics, bio-ceramics, batteries with greater power output, environmental protection, anti-corrosion agents, drug delivery, UV protection gels, as fire retardant material, in the production of lubricant and scratch free paints and in adsorptive studies with clear application in desulfurization.

There are various ways of synthesizing nanocomposites which will be outlined in this section. The processes do not take a specific method; the synthesis may involve combining two different methods or even more for the production. The mostly widely used methods are: Intercalation, sol-gel method, molecular composite formation method, high energy sonication, nanofiller direct dispersion method, hydrothermal synthesis, polymerized complex method, surfactant assisted processing, solution-evaporation methods,

electrochemical synthesis of polymers, chemical vapor deposition, microwave synthesis, and ball milling process. Figure 2.7 outlines the methods involved in the synthesis

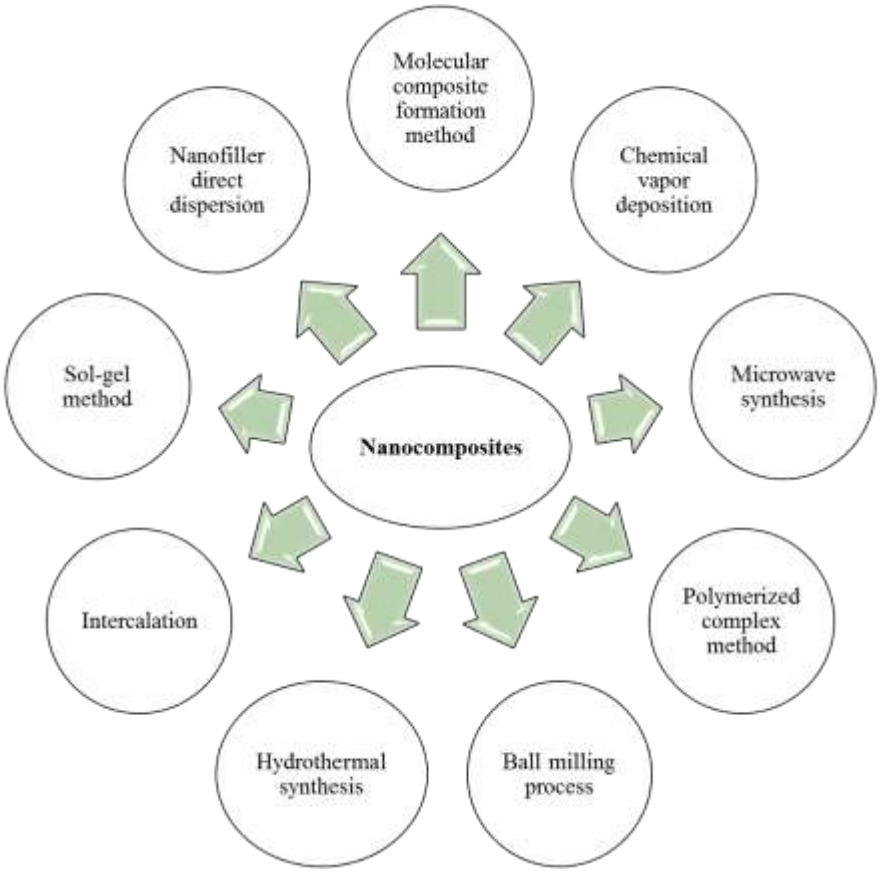

Figure 2.7: Synthesis routes of nanocomposites

Sol-gel synthesis

This is the most effective and cost reliable method of producing nanomaterial, nanocomposites and powders recently. Earlier it was widely used in glass and ceramic industries. It involves hydrolysis of the alkoxides by water, alcohol, ammonia, or acid followed by condensation of the products formed to produce a glass like material. It is utilized when forming inorganic or hybrid composites at low temperatures and pressures. The factors affecting this method include: pH, starting material, and solvent to be used.

Hydrothermal synthesis

This involves combining the starting materials intended for composites synthesis with certain amount of water followed by acid digestion in a reactor at high temperature and pressure. The reactants may not dissolve completely using this method.

Chemical vapor synthesis

This is a modification of the chemical vapor deposition where the process is directed towards the synthesis of nanomaterials instead of films. The whole idea of chemical vapor deposition is the attachment of solids produced from chemical reactions in the vapor phase to a heated surface. The energy needed for complete conversion of starting materials to nanoparticles is provided by hot walls, plasma, flame and laser reactors. The availability of appropriate starting material is the major limitation of this technology. It is currently used in the production of monoliths, powders and films.

Microwave synthesis

Microwave synthesis technique has been used in organic synthesis since time immemorial. More than 2000 papers have been published relating to the application of this technique (Kappe 2004). It is in use in pharmaceutical, biochemical, medical, food, ceramic industries and academic institutions. Use of microwave synthesis in the production of nanocomposites entails combining starting materials by microwave irradiation to yield desired nanomaterial. It is fast, economical and generate less by products.

Solution-evaporation method

This is a method of composites formation which involves mixing of nanotubes dispersion with a solution solely made up polymers that dissolves in solvents or thermoplastic polymers followed by evaporating the solvent. This will allow the nanotubes to move freely within the polymer matrix. The mixture can then be subjected to mixing and molding till desired shape is achieved. The mixing intensity and its duration will determine the distribution of the nanoparticles within the polymer. The major drawbacks of this technique is that the polymer has to be soluble in the same solvent used to disperse nanoparticles and the problem of solvent removal limits the application of this technique in major industries.

Ball milling process

This is a technique that has been used in almost all industries for size reduction of materials. Nanocomposites production is no exception considering the recent utilization of high energy ball milling process for the production. Powdered materials are normally immersed for ball milling in the appropriate machine through movement of the balls, collision to the supporting disc and centrifugal force exerted nanomaterials are easily formed. Mechanical alloying, mechanical milling and mechanochemical synthesis are the terms mostly used relating to the production of materials by ball milling. This method is perfect for the production of nanomaterials because it is efficient, and cost effective.

Intercalation method

This is the most widely known method for the synthesis of polymer nanocomposites. The desired outcome depends on whether an intercalated or exfoliated hybrid is required. The process involves combining a starting material (a polymer) within layers of clay of material. When intercalate is required the organic material is immersed within the layers of the clay such that there will be expansion within the component mixtures. While in

exfoliated mixture, the whole layers of the clay material will be separated from each other but tied within the matrix of the organic component.

Nanoparticle direct dispersion method

This is a method of producing nanocomposites by chemically modifying nanoparticle to increase compatibility with polymers. The advantage of using this method is that total homogeneity is achieved without compaction. Zinc oxide nanoparticles were prepared by combining zinc sulfate and ammonium bicarbonate in the study conducted by (Yujun *e*t *a*l., 2010).

Molecular composite formation

This is a method of producing nanocomposites that have extra mechanical stability due to the reinforcement provided by molecular rods. A strong and durable polymer is normally combined with a malleable polymer matrix at molecular dimension with a solvent that will later be precipitated. An equilibrium compound is required as the third component for this method which will aid in the formation and dispersing of fibrils within the composite.

2.7 Activated Carbon in desulfurization

AC is widely known as a versatile absorbent due to its surface area, wide availability, ease of preparation and its wide applications in adsorptive studies. It is said to have high selectivity for organosulfur compounds and organo-nitrogen compounds due to the presence of hydrogen bonding interactions in their surface functional groups (Jae *e*t *a*l., 2006). In addition ACs are said to have surface functional groups that aid in chemisorption (Roop *e*t *a*l., 2005; Rahimeh *e*t *a*l., 2012). AC is generally use in ADS due its low cost and high capacity for sulfur compounds. Local diesel fuel of 450ppm sulfur content was treated

using AC at room temperature and the sulfur concentration reduced to 210ppm using 5% adsorbent material (Isam *e*t *a*l., 2013).

The activity of removal of dimethyl sulfide (DMS) impurity from bioethanol using virgin AC and AC loaded with zinc oxide was investigated. The result indicates loaded AC having twice efficiency in comparison with the virgin AC due to the presence of larger mesopores (Jintawat *e*t *a*l., 2010). The beauty of AC over other adsorbents is that it can be synthesized from different parent materials (waste inclusive). AC derived from sewage sludge was tested for ADS of DBT from n-octane at room temperature. Time (30mins-2hrs), carbonization temperature (400-800°C) and different activating agents were varied in the study to fully understand the adsorption process. The result indicates that DBT adsorption increases with increase in carbonyl functional groups and around 70.6% DBT removal was achieved using potassium hydroxide activating agent, carbonized at 600°C for 1hr which is by far higher than the percentage removed by commercial AC. The adsorption of DBT on the sewage derived AC best fit Langmuir isotherm (Thitiwan *e*t *a*l., 2013). The efficiency of AC in desulfurization was compared with zeolite in a batch adsorber and the result indicates AC having better adsorption characteristics that fits with Langmuir and Freundlich isotherms (Marko *e*t *a*l., 2010). AC used in ADS of diesel fuel containing 72ppmw sulfur content in a batch system at 303.15K at atmospheric pressure and magnetic stirring for 18hrs presents result that best fit Sips and BET models and the sulfur content was reduced to 15ppmw (Celia *e*t *a*l., 2010).

Modification of AC with oxidizing agent, metals and metal oxides is known to improve selectivity, reactivity and capacity to sulfur compounds. Modification of ACs by nitric acid and nickel proves to have better efficiency compared to non-modified commercial AC in

the ADS of refractory sulfur compounds from diesel oil (Selvavathi *e*t *a*l., 2009). AC, activated alumina, and nickel based adsorbents have been tested for denitrogenation and desulfurization of aromatic compounds from model diesel fuels in a fixed bed system; the result indicates that AC has greater affinity and selectivity in the removal of both the most notorious refractory sulfur compounds and the nitrogen compounds compared to the other adsorbents used (Jae *e*t *a*l., 2006).

There are believes that other components in fuels such as (polyaromatic hydrocarbons) may compete with the sulfur compounds in fuels on the surface of AC thus resulting in impaired desulfurization. Due to this, adsorption affinity of polyaromatic sulfur heterocycles (PASHs) and polyaromatic hydrocarbon (PAHs) on AC and how PAHs affects the adsorption of PASHs in both batch and fixed bed systems was investigated. The result concludes that the electron-donor acceptor mechanism plays an important role in the adsorption of sulfur molecules and the presence of PAHs reduces the adsorption of PASHs. In addition, for better performance of the adsorbent, it should possess pore size higher than the adsorbate for effective adsorption of large molecules and reducing diffusional resistance (Jie *e*t *a*l., 2011). The side effects of aromatics, oxygen containing additives, nitrogen containing compounds and moisture on the efficiency of ADS from diesel fuel on AC have been tested and it reveals that sulfur adsorption by AC is due to the interaction of conjugated π electrons with the carbon surface and all the compounds have inhibitory effects on the adsorption which is due to the hydrogen bonding interaction between polar groups (Jing *e*t *a*l., 2012).

Nickel loaded on different sorbents was tested for desulfurization of diesel oil containing all the refractory sulfur compounds (250ppmw); the inhibitory effects of aromatics on

adsorption by AC was confirmed (Hernandez *et al*., 2010), despite the inhibition however, AC loaded with nickel gave higher breakthrough and uptake capacities compared to other sorbents due to the high selectivity of nickel on sulfur compounds and high surface area of AC. In addition, textural and chemical factors such as (level of micropores and acidic groups in macropores) affect the adsorption capacity of AC in diesel fuel (Mykola *et al*., 2009). The major concern about the use of ADS is the regeneration and disposal of the adsorbent. The regeneration methods to restore carbon adsorptive capacity of DBT are thermal, solvent and ultrasound approaches. In addition, maintaining the integrity of micropores is cardinal to regeneration. Thermal regeneration method result in the loss of micropores and the important surface functional groups of AC. Regeneration of AC by solvent extraction proves to be the best approach because it can restore its efficiency to about 70% fresh capacity after nine cycles of regeneration (Xue *et al*., 2014).

2.8 Nanocomposites in desulfurization

Doping of adsorbents with metals and metal oxides is known to enhance selectivity, reactivity and capacity for the sulfur compounds. Solid metal thiolates that are insoluble in hydrocarbons are formed when metal oxides react with thiophene derivatives; this allows there removal by filtration. Various nanocomposites have been reported of having potentials in ADS such as alkaline and alkaline earth metals, CuO, Cr_2O_3, NiO, Fe_2O_3, CeO_2, ZnO etc (Saha *et al*., 1995; Ramaswamy *et al*., 2004). Most of the adsorbents adsorbs at ambient conditions and the desulfurization efficiency is dependent on the amount of metals and the type of sorbents used. Varying the nickel/cupper loadings on Ni/Alumina and Ni/Aluminosilicate-5 in ODS using hydrogen peroxide as the oxidant shows a dramatic change in the desulfurization. Loading Ni on Alumina can completely

treat sulfur in oil from 350ppmw to 0ppmw (Sarda *et al*., 2012). Dispersion of metals and metal oxides on adsorbents increases adsorption efficiency. Ag/TiOx–Al_2O_3 and Ag/TiOx–SiO_2 have been used as remarkable adsorbents for the ADS of jet and diesel fuels at ambient conditions. Dispersion of TiOx and loading of Ag on alumina or silica increases desulfurization performance. Ag/TiOx–Al_2O_3 has greatest affinity to BT and it reduces the sulfur content of ULSD from 1170ppmw to 75ppmw. It is equally regenerable (Shahadat *et al*., 2013). A high performance sulfur adsorbent (NiO–CeO_2/Al_2O_3–SiO_2) has been used for the desulfurization of Jet A fuels at ambient conditions. The composite reduces the sulfur content from 1140ppmw to as low as 10ppmw; it has sulfur adsorption capacity of 1.4 and 3.22 mg-S/g-ads at breakthrough points of 10 and 50 ppmw respectively. The adsorbent was regenerated four times by calcinating helium gas for a short time before reaching half-life (Xinhai *et al*., 2014).

NiMCM-41 and NiY adsorbents have been used in vapor phase ADS of diesel under controlled condition. 1g of NiMCM-41 treated 20ml of diesel and the sulfur concentration was reduced from 450ppm to 50ppm while 1g of NiY treated 25ml of diesel and the sulfur concentration was reduced to <50ppm. Both composites were regenerated under controlled oxidation at approximately 450°C (Soumen *et al*., 2013). Zeolite-TiO_2 have been tested for the photodegradation of DBT in fuels, β-zeolite adsorbed almost all the degradation product while TiO_2 was used as a photo catalyst in the reaction. Over 88% of DBT was degraded (Faghihian *et al*., 2013).

π-complexation a form of a ADS using copper species on nanomaterials such as zeolites, AC, silica and alumina or nanocomposites to selectively remove thiophenic compounds in fuels at room temperature and pressure proves to be a promising approach in

desulfurization (Yang *et al*., 2006; Wen-Hang *et al*., 2010). Complexes are formed between the bulk materials and the cuprous ions which is an essential step in the removal of sulfur compounds from fuels. The extent of removal depends on the amount of the copper species and the limit of dispersion of the species on the nanomaterials. The cuprous species for ADS can be directly introduced or formed from the reduction of cupric species.

An area of interesting research currently focuses on the utilization of membranes for efficient desulfurization. Oleophilic polymer-inorganic nanocomposites are used for the pervaporative removal of organosulfur compounds from gasoline. The inorganic component (silica nanoparticles) can be synthesized in-situ through biomimetic mineralization in confined space using an alkaline inducer catalyst. The membrane has a good performance permeation flux of 7.36 kg/ (m^2h) and a selectivity of 4.98 to thiophene in gasoline (Ben *et al*., 2012). Table 2.3 outlines some of the selected literatures on the utilization of Ni, Ce and Fe nanocomposites in desulfurization.

Table 2.3: Selected literatures on the utilization of Ni, Ce and Fe nanocomposites in desulfurization

Referencce	Description	Material Used
Rachid *et al*., 2000	Coal flue gas desulfurization	CuO, Fe_2O_3, MnO, ZnO
Zeng *et al*., 2000	H_2S Removal	CeO_2
Rachid *et al*., 2001	H_2S removal by waste material	SnO, ZnO, Fe_2O_3, & Ash
Selvavathi *et al*. 2009	ADS of refractory sulfur compounds	Ni loaded on commercial AC
Hernandez *et al*., 2010	ADS of refractory sulfur compounds	Ni on AC
Sumathi *et al*., 2010	SO_2 removal from flue gas	Ce loaded on AC synthesized from palm shell
Wei *et al*., 2010	H_2S removal	Fe_2O_3 & CeO_2 on coal ash
Xiang *et al*., 2011	SO_2 removal	Carbons doped with Fe, Ni, Ce
Jia *et al*., 2012	SO_2 removal	Ni loaded on acid treated AC
Yuliang *et al*., 2013	Thiophene removal	Ni/MnO-ZnO
Fengkui *et al*., 2013	Sulfidation experiment	Fe_2O_3 on Activated Char
Jianglong *et al*., 2013	Sulfur removal	Fe-Mo on Activated Char
Lu *et al*., 2013	SO_2 removal	Fe_2O_3/AC from walnut shell
Xiao *et al*., 2014	SO_2 removal	Fe/AC, Fe/AC-HNO_3
Nan *et al*., 2015	Photo catalytic desulfurization	CeO_2 loaded on porous carbon derived from lignin

2.9 Mechanisms of Adsorptive desulfurization

ADS is based on physisorption or chemisorption process of organosulfur compounds on solid sorbents. The mechanism of desulfurization in general has not been extensively studied in full details. Most of the reports on this field proposed the mechanism theoretically or experimentally without proper insight into the subject. However, the studies of (Liang *e*t *a*l., 2010; Duan *e*t *a*l., 2014; Lichun *e*t *a*l., 2011) have outlined some of the mechanisms involved in ADS.

The mechanism of ADS based on the idea to regenerate sulfur-poisoned Ni catalyst in reduced atmosphere has been studied by (Tawara *e*t *a*l., 2000). Ni/ZnO and Ni/Al_2O_3 were utilized as catalysts for adsorptive ultra-deep hydro desulfurization of kerosene using hydrogen at 600K. The idea is based on the fact that sulfur poisoned nickel catalyst particles will be combined with ZnO or Al_2O_3 particles in the presence of hydrogen, then each poisoned catalyst will release a few ppb of H_2S which will be attached to the ZnO or Al_2O_3 particles. This process in turn will allow the effective regeneration of sulfur poisoned nickel catalyst. Residual sulfur was not detected in the treated kerosene with Ni/ZnO. The catalyst completely remove residual sulfur even after 800 h of operation and no methane was produced in contrast to the other materials used. Following the results outlined above, (Babich *e*t *a*l., 2003) further illustrates the mechanism. ZnO/Al_2O_3 was used as the main component of the sorbent while Ni was used as the main site for the hydro desulfurization. Thiophene in the second step of the reaction was decomposed on the Ni site after reacting with hydrogen. Further reaction with hydrogen lead to the removal and transfer of hydrogen sulfide to ZnO surface. Subsequent reactions with thiophene further converts ZnO completely to ZnS which may later be regenerated or discarded.

Reactive adsorption desulfurization of model oil containing DBT over a Ni/ZnO adsorbent has been outlined by (Lichun *e*t *a*l., 2011). The reaction mechanism under different atmospheres has been investigated. The result indicates different mechanisms when nitrogen and hydrogen were used respectively. Desulfurization over Ni/ZnO using nitrogen was achieved based on physical and chemical adsorption but the rate was very slow. However, the desulfurization under hydrogen turns out to be based on reactive adsorption desulfurization and the rate was very fast. Hydrogen is very important in reactive adsorption desulfurization when Ni/ZnO adsorbent is used, it aids in the decomposition of DBT on Ni species and in the formation of Ni_3S_2 and the transfer of sulfur moieties to ZnO. The kinetics of thiophene reactive adsorption on Ni/SiO_2 and Ni/ZnO via thermal gravimetric analysis at 280–360°C under 5–40 mbar of thiophene in H_2 was illustrated by (Bezeverkhyy *e*t *a*l., 2008). The interaction of Ni/SiO_2 with thiophene followed a two-step reactions: surface reaction followed by bulk transformation into Ni_3S_2 (nickel sulfidation). The interaction of Ni/ZnO with thiophene is similar to Ni/SiO_2 interaction, a surface reaction was noticed due to increase in weight but there was no nickel sulfidation transformation instead a nucleation-controlled ZnO surface transformation was noticed followed by complete particle sulfidation.

The sulfur transfer mechanism in the presence of hydrogen involves three step reactions: first step involves the decomposition of DBT in the model oil on Ni surface of Ni/ZnO to form Ni_3S_2, the second step involves the reduction of Ni_3S_2 in the presence of hydrogen to form H_2S followed by the release of active nickel species from Ni_3S_2. The final step involves the storage of H_2S in the adsorbent followed by the final conversion of ZnO into ZnS. The mechanism is illustrated in Figure 2.8.

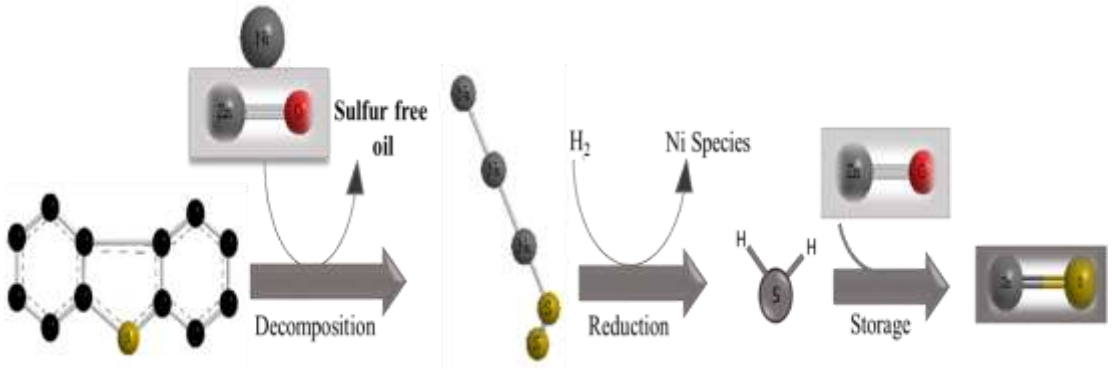

Figure 2.8: Mechanism of reactive ADS of DBT containing model oil over adsorbent of Ni/ZnO in hydrogen.

The mechanism involved in the removal of thiophene by reactive ADS from model fuels is illustrated by (Xuan *e*t *a*l., 2013). Reduced NiZnO/Al_2O_3-diatomite was used as the adsorbent in the studies and the result indicated that S-M bonding of thiophene to Ni sites of the adsorbent was decomposed to form Ni_3S_2 and C4 olefins formed were further saturated by hydrogen to CH_4 which was released back to the stream. The final step involves the transfer of sulfur from Ni_3S_2 to ZnO in a reduced atmosphere which will yield ZnS and a free Ni specie ready for another round of the reaction.

Zeolites are acid catalyst used in olefin hydroforming and aromatic conversion. They are also used in HDS and as bi-functional catalyst. Zeolites contains both acidic and a basic site. The lewis basic site on zeolites is responsible for the catalytic hydrogen desulphurization of most sulfur compounds in fuels; the bronsted acidic site has little or no role to play in the catalysis. Thiophenic ring cracking is the rate determining step in HDS of thiophene and DBT (Rozanska *e*t *a*l., 2003). A periodic density functional theory study of the thiophenic derivative cracking catalyzed by proton or lithium exchanged modernite (zeolite) can be a good method to prove the cracking of thiophene derivatives; benzothiothiophene is cracked by a catalyst where one of the oxygen atoms in the catalyst

is the catalytic center for the reaction. The mechanism of BT cracking is illustrated in Figure 2.9.

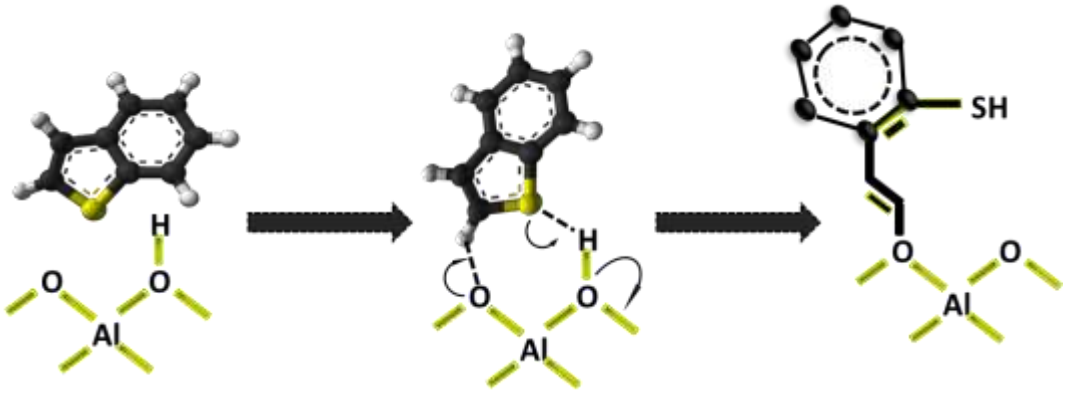

Figure 2.9: Mechanism of BT cracking by zeolites

Mechanism of adsorption of DMDBT from solutions in hexadecane on three different nanopourous AC has been illustrated by (Kostas *e*t *a*l., 2014). Each of the nonporous carbons has microporous or combined micropores and mesopores structures. The capacity for 4, 6-DMDBT adsorption increases with increase in the volume of pores. The pores with diameter lower than 10 Å are said to adsorb better because the diameter is similar to that of 4, 6 DMDBT molecule. Acidic functional groups on the surfaces of the larger pores are said to contribute to the adsorption via polar interactions. Most noticeable functional groups are carboxylic acids because they interact with the oxidation products of 4, 6 DMDBT (sulfoxides, sulfones, and sulfonic acids) via hydrogen bond. Dispersive interactions between the delocalized π-electrons within the benzene rings of 4, 6 DMDBT and the electron rich region on the nanoporous carbon aromatic ring also plays a major role in the adsorption. Figure 2.10 illustrates the mechanism

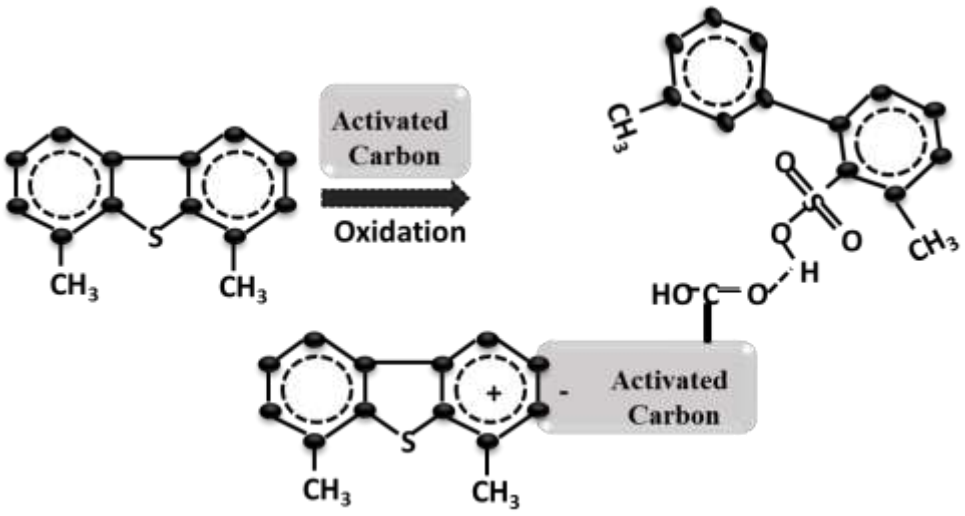

Figure 2.10: The possible adsorption mechanism of 4, 6 DMDBT on AC

Molecular simulation techniques are used for the illustration of reaction mechanisms involved in desulfurization using density functional theory. These techniques are reported by (Hideo *e*t *a*l., 2004; Shengli *e*t *a*l., 2012) and they provide useful information for better optimization and improvement of materials used in the desulfurization technology. The reactive adsorption desulfurization mechanism of thiophene over Zn_3NiO_4 (bimetallic oxide adsorbent) is illustrated using density functional theory. The gas phase thiophene molecule is adsorbed on the Ni site instead of the Zn-site on the adsorbent. Hydrogen plays a fundamental role in the cleavage of the C-S bond of the sulfur compound. The result indicates that thiophene is first decomposed on the Ni site of the adsorbent followed by reduction to nickel sulfide via two pathways. The first pathway is that nickel sulfide is reduced to H_2S in the presence of H_2 while the second pathway allows the transfer of sulfur from nickel site of the adsorbent to zinc site. A further illustration on the adsorption of thiophene on icosahedral Ni_{13} and Zn doped Ni_{13} clusters ($Zn@Ni_{13}$ and $Ni@Ni_{11}Zn_1$) is shown using density functional theory by (Ping *e*t *a*l., 2013). The results indicates that thiophene is preferentially adsorbed on Ni_{13} and $Zn@Ni_{12}$ clusters

with the whole ring π-bond to the hollow site (η^5 bonding model) and the introduction of Zn to Ni_{13} leads to a small decrease in the bonding energy. Thiophene is preferred to be adsorbed on the Ni rather than on the Zn site.

2.10 Research Objectives

The main aim of this research was to synthesize AC from WRTs, load it with nanoparticles and test its suitability as an adsorbent in desulfurization. The specific objectives were:

1. To set a design-of-experiment for preparing porous carbon (PC) from WRTs.

2. To synthesize nanoparticles of PC; including Ni, Ce, Fe and a combination of nanoparticles supported on the prepared PC.

3. To characterize the prepared materials in terms of surface morphology and structural properties.

4. To evaluate the sorption activity of the prepared materials.

CHAPTER 3

EXPERIMENTAL

This chapter describes the materials, chemicals, solvents and experimental equipment used in this work. It also outlines the synthesis, characterization and evaluation of the sorption abilities of the synthesized materials. The methodology employed to achieve the set objectives of this work is also elucidated. Adsorbents characterization consisted of boehm's titration experiment, scanning electron microscope equipped with energy dispersive x-ray detector (SEM-EDX), Fourier Transform Infrared Spectroscope (FT-IR), X-ray diffraction analyzer (XRD), BET surface area analyzer and thermogravimetric analyzer (TGA). ADS tests were conducted in batch mode and fixed bed adsorption systems, Gas chromatography sulfur chemiluminescence detector was used throughout the adsorption experiments to monitor the level of sulfur.

3.1 Chemicals and solvents

The following chemicals were used in the current work:

Ethanol (C_2H_6O, 99.8%, 46.07 g/mol Fluka AG),

Ethylene glycol monomethyl ether ($CH_3OCH_2CH_2OH$ 76.10 g/mol J. T Baker Chemical),

Toluene (C_7H_8, 99.81%, 92.14 g/mol, Chem Lab),

N-Hexane ($C_6H_{14,}$ 95%, 86.18 g/mol, Fischer Scientific),

Nickel Acetate tetrahydrate ($NiC_4H_6O_4 \cdot 4H_2O$, 99%, 248.86 g/mol, Fischer Scientific),

Ferric Nitrate ($Fe(NO_3)_3 \cdot 9H_2O$, 99.5%, 403.9 g/mol Sigma Aldrich),

Cerium Nitrate hexahydrate ($Ce(NO_3)_3 \cdot 6H_2O$, 99.0%, 434.22 g/mol, Sigma Aldrich), Thiophene (C_4H_4S, 99%, 84.14 g/mol, Sigma Aldrich),

BT (C_8H_6S, 99%, 132.4 g/mol Sigma Aldrich),

DBT ($C_{12}H_8S$, 99%, 184.26 g/mol, Sigma Aldrich),

Manganese chloride tetra hydrate ($MnCl_2 \cdot 4H_2O$, 99%, 197.91 g/mol, Fischer Scientific),

Sodium bicarbonate ($NaHCO_3$, 99.5%, 84.01 g/mol, Panreac),

Sodium carbonate Anhydrous (Na_2CO_3, 99.99%, 105.9888 g/mol Sigma Aldrich),

Sodium hydroxide (NaOH, 98%, 40 g/mol, Panreac),

Hydrochloric acid (HCl, 37%, 36.46 g/mol, Sigma Aldrich), and

Nitric Acid (HNO_3, 70%, 63.01 g/mol, Sigma Aldrich).

3.2 Carbon Production

3.2.1 Conversion of WRTs to Porous Carbon

As received used tires were cut into small pieces. In this step iron wires were removed from tire to make small pieces. WRTs were cleaned and thoroughly washed with deionized water many times to remove impurities till it became neat and clean. The material was dried in an oven at 110◦C for 2 h. The tire pieces were then cut to smaller pieces to fit into crucible. Approximately 20g of the sample was taken for carbonization (exact weight was noted and recorded) then kept inside batch adsorber in air atmosphere at 250, 300, 350, 400, 450, 500 and 550°C for 2 h. The liquid hydrocarbon produced was trapped and weighed

appropriately. The % yield of both carbon black and liquid hydrocarbon was calculated. The gases produced convert the air atmosphere inside the closed system into a mixture of gases and the % yield was calculated by subtraction. The sample was taken out of the batch adsorber and the carbon particles were allowed to cool then later grounded to fine particles using pestle and mortar. The procedure was repeated for different samples by keeping the temperature constant at 500℃ and varying the time to 30mins, 1 h, 2 h, 2 h, 4 h and 5 h in a muffle furnace. Adhering impurities on the surface of the adsorbent were oxidized upon treatment with hydrogen peroxide solution. The material was washed with deionized water and dried in a vacuum oven. The dried material was then activated at different temperatures viz: 400, 500, 600, 700, 800 and 900◦C at a fixed time 5 h in a muffle furnace. The material was then treated with nitric acid and sodium hydroxide solutions to remove the ash content and for the development of oxygen functional groups on the surface of the adsorbent. The following formulas were used for the calculation of percentage yield and percentage recovery:

$$\%\, Yield = \frac{actual\ yield\ (g)}{theoretical\ yield} * 100$$

$$\%\, Recovery = \frac{amount\ of\ pure\ product\ recovered}{amount\ of\ crude\ material\ used} * 100$$

The adsorbent was washed with deionized water and dried in an oven at 120◦C overnight. The procedure used for the synthesis is depicted in figure 3.1 and figure 3.2 depicts the image of the adsorber used in the synthesis of AC from WRTs.

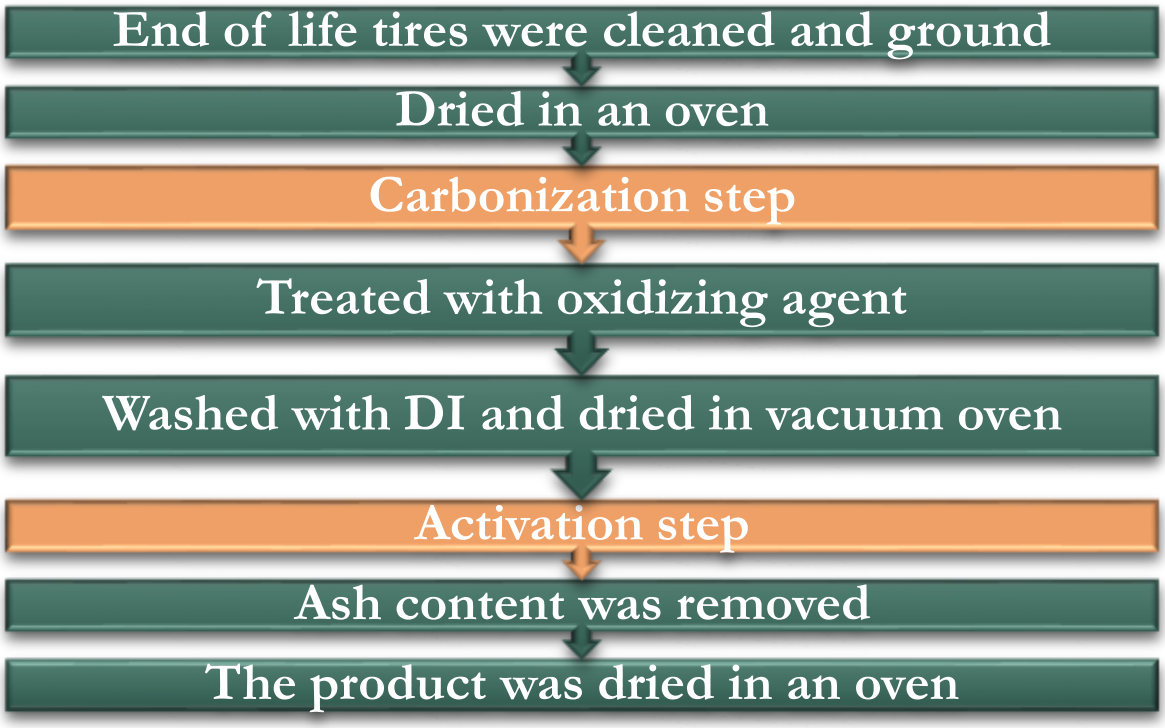

Figure 3. 1: Steps in the conversion of waste rubber tires to porous carbon

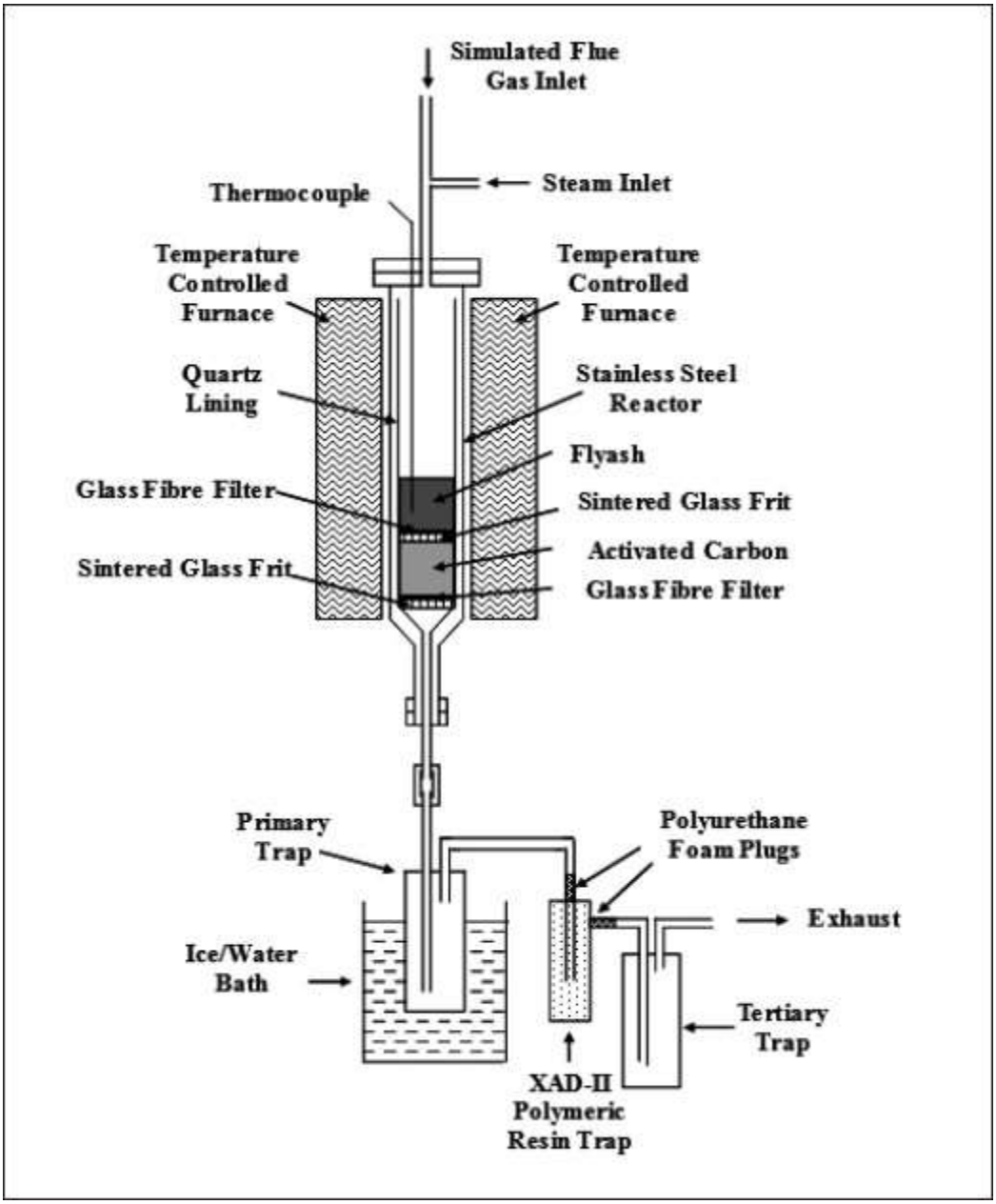

Figure 3. 2: Stainless steel adsorber used in the synthesis of AC from waste rubber tires

3.2.2 Oxidation of the synthesized AC

Chemical activation was conducted on the prepared material using 4M HNO_3 and 4M NaOH at three different temperatures respectively (30, 60, and 90°C). 42 grams of the synthesized material were divided into six round bottom flasks each containing 7grams of the adsorbent. The first 3 flasks were filled with 70ml each of concentrated HNO_3 while

the second sets were filled with 70ml each of concentrated NaOH respectively. The set up was stirred and allowed to stand for 3h in a reflux condenser. The samples were then washed thoroughly after the oxidation treatment with deionized water till neutral pH was achieved and dried at 110°C overnight. The samples were stored and covered in a glass bottle before use. The samples after acid and base treatment were labelled as AC-HNO_3-t and AC-NaOH-t respectively (t signifying the temperature).

3.3 Synthesis of Nanomaterials

3.3.1 Loading of 0.5%, 5%, 10% and 30% Manganese oxide on AC (Mn/AC).

28.0 g of AC were divided into four separate round bottom flasks. 150 mL of deionized water and 100 mL of ethanol were added to each flask and stirred for 3 h. Manganese chloride tetra hydrate ($MnCl_2 \cdot 4H_2O$) was used as the precursor for loading of different ratios of Mn on AC.

For 0.5% Mn/AC

$$\frac{0.5}{100} * 7g = 0.035g\ of\ MnO$$

$$\frac{Mn}{MnCl_2.4H_2O} = \frac{54.94\ g/mol}{197.9\ g/mol} = \frac{0.035g}{x}$$

$$x = 0.126\ g\ of\ precaussor$$

The volume required to prepare 0.1 M solution of $MnCl_2.4H_2O$ (0.126g) can be calculated using

$$vol\ in\ mL = \frac{mass\ (g) * 1000}{Molar\ mass * concentration\ \left(\frac{mol}{dm^3}\right)} = \frac{0.126 * 1000}{197.9 * 0.1} = 6.36\ mL$$

So, 6 mL solution containing 0.126 g of the precursor was added to the first round bottom flask containing 7g AC, 10 mL ethylene glycol was later added to the mixture to ensure adequate binding of the metals to the adsorbent. The set up was allowed to stand for 2 h and maintained at a basic pH, then later refluxed at 80°C for 6 h. the precipitate was filtered, washed and dried at 120°C for 6 h. Similar set up was carried out to the remaining flasks for the synthesis of 5% (1.26g of precursor in 6 mL), 10% and 30% Mn on AC respectively. The effect of metal ratio and calcination on the desulfurization performance of the prepared adsorbents was evaluated.

3.3.2 Loading of 10% Nickel on AC (AC/Ni)

Sol–gel method was used for loading of nanoparticles on the porous carbon. 7.0 g of AC was dispersed in 150 mL of deionized water and 100 mL ethanol by the use of sonicator. Then, a 9.36 mL solution containing 2.96 g of Nickel Acetate (Ni $(C_2H_3O_2)_2.4H_2O$ (1M) was drop-wise added into the dispersed AC to make a 1 M solution. 20 ml of ethylene glycol was added followed with stirring for 2h, maintaining pH at 8-9 followed by heating to 80°C for 6h under stirring. The precipitate was filtered, washed and dried at 110°C overnight.

3.3.3 Loading of 10% Cerium on AC (AC/Ce)

7.0 g of AC was dispersed in 150 mL of deionized water and 100 mL ethanol by the use of sonicator and stirred for 5 h. Then, a 5 mL solution containing 2.17 g of Cerium nitrate hexahydrate (Ce $(NO_3)_3 \bullet 6H_2O$) to make 1M solution was drop-wise added into the dispersed AC, 20 ml of ethylene glycol was added followed with stirring for 2h, maintaining pH at 8-9 followed by heating to 80°C for 6h under stirring. The precipitate was filtered, washed and dried at 110°C overnight.

3.3.4 Loading of 10% Iron on AC (AC/Fe)

7.0 g of AC was dispersed in 150 mL of deionized water and 100 mL ethanol by the use of sonicator and stirred for 5 h. Then, a 12.53 mL solution containing 5.06 g of Ferric Nitrate (Fe $(NO_3)_3$•$9H_2O$) solution was drop-wise added into the dispersed AC to make a 1 M solution. 20 ml of ethylene glycol was added followed with stirring for 2h, maintaining pH at 8-9 followed by heating to 80°C for 6h under stirring. The precipitate was filtered, washed and dried at 110°C overnight. The steps employed for loading of metals on AC are depicted in figure 3.3.

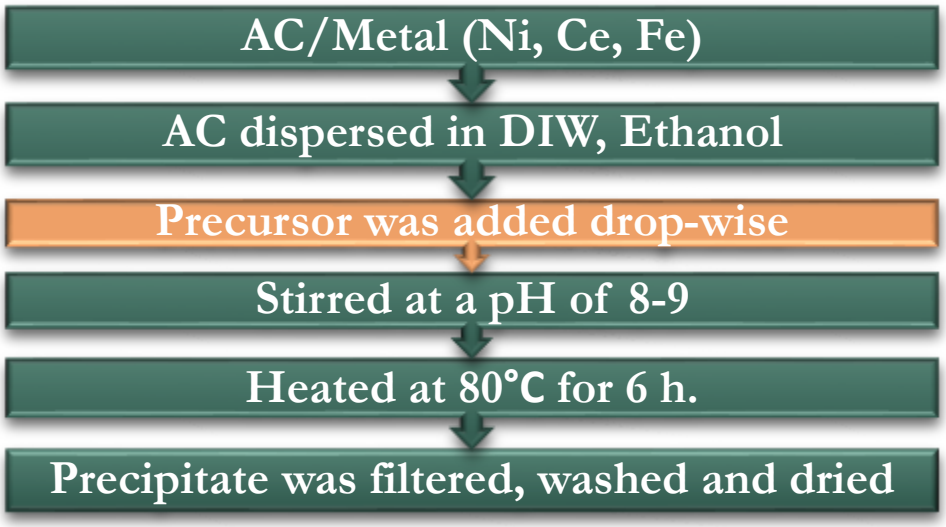

Figure 3. 3: Steps used for loading metals on AC

Nanocomposites preparation

3.3.5 Preparation of AC /NiO (5%)/ Ce (10%)

7.0 g of AC was dispersed in 150 mL of deionized water, 100 mL ethanol and 20 mL ethylene glycol and stirred for 5 h. Then, a 10 mL solution containing 1.16 g of Nickel Acetate (Ni $(C_2H_3O_2)_2$.4H2O solution was added drop-wise into the dispersed AC and

maintained at a pH of 8-9. The mixture was refluxed at 90°C for 5 h. The precipitate was filtered, washed and dried at 110°C overnight. The dried material was dispersed in 150 mL deionized water, 100 mL ethanol and 20 mL ethylene glycol. 5 mL solution containing 2.17 g of Cerium nitrate hexahydrate was added to the mixture and stirred for 2 h. The set up was refluxed at 90°C for 5 h and the precipitate was filtrated washed and dried at 110°C overnight.

3.3.6 Preparation of AC /CeO_2 (5%)/ Fe (10%)

7.0 g of AC was dispersed in 150 mL of deionized water, 100 mL ethanol and 20 mL ethylene glycol and stirred for 5 h. Then, a 5 mL solution containing 0.88 g of Cerium nitrate hexahydrate solution was added drop-wise into the dispersed AC and maintained at a pH of 8-9. The mixture was refluxed at 90°C for 5 h. The precipitate was washed and dried at 110°C overnight. The dried material was dispersed in 150 mL deionized water, 100 mL ethanol and 20 mL ethylene glycol. 13 mL solution containing 5.06 g of Cerium nitrate hexahydrate was added to the mixture and stirred for 2h at pH of 8-9. The set up was refluxed at 90°C for 5 h and the precipitate was filtered, washed and dried at 110°C overnight.

3.3.7 Preparation of AC /FeO (5%)/ Ni (10%)

7.0 g of AC was dispersed in 150 mL of deionized water, 100 mL ethanol and 20 mL ethylene glycol and stirred for 5 h. Then, a 5 mL solution containing 1.96 g of ferric nitrate solution was added drop-wise into the dispersed AC and maintained at a pH of 8-9. The mixture was refluxed at 90°C for 5 h. The precipitate was washed and dried at 110°C overnight. The dried material was dispersed in 150 mL deionized water, 100 mL ethanol and 20 mL ethylene glycol. 12 mL solution containing 2.95 g of nickel acetate was added

to the mixture and stirred for 2h at pH of 8-9. The set up was refluxed at 90°C for 5 h and the precipitate was filtered washed and dried at 110°C overnight.

3.4 Characterization

Several instrumental methods were used to characterize the synthesized materials including BET surface area analysis, XRD patterns, SEM equipped with EDX detector to understand the morphology and elements that constitute the adsorbent, TGA, and FT-IR analysis to understand the functional groups present in the synthesized materials. In addition, measurement of surface pH, boehm's titration experiment was performed to understand the amount of surface oxygen containing functional groups.

3.4.1 Surface pH.

The carbon samples were tested by HI 3512 benchtop pH meter equipped with a graphic LCD display to gain insight about the acidity and basicity of the samples. A suspension of 0.2 g of each sample was added to 10 mL of water and the suspension was stirred overnight to reach equilibrium. The samples were then filtrated and the pH of the each solution was measured.

3.4.2 Boehm's method

The amount of oxygen surface functional groups (both acidic and basic) were determined according to Boehm's method (Boehm 1966) after slight modification. 0.5g of raw and treated carbon samples were added to beakers each containing 25 mL of the following 0.05 M solutions: NaOH, Na_2CO_3, $NaHCO_3$ and HCl. The beakers were sealed and shaken for 24 h and then 10 mL of each filtrate was pipetted in an excess of 20ml 0.05M HCl for the determination of acidic functional groups or NaOH for the basic functional groups. The filterate was titrated with 0.05M NaOH or HCl using phenolphthalein indicator and the

volume required to reach the endpoint was noted. For Na_2CO_3 reaction base, an excess of 30ml 0.05M HCl was added rather than 20ml due to diprotic property of the base to ensure complete reaction with acid. The number of acidic sites was calculated under the assumption that NaOH neutralizes carboxyl, phenolic, and lactonic groups; Na_2CO_3 neutralizes carboxyl and lactonic; and $NaHCO_3$ neutralizes only carboxyl groups. The number of surface basic sites was calculated from the amount of hydrochloric acid required.

The following formula was used to calculate the amount of surface acidic and basic groups neutralized by NaOH and HCl respectively (Paul *et al*., 2004):

$$Moles\ of\ Carbon\ functionality = \frac{\left(\left[R\ a\ or\ b\right] V_r - \left([X]\ V_x - [T]\ V_t\right)\right)}{m}$$

Where: $\left[R\ a\ or\ b\right]$ & V_r denote the concentration and volume of the reaction base or acid in mol/L and Litres respectively

$[X]$ & V_x denote the concentration and volume of the excess acid or base added to the aliquot

$[T]$ & V_t denote the concentration and volume of the titrant required to reach the endpoint

m stands for the mass of the carbon used in grams

The amount of surface acidic groups neutralized by Na_2CO_3 and $NaHCO_3$ was calculated using the following formula (Alicia *et al*., 2010; Sarah *et al*., 2010):

$$n_{csf} = \frac{n_{HCl}}{n_B}[B]V_B - ([HCl]V_{HCl} - [NaOH]V_{NaOH})\frac{V_B}{V_a}$$

n_{csf} = the moles of carbon surface functionalities on the surface of the carbon that reacted with base during the mixing step.

$\frac{n_{HCl}}{n_B}$ = molar ratio of acid to base

$[B]$ & V_B = are the concentration and volume of the reaction base mixed with the carbon

$[HCl]$ & V_{HCl} = are the concentration and volume of the acid added to the aliquot taken from the original sample

$[NaOH]V_{NaOH}$ = the concentration and volume of the titrant in the back titration

V_a = the volume of the aliquot taken from V_B

3.4.3 BET surface area analysis

The porous structure of the synthesized materials were characterized by adsorption/desorption of nitrogen at (−196 ^{0}C) on a Micromeritics ASAP 2020 surface area and porosimetry analyzer (Micromeritics, USA) to determine surface area (BET), pore volume and pore size distribution of the treated sorbents. The image of the equipment is showed in figure 3.4

Figure 3. 4: Micromeritics ASAP 2020 surface area analyzer

3.4.4 XRD

X ray diffraction patterns of the adsorbents were taken using (Rigaku Miniflex II desktop X-ray diffractometer) using Cu-Kά radiation and an X-ray gun operated at 40 kV (voltage) and 200 mA current. Data was collected from 2θ = 0 - 80° at a scan rate of 4°/min. The equipment is shown is figure 3.5.

Figure 3. 5: Rigaku Miniflex II Desktop X-ray Difractometer

3.4.5 SEM and EDX

Scanning electron microscopy (SEM) analysis of the treated samples was conducted using low vacuum JEOL (JSM-6610LV Scanning Electron Microscope (SEM) equipped with tungsten electron gun. Energy dispersive X-ray spectroscopy (EDX) analysis was conducted to understand the composition of the synthesized materials. EDX is an analytical technique used for chemical characterization and elemental analysis based on the fact that each element has unique characteristics and composition that allow unique set of peaks to appear upon interaction with X-ray light. The image of the instrument is given in figure 3.6.

Figure 3. 6: JEOL (JSM-6610LV Scanning Electron Microscope)

3.4.6 FT-IR

The FT-IR spectra of the prepared acid and base treated samples were recorded using Nicolet 6700 spectrometer (Thermo electron, USA) with a resolution of 2.0 cm^{-1} well equipped with Deuterated triglycine sulfate detector and an OMNIC program. The experiments were conducted on the powdered samples ground in an agate mortar to produce KBr pellets and spectra were obtained by adding 64 scans and corrected for the background noise. The spectra of the samples were recorded in transmission mode and the wavenumber range of 4000–400cm^{-1}. The instrument used for this characterization is shown in figure 3.7.

Figure 3. 7: Nicolet 6700 spectrometer (Thermo electron, USA)

3.4.7 Thermal Gravimetric Analysis (TGA)

TGA analysis was conducted to understand the thermal stability of the adsorbent. The thermal stability of sorbents was tested by heating to 800 °C. About 10-15 mg of sorbent was heated with a heating rate of 20°C/ min in N_2 atmosphere at a flow rate of 100 ml/min.

3.5 Adsorption experiment

A model diesel fuel was prepared by adding the refractory sulfur compounds viz thiophene, BT and DBT in hexane (85%) and toluene (15%). The sulfur concentration in the model fuel was 150ppm prepared by dissolving 50 mg each of thiophene, BT and DBT in 1 L of hexane/toluene mixture. The adsorption experiment was conducted both in batch and column mode. The amount of sulfur in thiophene, BT and DBTwas calculated using the formula below:

$$(T, BT\ or\ DBT\ concentration\ (ppm) = \frac{molecular\ weight\ of\ sulfur}{molecular\ weight\ of\ (T, BT\ or\ DBT)}$$

3.5.1 Batch mode adsorption experiment

In a typical run using the batch mode adsorption studies, various amounts, in the range between 0.1 to 0.5g of adsorbents was introduced into 15ml of the fuel solution. The total T, BT and DBT initial concentration was 50ppm. The refractory sulfur compounds solutions containing the adsorbents were mixed well under stirring at room temperature till equilibrium. After adsorption for certain period of time, samples were collected using a syringe filter (hydrophobic polytetrafluoroethylene) and the concentrations of the sulfur compounds were measured by gas chromatography coupled with sulfur chemiluminescence detector.

3.5.2 Fixed bed adsorption experiment

Fixed bed flowing system was used to test the ADS of the treated AC samples using a column 11 cm (length) x 1 cm diameter. 0.5g of the adsorbents was packed inside the column, model fuel sample was then passed into the column by a peristaltic pump with a controlled flow rate (50rpm) at a temperature of 25°C. Once the adsorption process was started, treated fuels were sampled at different time intervals and injected to the GC-SCD for analysis. The process was halted after breakthrough was reached.

3.6 Gas chromatography

A gas chromatograph equipped with sulfur chemiluminescence detector was used for identifying and measuring the sulfur compounds in the model diesel fuel. Chromatography is a technique for separating mixtures into their components based on their interactions with mobile and stationary phases in order to analyze, identify, purify, and quantify the mixture. Chromatography involves packing of stationary phase in a column where the mobile phase in form of liquid or gas along with the analytes can pass through. The equilibration between the mobile and stationary phase accounts for the separation of

different analytes. The column conditions can be kept constant (isocratic) or variable (gradient elution). The gradient elution methods involves temperature and pressure programming where temperature will start initially at some point and reach final temperature at certain period of time for effective separation of component mixtures. A detector provides a signal of the analytes based on their concentration after eluding the column and a peak corresponding to the analyte concentration will be shown on the data system. Figure 3.8 illustrates the GC instrumentation setup

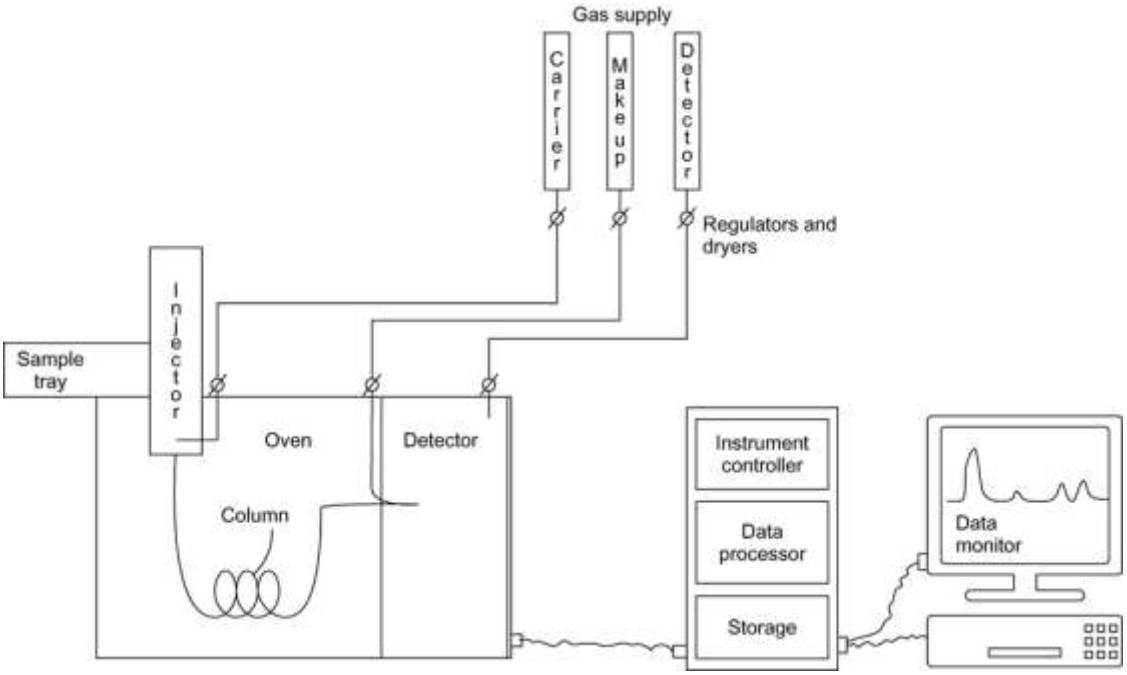

Figure 3. 8: GC Instrumentation set up

3.6.1 Sulfur Chemiluminescence Detector

Chemiluminescence refers to the emission of light resulting from a chemical reaction without apparent change in temperature. The detector is composed of O_2/H_2 supply, pyrolyzer, ozone generator, and a reaction chamber. The overall reaction that takes place in the pyrolysis chamber is RS (sulfur compound) + O_2 + H_2 → SO + CO_2 + H_2O, the ozone generator then generates ozone that reacts with SO to yield SO_2* in the reaction

chamber. The SO_2* then emits light in the UV region (around 360nm) to give SO_2. The light emitted is then detected by a photomultiplier. Figure 3.9 illustrates sulfur chemiluminescence detector.

Figure 3. 9: Sulfur chemiluminescence detector

3.6.2 Gas Chromatograph linearity response

The GC-sulfur chemiluminescence detector was calibrated using standards of thiophene, BT and DBT. Standards (1 to 75 ppm) were prepared and the dynamic range was established for thiophene, BT and DBT respectively from the result obtained. The calibration plots are shown in figure 3.10 (a,b and c) and they signify the linearity of the instrument in the experiment.

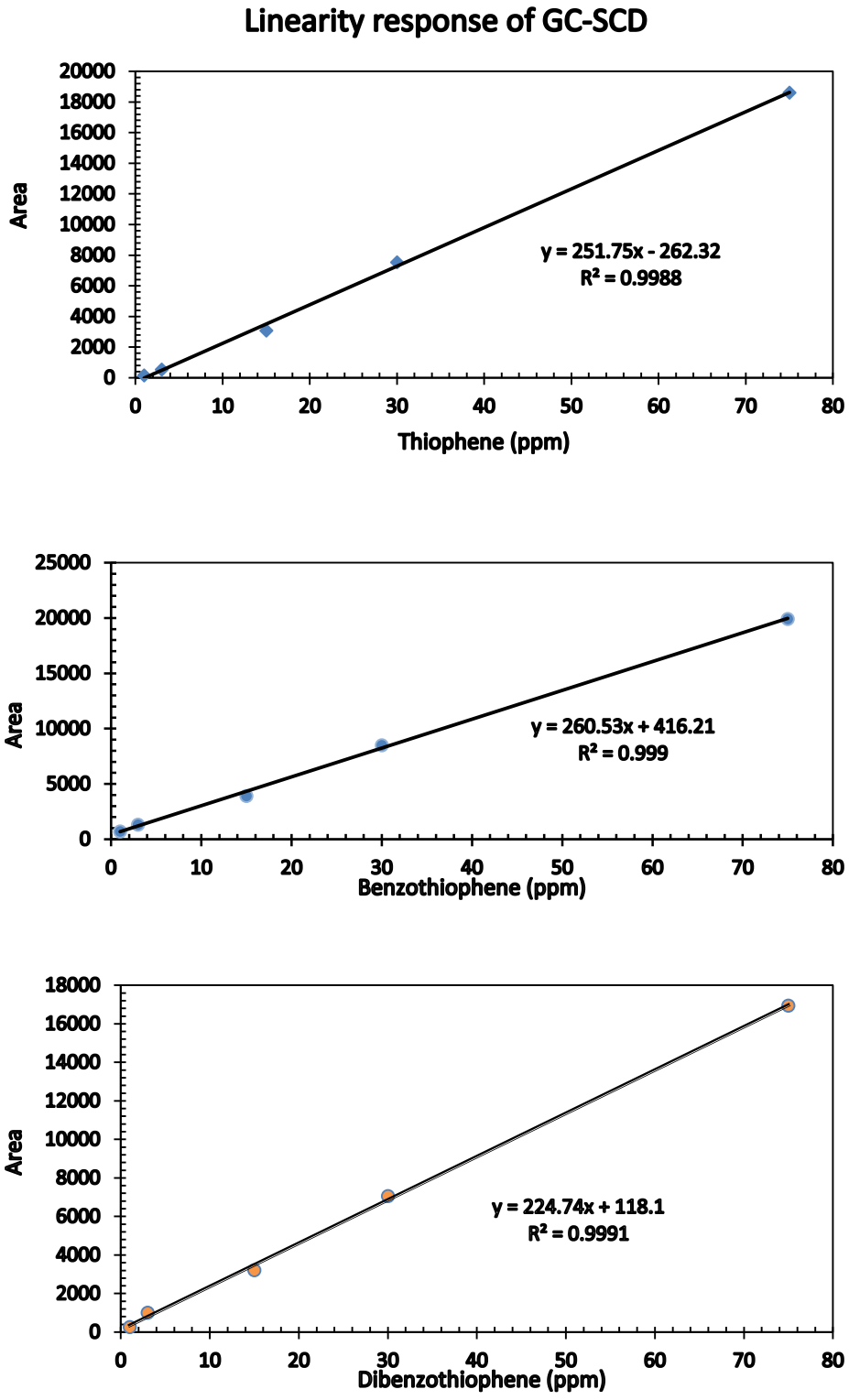

Figure 3.10: Linearity response of GC-SCD for thiophene (a), BT (b) and DBT (c) respectively

3.6.3 GC-SCD Analysis Method

The concentration of the refractory sulfur compounds was analyzed by GC-SCD (Model 7890A) system (Agilent) equipped with auto sampler (7693) and splitless injector. The column used was Agilent 19091S-001: 2638-45555 50 m × 0.2 mm dimensions and a film thickness of 0.5 μm methyl siloxane stationary phase. The injection volume was 1 uL with flow rate of 0.839 mL/min. Table 3.1 gives the details of the method used for the analysis.

Table 3.1: GC-SCD analysis method

Column description	Agilent 19091S-001: 2638-45555
	HP-PONA Methyl Siloxane
Length	50 m
Diameter	200 um
Film thickness	0.5 um
Maximum temperature	325°C
Back MM Inlet He	
Mode	Splitless
Heater	On 150°C
Pressure	On 30.385 psi
Total flow	15.839 mL/min
Septum purge flow	Off
Temperature program	On 150°C
Run time	20 mins
Purge flow to split vent	15 mL/min
Oven Program	60°C for 1 min then 10°C/min to 230°C for 2 mins
Back Detector FID	
Inlet temperature	60°C
Pressure	30.385 psi
Flow	0.839 mL/min
Avergae Velocity	22.742 cm/sec
Hold up time	3.6643 min
Flow program	On 0.839 mL/min
Front Detector AIB	
Heater	On 250°C
Electrometer	On

The sulfur removal efficiency of the AC treated samples was calculated using the formula below:

$$x = {}^{(Co - Ce)}/_{Co} * 100\%$$

where x = Sulfur removal percentage (%) C_0 = Initial concentration of sulfur in model oils (ppmw), Ce = final sulfur concentration

The amount of sulfur compounds adsorbed per unit mass of the adsorbent at equilibrium (q_e mg/g) and at any time t (q_t mg/g) termed as the adsorption capacity was calculated from the formulas:

$$q_e = \frac{\mathrm{V}(C_0 - C_e)}{\mathrm{m}}$$

$$q_t = \frac{V(C_0 - C_t)}{m}$$

where V (L) is the volume of the liquid phase, C_0 (mg/L) is the initial concentration of the sulfur compounds before they come in contact with the adsorbent, Ce and C_t (mg/L) are the concentration at equilibrium and at any time t, and m (g) is the amount of the adsorbent.

3.7 Adsorption Kinetics

Adsorption kinetics is a useful tool in the determination of adsorption mechanism and its pathways. It gives the rate of solute uptake by the solid-solution interface. Contact time and adsorbent dosage are useful tools in the determination adsorption kinetics of the refractory sulfur compounds from model fuel. The kinetics of the refractory sulfur compounds on the prepared sorbents viz: AC, AC/Ni, AC/CeO_2/Fe, and AC/NiO/Ce were analyzed using pseudo first order, pseudo second order and intraparticle diffusion models.

R-square values (correlation coefficients) were used to determine the level of conformity between the experimental data and the predicted values.

3.8 Adsorption Isotherms

Adsorption is mainly described through isotherms, i.e. the amount of adsorbate on the surface of the adsorbent as a function of pressure for gasses or concentration for liquids at isothermal conditions. Comparison of different materials can then be carried out based on the quantity adsorbed to the mass of the adsorbent. There are fifteen different isotherm models but this work will be restricted to only three i.e. Langmuir and Freundlich isotherm (Foo *e*t *a*l., 2010). The isotherms were fitted to the following adsorbents: AC, AC/Ni, and AC/CeO_2/Fe.

3.9 Regeneration of the Adsorbents

The major environmental concern of ADS is the disposal of spent adsorbents. Regenerable adsorbents therefore hold a great promise for an environmentally friendly ADS. The regeneration of the synthesized materials was evaluated after saturation of the sorbents with refractory sulfur compounds. Thermal regeneration method was used to determine the recycling potentials of the sorbents. The boiling points of thiophene, BT and DBT are 84°C, 221°C and 333°C. The sorbents were then treated to 350°C for 3 h for effective disposal of the compounds and the regenerated adsorbents were tested further for the removal of the refractory sulfur compounds in batch mode. Aliquots were taken at intervals and analyzed by the GC-SCD.

CHAPTER 4

RESULTS AND DISCUSSION

4.1 Carbonization

Effect of temperature

The results of the effect of pyrolysis temperature on the yield of carbon black, liquid hydrocarbons and gases are presented in table 4.1 and figure 4.1. It can be clearly seen that the yield of gases and liquid hydrocarbons increases with temperature till around 500°C where the % yield starts declining, this can be attributed to the fact that higher temperatures tend to give stronger thermal pyrolysis and in turn reducing the yield of the liquid hydrocarbons and gasses. The yield of carbon black decreases till the temperature range of 500-550°C where it started stabilizing. This means that treating WRTs to 500°C was the optimum for effective decomposition of all its components and the sole production of aggregates of carbon that are randomly linked together (Jasmin *et al*., 2006).

Table 4.1: Effect of pyrolysis temperature on the production of carbon black, liquid and gas

Temperature (°C)	Carbon black (% yield)	Liquid hydrocarbons (% yield)	Gasses(% yield)
250	85	15	5
300	72	18	10
350	65	20	15
400	60	22	18
450	54	27	19
500	51	28	21
550	51	27	22

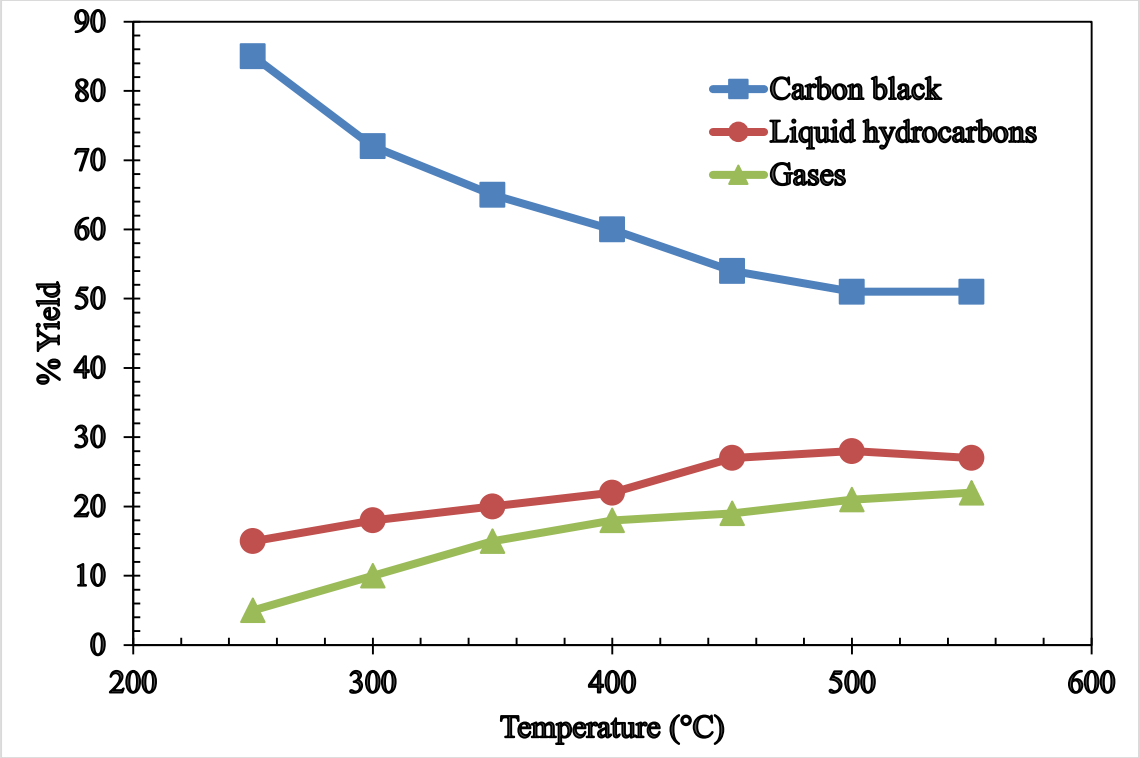

Figure 4.1: Effect of temperature on the yield of carbon black, liquid hydrocarbons and gases from waste rubber tires.

Effect of time

The effect of time on the development of carbon black was studied and the results are shown in Table 4.2 and figure 4.2. The temperature was fixed at 500℃ and the time was varied from 30 mins to 5 h. It can be seen from figure that treatment from 30 mins to 1 h had the greatest effect on the carbon black recovery. Increasing the timing from 2 h to 5 h did not show any significant effect. However, the current work fixed the timing at 5 h for effective decomposition of the WRTs.

Table 4.2: effect of time on pyrolysis of waste rubber tires.

Time (hours)	Initial weight (g)	Final Weight (g)	% of Recovery (as Carbon)
0.5	20.6885	11.1792	54.0358
1	20.2956	8.0959	39.8884
2	20.7431	8.6383	41.6442
3	20.6584	7.9864	38.6593
4	20.6175	8.0348	38.9707
5	20.2755	8.3479	41.1724

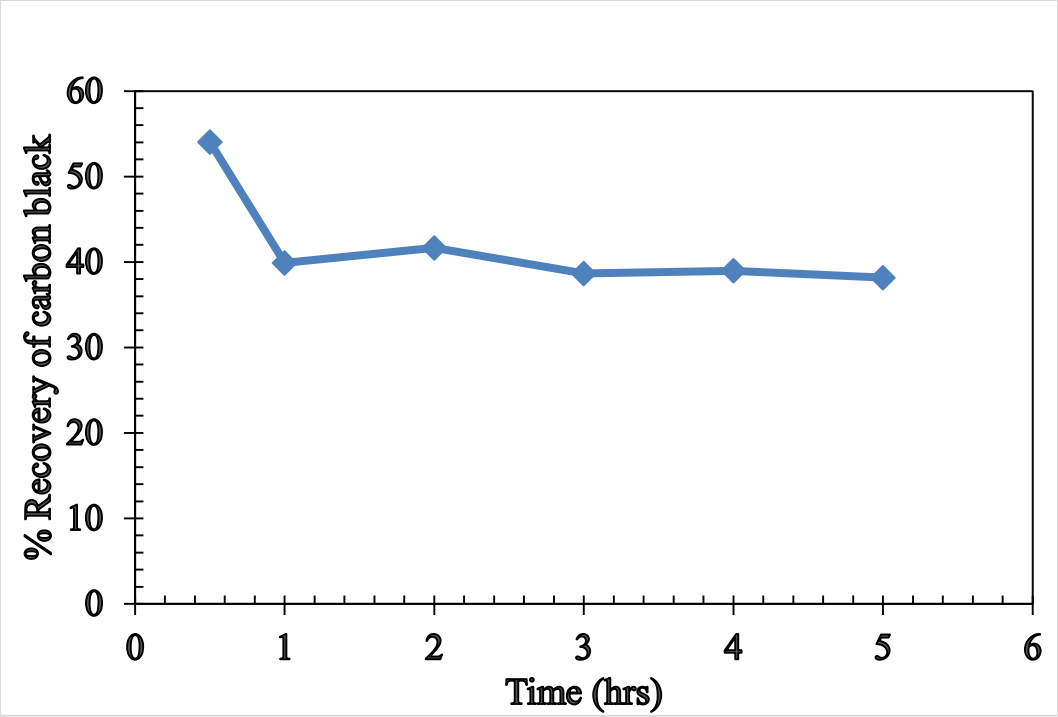

Figure 4. 2: Effect of pyrolysis time on the % recovery of carbon black derived from used tires.

4.2 Activation

The result of the activation carried out on the pyrolyzed waste rubber tire to enhance porosity and surface area is shown in Table 4.3 and Figure 4.3. The time was fixed at 5 h for each experiment and the temperature was varied from 400 to 500°C. Initial weight and final weight were recorded and the % recovery was calculated. Figure 4.3 showed continued reduction in the % recovery of the AC signifying continuous enhancement of the porosity and the decomposition of functional groups present in the WRTs. The adsorbent produced at 900°C having 27.20 recovery was believed to be the best and its surface area was taken after the experiment. Subsequent modifications on the surface of the adsorbent using acids and bases were conducted to enhance the surface area and all other experiments were carried out using the adsorbent with the highest surface area.

Table 4.3: Effect of activation temperature on the development of activated carbon

Temperature (°C)	Initial weight (g)	Final Weight (g)	% of Recovery
400	21.1291	8.4319	39.9066
500	20.2755	8.3479	41.1724
600	19.8128	7.2219	36.4507
700	22.0971	7.9013	35.7572
800	27.9802	8.5092	30.4115
900	29.6855	8.0756	27.2039

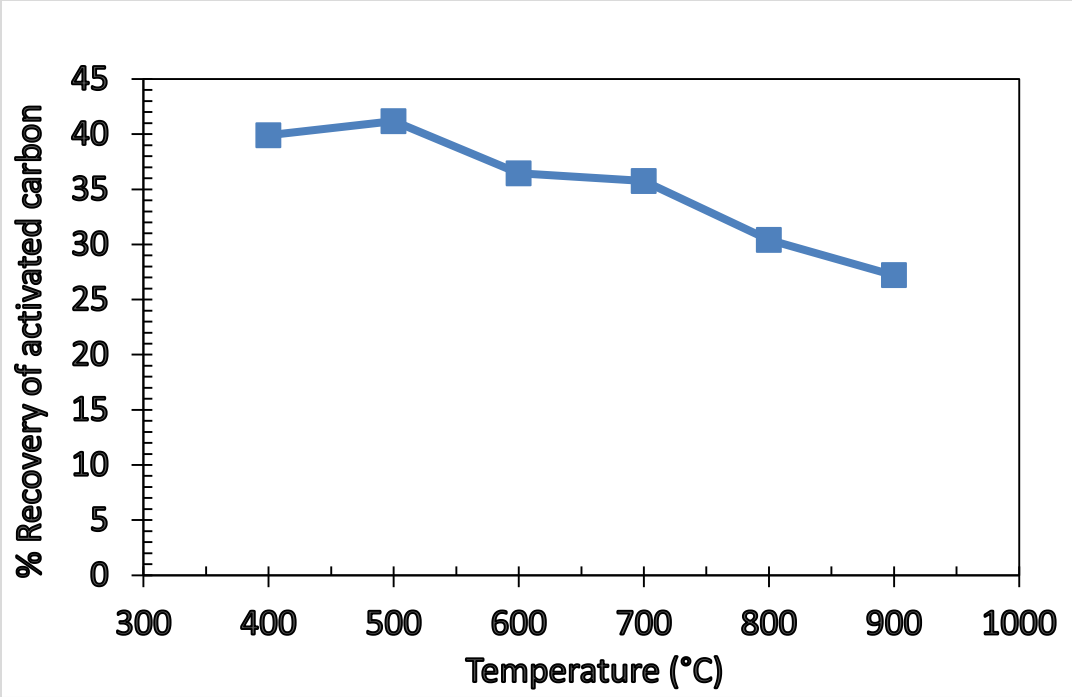

Figure 4.3: Effect of activation temperature on the enhancement of surface porosity of AC derived from used tires.

4.3 Effect of treatment conditions

The surface areas and porosities of AC are greatly influenced by the parent material and the method employed in the production. Better adsorption capacities and adsorption rates of AC are directly linked to larger surface areas and pore size distributions (Chiang *e*t *a*l., 1999). Mesoporous and microporous volumes of AC also play a crucial role in the adsorption of larger molecules (Costas *e*t *a*l., 2001) In general, the selective adsorption of inorganic molecules on the surface of AC directly depends on the amount of oxygen containing complexes. The oxygen containing complexes are mostly created using dry or wet oxidations methods (Zongxuan *e*t *a*l., 2003). Dry oxidation methods involves the utilization of oxidizing gases at high temperatures (>700°C) to bring about the surface modification of the AC. However, this method is not so effective because some of the oxygen complexes such as carbonyl groups are unstable and they decompose at high temperatures to carbon dioxide leading to the loss of important oxygen species on the surface of the adsorbent. Wet oxidation methods involves the reactions of aqueous solutions such as (H_2SO_4, HNO_3, H_2O_2, NaOH, NaOCl $(NH_4)S_2O_8$, $AgNO_3$, H_2PtCl_6 etc.) on the carbon surface at mild temperatures (≤100°C) to bring about the development of oxygen containing complexes (Beom *e*t *a*l., 2015; Garcia *e*t *a*l., 2004; Boehm 2002). The major drawback of this method is that it reduces the specific surface areas and porosities of AC, damages the mesoporous structure at temperatures above 80°C and yield off unwanted gasses during the reaction (Moreno *e*t *a*l., 2000). HNO_3 is believed to have better oxidizing properties by simply adjusting its concentration and temperature.

Despite the drawbacks of the wet oxidation methods, studies have shown that aqueous treatment of AC with concentrated acids does have better adsorption capacity and

negligible if not none effect to surface areas and pore volumes. Adsorptive capability of AC modified with HNO_3 at 120°C was increased significantly and modification using HNO_3 even at high temperatures showed a promising result in the removal of thiophene from oil (Chang *et al*., 2008). The surface properties, porosities, and adsorption capacities of AC showed significant improvement for the removal of DBT after modification with concentrated H_2SO_4 at temperatures 150−270 °C in the report of (Zongxuan *et al*., 2003) The treatment of AC with concentrated H_2SO_4 at 250 °C greatly increases the specific surface areas from 393 m^2/g to 745 m^2/g, mesoporous volume from 0.243 mL/g to 0.452 mL/g, and acidic surface oxygen complexes from 0.071 meq/g to 1.986 meq/g as compared with the unmodified AC. The amount of the oxygen containing complexes (phenols and carboxyls) on the surface of AC increases with treatment temperature. The report of (Ku *et al*., 1994) modified AC using ammonium sulfate and the result showed increase in specific surface area after the treatment, however, the amount of oxygen containing functional groups diminished with temperature.

This clearly shows that the effect of wet oxidation treatment on the performance of AC in ADS and the mechanism employed by different researchers is quite different. Despite all the reports available, reports addressing the effects of modification conditions to the performance of AC in ADS are still needed. The goal is to produce as much surface oxygen functional groups as possible on the surface of the adsorbent regardless of the wet oxidation method employed while at the same time increasing the specific surface area and porosity of the adsorbent.

The aim of this section is to produce AC from ELTs and to treat the AC using HNO_3 and NaOH at various temperatures. The effect of acid/base treatment of AC on the removal of

DBT was examined. The samples were characterize based on surface chemistry surface area and porosity by FTIR, surface pH measurement, boehm's titration experiment, EDX, XRD and SEM. The adsorption performance of the AC samples was evaluated in batch and column system. The Effects of surface chemistry and porous structure on the adsorption capacity was examined.

4.3.1 Surface pH

The surface pH of all the raw and treated AC samples was taken to have a clear understanding of the acidity or basicity of the adsorbents. Table 4.4 shows that the raw sample has acidic pH of 4.92 corresponding with total surface acidic and basic groups of 1.71 and 1.62 mmol/g respectively obtained from Boehm's titration experiment. Treatment with NaOH increases the basicity from 4.92 to 10.66 and 10.69 at 30°C and 90°C respectively however, there is a noticeable difference on the surface pH at 60°C as depicted in table 4.4 and this corresponds with the FT-IR results obtained for this adsorbent. It implies that modification using NaOH at temperatures above 60°C has a negative effect on the development of acidic functional groups of AC that are responsible for the adsorption of thiophenes and it contributed to the formation of positive charges on the surface of AC samples as depicted in equation 3. Treatment with HNO_3 on the contrary has been observed to substantially increase the acidity on the surface of the adsorbents at various temperatures. Increase in treatment temperature played a major role in the enhancement of acidity as shown in table 4.4. The pH rose from 4.92 (value of the raw sample) to 4.21 at 30°C, 4.05 at 60°C and finally to 3.09 at 90°C respectively. The increase in surface pH can be attributed to the reduction in total basic groups and the introduction of new acidic functional groups on the surface of the AC samples this is evident with the result obtained

from the Boehm's titration experiment showing increase in the carboxyls and lactonic groups with temperature. The FT-IR and XRD results also confirms the increase in surface acidic groups due to the increase in relative intensities of the peaks depicting the presence of phenols, carboxyls and lactones.

4.3.2 Boehm's titration

There are surface acidic and basic functional groups on the AC and they can be determined by titration methods. The most widely known method is the Boehm's titration for the determination of surface acidic functional groups. The acidic functional groups are due to the presence of phenols, lactols, lactones and carboxylic acids. The acidic groups are said to differ in their acidity which can be determined by reaction with 0.05 M NaOH, Na_2CO_3 and $NaHCO_3$ respectively (Boehm 2002; Chang *e*t *a*l., 2008). Phenols are neutralized by NaOH, while lactones and carboxylic acids are neutralized by Na_2CO_3, and $NaHCO_3$ neutralizes only carboxyl groups. All the surface acidic functional groups therefore can be determined both qualitatively and quantitatively. The surface acidic functional groups of all the treated AC samples are shown in table 4.4, the results clearly show the increment in total acidic functional groups with treatment temperature. The raw AC is relatively acidic with high amount of phenolic groups and a total acidic groups of 1.71 mmol/g, however upon treatment with NaOH at 30°C the total acidic groups decreased to 1.21 mmol/g but the phenolic groups were greater than the raw samples. This is because temperature has an effect in the development of the oxygen containing functional groups. The total basic functional groups on the surface of the AC-NaOH 30°C were the highest in all the samples modified (2.48 mmol/g). It is clearly noticed that the treatment at 60°C which seems to be the best temperature for NaOH modification gave the highest surface acidic functional

groups (1.72 mmol/g) and the lowest surface basic groups (1.98 mmol/g). Samples treated with HNO_3 showed a better performance, total acidic functional groups increased with treatment temperature from 2.11 to 2.22 and finally 2.39 mmol/g for AC-HNO_3 at 30, 60 and 90°C respectively. The total basic groups reduced from 1.37 to 1.36 and finally to 1.33 mmol/g for the same samples respectively. The results are in accordance with the findings of Gil *et al*., 1997 and Chang *et al*., 2008. They believe that raw AC samples are acidic in nature with high amount of phenolic groups and that AC treated with HNO_3 gives high amount of acidic functional groups and yield better results in adsorptive studies as seen in the next section.

Table 4.4: Surface pH, total basic and acidic groups on the raw and treated AC samples

Sample	**Surface pH**	**Total Basic groups (mmol/g)**	**Surface acidic groups (mmol/g)**			
			Phenol	**Lactone**	**Carboxyl**	**Total**
Raw AC	4.92	**1.62**	0.81	0.22	0.68	**1.71**
AC-NaOH 30°C	10.66	**2.48**	1.07	0.16	0.00	**1.23**
AC-NaOH 60°C	10.18	**1.98**	1.21	0.33	0.18	**1.72**
AC-NaOH 90°C	10.69	**2.46**	1.13	0.25	0.00	**1.38**
AC-HNO_3 30°C	4.21	**1.37**	0.80	0.64	0.67	**2.11**
AC-HNO_3 60°C	4.05	**1.36**	0.82	0.71	0.69	**2.22**
AC-HNO_3 90°C	3.09	**1.33**	0.69	0.81	0.89	**2.39**

4.3.3 FTIR spectroscopy

FTIR spectra of the raw, HNO_3 and NaOH treated AC at various temperatures (30°C, 60°C and 90°C) were taken to understand the presence of functional groups on the AC samples and they are given in Figure 4.4. The three samples (Raw AC, NaOH and HNO_3 treated AC) have displayed varying degrees and intensities of their bands though they all have similar pattern but the bands increases with increasing treatment temperature. This implies that temperature has a great effect on the development of oxygen containing functional groups and acidic and basic sites on the surface of the AC samples (Yi *e*t *a*l., 2012; Jia-Xiu *e*t *a*l., 2015, 2012). It can be seen that the samples showed a sharp peak centering around 3430cm^{-1} which can be ascribed to O-H stretching vibrations of hydroxyl or carboxylic groups or due to chemisorbed water. There is a noticeable development peaks at 2854 cm^{-1} and 2924 cm^{-1} as temperature increases and these peaks can be due to the presence of aliphatic C-H stretch of CH, CH_2 and CH_3. The small and broad peaks at 1700 and 1640 cm^{-1} are due to C=O stretching vibrations in ketones (such as ion radical or quinone structure that are highly conjugated) and carboxyl groups in carboxylic acid respectively. The peak around 1400cm^{-1} appeared in HNO_3 treated samples and may be attributed to the presence of C=O stretching vibrations of the O=C-OH and nitrate structures (Paul *e*t *a*l., 2004; Wu *e*t *a*l., 2013). This confirms the effect of temperature on the development of carbonyl groups (Tazibet *e*t *a*l., 2013). The NaOH treated AC samples at (30°C, 60°C and 90°C) have showed similar pattern as depicted in but the intensities are not well developed as compared to the HNO_3 treated samples and the results also confirms the effect of temperature and HNO_3 on the development of surface functional groups such as nitrate, carboxyl, and carbonyl groups. In addition to the absorption peaks already discussed, the NaOH treated samples showed peaks around 2200-2400 cm^{-1} and 500-700 cm^{-1} which can

be ascribed to the presence of double bonded carbon oxygen groups and alkenes respectively. The proposed reactions for the development of surface functional groups on the AC samples by NaOH and HNO_3 are given below:

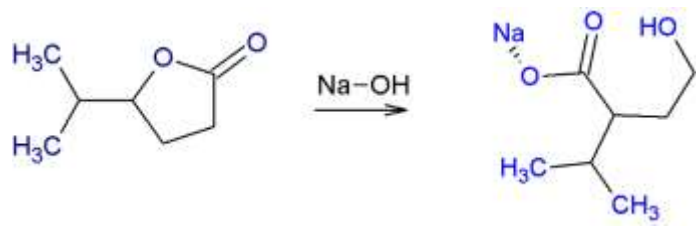

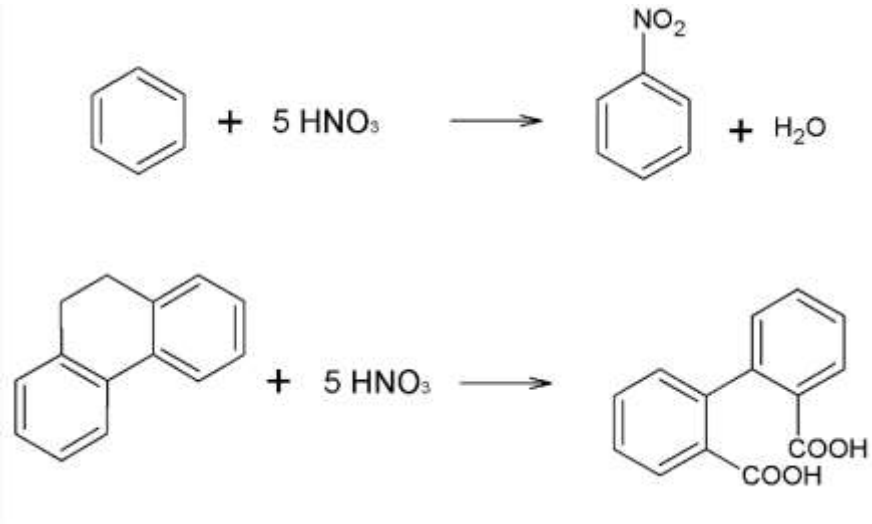

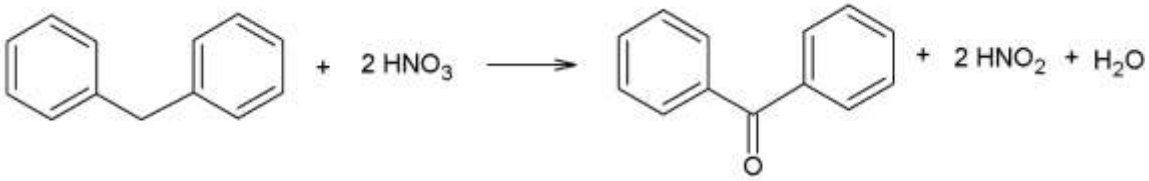

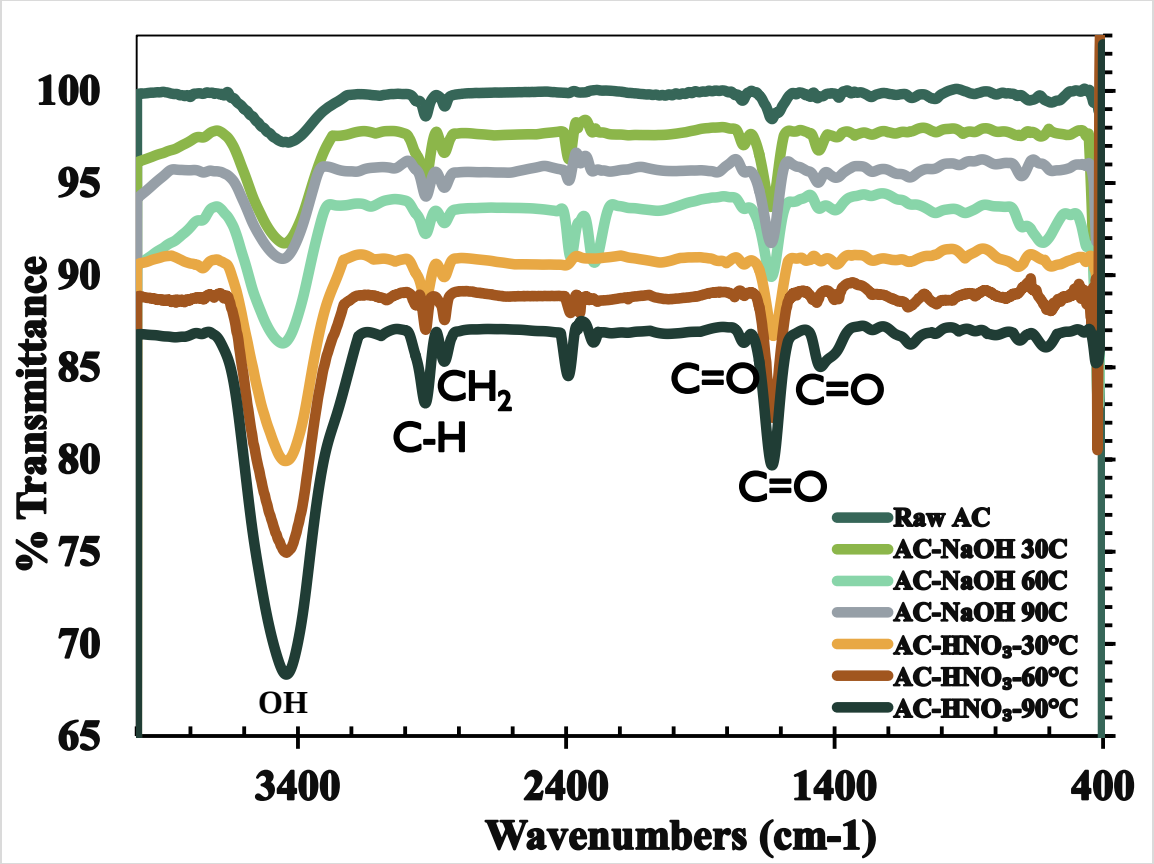

Figure 4.4: ***FTIR spectra of treated AC samples at various temperatures with NaOH and HNO_3***

4.3.4 SEM/EDX Result on the treated AC samples.

The SEM/EDX results of the raw and treated AC samples are depicted in figure 4.5 and 4.6 (a, b, c, d, e, f) respectively. Raw AC showed the presence of sulfur in the EDX analysis and this is because of the vulcanization process that uses sulfur to bind most of the polymers such as styrene and butadiene together in the tire formation process. This means that the pyrolysis and activation processes did not purely convert the waste materials into carbon though the concentrations of the sulfur from the EDX analysis is very low. However, upon subsequent treatment with acids and bases all the impurities were removed completely. Treatment with HNO_3 at 30, 60, and 90°C showed the presence of carbon and oxygen as the only elemental composition of the adsorbents and they showed significant improvement

trend in the wt% of oxygen from 11.01 to 11.86 and finally 14.39 meaning that oxygen containing functional groups kept on increasing with temperature upon acid treatment. This result is in accordance with the result obtained from the FT-IR, bohms titration experiment and XRD results. EDX results on the NaOH treated samples showed the presence of carbon, oxygen and sodium in different proportions. The appearance of sodium confirmed the NaOH used in the modification which upon treatment will release the H^+ present and attach the Na^+ to the surface of the carbons. Increase in treatment temperature shows significant reduction in the wt% of oxygen from 18.33 to 17.72 and finally 13.63 for AC-NaOH 30°C, 60°C and 90°C respectively.

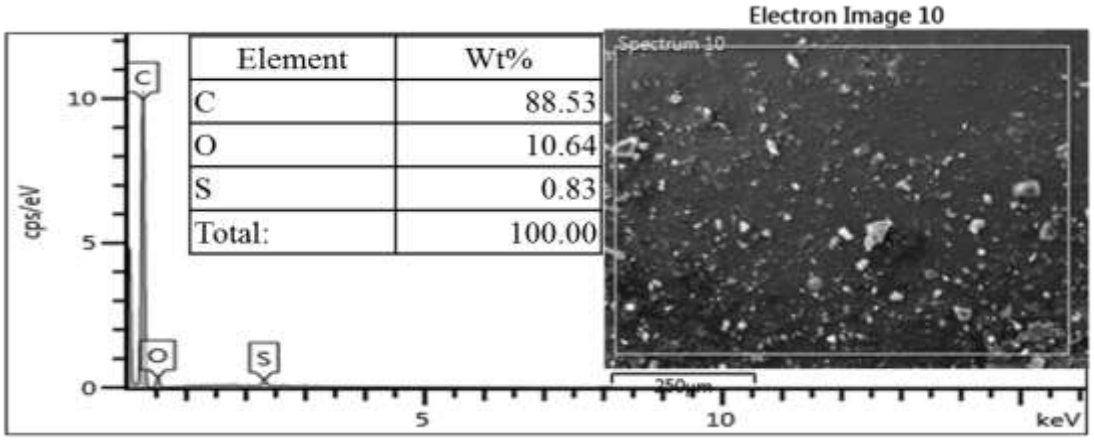

Figure 4.5: SEM/EDX result of Raw AC sample after pyrolysis and activation

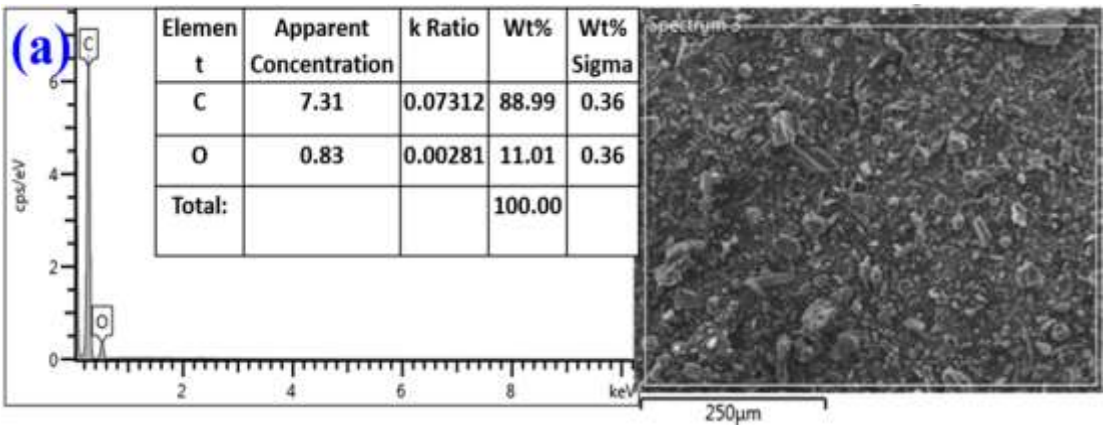

(b)

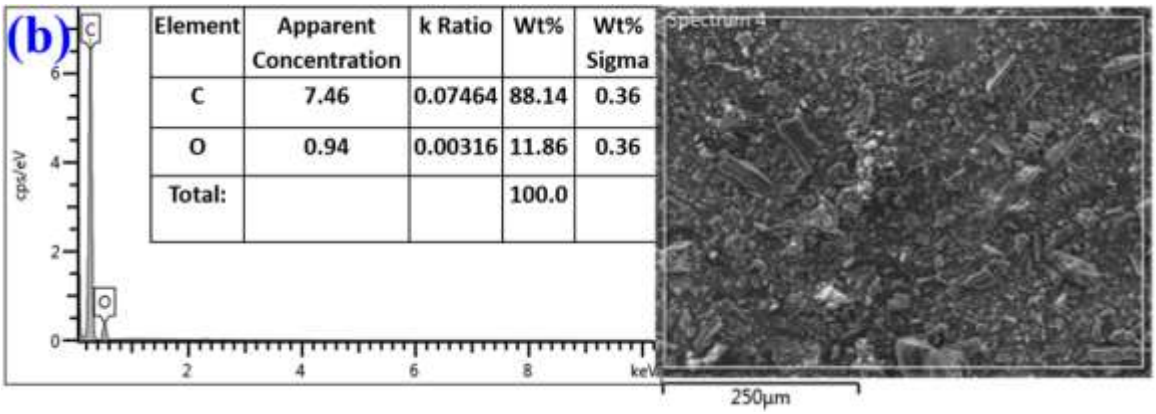

Element	Apparent Concentration	k Ratio	Wt%	Wt% Sigma
C	7.46	0.07464	88.14	0.36
O	0.94	0.00316	11.86	0.36
Total:			100.0	

(c)

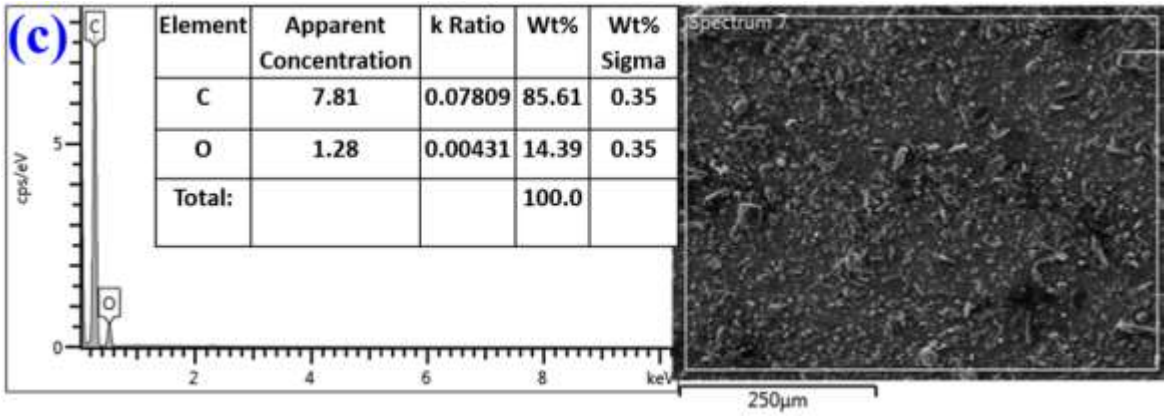

Element	Apparent Concentration	k Ratio	Wt%	Wt% Sigma
C	7.81	0.07809	85.61	0.35
O	1.28	0.00431	14.39	0.35
Total:			100.0	

(d)

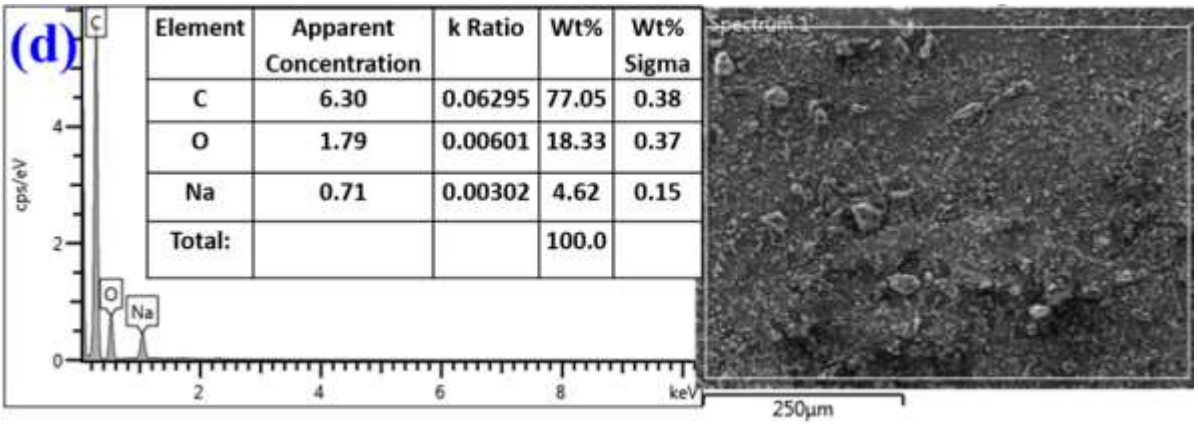

Element	Apparent Concentration	k Ratio	Wt%	Wt% Sigma
C	6.30	0.06295	77.05	0.38
O	1.79	0.00601	18.33	0.37
Na	0.71	0.00302	4.62	0.15
Total:			100.0	

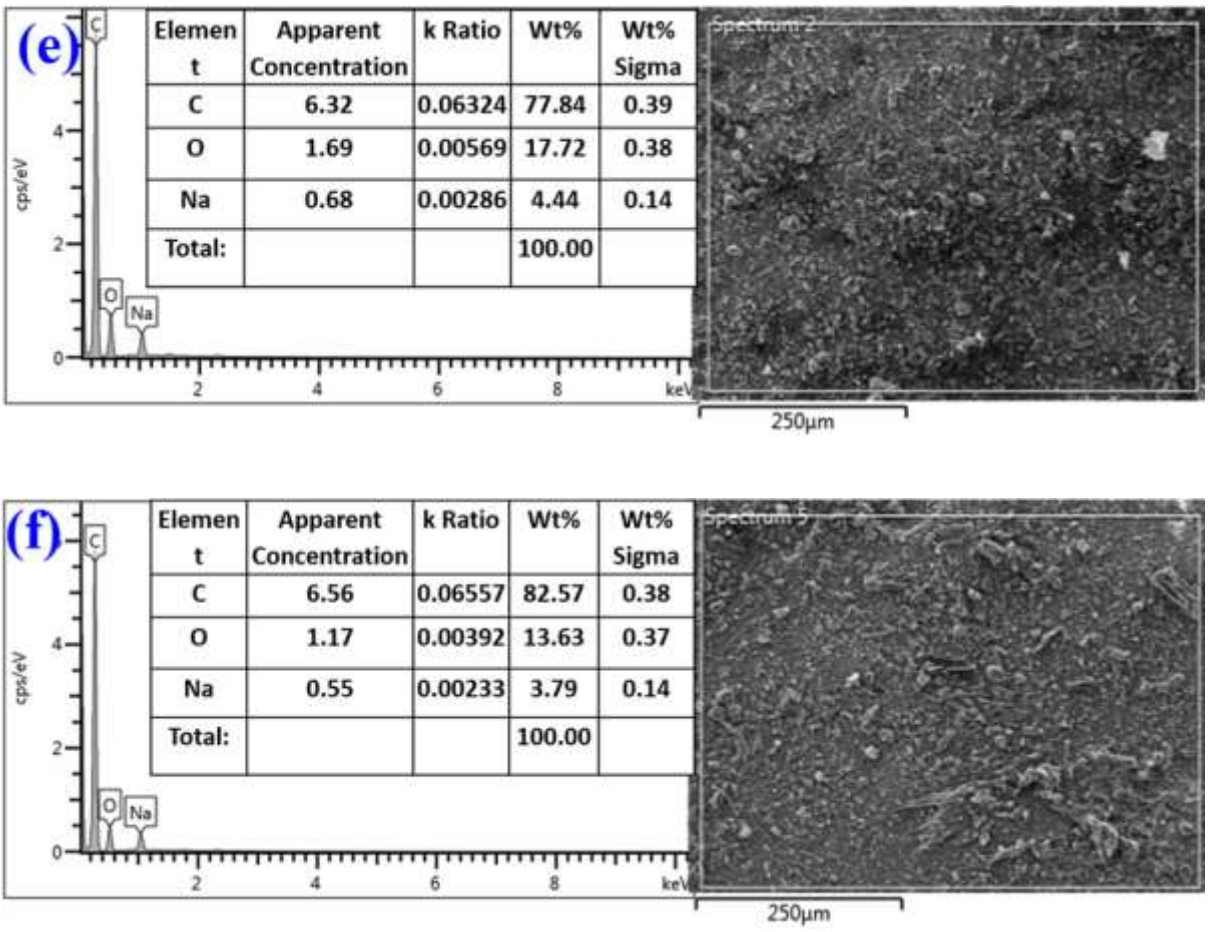

Figure 4.6: SEM/EDX images of AC samples treated at various temperatures with NaOH and HNO_3; (a) AC-HNO_3 30°C (b) AC-HNO_3 60°C (c) AC-HNO_3 90°C (d) AC-NaOH 30°C (e) AC-NaOH 60°C (f) AC-NaOH 90°C

4.3.5 XRD patterns of the treated AC samples

XRD is a useful characterization tool for the elucidation of elemental composition of a sample. Each atom in an element has a distinct pattern upon which it diffracts X-ray light. Figure 4.7 shows the XRD pattern of raw AC and treated AC samples with NaOH. All the samples showed a broad diffraction peaks at 2 theta values of between 20 to 30° (002) and 40 to 50° (100) signifying the presence of amorphous carbon. The relative intensities on the other hand gives an account of the carbon and oxygen containing functional groups present in the samples. Figure 4.8 shows the patterns for the AC-HNO_3 treated samples and

the result showed similar pattern of diffraction peaks at 2theta values of 20-30° and 40-50° (Xiaojun *et al*., 2014). The relative intensities also increased upon treatment signifying the improvement in treatment conditions and surface morphologies.

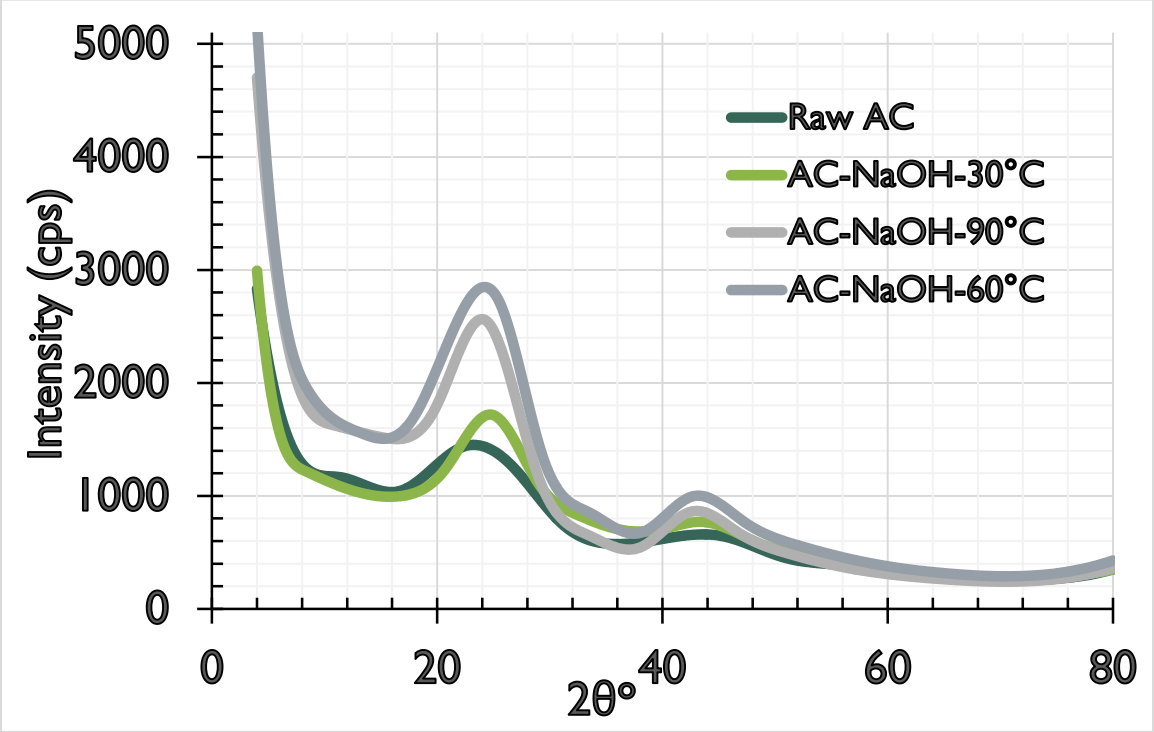

Figure 4.7*: XRD pattern of Raw AC and AC samples treated with NaOH at 30, 60 and 90°C.*

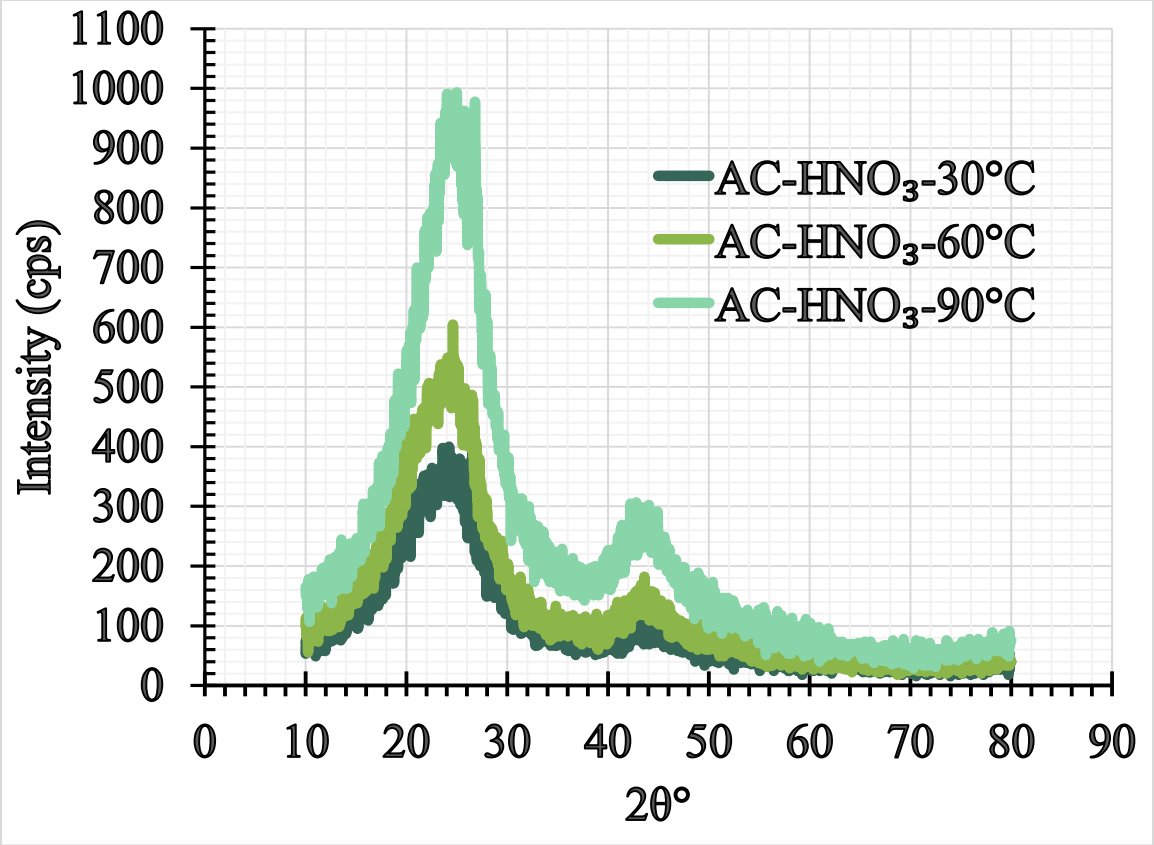

Figure 4.8*: XRD pattern of AC samples treated with HNO_3 at 30, 60 and 90°C*

4.3.6 Brunauer-Emmett-Teller (BET) Surface Area and Porosity Studies

Nitrogen adsorption desorption isotherm is a useful tool in the characterization of amorphous materials. The nitrogen adsorption isotherms of the raw and treated AC samples are shown in figure 4.9. All the samples can be seen to express Type I isotherm according to Brunauer *et al*., 1940 and Deng *et al*., 2009, however, the surface area and pore volumes were significantly enhanced upon NaOH and HNO_3 treatments. Temperature also enhanced the development of the surface area in the acid treated samples. The N_2 adsorption capacity followed the order: Raw < AC-NaOH 30°C < AC-NaOH 90°C < AC-NaOH 60°C < AC-HNO_3-30°C < AC-HNO_3-60°C < AC-HNO_3-90°C. A hysteris loop can be observed in figure 4.9 in all the samples at the relative high pressure (0.8 to 1) indicating

the presence of mesopores. In addition, a minor uptake of nitrogen can be observed at relative pressures between 0 and 0.2 signifying the presence of little amount of micropores within the samples. The change in surface area caused by different treatments is summarized in Table 4.5. It can be clearly seen that AC-NaOH-60°C sample has the highest surface area (369 m^2/g) and pore volume (0.69 cm^3/g) in the base treated samples. AC-HNO_3-90°C on the other hand has the highest surface area (473.35 m^2/g) and pore volume (0.70 cm^3/g) in all the samples used which confirms the significance of temperature and acid treatment of AC in the development of surface area and porosity. The results are in agreement with the results obtained from the XRD, FT-IR and boehm's experiment.

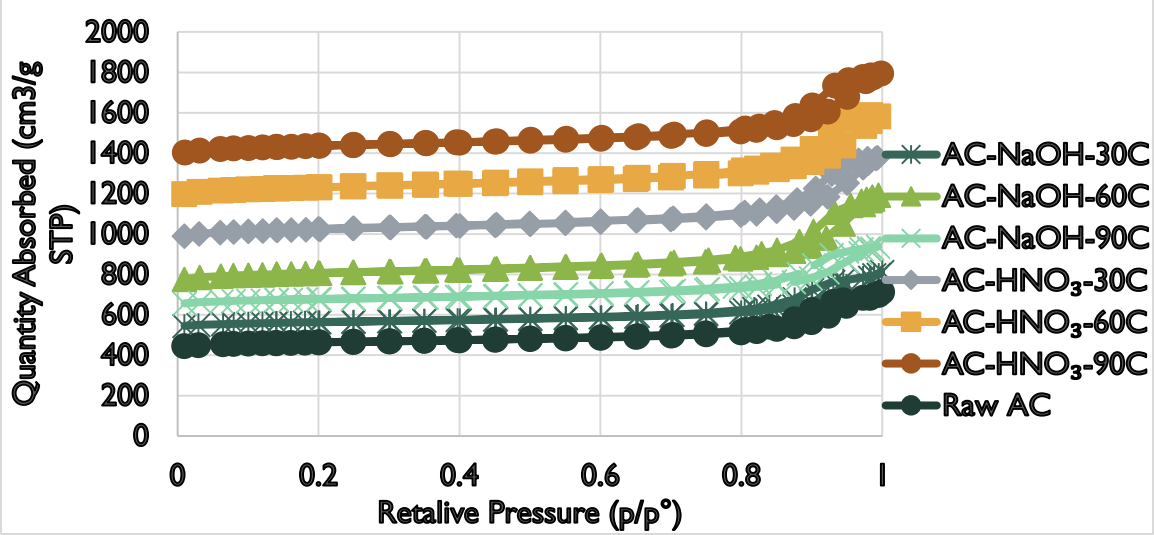

Figure 4.9: Effect of acid and base treatment conditions on N_2 adsorption–desorption isotherms of AC

Table 4.5 : Surface area and pore volume analysis		
Adsorbents	BET Surface Area (m^2/g)	Pore volume (cm^3/g)
Raw AC	183.21	0.30
AC-NaOH 30°C	220.48	0.48
AC-NaOH 60°C	369.27	0.7
AC-NaOH 90°C	268.11	0.52
AC-HNO_3 30°C	427.05	0.73
AC-HNO_3 60°C	454.81	0.74
AC-HNO_3 90°C	473.35	0.76

4.3.7 TGA Result

The TGA analysis curve is given in figure 4.10 to understand the optimum temperature for pyrolysis and the pattern of decomposition the functional groups on the surface of the AC employ. It can be clearly seen that there is around 8% weight loss between 20°C to 80°C signifying the desorption absorbed water (Chang *e*t *a*l., 2013). 10% weight loss was recorded between 150°C to 450°C and this is due to CO_2 desorption representing decomposition of carboxyl, lactone and lactol groups (Chang *e*t *a*l., 2008). 80% weight loss was recorded after 450°C signifying CO desorption corresponding to decomposition of carbonyl, ether, quinine and phenol groups on carbon surface at higher temperatures. This means that more CO was released from the decomposition process signifying the relative abundance of carbonyl and phenolic groups on the surface of synthesized AC. In addition, AC completely decomposed after about 550°C.

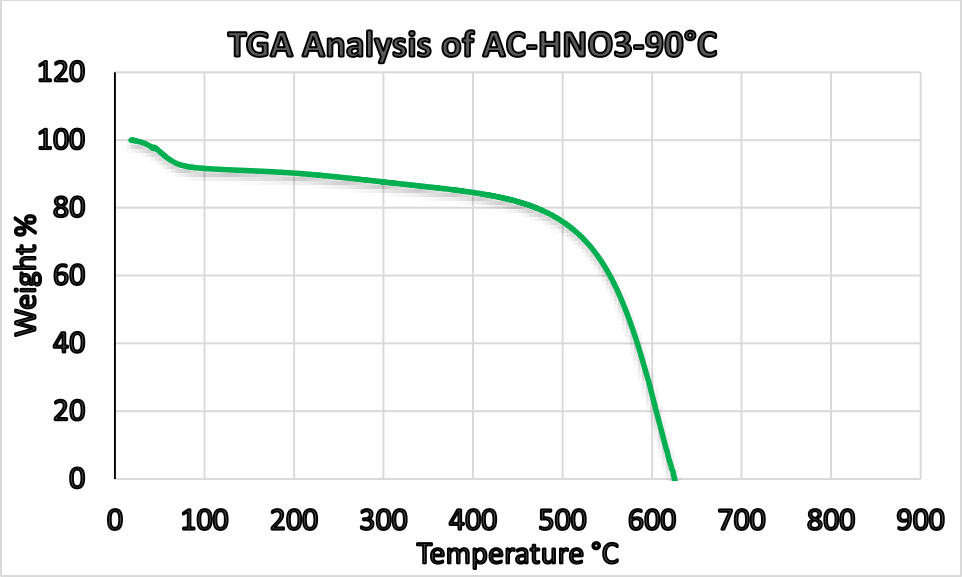

Figure 4. 10: ***TGA analysis of AC-HNO_3-90°C***

4.4 Adsorption evaluation of the treated AC samples

The raw and treated samples of AC both with NaOH and HNO_3 were compared for their desulfurization efficiency. 0.5g of each sample was taken and added to 50ppm mixture of thiophene, BT and DBT in 20 mL (85% hexane and 15% toluene). The set ups were stirred and samples were taken after 30 mins and analyzed with GC-SCD. The result is shown in figure 4.11 and the percentage removal of thiophene, BT and DBT from the raw and treated samples at various temperatures was reported. It can be clearly seen that raw sample performed the least. AC-NaOH-60°C showed the best performance among the base treated samples and this can be attributed to the presence of oxygen containing functional groups, high surface area, pore volume, and pore size exhibited by the sample compared with other base treated samples. AC-HNO_3-90°C showed the best performance. This can be explained because the sample showed the highest total acidic groups, the largest intensity in XRD analysis, and the highest in % transmittance in FT-IR. It also possess the highest surface area and pore volume. The percentage removal of the refractory sulfur compounds in all

the samples followed the order: DBT > BT > T, while the adsorbent performance followed the order: AC-HNO_3-90°C > AC-HNO_3-60°C > AC-HNO_3-30°C > AC-NaOH-60°C > AC-NaOH-90°C > AC-NaOH-30°C > Raw AC. All the treated samples showed at least 80% or greater percentage removal of DBT and this is due to the size of the molecule and acidic functional groups on the AC surfaces which contributes to polar interactions (Kostas *et al.*, 2014). Dispersive interactions between the delocalized π-electrons within the benzene rings of DBT and the electron rich region on the nanoporous carbon aromatic ring also plays a major role in the adsorption. The result also confirms the effect of treatment conditions on the overall performance in adsorptive studies.

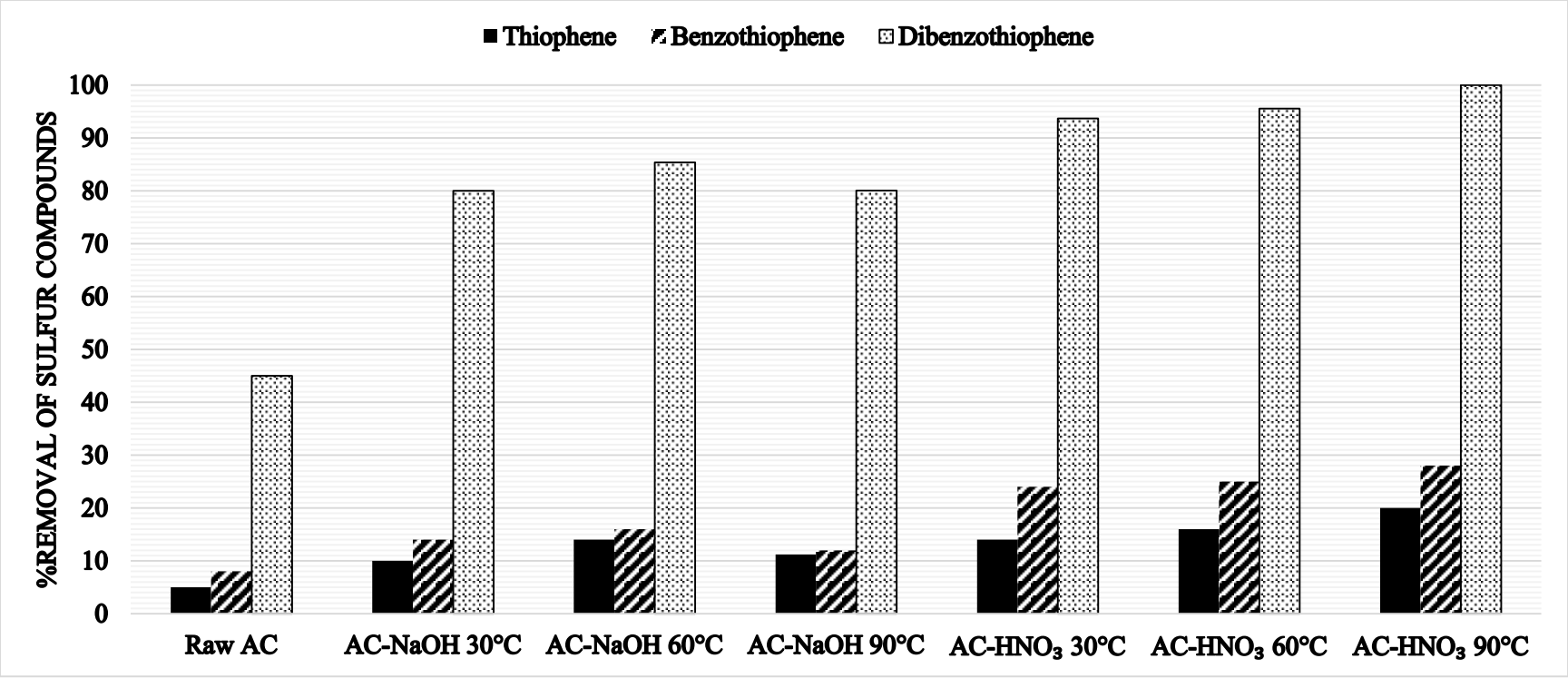

Figure 4.11*: Percentage removal of Thiophene, BT, and DBT (initial concentration of 50ppm each) on acid and base treated AC samples after 30 mins (dosage of each sample was 0.5g in 20ml initial solution volume) @ 25°C.*

4.4.1 Effect of processing time of AC-HNO_3-90°C on ADS.

The effect of refluxing time on the adsorptive performance of AC-HNO_3-90°C is depicted in figure 4.12. It can be clearly seen that increasing the refluxing time from 3hrs to 12 hr. has an overall net negative effect on the removal of the refractory sulfur compounds. This can be due to the effect of temperature on the destruction of AC surface. This confirms that selecting temperature and appropriate time of processing contributes to the better performance of the AC. The adsorption performance followed the order: AC-HNO_3-90°C 3hrs > AC-HNO_3-90°C 6hrs > AC-HNO_3-90°C 12hrs.

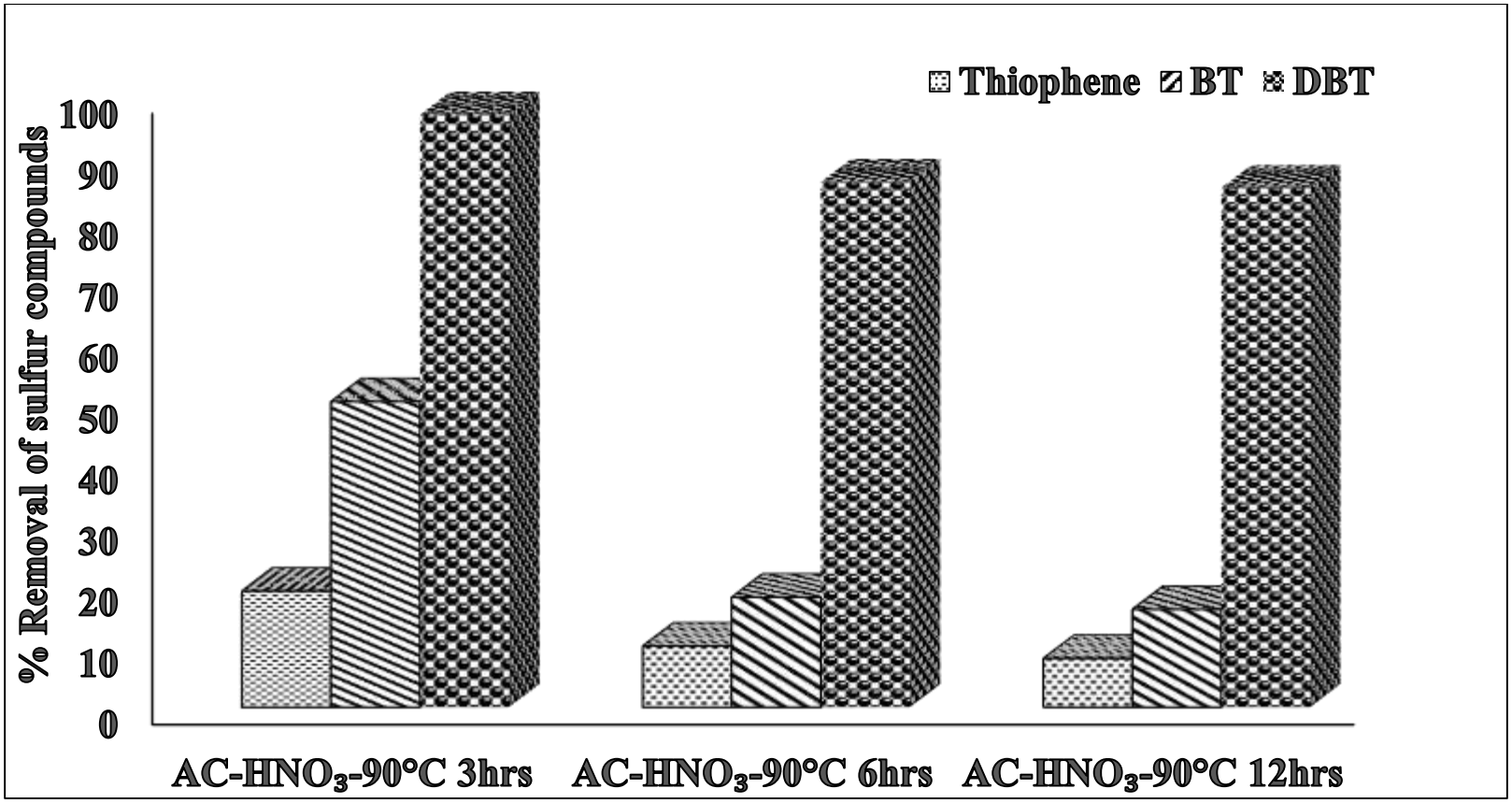

Figure 4.12: ***Effect of processing time on the performance of HNO_3 treated AC at 90°C (0.5 g dosage, initial concentrations of Thiophene 50ppm, BT 50ppm and DBT 51 ppm, 18 ml volume of solution and 30 min contact time)***

4.4.2 Effect of adsorbent dosage on the performance of AC-HNO_3-90°C and AC-NaOH-60°C

Adsorbent dosage is an important parameter in adsorptive studies because it determines maximum adsorptive capacity of a giving adsorbent using a starting concentration of analyte of interest. Best NaOH and HNO_3 treated samples were selected for testing the effect of adsorbent dosage. The effect of AC-HNO_3-90°C and AC-NaOH-60°C dosage on the uptake of refractory sulfur compounds (Thiophene 52 ppm, BT 50 ppm and DBT 51 ppm at room temperature) was studied and the results are shown in figure (4.13 a & b). The mass of the adsorbent was varied from 0.1g to 0.5g and the amount of refractory sulfur compounds adsorbed was found to be increasing with adsorbent dosage. The increase in adsorption capacity of sulfur compounds with dosage is expected because more active surface areas and sites for sulfur adsorption are introduced in the medium (Xinhai *e*t *a*l., 2014; Ankur *e*t *a*l., 2009). The removal efficiency after 0.25g was less becoming almost constant after 0.5 g, due to this we fix the rest of the experiments at adsorbent dosage of 0.5 g. The trend of adsorption of the refractory sulfur compounds followed the same order with the previous experiments DBT > BT > T. For all the adsorbent dosages tested, DBT was removed higher than all other refractory sulfur compounds this is due to the dispersive interactions formed between the AC and DBT and due to the presence of double benzene rings in DBT (Jie *e*t *a*l., 2011).

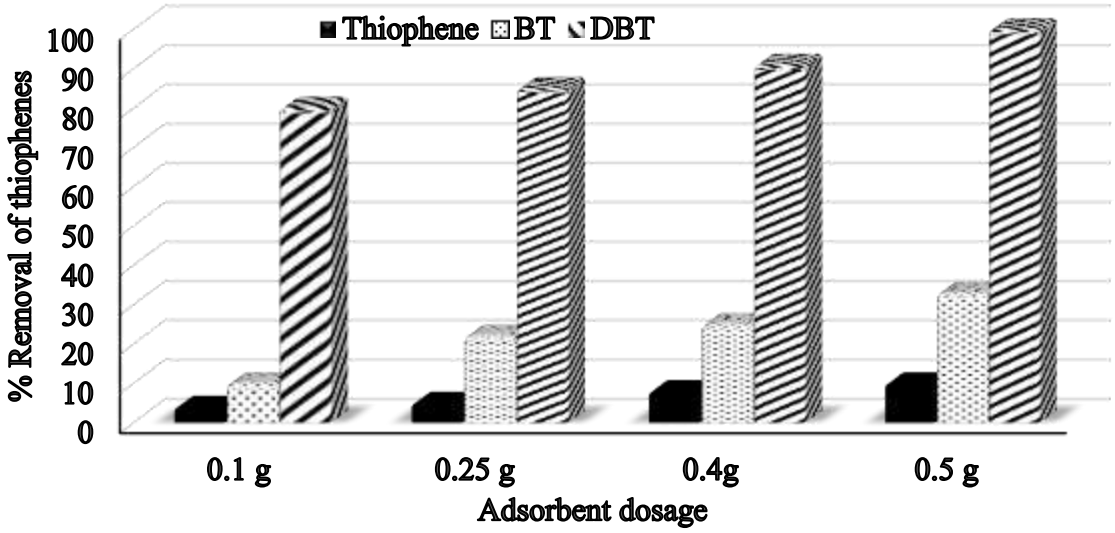

Figure 4.13 a*: Effect of adsorbent dosage AC-HNO_3-90°C on the adsorptive removal of thiophene, BT and DBT (initial concentrations 51, 50 and 51 ppm respectively, 15 ml volume of solution and 30 min contact time)*

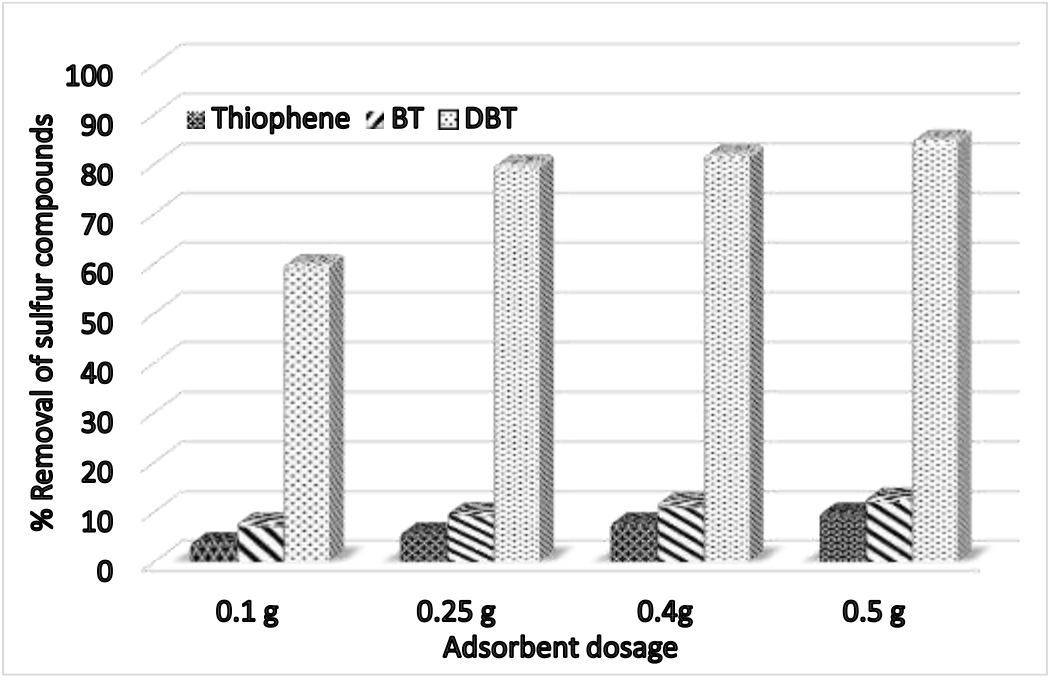

Figure 4.13 b*: Effect of adsorbent dosage AC-NaOH-60°C on the adsorptive removal of thiophene, BT and DBT (initial concentrations 51, 50 and 51 ppm respectively, 18 ml volume of solution and 30 min contact time)*

4.4.3 Effect of contact time

The effect of contact time on the efficiency of AC-HNO_3-90°C on the removal of refractory sulfur compounds is depicted in figure 4.14. It can be seen that the removal is very rapid, nearly 95% of all the adsorption process occurs in the first 5 mins of the process and this is because of the available free sites for adsorption of the sulfur compounds at the beginning of the adsorption process. Equilibrium was achieved at around 30 mins of adsorption process and afterwards the adsorption of the refractory sulfur compounds was noticed to decline due to desorption process of the analytes from the adsorbent. Size of the adsorbent, concentration of the sulfur compounds, degree of mixing, the affinity of the adsorbent to the sulfur compounds and the diffusion coefficient of the adsorbent in bulk and solid phases play a cardinal role in the percentage of sulfur compounds adsorbed on the surface of the adsorbent (Ankur *e*t *a*l., 2009). The adsorption capacity followed the order: DBT > BT > T. The vast majority of the area on the samples are mesoporous which makes it easier for adsorption at the initial time, however when the contact time increases the refractory sulfur compounds are faced with much larger resistance to pass through the micropores.

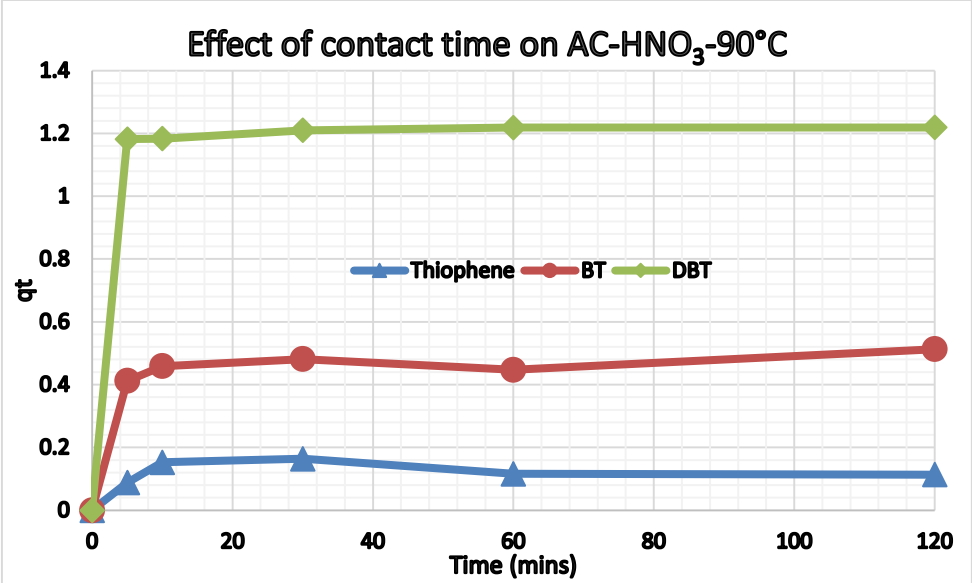

Figure 4.14*: Effect of contact time on removal of thiophene, BT and DBT by AC-HNO_3-90℃ (adsorbent dosage 0.5g, 20ml volume of model fuel containing 52 ppm thiophene, 50 ppm BT and 51 ppm DBT)*

4.5 Design of experiment (DOE) results

Minitab software version 16 was used for the DOE to understand the most significant factors affecting the adsorption experiment. Five factors with high and low values namely concentration (50 ppm and 150 ppm), flow rate (50 rpm and 150 rpm), column length (6 cm and 11 cm), dosage (0.1 g and 0.5 g) and contact time (5 mins and 120 mins) were selected having in mind that they are indeed the most significant factors affecting adsorption experiment. Half factorial design $2^{(5-1)}$ with 16 experimental runs without center point and randomization was used for the analysis. Main effect plots, interaction plots and pareto charts of these experimental factors were obtained and the results are depicted in figures 4.15, 4.16 and 4.17 respectively. The main effect plot showed that the column studies is best conducted at higher column length and dosage because the longer the column the better the interaction between the sulfur compounds and the adsorbent while the higher the dosage the more active sites available for sulfur compounds adsorption. On the contrary the lower the concentration and flow rate the better the percentage removal. This is because the adsorbent can only take the maximum sulfur compounds at any given time before reaching saturation. In addition, the lower the flow rate the better the interaction of the model fuel with the adsorbent. Contact time did not show any significant effect because as shown previously in this report the adsorption of the refractory sulfur compounds on the surface of the AC is a rapid process attaining equilibrium sometimes at 10 minutes.

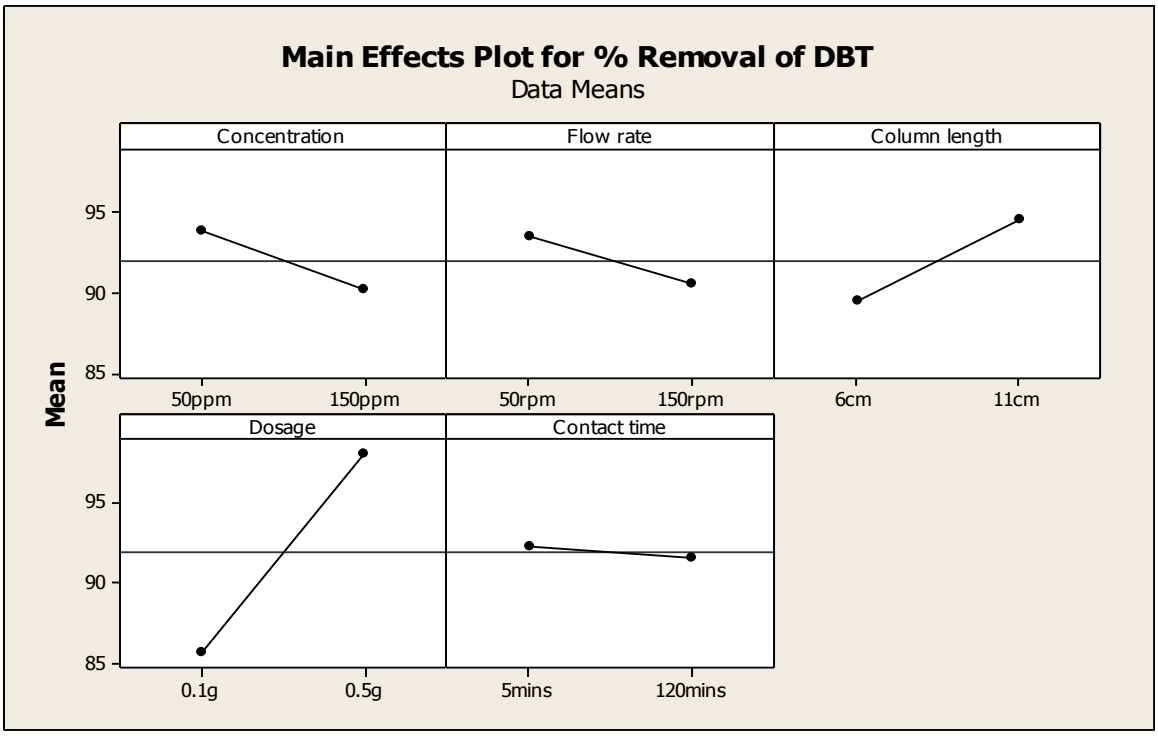

Figure 4.15: ***Main effects plot for the removal of DBT obtained from Minitab software***

Results from the interaction plot (figure 4.16) showed that the interaction between dosage and concentration, dosage and flow rate, dosage and column length gave the most profound effect on the adsorption experiment. It shows that whether column length, concentration and flow rate are high or low when the dosage of the adsorbent is high the percentage removal of the refractory sulfur compound tends to be very high.

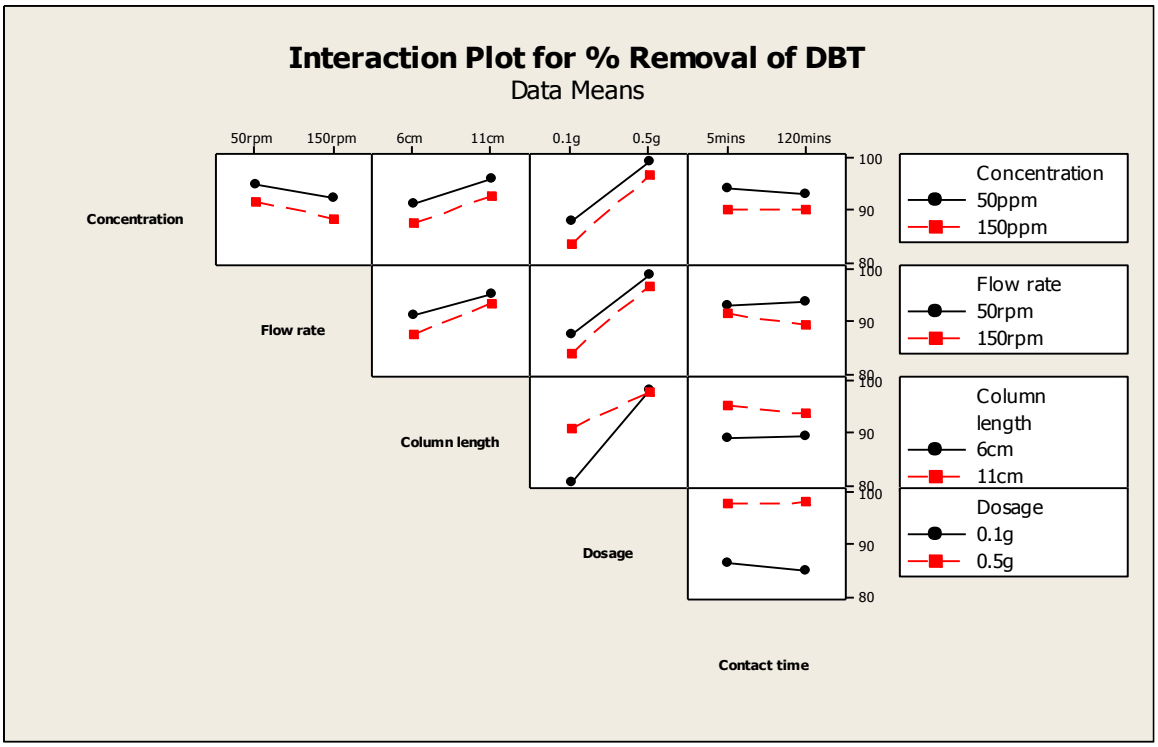

Figure 4.16: ***Interaction plot for the removal of DBT obtained from Minitab software***

The significance of the Pareto plot (figure 4.17) is that it gives a summary of the whole factors that affect a particular experiment. All the bars that exceeds the red line in the plot are said to be significant in the experiment and they should be taken into account with much in depth attention. The results obtained in this experiment showed that dosage (D) had the highest effect on the percentage removal of the sulfur compounds followed by the interaction of column length and dosage (CD) followed by column length (C) alone and finally concentration (A) of the sulfur compound used in the experiment. All other bars below the red line are presumed to be less significant on the experimental result.

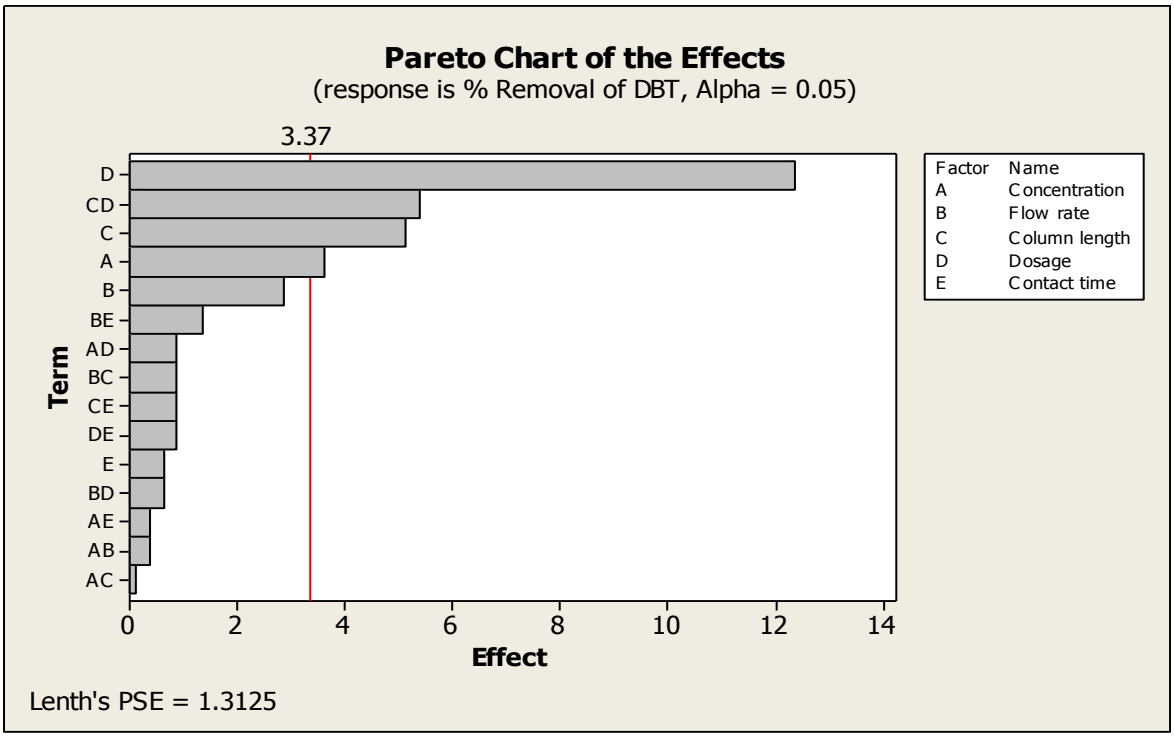

Figure 4. 17: ***Pareto chart for the removal of DBT obtained from Minitab software.***

4.6 Breakthrough Curves

The performance of AC-NaOH-60°C and AC-HNO_3-90°C were further studied in a fixed bed mode. Breakthrough curves were generated by plotting transient total sulfur concentration normalized by the feed total sulfur concentration (C/Co) vs. cumulative time. The breakthrough curves for thiophene, BT and DBT in the base and acid treated samples are depicted in figure 4.18 (a & b). The starting concentrations of thiophene, BT and DBT were 50 ppm, 51 ppm and 52 ppm respectively. The acid treated sample showed higher breakthrough times compared to the base treated sample. DBT was lowered to 0 ppm after 5mins of adsorption in all the samples tested however breakthrough was not achieved even after 400mins of adsorption. This indicates the suitability of acid treatment in the adsorption of this compound. Breakthrough was achieved after 180mins for DBT using AC-NaOH-60°C. The breakthrough of thiophene and BT in both AC-NaOH-60°C and AC-HNO_3-90°C was achieved after 5mins and 10mins respectively. For AC-NaOH-60°C, thiophene returned to its initial concentration after the first 120mins while BT returned to its initial concentration after 50 mins signifying no further adsorption that has taken place after this time. This is in contrast with the AC-HNO_3-90°C performance, both thiophene and BT did not reach their initial concentration even after 400mins of the column adsorption process. The breakthrough for all the adsorbent followed the order DBT > BT > T. This means that AC treated with HNO_3 is good in both batch and fixed bed mode. Some of the selected chromatograms before and after breakthroughs from the GC instrument are given in figure (4.19 a, b, c, d, e, & f)

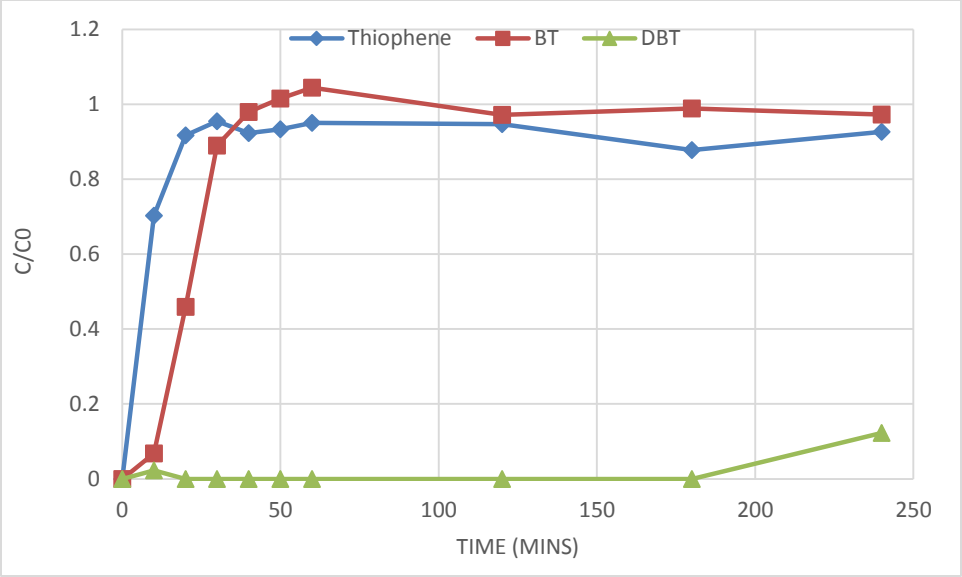

Figure 4.18 a*: Breakthrough curve for AC-NaOH-60℃*

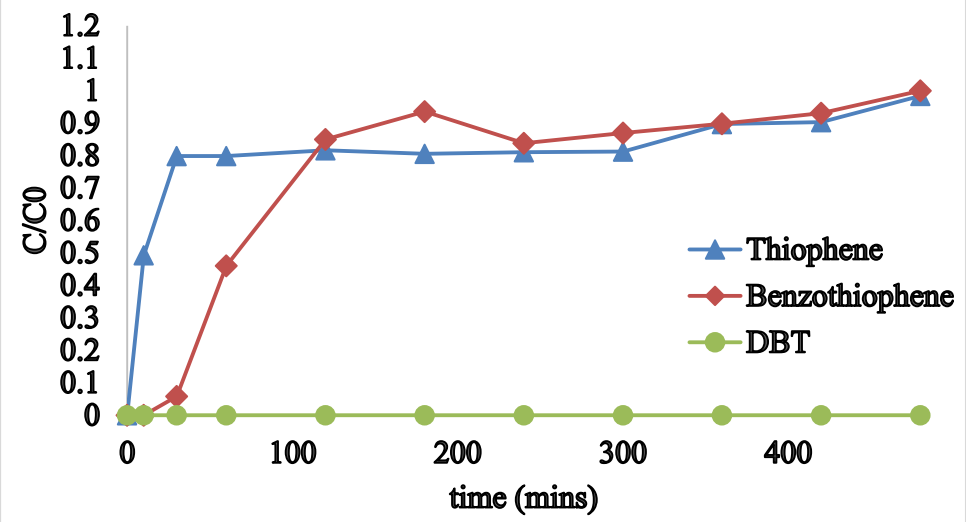

Figure 4.18 b*: Breakthrough curve for AC-HNO_3-90℃*

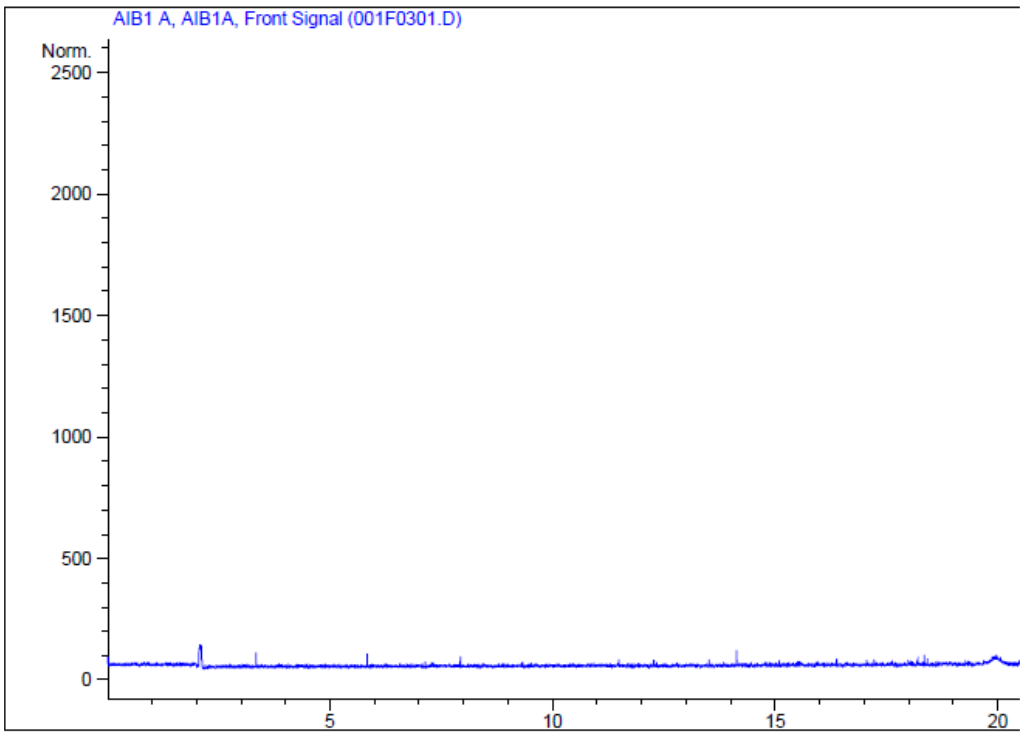

Figure 4.19 a*: GC-SCD Chromatogram of the blank*

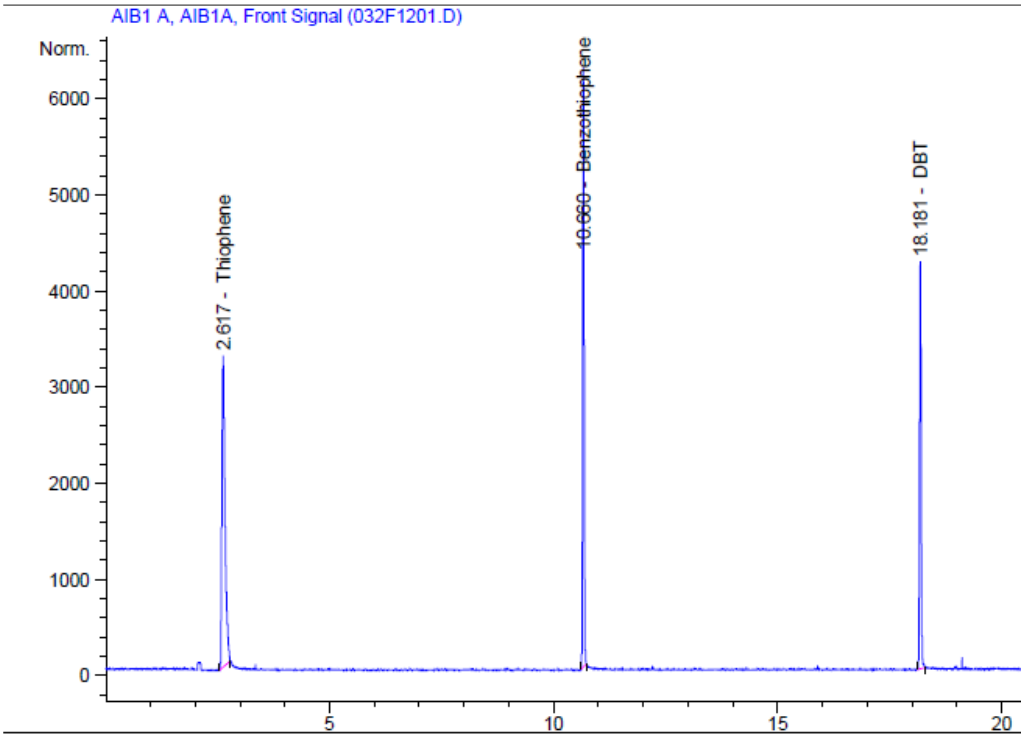

Figure 4.19 b*: GC-SCD chromatogram of the refractory sulfur compounds before adsorption*

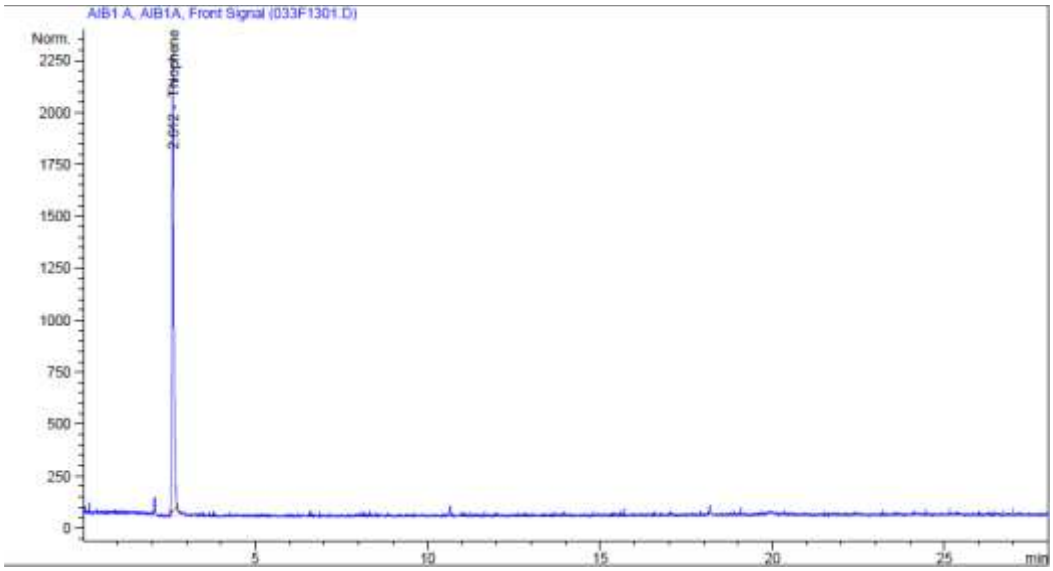

Figure 4.19 c*: GC-SCD chromatogram of AC-HNO₃-90℃ after 10mins (column)*

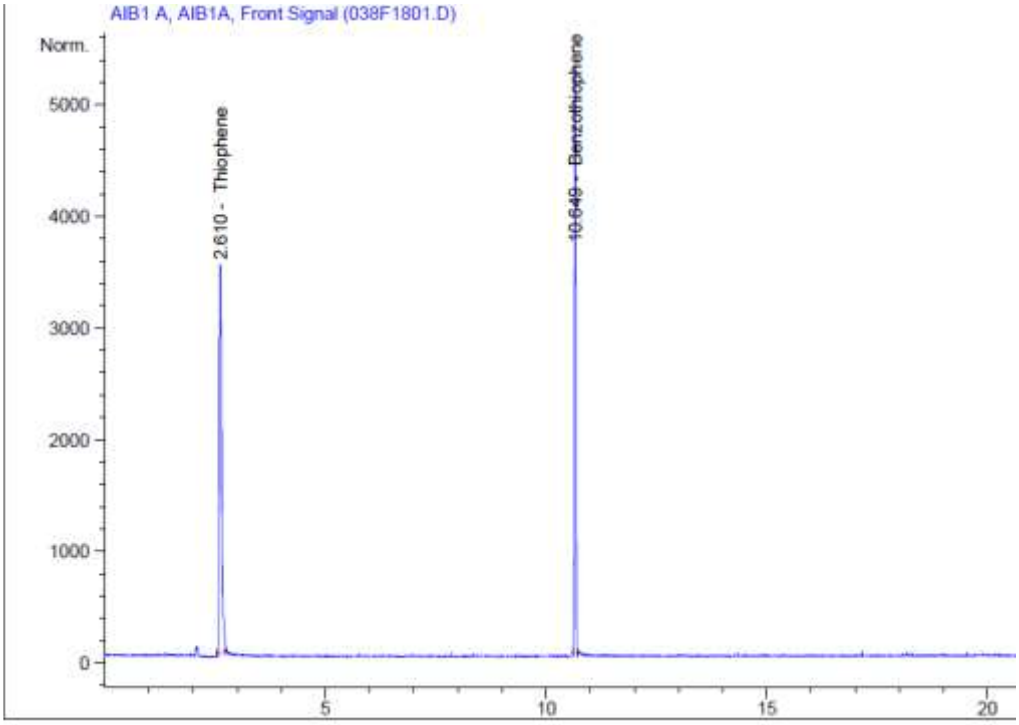

Figure 4.19 d*: GC-SCD chromatogram of AC-HNO₃-90℃ after 4 hours* **(column)**

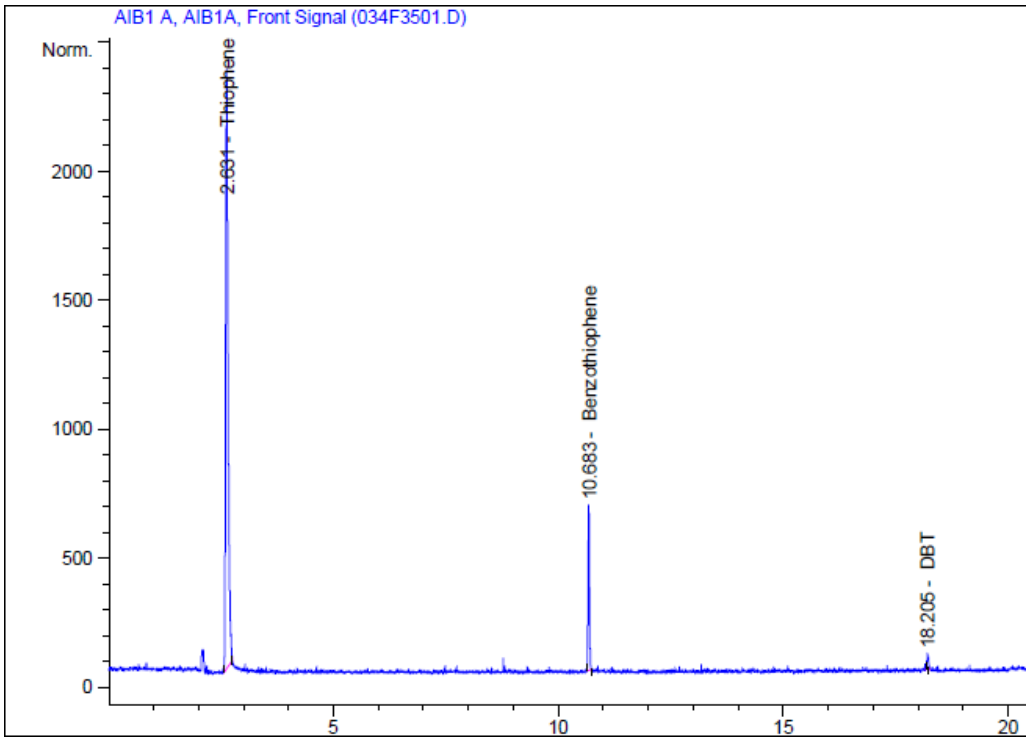

Figure 4.19 e*: GC-SCD chromatogram of AC-NaOH-60℃ after 10mins (column)*

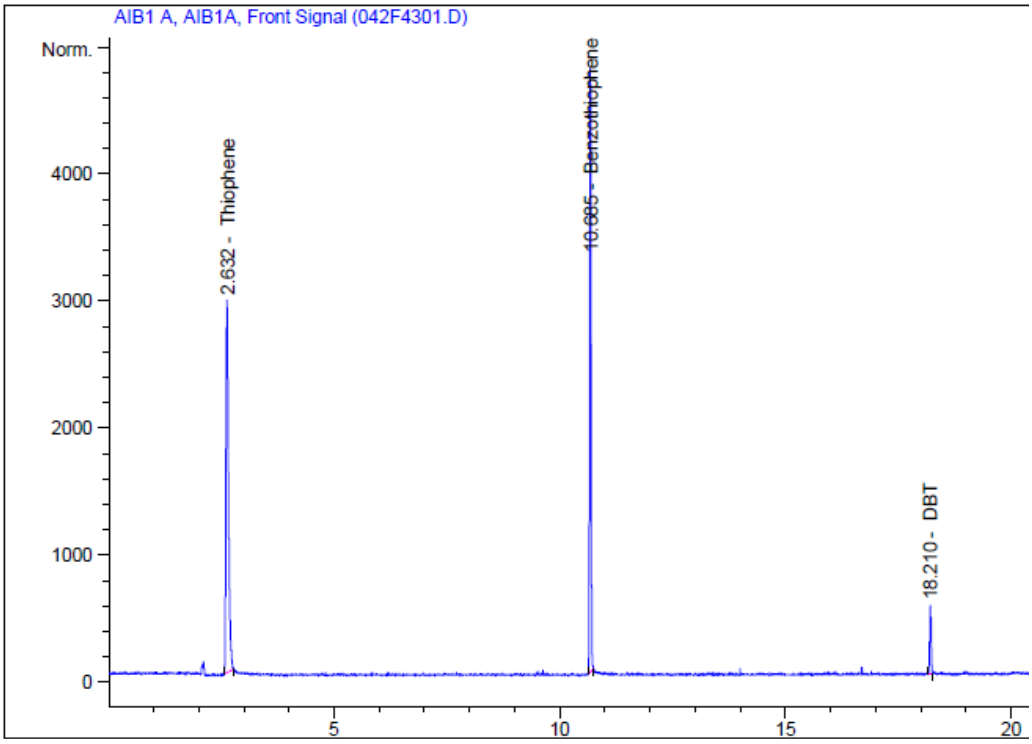

Figure 4.19 f*: GC-SCD chromatogram of AC-NaOH-60℃ after 4 hours (column)*

4.7 Adsorption kinetic study

Results from batch adsorption kinetics are important for the design of industrial adsorption columns. AC-HNO_3-90°C was selected for the kinetic studies since it showed the best performance among all the adsorbent synthesized. In order to understand the adsorption process, the commonly used kinetic models including the pseudo-first order model, the pseudo-second order model, and the intraparticle diffusion model were examined to best describe the sulfur adsorption kinetics of the new developed adsorbents. Pseudo first order kinetic model is used to describe the initial stages of adsorption process where as pseudo second order models gives the description of the whole adsorption process and overall adsorption capacity (Anbia *e*t *a*l., 2011).

Pseudo-first-order equation was first given by Lagergren 1898. The equation is as follows:

$$\ln(q_e - q_t) = lnq_e - k_1 t$$

Where, qe (mg/g) and qt (mg/g) are the amounts of analyte adsorbed at equilibrium and time t (min), respectively; and k_1 (min^{-1}) is the rate constant of the Lagergren-first-order kinetics model. The k_1 and qe were calculated from the slope and intercept of the plot $\ln(q_e - q_t)$ versus t. Figure 4.20 and Table 4.6 summarizes the parameters of the first order kinetic parameters of AC/HNO_3/90°C. The results were compared with the second order model and the experimental q_e. It can be clearly seen that the correlation coefficients for the thiophene, BT and DBT in the first order kinetic model are lower than the second order model. In addition, the calculated q_e values are not in accordance with the experimental q_e. It can therefore be concluded that the adsorption process does not obey the pseudo first order kinetics.

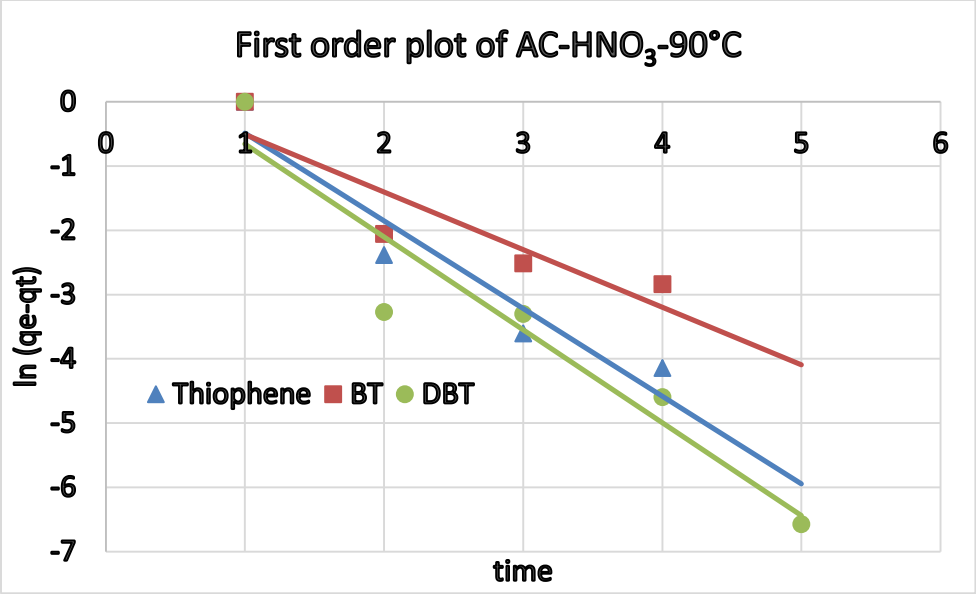

Figure 4.20*: First order pseudo kinetics for adsorption of thiophene, BT and DBT by AC-HNO₃-90°C*

The pseudo second order model is based on the assumption that the rate limiting step of a reaction may be chemisorption which involves valence forces by sharing or electron exchange between the adsorbent and the adsorbate (Wang *et al*., 2008). The pseudo second order kinetics can be expressed from the equation given by (McKay *et al*., 1999), as:

$$\frac{t}{q_t} = \frac{1}{k_2 q_e^2} + \frac{t}{q_e}$$

Where qt is the amount of adsorption thiophene, BT and DBT (mg/g) at time (min) and k_2 (g/ (mg min)) is the adsorption rate constant of pseudo-second-order adsorption. The slope and intercept of the linear plots of t/qt against t yield the values of 1/qe and $1/k_2q_e^2$. The qe and k_2 can be obtained from the slope and intercept. The values of the rate constants, maximum amount adsorbed and the correlation coefficients are given in Table 4.6. It can be clearly seen that the R^2 and calculated q_e values of thiophene, BT and DBT agrees with the second order kinetic model. The plot of the second order model in given in figure 4.21

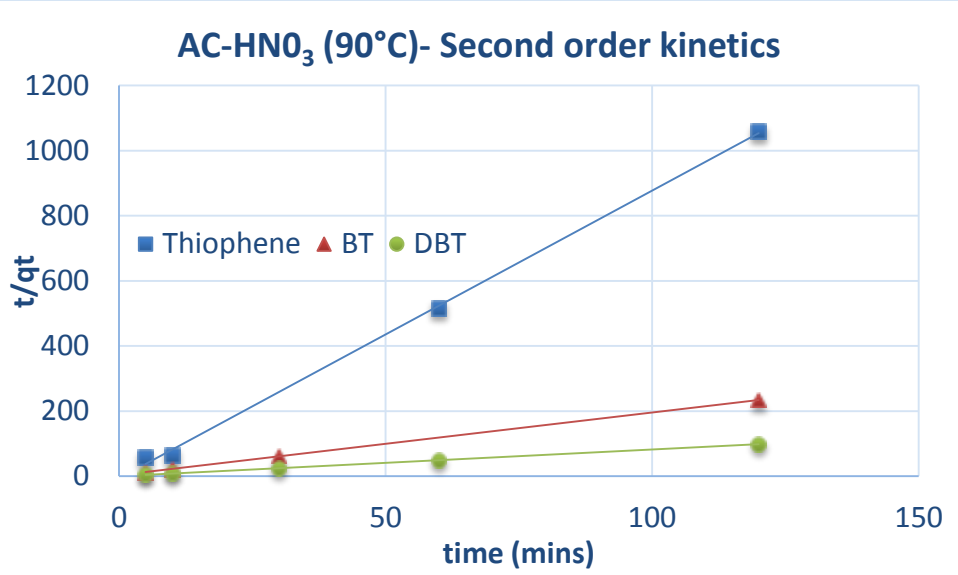

Figure 4.21*: Second order pseudo kinetics for adsorption of thiophene, BT and DBT by AC-HNO$_3$-90°C*

The kinetic experimental results were also fitted to the Weber's intraparticle diffusion mechanism to gain insight understanding to the mechanisms and rate controlling steps affecting the adsorption kinetics (Weber *et al*., 1963).

The kinetic results were analyzed by the intraparticle diffusion model to elucidate the diffusion mechanism. The following equation was applied:

$$q_t = k_{id} t^{1/2} + C$$

where C is the intercept (mg/g) which is related to the boundary layer thickness and k_{id} is the slope which represents the intraparticle diffusion rate constant (mg/g h1/2), which can be calculated from the slope of the linear plot of q_t versus $t^{1/2}$. The intraparticle diffusion plots of the adsorbents AC/HNO$_3$/90°C is depicted in figure 4.22.

The results indicate that the adsorbent have higher adsorption efficiency toward DBT over the other two refractory sulfur compounds. This can be concluded from the intercept as presented in (table 4.6). The correlation coefficient (R^2) and intercept of DBT are higher

than that of thiophene and BT table (4.6) indicating greater contribution of the surface sorption is the rate controlling step in case of DBT adsorption. If the regression of qt versus $t^{1/2}$ is linear and passes through the origin, then intraparticle diffusion is the sole rate-limiting step. However, the linear plots at each dosage did not pass through the origin. This indicates that the intraparticle diffusion was not only rate controlling step (Hameed *et al*., 2008)

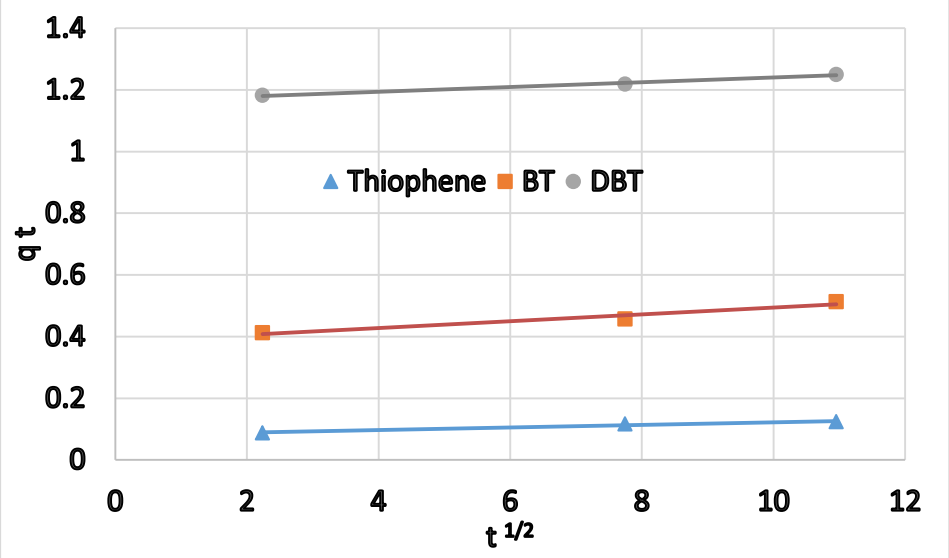

Figure 4.22: Plots for evaluating intraparticle diffusion rate constant for sorption of Thiophene, BT and DBT onto AC-HNO_3-90°C

Table 4. 6: Pseudo first order, pseudo second order and intraparticle diffusion parameters for adsorption of thiophene, BT and DBT on AC/HNO_3/90°C

			Pseudo first order			Pseudo second order model			Intraparticle diffusion		
Adsorbent	Compound	Experimental qe (mg/g)	K_1	Calculated qe	R^2	K_2 (g/mg min)	Calculated qe	R^2	Ki.d	C	R^2
AC-HNO_3-90°C	Thiophene	0.18	0.0579	0.08	0.7228	11.7655	0.11	0.9989	0.0042	0.0798	0.968
	BT	0.54	0.0115	0.1	0.891	1.2	0.52	0.9999	0.0112	0.3827	0.9555
	DBT	1.22	0.062	0.06	0.9935	3.375	1.22	1	0.0077	1.163	0.9886

4.8 Adsorption Isotherms

Equilibrium study on adsorption provides information on the capacity of the adsorbent. An adsorption isotherm is characterized by certain constant values, which express the surface properties and affinity of the adsorbent and can also be used to compare the adsorptive capacities of the adsorbent for different pollutants. Equilibrium data can be analyzed using commonly known adsorption systems. Several mathematical models can be used to describe experimental data of adsorption isotherms. The Freundlich and Langmuir models were employed for the analysis of adsorption that occurred in the experiment.

4.8.1 Langmuir adsorption isotherm

This is the most common model used to quantify the amount of adsorbate on the surface of the adsorbent as a function of partial pressure or concentration at a given temperature. It describes quantitatively the formation of a monolayer adsorbate on the outer surface of the adsorbent and no further adsorption takes place after the monolayer formation. The Langmuir isotherm is valid for monolayer adsorption onto a surface containing a finite number of identical sites. The model assumes uniform energies of adsorption onto the surface and no transmigration of adsorbate in the plane of the surface. The Langmuir equation that governs the adsorption of thiophene, BT and DBT is given as:

$$\frac{C_e}{q_e} = \frac{1}{K_L q_m} + \frac{C_e}{q_m}$$

Where q_e (mg g^{-1}) is the amount adsorbed at equilibrium concentration C_e (mg L^{-1}), q_m (mg g^{-1}) is the Langmuir constant representing maximum monolayer capacity and K_L is the Langmuir constant related to the energy of adsorption. The slope and intercept of linear plots of Ce/qe against Ce (figure 4.23) yield the values of $1/q_m$ and $1/K_L q_m$

The adsorption capacity q_m for the refractory sulfur compounds on AC/HNO_3/90°C followed the order thiophene < BT < DBT. The dimensionless constant separation factor R_L is considered an integral part of Langmuir isotherm. The equation is given below:

$$R_L = \frac{1}{1 + K_L C_0}$$

Where C_0 = is the initial concentration of the analytes (mg/L), and K_L (L/mg) is Langmuir constant. The shape of the isotherm can better be represented by R_L value where $R_L > 1$ indicates an unfavorable process, $R_L = 1$ indicates linearity and $R_L < 1$ but > 0 indicates a favorable process. The results obtained from table 4.7 shows that the adsorption of DBT on the adsorbent is a favorable process.

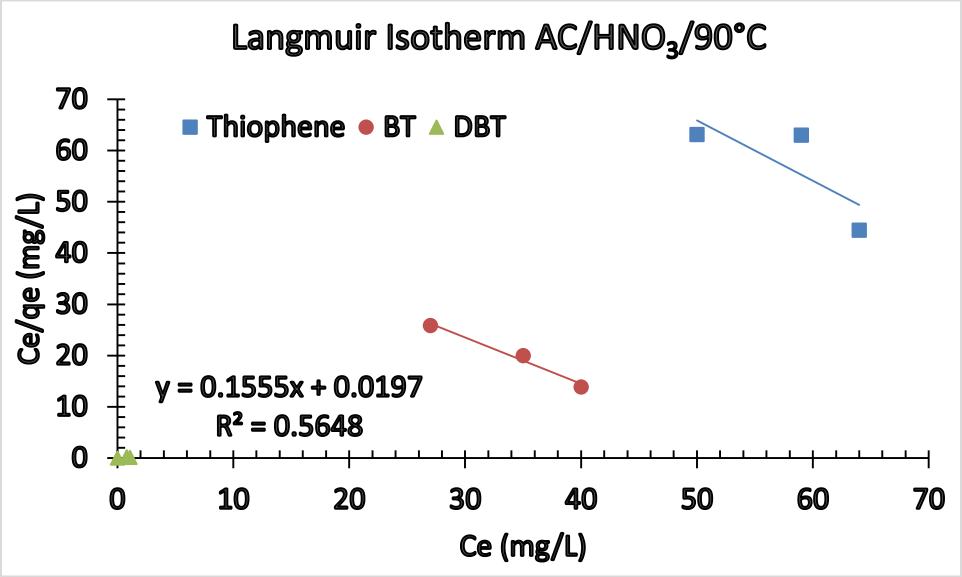

Figure 4.23*: Plot of Langmuir isotherm for adsorption of thiophene, BT and DBT by AC/HNO_3/90°C*

Table 4.7: Langmuir and Freundlich Isotherms constant for AC-HNO3-90°C

Adsorbents	Compounds	Langmuir Isotherm constant				Freundlich Isotherm constant			
		q_m (mg/g)	K_L (L/mg)	R^2	R_L	K_f	1/n	n	R^2
AC-HNO3-90°C	Thiophene	0.7790589	0.0100117	0.9442	0.5811	6.51E-05	2.4066	0.415524	0.9914
	BT	1.10680686	0.017843	0.9793	0.5002	0.001356	2.0102	0.497463	0.9945
	DBT	6.43086817	7.893401	0.5648	0.002527	4.611255	8.9311	0.111968	0.9986

4.8.2 Freundlich adsorption isotherm

Freundlich isotherm is an empirical equation employed to describe heterogeneous systems or multilayer sorption (Freundlich *e*t *a*l., 1906). The Freundlich isotherm can be expressed in the following equation:

$$q_e = K_F C_e^{1/n} \rightarrow \ln q_e = \ln K_F + \frac{1}{n} lnC_e$$

Where q_e ($mg.g^{-1}$) is amount of absorbed material in absorbent surface, K_F and n are Freundlich constants with K_F (mg/g) is the adsorption capacity of the sorbent and n giving an indication of how favorable the adsorption process. The magnitude of the exponent, 1/n (g/L), gives an indication of the favorability of adsorption. Values of n > 1 represent favorable adsorption condition (Poots *e*t *a*l., 1978). To determine the constants K_F and n, the linear form of the equation may be used to produce a graph of $\ln(q_e)$ against $\ln(C_e)$ figure 4.24. Values of K_F and n are calculated from the intercept and slope of the plot.

Results in (table 4.7) showed the value of n are more than one which means that it is a favorable adsorption process. As it is shown in (table 4.7), the adsorption capacity of the AC/HNO_3/90°C toward DBT is higher than that toward BT and thiophene. The comparison of the R^2 values from (table 4.7) indicate that Freundlich isotherm model yields a better fit to the experimental data than Langmuir isotherm.

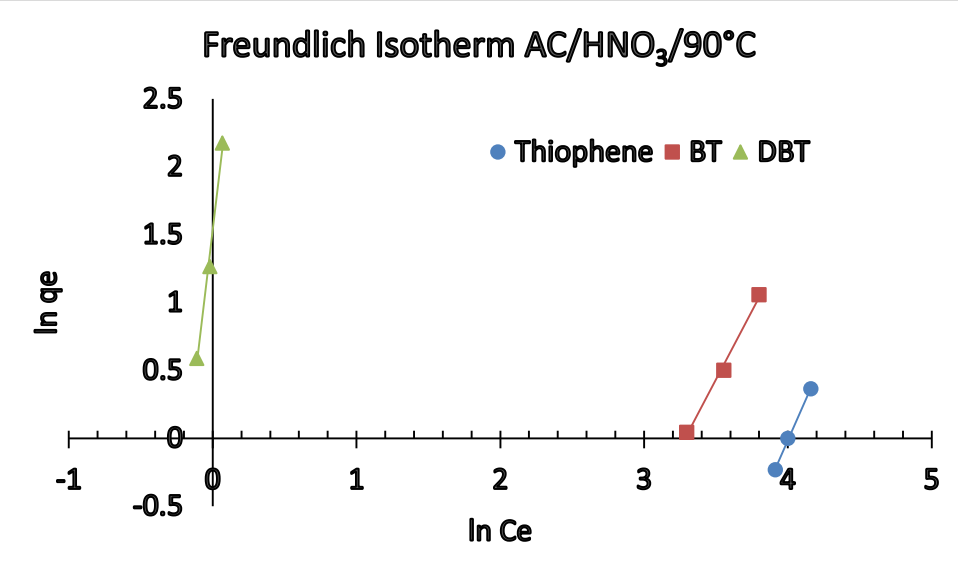

Figure 4.24*: Plot of Freundlich isotherm for adsorption of thiophene, BT and DBT by AC/HNO₃/90℃*

4.9 Comparison of desulfurization abilities between coal based AC and AC synthesized from WRTs.

GC IPH coal based AC commercially available for desulfurization was used as a basis for comparison of the potential of AC synthesized from WRTs to serve as a replacement in desulfurization. As received coal based AC pellets were crushed to fine powdered particles and they were subjected to the same treatment as the synthesized carbon from WRTs i.e. (treatment with nitric acid at 90°C). Table 4.8 summarizes the properties of the coal based AC used for the comparison.

Table 4. 8: Properties of GC IPH Pelletized Activated Carbon

Particle type	Pelletized
Typical particle size (diameter) mm	4
Length (mm)	6
Mean Particle diameter (mm)	4.7
Iodine number (mg/g)	1000
Surface Area m2/g	1000
Hardness	95
Bulk density g/cc	0.55
Moisture %	15

The results are shown in figure 4.25. It can be clearly seen that as-received coal based AC performed better than the raw carbon from WRTs and this can be attributed to industrial enhancement techniques employed for the production of the commercial carbon. Treatment of the samples with nitric acid at 90°C on the other hand significantly improved the performance of the AC derived from WRTs but it had net negative effect on the desulfurization performance of the coal based AC. The desulfurization of the sulfur compounds in all the samples followed the order DBT > BT > T. The result from this study showed the possibility of replacing the commercially expensive AC with simple, cost effective, efficient and easily regenerated adsorbent for adsorption studies.

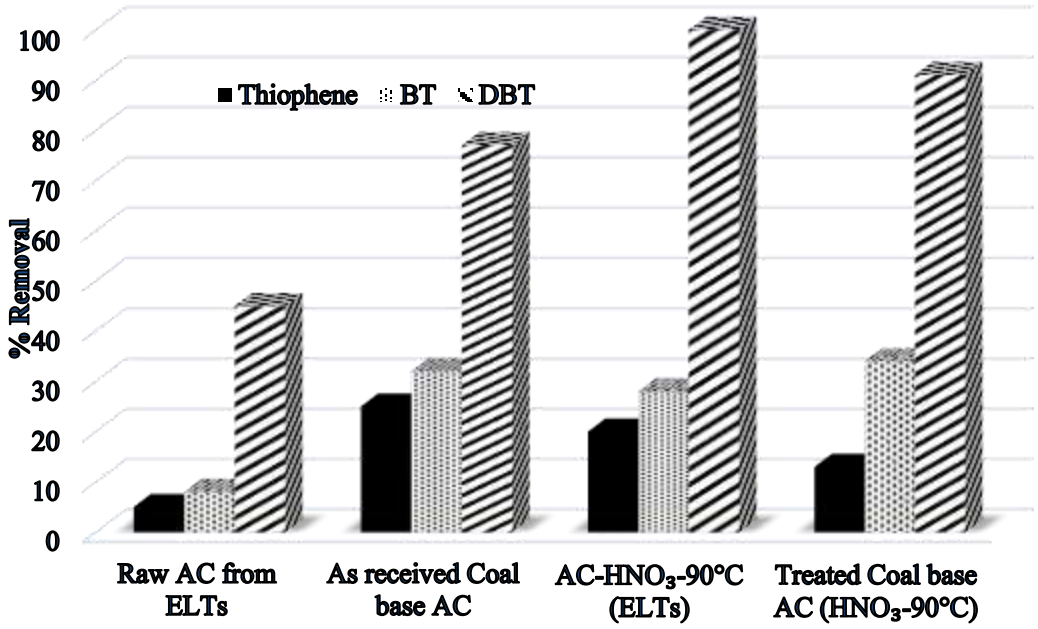

Figure 4.25*: Efficiency of raw and treated ACs derived from waste rubber tires compared with commercial coal base AC (GC IPH).*

4.10 Regeneration of the used adsorbent

The synthesized AC (AC-HNO_3-90C) was evaluated for its regeneration abilities. The regeneration was done by heating the adsorbent in closed system for 3 h at 350°C. The temperature which is said to vaporize all the sulfur compounds from the adsorbent (thiophene 84°C, BT 221°C and DBT 333°C). The results are showed in figure 4.26, the percentage removal of the sulfur compounds showed continued decrease in the adsorptive capacity of the adsorbent. However it still showed great promise in the removal DBT even after three cycles of regeneration. The order of desulfurization after three cycles of regeneration followed the sequence: DBT (59%) > T (6%) > BT (5%).

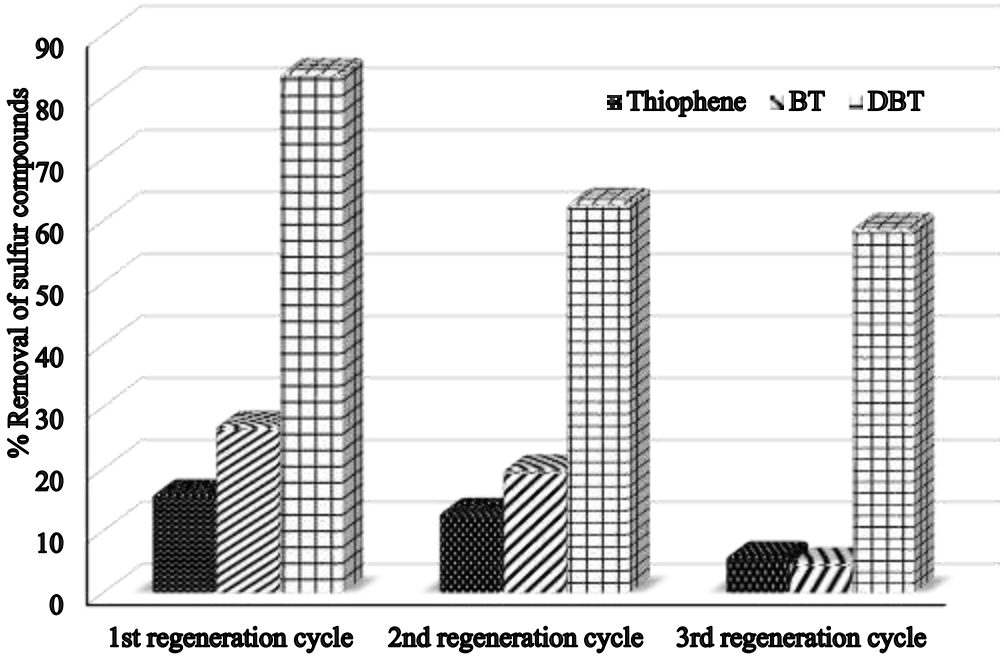

Figure 4.26*: Regeneration efficiency of AC-HNO_3-90℃ on the adsorption of sulfur compounds*

4.11 RESULTS ON THE NANOPARTICLES NICKEL, CERIUM and IRON LOADING ON AC.

4.11.1 Characterization of Nickel loaded on AC

The result of the SEM/EDS of nickel loaded on AC is given in figure 4.27, the elemental composition from the result indicated the presence of carbon peak at 0.25 keV, oxygen at 0.5 keV and nickel peak at 0.9 keV with percent weight of (80%) for carbon, oxygen (15.6%) and nickel (3.78%).

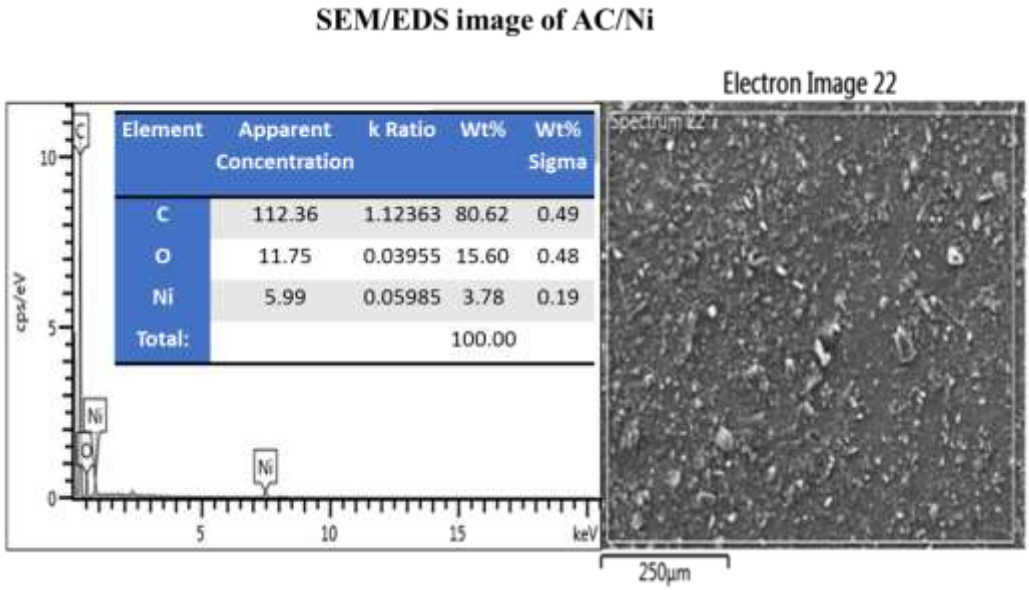

Figure 4.27*: SEM/EDS image of AC/Ni*

The XRD pattern of the synthesized adsorbent (AC/Ni) is depicted in figure 4.28, the results showed characteristic peaks centered at 2 theta values of around 26° and around 43° denoting the presence of graphitic carbon. In addition to these peaks other peaks are also visible at the 2 theta values of 35, 42 and 62° signifying the presence of NiO while the peaks at around 44.51, 51.85 and 76.34 corresponding to the 111, 200 and 220 planes respectively denotes the presence of Ni crystal within the sample (Zhifeng *et al*., 2013).

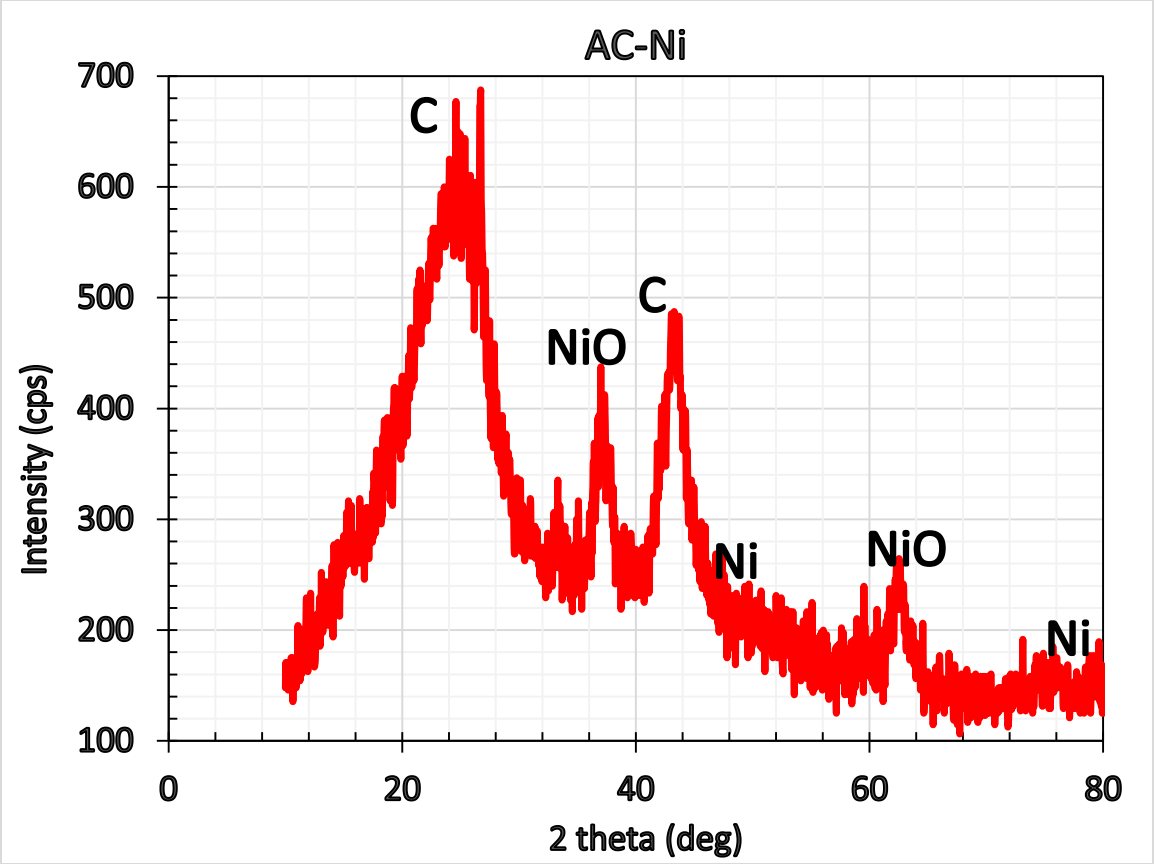

Figure 4.28*: XRD pattern of AC/Ni*

The FTIR spectrum of the AC/Ni sample is given in figure 4.29. There are noticeable bands at 3400 cm^{-1} signifying the presence of OH stretching vibration, 2800 cm^{-1} and 2900 cm^{-1} denoting the presence of C-H stretch of CH, CH_2 and CH_3, 2100-2000 cm^{-1} due to the presence of nitriles or double bonded carbon oxygen groups and alkenes (Estrella *et al.*, 1996, Morlanes 2013). Peaks at 1600 cm^{-1} and 1700 cm^{-1} are due to C=O stretching vibrations in ketones and carboxylic acids. Bands at 1300 cm^{-1} to 1100 cm^{-1} are due to the presence of a C-O bond. Bands around 400 to 500 cm^{-1} denote the stretching of NiO bond.

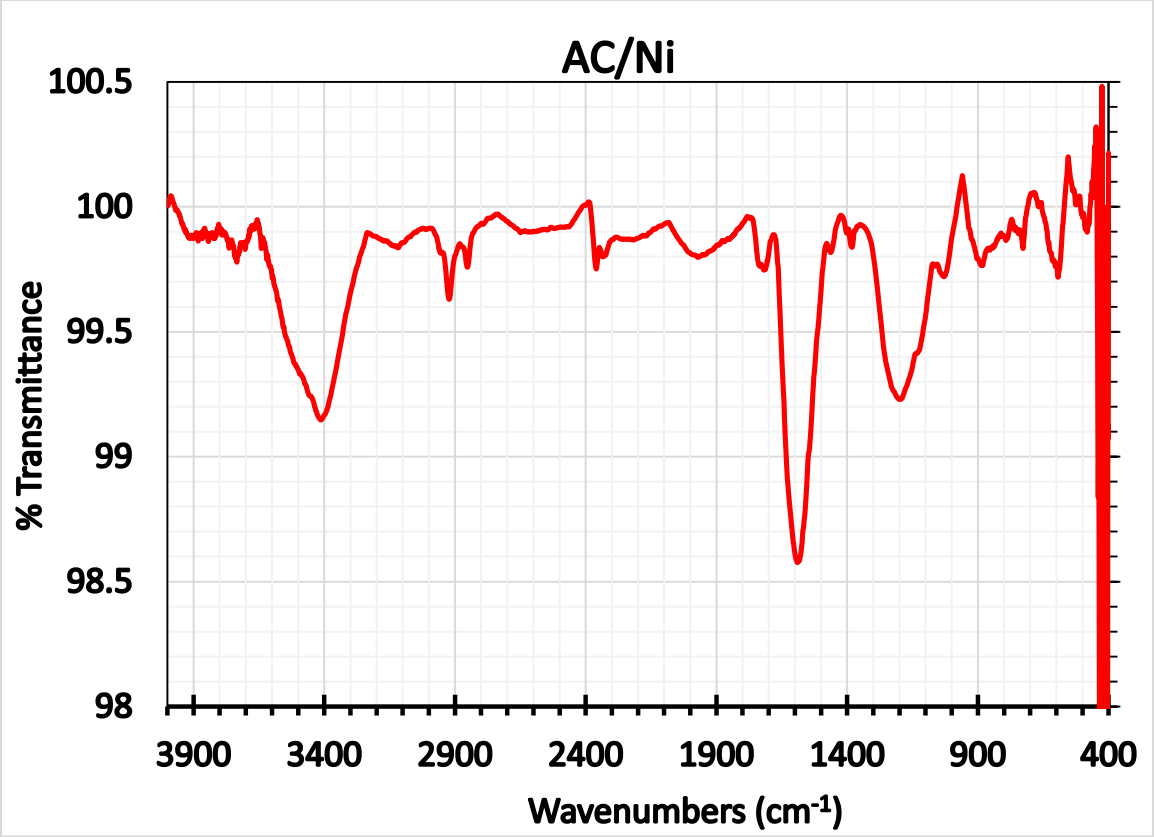

Figure 4.29*: FTIR spectrum of AC/Ni*

4.11.2 Characterization of AC/Ce

The result of the SEM/EDS of nickel loaded on AC is given in figure 4.30. The elemental composition from the result indicated the presence of carbon (82.81%), oxygen (16.14%) and cerium (0.89%), with main peaks at 0.25 for C, 0.5 for O and 1, 3.6, 5, 6 KeV for Ce.

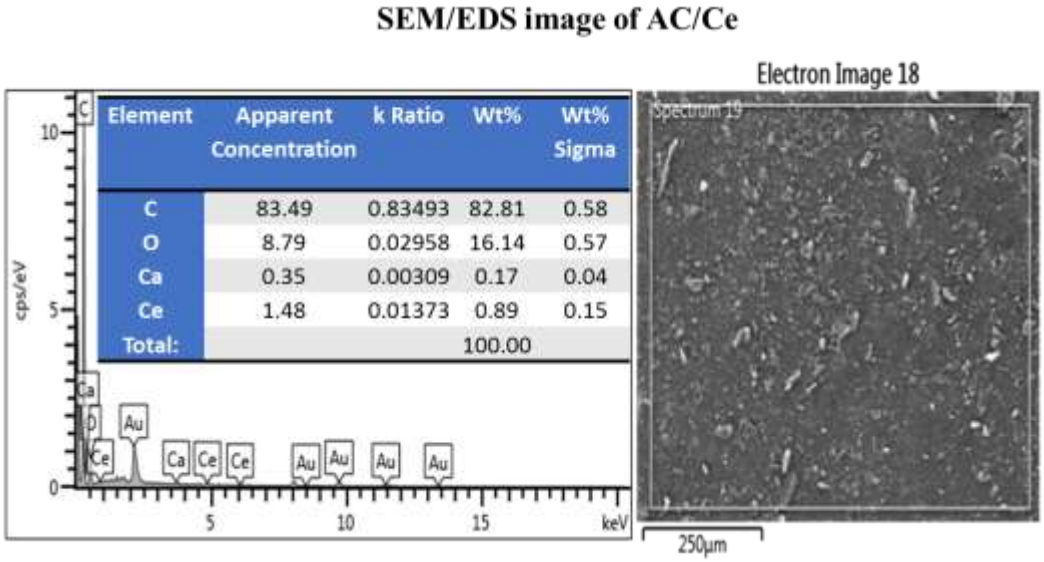

Figure 4.30: ***SEM/EDS image of AC/Ce***

The XRD pattern of the synthesized adsorbent in shown in figure 4.31, the normal carbon peaks quantifying the presence of carbon based material. Other peaks are also visible at the 2 theta values of 28.53 (111), 33 (200), 47 (220), 56 (311) signifying the presence of CeO_2 crystals. The pattern is in accordance with JCPDS No: 34-0394. (Girija *et al*., 2011; Renu *et al*., 2012).

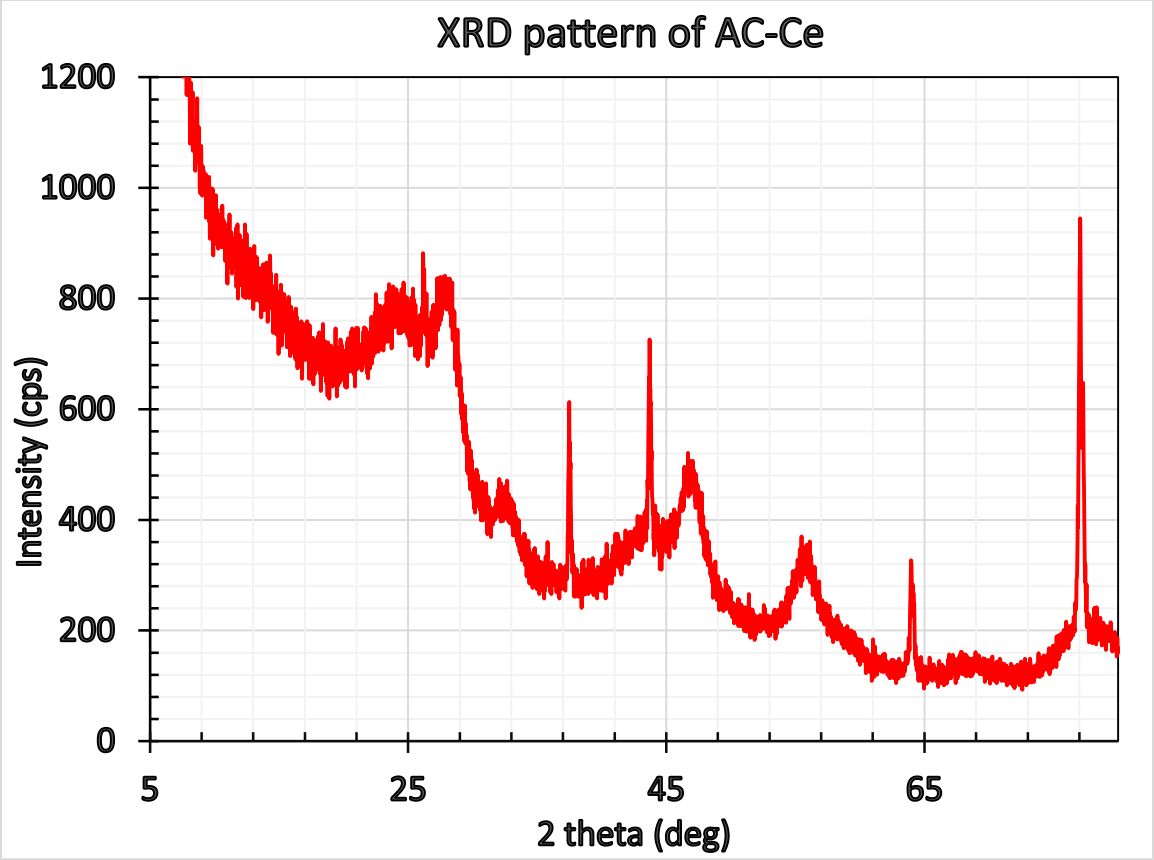

Figure 4.31*: XRD pattern of AC/Ce*

The FT-IR spectrum of AC/Ce is depicted in figure 4.32. There are noticeable bands at 3400 cm^{-1} signifying the presence of OH stretching vibration, 2800 cm^{-1} and 2900 cm^{-1} denoting the presence of C-H stretch of CH, CH_2 and CH_3, 2100-2000 cm^{-1} due to the presence of double bonded carbon oxygen groups or alkenes (Estrella *et al*., 1996, Morlanes 2013). Bands at 1600 cm^{-1} and 1700 cm^{-1} are due to C=O stretching vibrations in ketones and carboxylic acids. The band at 1300 cm^{-1} represents N-O stretch due to the HNO_3 treatment. The peak at 550.84 cm^{-1} signifies the presence of Ce-O within the sample (Ansari *et al*., 2009).

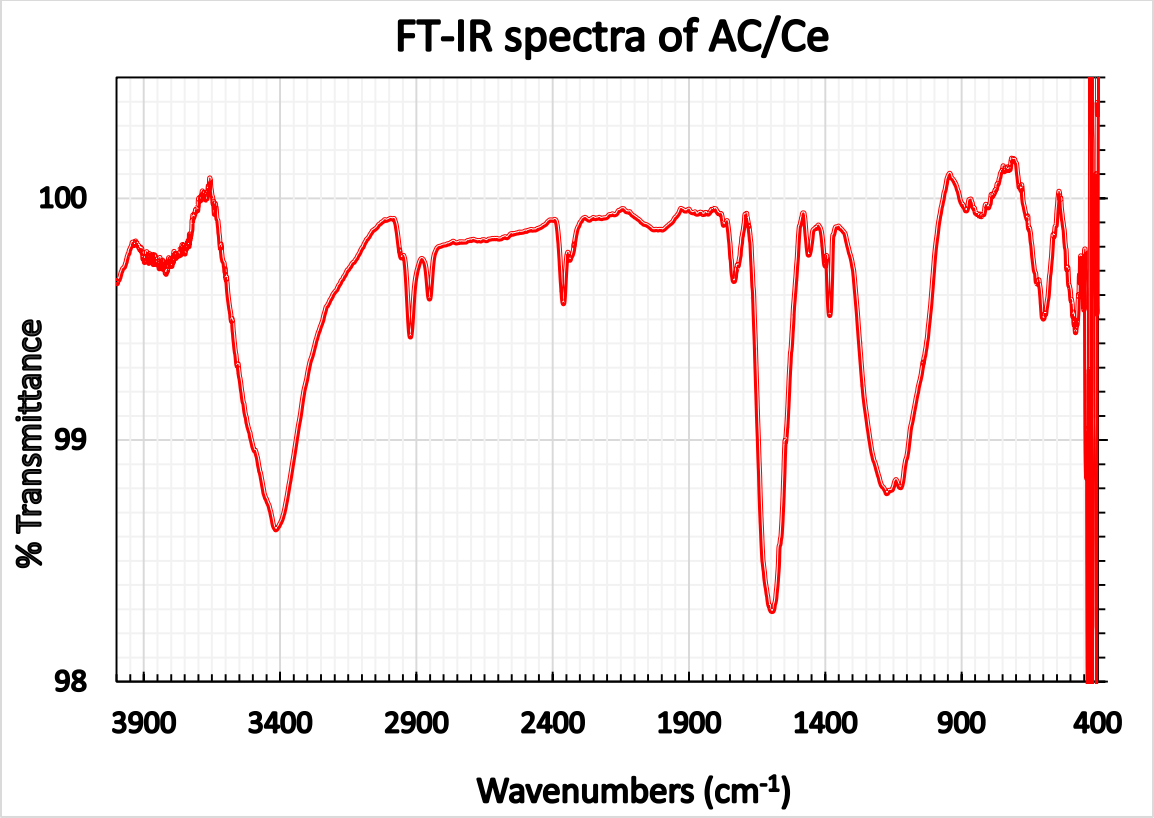

Figure 4.32*: The FTIR spectrum of AC/Ce*

4.11.3 Characterization of AC/Fe

The result of the elemental composition obtained from the SEM/EDS analysis of AC/Fe is shown in figure 4.33, the elements found on the surface of the adsorbent are carbon (81.04%), oxygen (15.18%) and iron (3.78%).

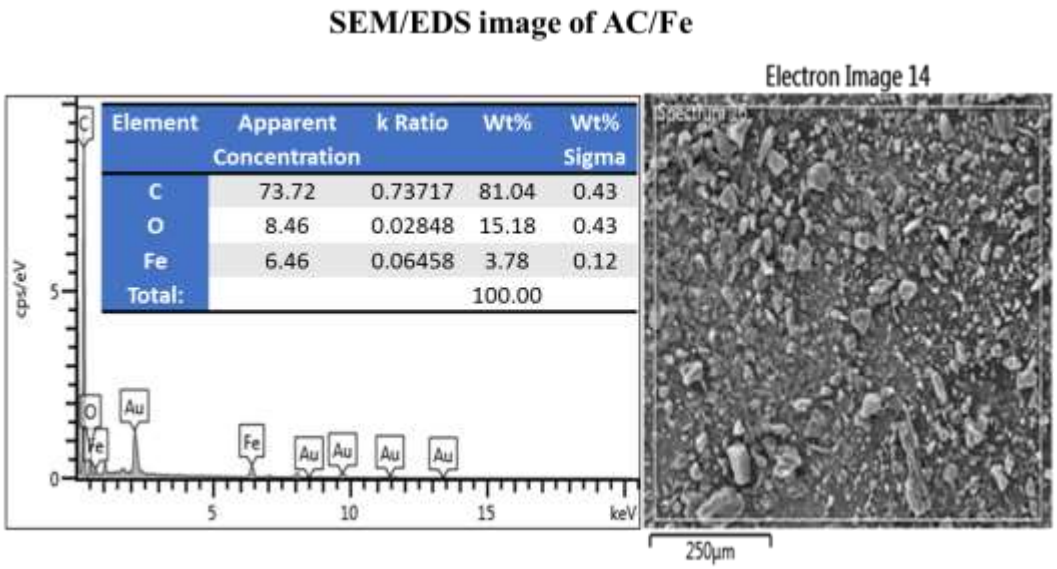

Figure 4.33*: **SEM/EDS image of AC/Fe***

The XRD spectrogram of AC/Fe showed the presence of broad graphitic carbon peaks at 2 theta values at around 26° and around 43°. In addition peaks were also noticed at 2 theta values of 43° and 63° corresponding to 400 and 440 plane of iron oxide (Mahadevan *e*t *a*l., 2012). Figure 4.34 depicts the XRD pattern.

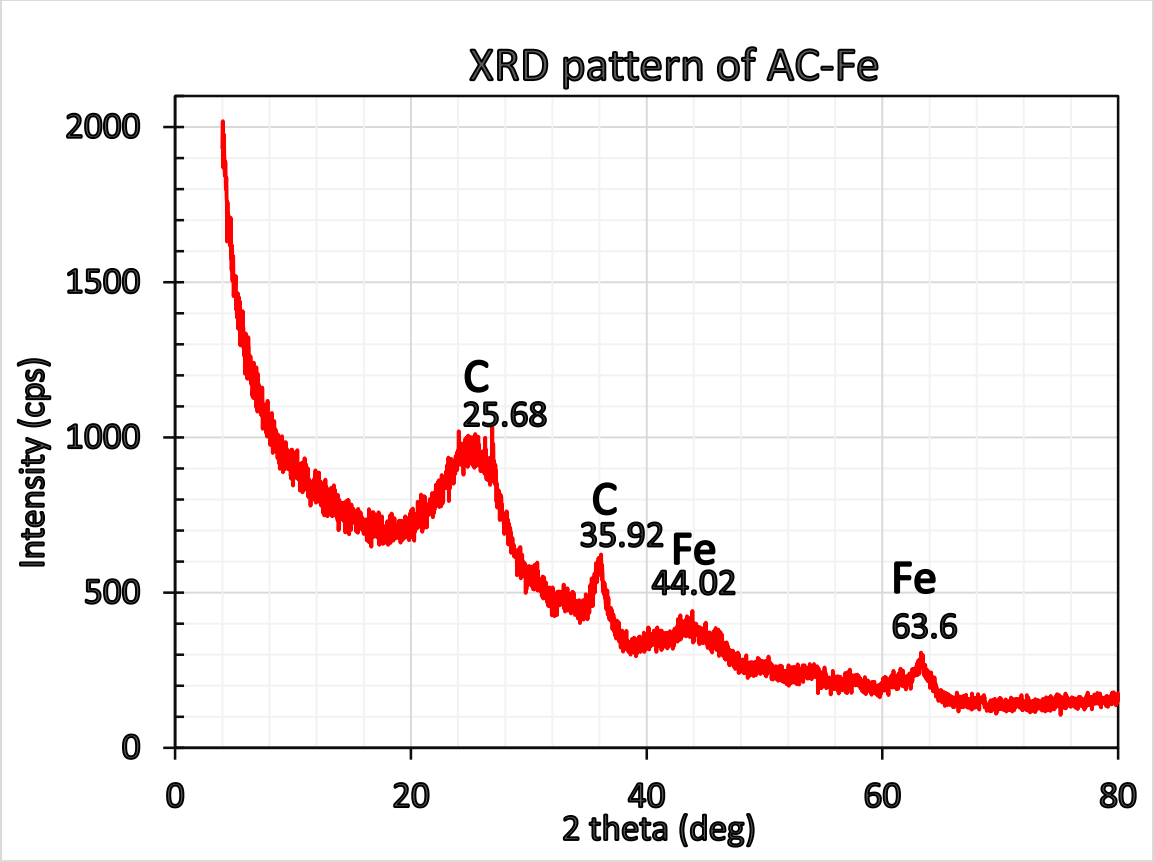

Figure 4.34*: XRD pattern of AC/Fe*

The FT-IR spectrum of AC/Fe is depicted in figure 4.35, the broad band at 3400 cm^{-1} signifies the presence of OH stretching vibration. The peaks at 2800 cm^{-1} and 2900 cm^{-1} denotes the presence of C-H stretch CH_2 and CH_3 while the peaks at around 2100-2000 cm^{-1} arise due to the presence of double bonded carbon oxygen groups and alkenes respectively (Estrella *et al*., 1996, Morlanes 2013). C=O stretching vibrations in ketones and carboxylic acids appeared at 1600 cm^{-1} and 1700 cm^{-1}. The characteristic peaks that appeared at 798 and 895 cm^{-1} are attributed to the Fe-O bending vibrations while the peak at 624 cm^{-1} is due to the Fe-O stretching vibrations within the sample (Marijan *et al*., 2007).

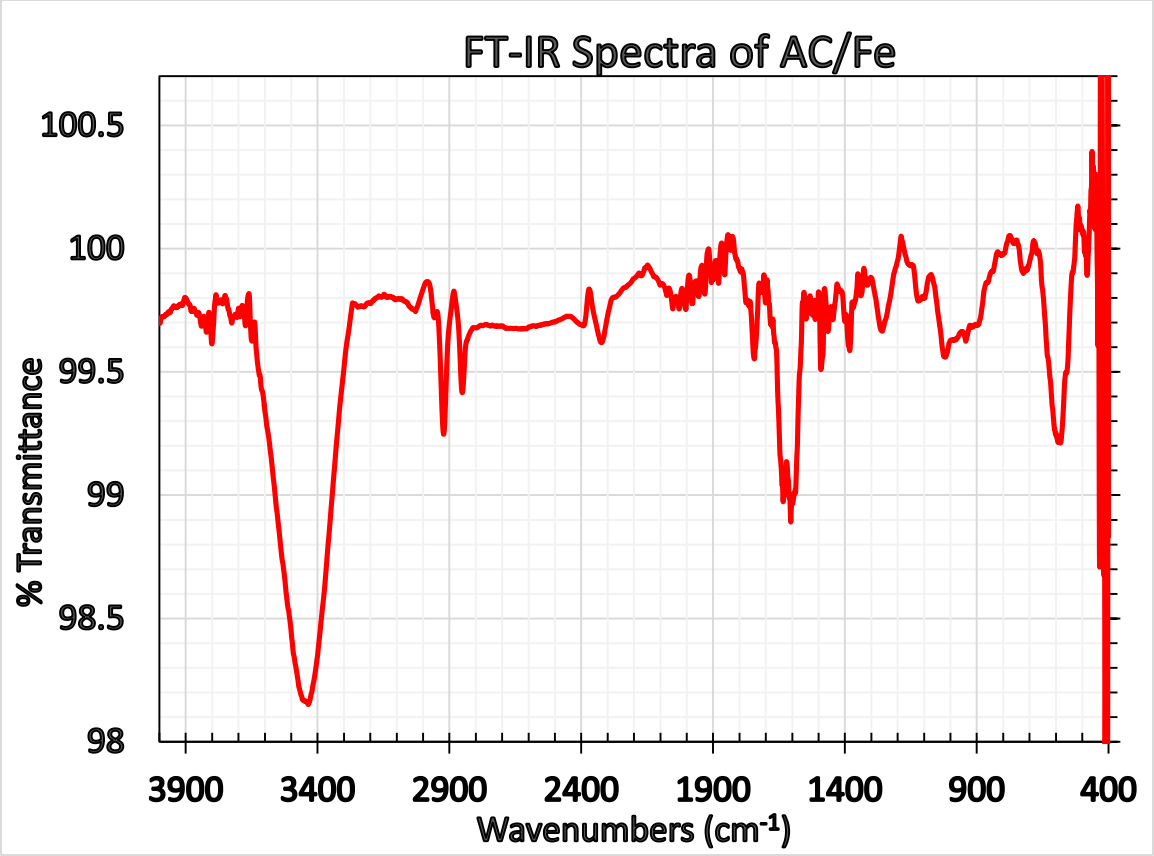

Figure 4.35*: The FTIR spectrum of AC/Fe*

4.11.4 Characterization of AC/NiO/Ce

The result of the elemental composition obtained from the SEM/EDS analysis of AC/NiO/Ce is shown in figure 4.36, the elements found on the surface of the adsorbent are carbon (85.04%), oxygen (13.69%) nickel (0.12%) and cerium (1.15%).

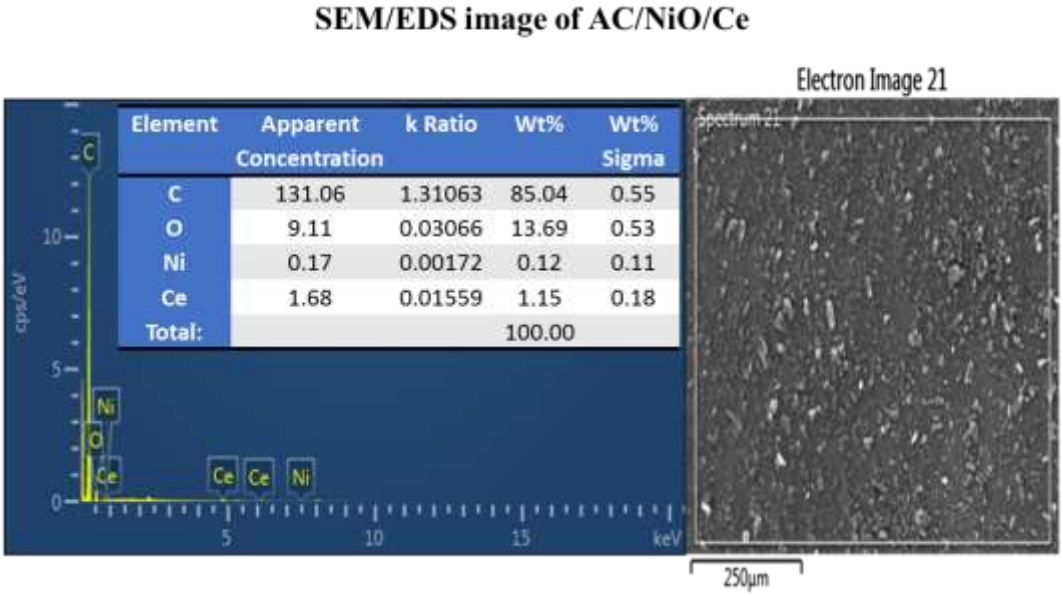

Figure 4.36*: SEM/EDS image of AC/NiO/Ce*

The XRD pattern of the synthesized adsorbent in shown in figure 4.37. The graphitic carbon peaks at 26 and 43° indicates the presence of carbon based material. Peaks at 2 theta value 62° proves the presence of NiO while the peaks at 44.51 and 76.34 corresponding to the 111 and 220 planes respectively denotes the presence of Ni within the sample (Zhifeng *et al*., 2013). Peaks appearing at 28.53 (111), 33 (200), 47 (220), 56 (311) signify the presence of CeO_2 crystals. The pattern is in accordance with JCPDS No: 34-0394. (Girija *et al*., 2011; Renu *et al*., 2012).

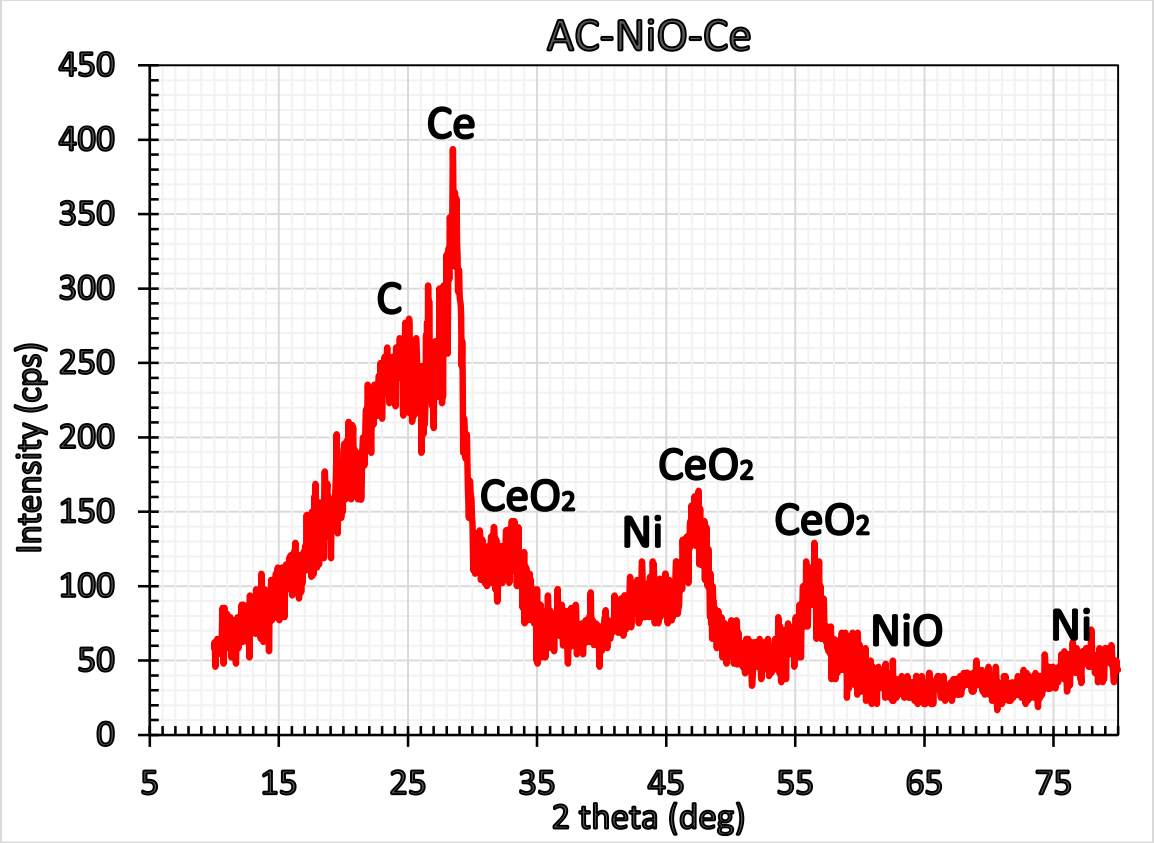

Figure 4.37*: XRD pattern of AC/NiO/Ce*

The FTIR spectrum of the AC/NiO/Ce, Figure 4.38, indicates bands at 3400 cm^{-1} due to the presence of OH stretching vibration, 2800 cm^{-1} and 2900 cm^{-1} denoting the presence of C-H stretch of CH, CH_2 and CH_3, 2100-2000 cm^{-1} due to the presence of NiO species, nitriles or double bonded carbon oxygen groups and alkenes (Estrella *et al*., 1996, Morlanes 2013). Bands appearing at 1600 cm^{-1} and 1700 cm^{-1} are due to C=O stretching vibrations in ketones and carboxylic acids, and 1300 cm^{-1} to 1100 cm^{-1} due to the presence of a N-O stretch. Bands around 400 to 500 cm^{-1} denote the stretching of NiO. The peak at 550.84 cm^{-1} signifies the presence of Ce-O within the sample (Ansari *et al*., 2009).

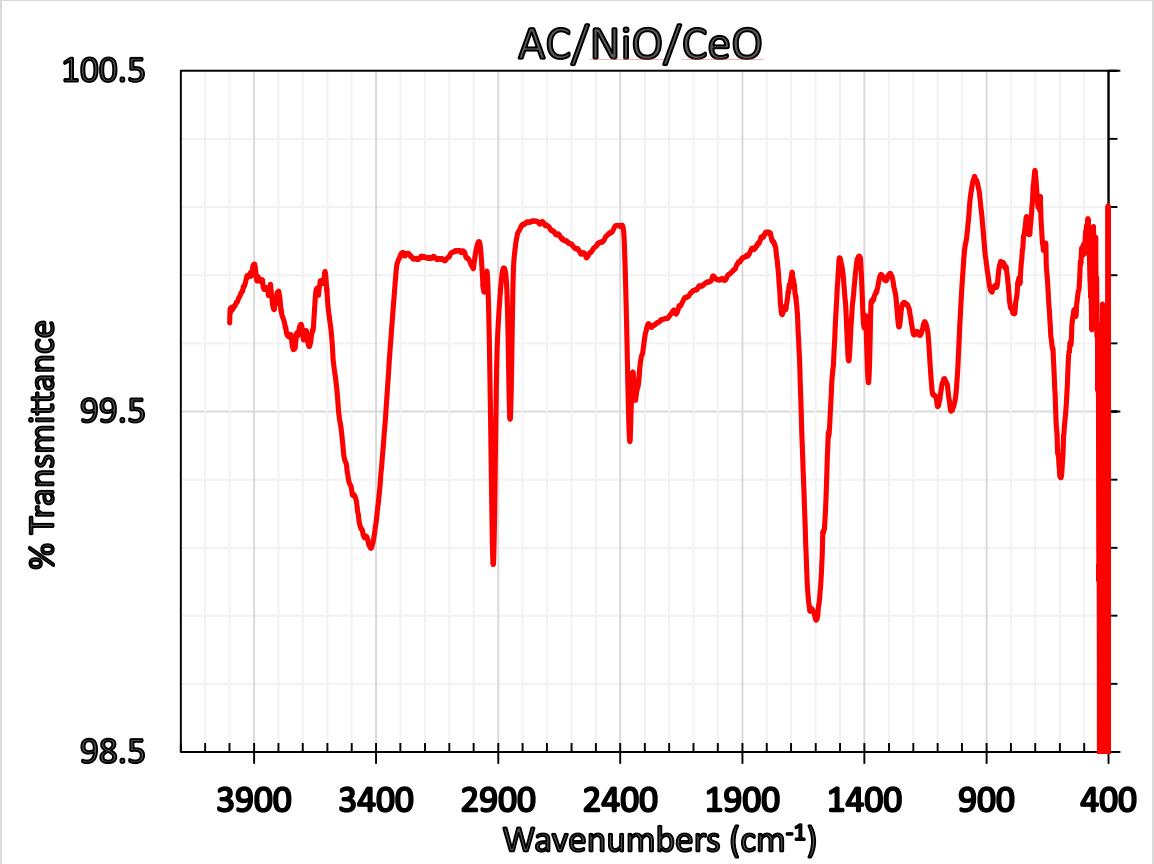

Figure 4.38*: The FTIR spectrum of AC/NiO/Ce*

4.11.5 Characterization of AC/FeO_2/Ni

The result of the elemental composition obtained from the SEM/EDS analysis of AC/FeO_2/Ni is shown in figure 4.39. The elements found on the surface of the adsorbent are represented by weight percent as carbon (82.87%), oxygen (16.15%) iron (0.54%) and nickel (0.43%) summing up to a total of 100%.

SEM/EDS image of AC/FeO_2/Ni

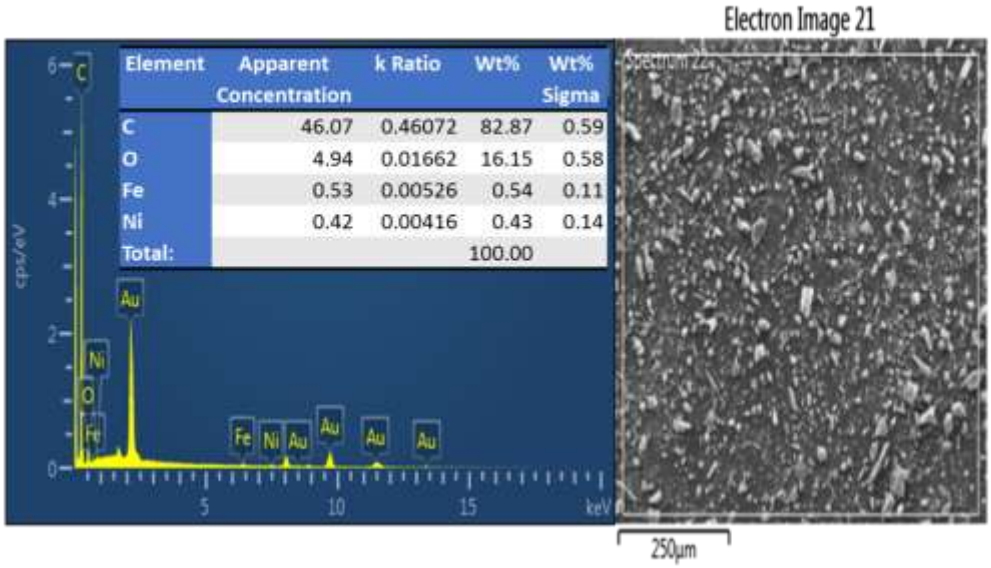

Figure 4.39*: SEM/EDS image of AC/FeO_2/Ni*

The XRD spectrogram of AC/FeO_2/Ni depicted in figure 4.40 showed the presence of broad graphitic carbon peaks at 2 theta of 26° and at 43°. In addition, peaks were also noticed at 2 theta values of 34° and 50° corresponding to the presence of iron oxide (Mahadevan *et al*., 2012). In addition peaks are also visible at the 2 theta values of 35 and 42° signifying the presence of NiO while the peak at 51.85° corresponding to the 200 planes denotes the presence of Ni within the sample (Zhifeng *et al*., 2013).

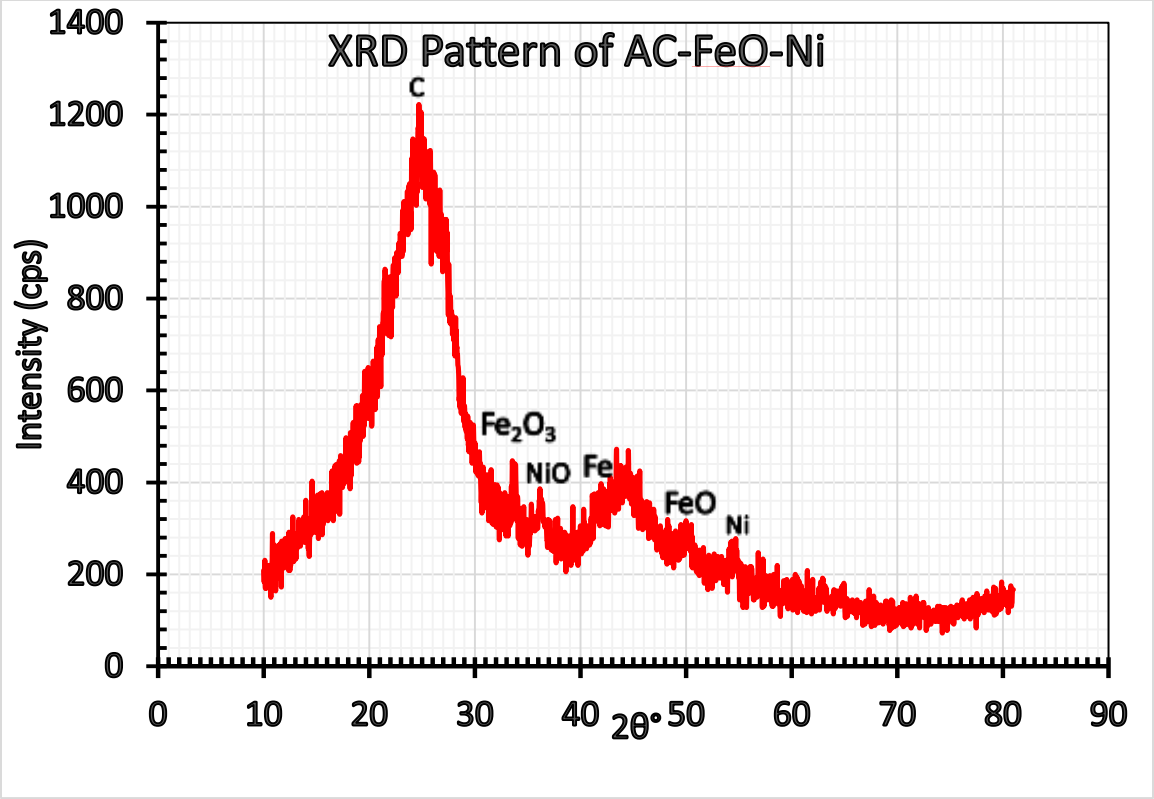

Figure 4.40: ***XRD pattern of AC/FeO$_2$/Ni***

The FT-IR spectrum of AC/Fe is depicted in figure 4.41. The broad band at 3400 cm^{-1} signifies the presence of OH stretching vibration. The peaks at 2800 cm^{-1} and 2900 cm^{-1} denote the presence of C-H stretch of CH_2 and CH_3. The C=O stretching vibrations in ketones and carboxylic acids appeared at 1600 cm^{-1} and 1700 cm^{-1}. The characteristic peak that appeared at 798 is attributed to the Fe-OH bending vibrations while the peak at 624 cm^{-1} is due to the Fe-O stretching vibrations within the sample (Marijan *et al*., 2007). The band around 1300 cm^{-1} to 1100 cm^{-1} is due to the presence of a C-O bond, and bands around 400 to 500 cm^{-1} denotes the stretching of NiO (Estrella *et al*., 1996, Morlanes 2013).

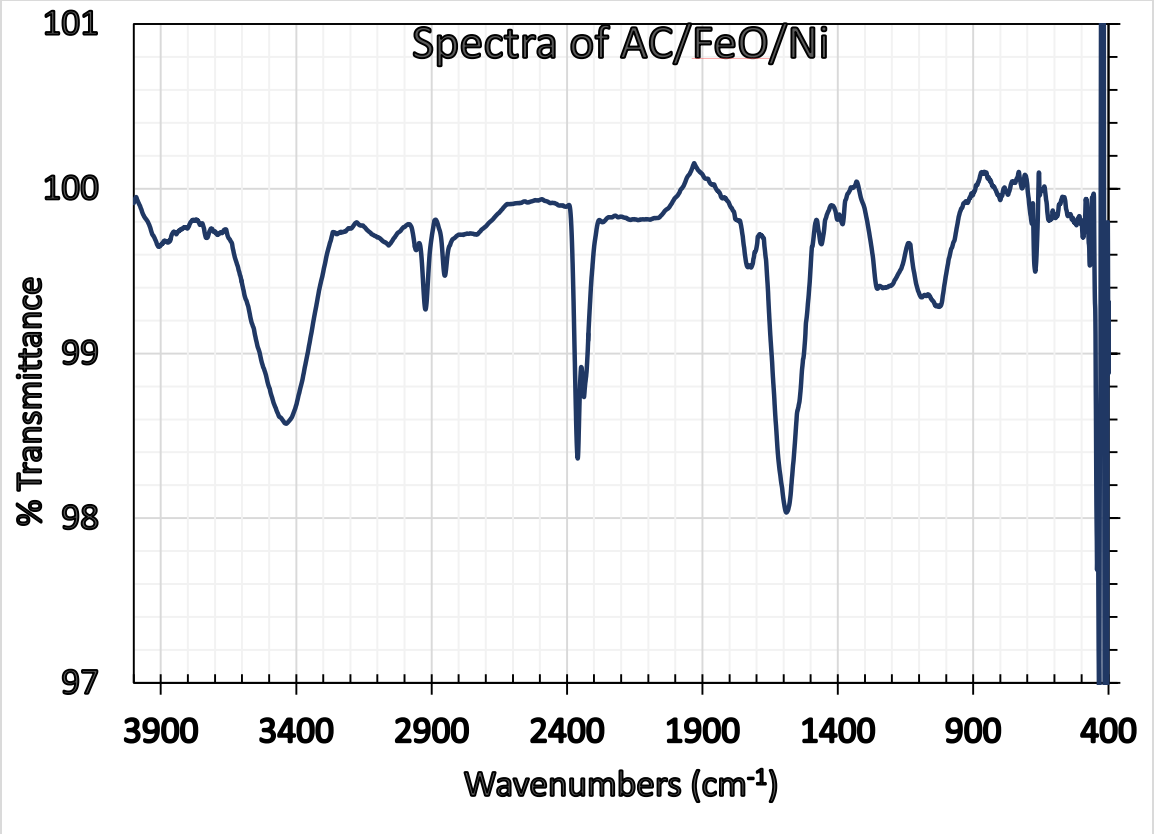

Figure 4.41*: The FTIR spectrum of AC/FeO/Ni*

4.11.6 Characterization of AC/CeO_2/Fe

The result of the elemental composition obtained from the SEM/EDS analysis of AC/CeO_2/Fe is shown in figure 4.42. The elements found on the surface of the adsorbent are represented by weight percent as carbon (81.23%), oxygen (15.49%) iron (2.41%) and cerium (0.87%) summing up to a total of 100%.

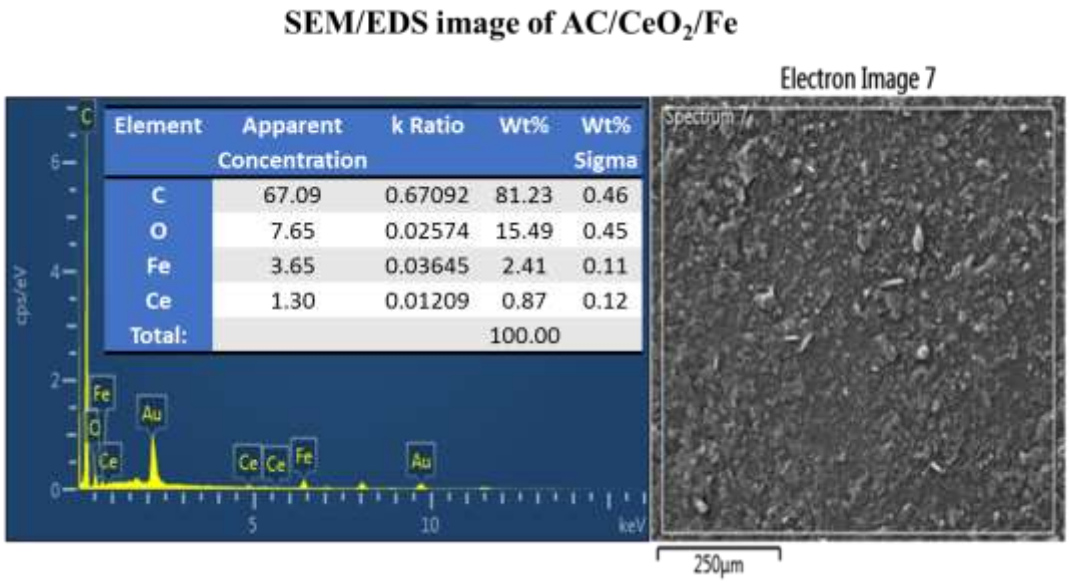

Figure 4.42*: SEM/EDS image of AC/CeO_2/Fe*

The XRD pattern of the synthesized adsorbent in shown in figure 4.43. The graphitic carbon peaks are seen at 2 theta 26° and 43°. Peak at 33° (200) denotes the presence of Ce-O particles. The pattern is in accordance with JCPDS No: 34-0394. (Girija *e*t *a*l., 2011; Renu *e*t *a*l., 2012). Peaks noticed at 2 theta values of 63° (440) and 50° signifies the presence of iron oxide (Mahadevan *e*t *a*l., 2012).

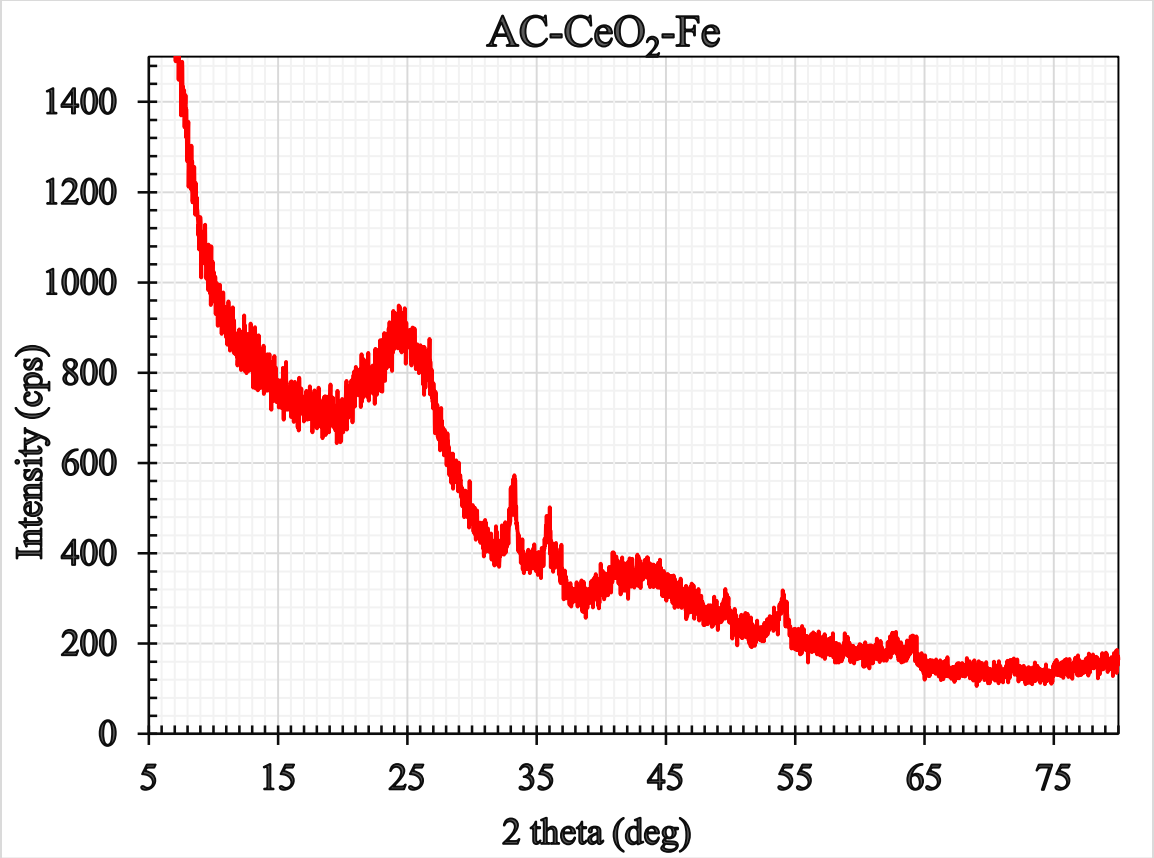

Figure 4.43*: XRD pattern of AC/CeO₂/Fe*

The FT-IR spectrum of AC/Ce is depicted in figure 4.44. Bands at 3400 cm^{-1} are assigned to OH stretching vibration. Bands at 2800 cm^{-1} and 2900 cm^{-1} denote the presence of C-H stretch of CH, CH_2 and CH_3. Band at 2100-2000 cm^{-1} is due to the presence of double bonded carbon oxygen groups and alkenes respectively (Estrella *et al*., 1996, Morlanes 2013). The bands at 1600 cm^{-1} and 1700 cm^{-1} are due to C=O stretching vibrations in ketones and carboxylic acids. The peak at 550.84 cm^{-1} is attributed to the presence of Ce-O within the sample (Ansari *et al*., 2009). The characteristic peak that appeared at 798 cm^{-1} can be attributed to the Fe-OH bending vibrations while the peak at 624 cm^{-1} appeared due to the Fe-O stretching vibrations within the sample (Marijan *et al*., 2007).

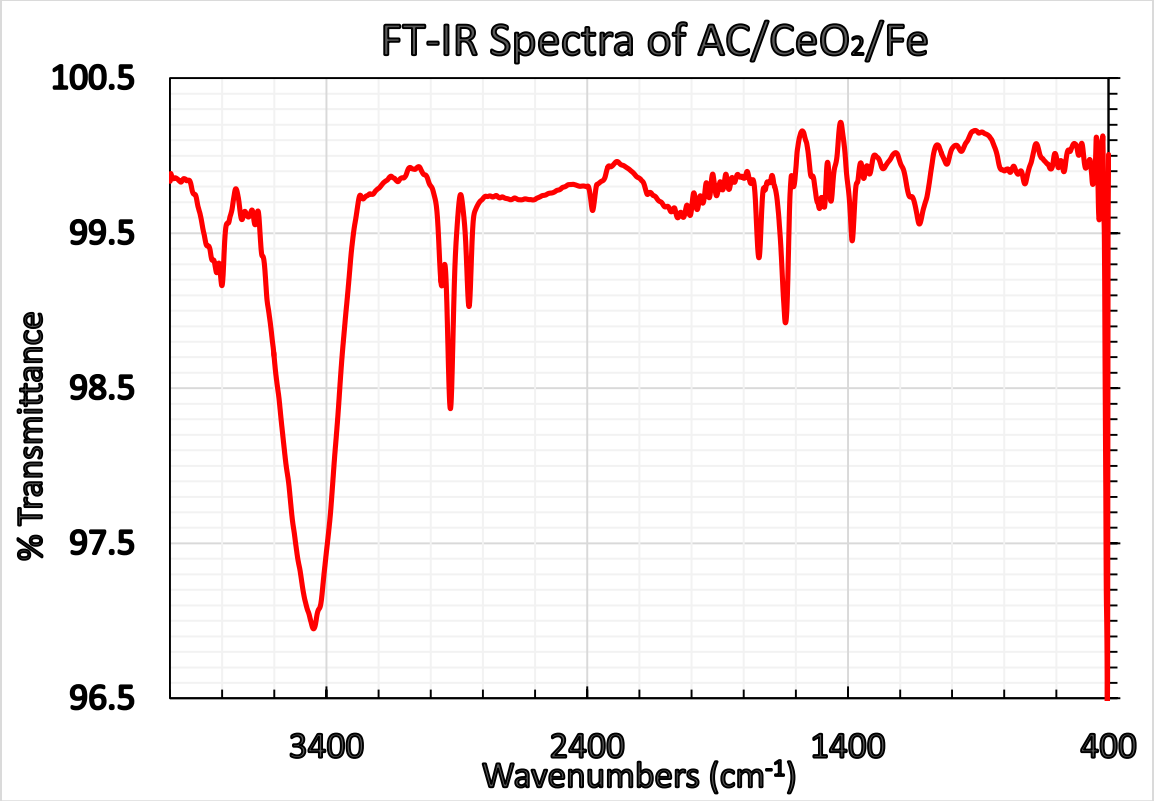

Figure 4.44: ***The FTIR spectrum of AC/CeO₂/Fe***

4.11.7 Surface area

Nitrogen adsorption desorption isotherm is a useful tool in the characterizing the surface of the materials. The nitrogen adsorption isotherms of the AC/Ni, AC/Ce, AC/Fe, AC/NiO/Ce, AC/FeO/Ni and AC/CeO_2/Fe are shown in figure 4.45 (a, b, c, d, e and f): respectively. All the samples can be seen to express Type I isotherm according to Brunauer *et al*., 1940 and Deng *et al*., 2009, however they express different degrees of surface areas, pore sizes and pore volumes. The range of the surface area is between (434.19 to 459.16 m^2/g). A hysteris loop can be observed in the samples at the relative high pressure indicating the presence of mesopores. In addition, all the samples showed uptake of nitrogen at relative pressures below 0.2 signifying the presence of micropores within the samples. The change in surface area caused by metal loadings is summarized in Table 4.9.

It can be clearly seen that AC-Ni sample has the highest surface area (459.96 m^2/g), pore volume (0.70 cm^3/g) and pore size (49.12 Å).

Table 4. 9: Surface area and pore volume analysis of metals loaded on AC

Adsorbents	BET Surface Area (m^2/g)	Pore volume (cm^3/g)	Pore size (Å)
AC-Ni	459.16	0.70	49.12
AC-Ce	451.08	0.66	59.83
AC-Fe	434.19	0.67	62.44
AC-NiO-Ce	440.66	0.69	63.39
AC-CeO2-Fe	436.44	0.64	59.61
AC-FeO-Ni	458.86	0.58	50.88

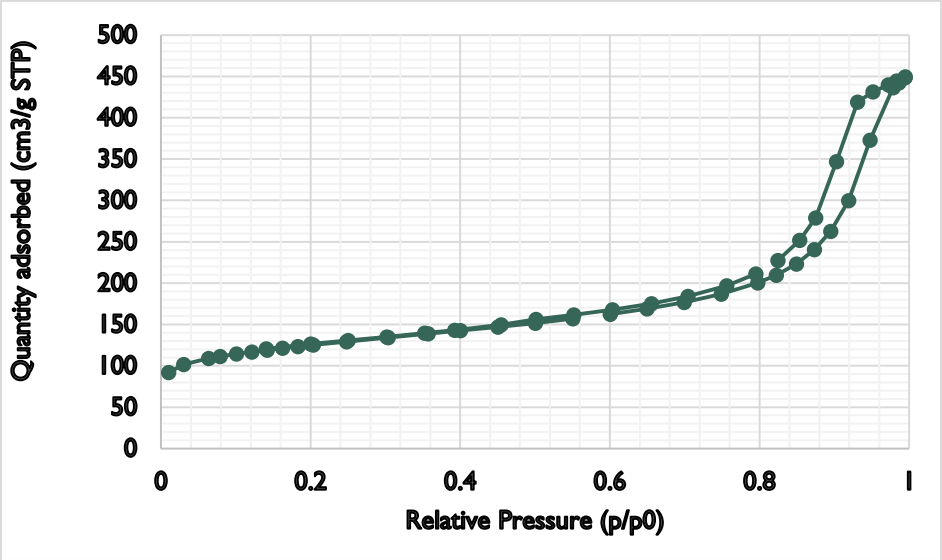

Figure 4.45 a*: Nitrogen adsorption/desorption isotherm for AC-Ni*

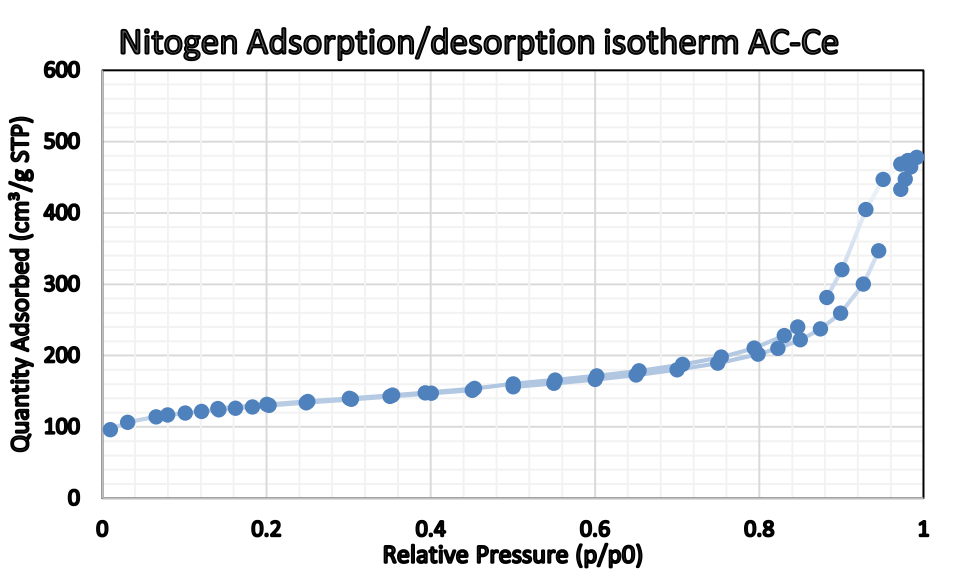

Figure 4.46 b: *Nitrogen adsorption/desorption isotherm for AC-Ce*

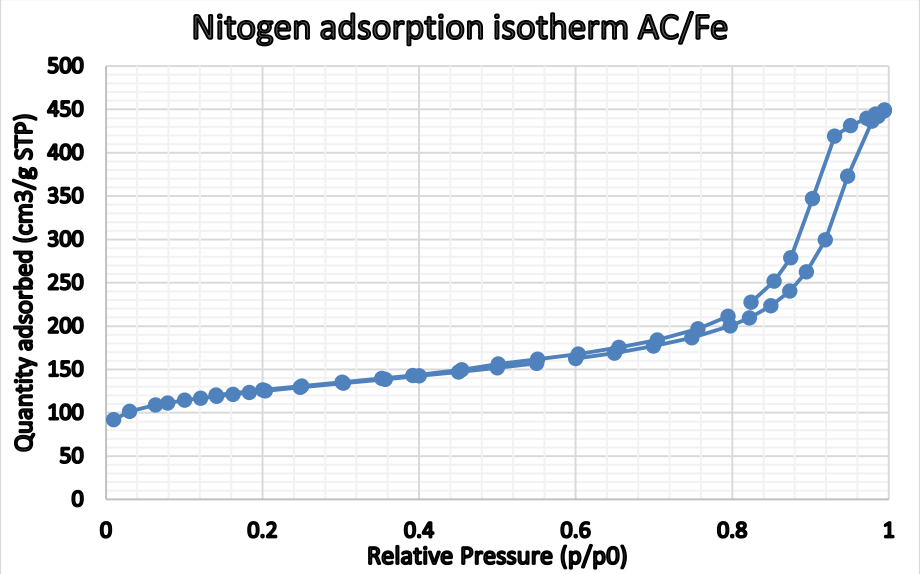

Figure 4.47 c*: Nitrogen adsorption/desorption isotherm for AC-Fe*

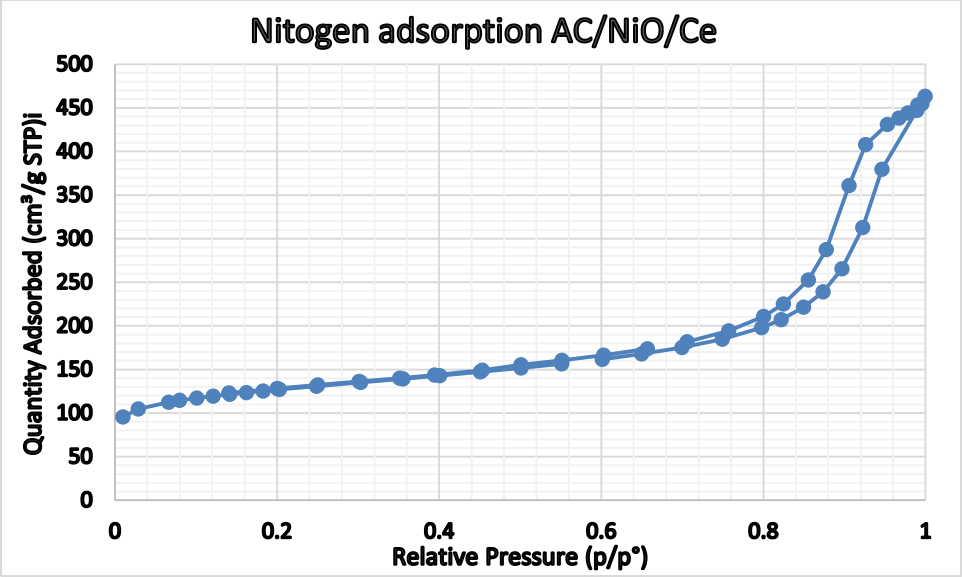

Figure 4.48 d: *Nitrogen adsorption/desorption isotherm for AC-NiO-Ce*

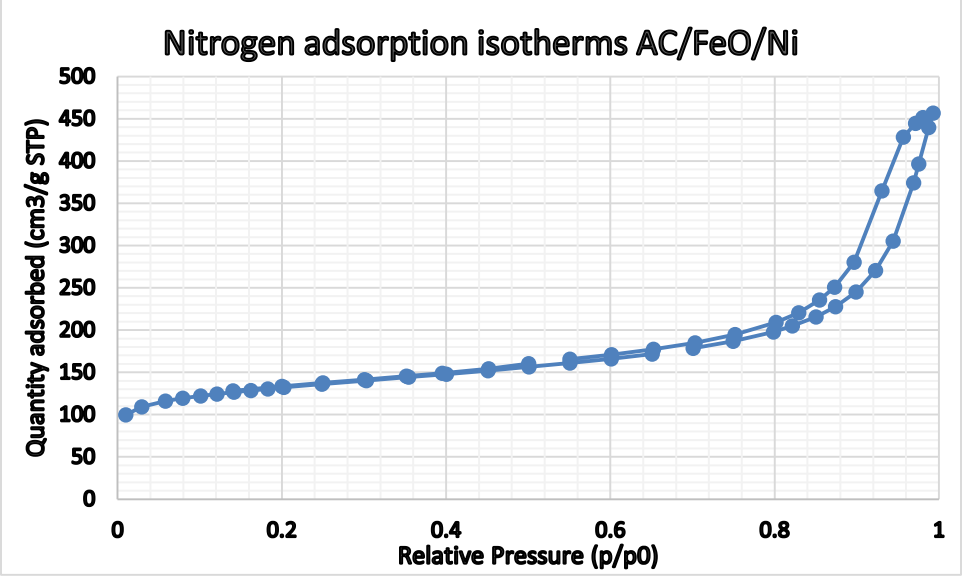

Figure 4.45 e: *Nitrogen adsorption/desorption isotherm for AC-FeO-Ni*

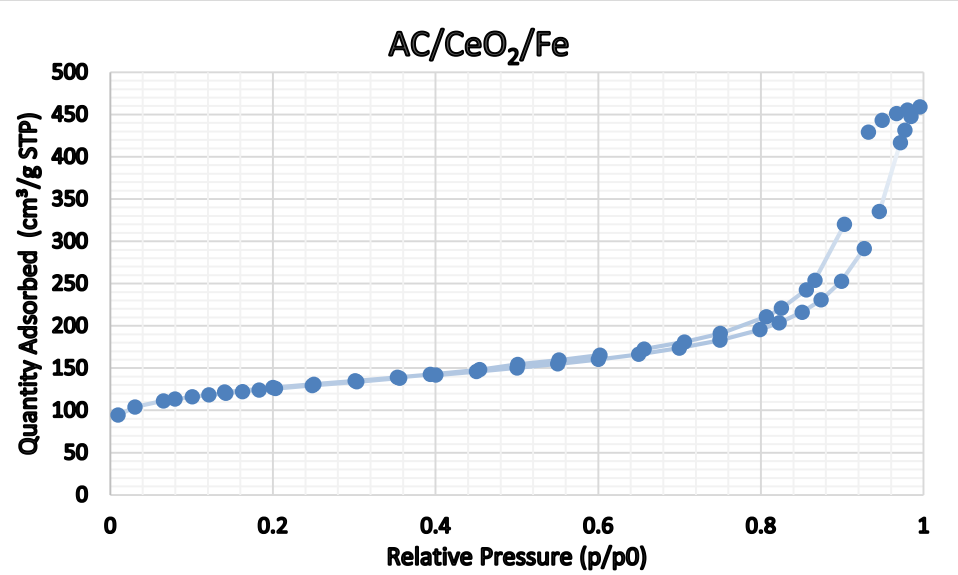

Figure 4.45 f*: Nitrogen adsorption/desorption isotherm for AC-CeO₂-Fe*

4.12 Adsorption evaluation of the loaded AC samples

AC/HNO_3/90°C loaded with nickel (AC-Ni), cerium (AC-Ce), iron (AC-Fe) and in combination of this metals (AC/NiO/Ce, AC/CeO_2/Fe and AC/FeO/Ni) were tested for their desulfurization efficiency. 0.5g of each sample was taken and added to 50ppm mixture of thiophene, BT and DBT each in 20 mL (85% hexane and 15% toluene). The set ups were stirred and samples were taken after 30 mins and analyzed with GC-SCD. The result is shown in figure 4.46 and the percentage removal of thiophene, BT and DBT from the metal loaded samples was reported. It can be clearly seen from the results that different metals have varying degrees of affinities to the refractory sulfur compounds, however each of the metal loaded adsorbent performed excellently well in DBT removal. The desulfurization efficiency followed the order DBT > BT > Thiophene. The performance of the adsorbents followed the order: AC/Ni > AC/CeO_2/Fe > AC/NiO/Ce > AC/Ce > AC/Fe > AC/FeO/Ni. Nickel loaded on AC showed the best performance and selectivity to the

refractory sulfur compounds and this is in accordance with the results obtained by Selvavathi *e*t *a*l., 2009 and Hernandez *e*t *a*l., 2010. Other reports believed that nickel serves as an active sites for the removal of thiophenic compounds (Moosavi *e*t *a*l., 2012; Xuan *e*t *a*l., 2013). Presence of oxygen containing functional groups, the surface area, pore volume and sulfur to metal interaction (S-M) plays an important role in the adsorption of thiophene and BT by AC/Ni and AC/CeO_2/Fe. Chemical interaction between metals and the sulfur compounds plays an important role in the selectivity and enhanced adsorption capacities of the adsorbents. All the adsorbents showed at least 65% percentage removal or greater for DBT and this is due to the size of the molecule and acidic functional groups on the surfaces of the larger pores which contributes to polar interactions (Kostas *e*t *a*l., 2014). Dispersive interactions between the delocalized π-electrons within the benzene rings of DBT and the electron rich region on the nanoporous carbon aromatic ring also plays a major role in the adsorption.

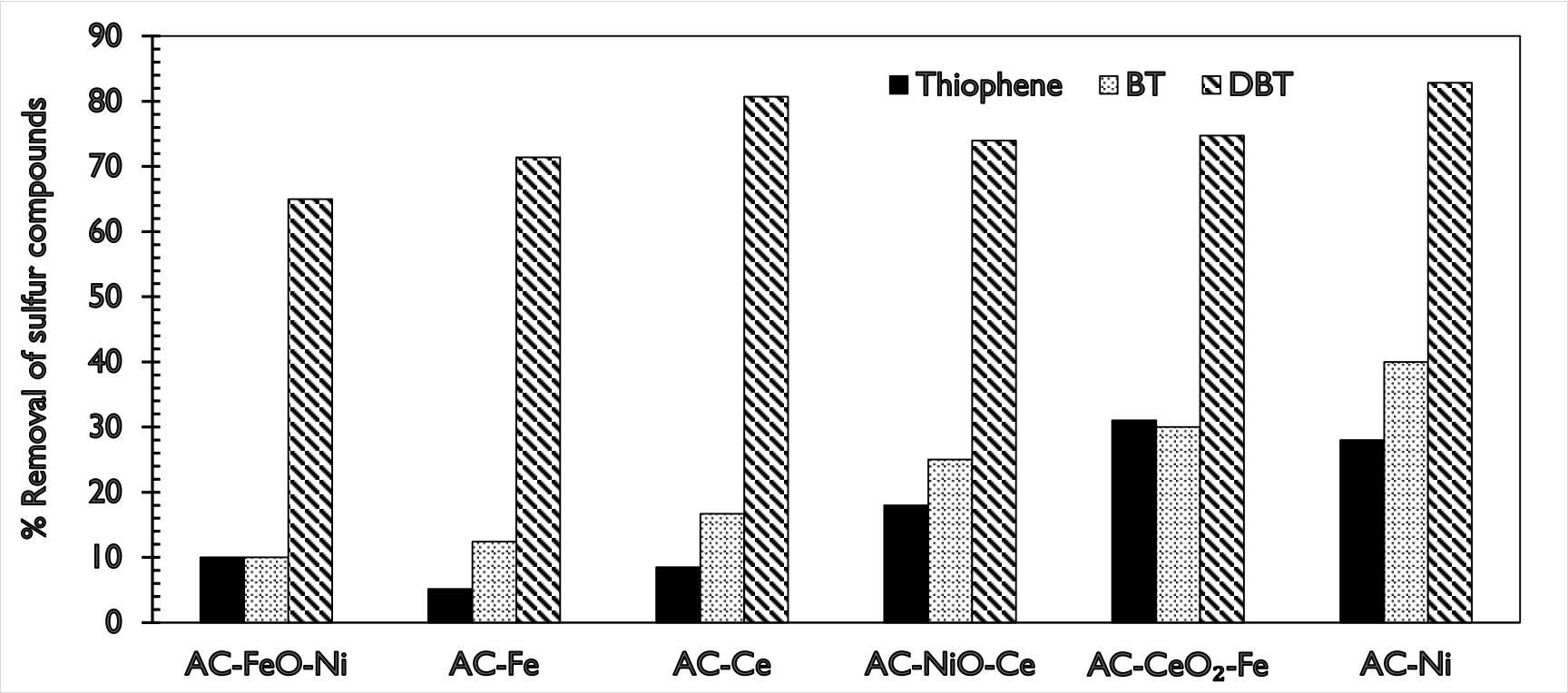

Figure 4.46*: Percentage removal of Thiophene, BT, and DBT (initial concentration of 50ppm each) on AC loaded with metal species after 30 mins (dosage of each sample was 0.5g in 20ml initial solution volume) @ 25°C*

One of the adsorbents AC/CeO_2/Fe was selected for SEM image to confirm the efficiency of the adsorption process. The result from the SEM//EDX analysis is given in figure 4.47 and the image confirms the presence of elemental sulfur after the adsorption process. The weight percent of the elements found on the surface of the adsorbent is as follows: Carbon (80.37), oxygen (15.85), sulfur (0.43), iron (2.44) and cerium (0.91)

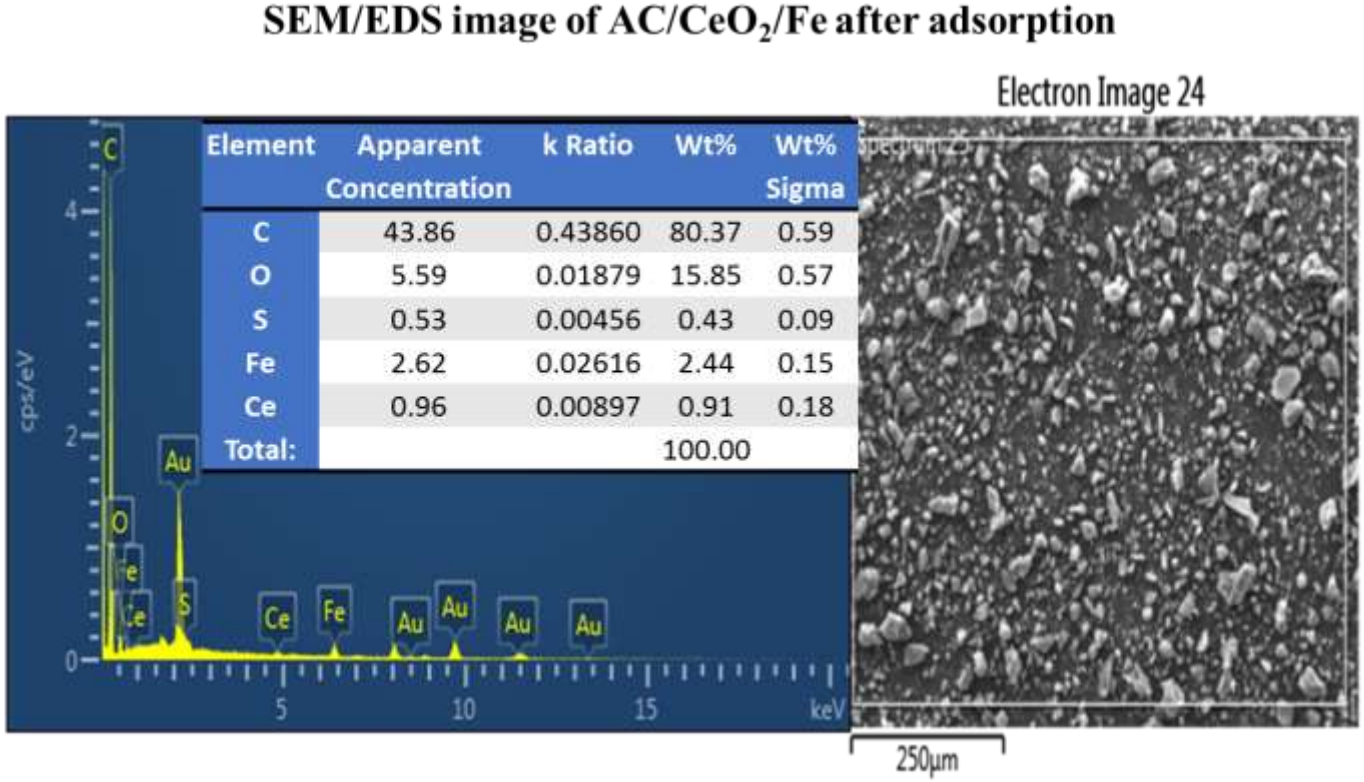

Figure 4.47: *SEM/EDX image of AC/CeO_2/Fe after adsorption of refractory sulfur compound*

4.13 Effect of metal ratio and calcination on the desulfurization performance of MnO/AC

It is known that dispersion of metals and metal oxides on adsorbents increases adsorption efficiency and most of the adsorbents adsorbs at ambient conditions and the desulfurization efficiency is dependent on the amount of metals and the type of sorbents used. (Shahadat *e*t *a*l., 2013). Varying the amount of nickel loading on alumina showed a dramatic change in the desulfurization (Sarda *e*t *a*l., 2012). The current study varied the loadings of MnO on AC from 0.5 to 30%. Each of the adsorbent was tested both before and after calcination at 350°C for 3 h. The result is shown in figure 4.48. It can be seen that calcination has a net negative effect on the desulfurization of the refractory sulfur compounds and this may be due to the effect of temperature on the destruction of the oxygen containing functional groups on the surface of the AC. In addition the AC used in this study had undergone pyrolysis, activation and treatment all at high temperatures which is why further calcination after loading with metals may have contributed to the reduced efficiency of the adsorbents. Increasing the metal loading on the surface of the AC can be seen to have an overall positive effect on the desulfurization efficiency. However, metal loading after 10% did not have any significant change to the desulfurization efficiency, and due to this outcome most of the experiments were set at 10% metal loadings. The order of metal loadings can be seen to follow: 0.5% < 5% < 10% < 30%.

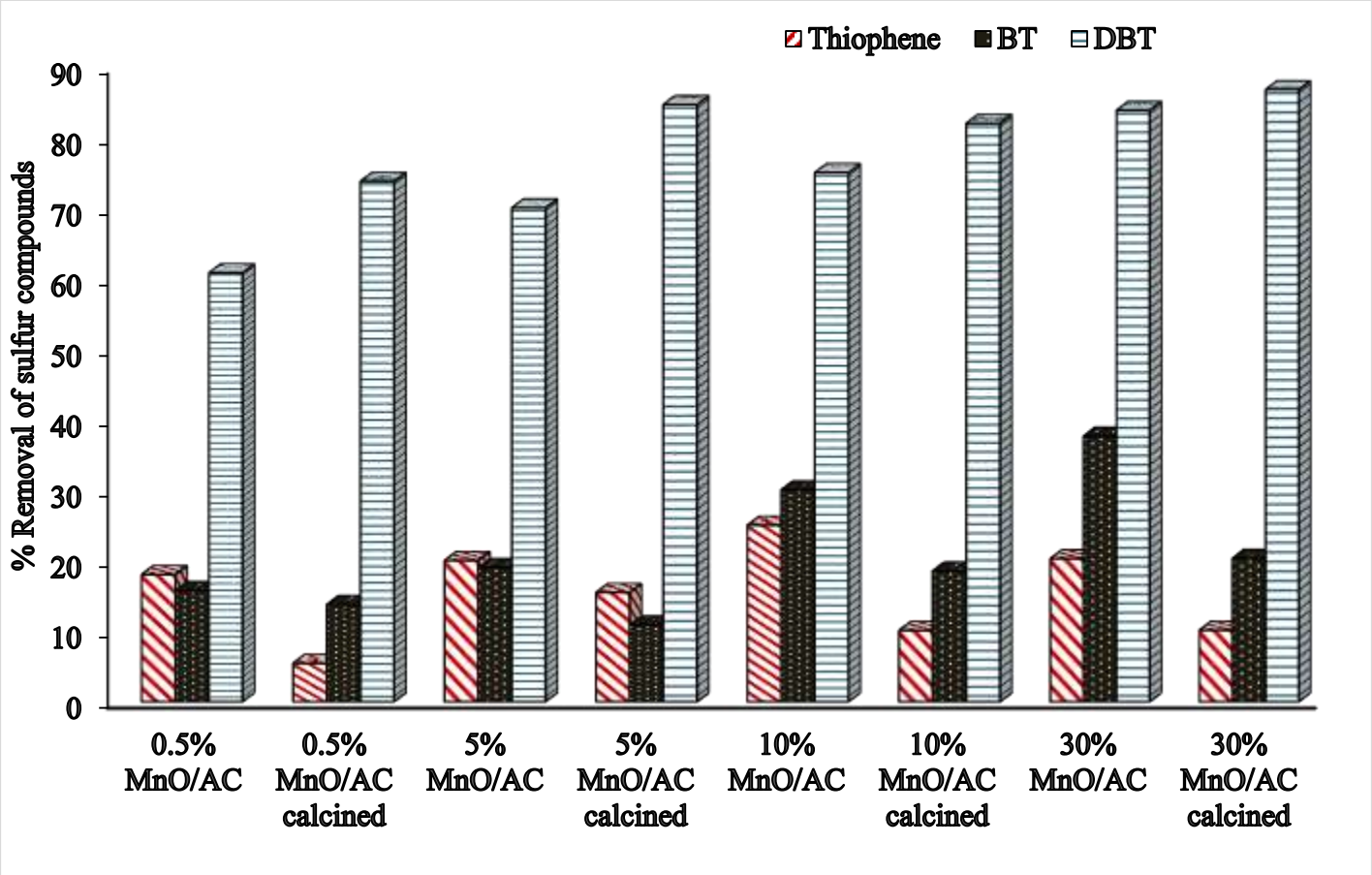

Figure 4.48: *effect of MnO loading on AC and calcination effect on the desulfurization of refractory sulfur compounds (concentration of thiophene, BT and DBT is 50ppm each) after 30 mins dosage of each sample was 0.5g in 20ml initial solution volume @ 25°C.*

4.14 Effect of adsorbent dosage

The efficiency of desulfurization depends upon the mass of the adsorbent present in the medium. From the results obtained, the best metal loading AC/Ni and the best metal combinations on AC i.e AC/CeO_2/Fe were selected and tested for the effect of adsorbent dosage and contact time. The amount of thiophene, BT and DBT adsorbed on the surface of AC/Ni and AC/CeO_2/Fe are depicted in figure 4.49 (a and b) respectively. It can be seen that with increment of adsorbent dosage from 0.1g to 0.5g the removal of thiophene, BT and DBT increases however the increment was not so significant. The initial increase in adsorption capacity with increment in adsorbent dosage is due to the available active sites and increase in surface area on the surface of the adsorbent for refractory sulfur compounds attachement. DBT exhibits higher percentage of removal for each dosage and on all adsorbents due to the ability of DBT to form π-π dispersive interactions between the aromatic ring in DBT and the surface of AC and also due to its large size compared to the other refractory sulfur compounds.

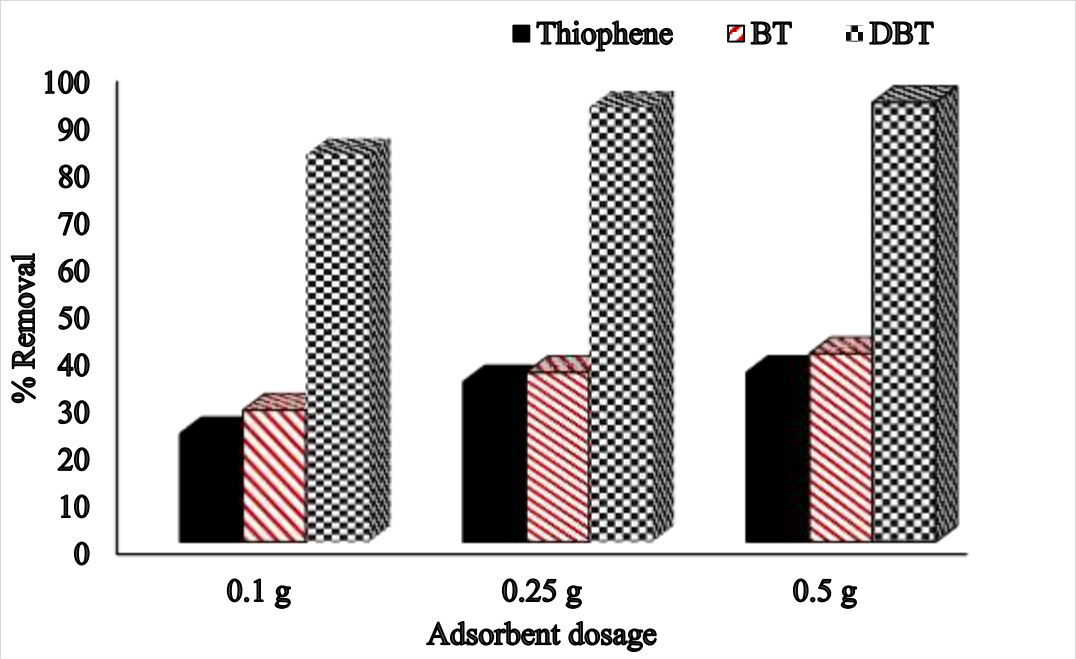

Figure 4.49 a: ***effect of*** **AC/Ni** ***concentration on the removal of sulfur compounds in batch mode***

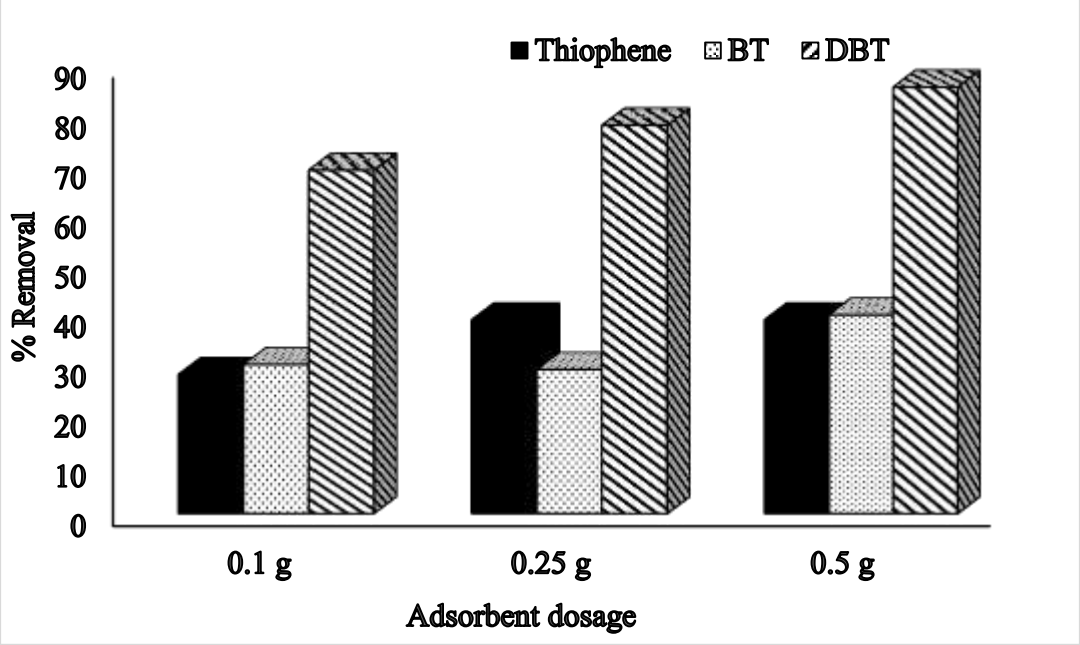

Figure 4.49 b***: effect of AC-CeO₂-Fe concentration on the removal of sulfur compounds in batch mode***

4.15 Effect of contact time on adsorption of sulfur compounds by AC/Ni and AC/CeO_2/Fe

The effect of contact time on the amount of sulfur compounds adsorbed by AC/Ni and AC/CeO_2/Fe is depicted in figure 4.50 respectively. The removal of refractory sulfur compounds in both adsorbents was found to be a rapid process reaching maximum value and equilibrium with increase in contact time at 10 mins for AC/Ni and 30 mins for AC/CeO_2/Fe. DBT showed the maximum adsorption capacity in both adsorbents followed by thiophene and BT. A large number of vacant surface sites are available for adsorption during the initial stage, and after a lapse of time, the remaining vacant surface sites are difficult to be occupied due to repulsive forces between the solute molecules on the solid and bulk phases. After sometime, the sulfur compounds molecules have to traverse further and deeper into the micro-pores encountering much larger resistance which results in the slowing down of the adsorption rate during later period.The adsorbents showed a slight decrease in adsorption after 60mins on all the sulfur compounds indicating the setting of a desorption process. The rate and quantity of sulfur adsorbed by the adsorbent is limited by the size of adsorbent molecules, concentration of adsorbate and its affinity towards the adsorbent, diffusion coefficient of the adsorbent in the bulk and solid phase and the degree of mixing. With increasing contact time, the number of available adsorption sites decreased as the number of sulfur ions adsorbed increased.

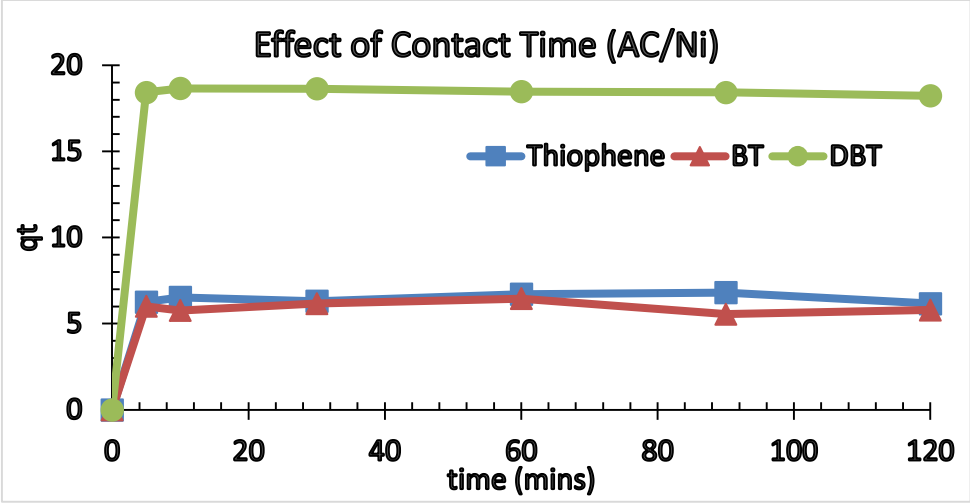

Figure 4.49 a*: effect of time on the adsorption of refractory sulfur compounds by AC/Ni in batch mode*

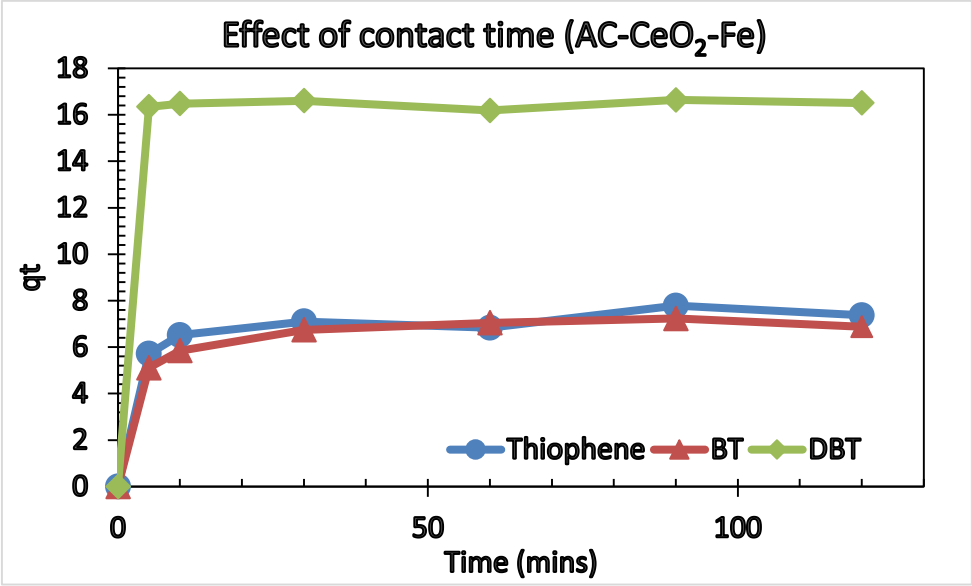

Figure 4.50b*: effect of time on the adsorption of refractory sulfur compounds by AC/CeO₂/Fe in batch mode*

4.16 Breakthrough curves of AC/Ni and AC/CeO_2/Fe

The effectiveness of AC/Ni and AC/CeO_2/Fe was further investigated in column mode (continous flow mode). The breakthrough curves were generated by plotting transient total sulfur concentration normalized by the feed total sulfur concentration (C_t/C_o) vs. cumulative time. The plots are given in figure 4.51 and 4.52 respectively. DBT showed a better performance in all the adsorbents. The brakthrough for DBT was reached after 180 mins and 60 mins using AC/Ni and AC/CeO_2/Fe respectively. However, the concentration of DBT did not return to the initial concentration even after 240 mins meaning that adsorption of DBT still continued through out the time used for the column studies. Breakthrough of BT was reached after 120 mins using AC/Ni but the concentration returned to the initial concentration after 240 mins of adsorption. The breakthrough for BT was reached after 30 mins using AC/CeO_2/Fe and it almost returned to the initial concentration after 60 mins of adsorption. The breakthrough for thiophene was around 30 mins and 5 mins in AC/Ni and AC/CeO_2/Fe. This means that the breakthroughs of the refractory sulfur compounds in all the metal loaded AC followed the order DBT > BT > thiophene.

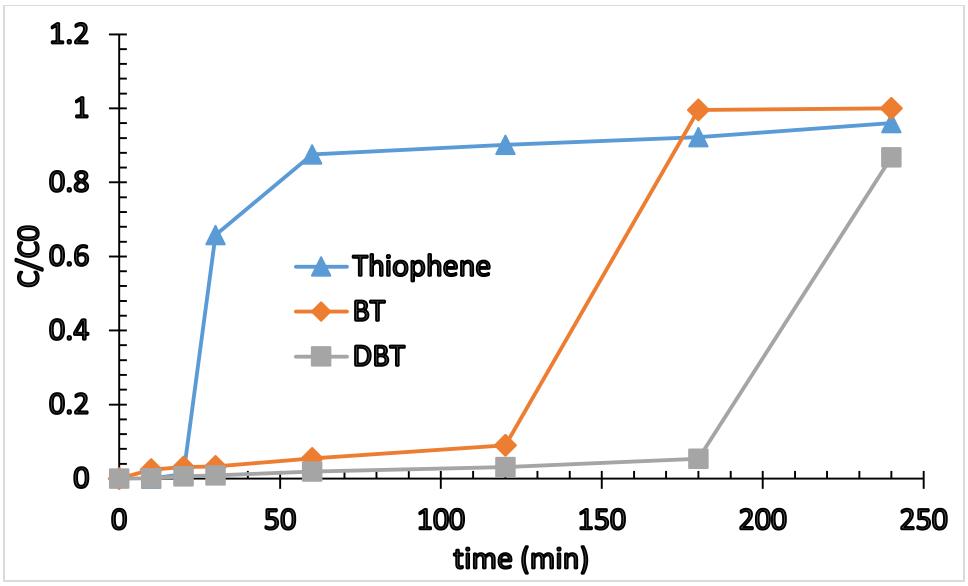

Figure 4.51*: Breakthrough curve for thiophene, BT and DBT using AC/Ni adsorbent (initial concentration of each compound was 50 ppm in 20 mL solution*

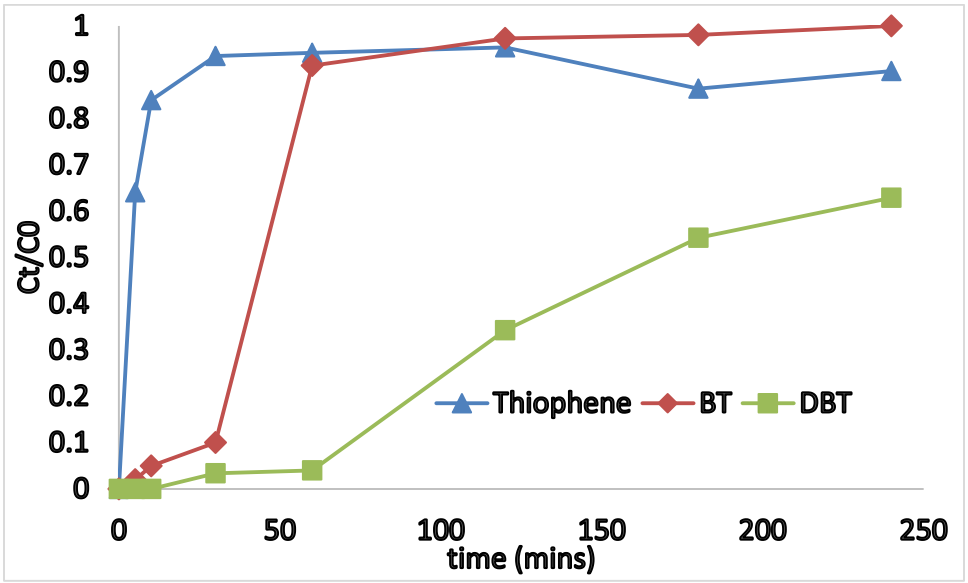

Figure 4.52: ***Breakthrough curve for thiophene, BT and DBT using AC/CeO_2/Fe adsorbent (initial concentration of thiophene, BT and DBT was 50 ppm each in 20mL solution.***

4.17 Adsorption Kinetics

In order to understand the adsorption process, the commonly used kinetic models including the pseudo-first order model, the pseudo-second order model, and the intraparticle diffusion model were examined to best describe the sulfur adsorption kinetics of AC/Ni and AC/CeO_2/Fe. Pseudo first order kinetic model was used to describe the initial stages of adsorption process where as pseudo second order models gives the description of the whole adsorption process and overall adsorption capacity (Anbia *e*t *a*l., 2011).

Pseudo-first-order equation was first given by Lagergren 1898. The equation is as follows:

$$\ln(q_e - q_t) = lnq_e - k_1 t$$

Where, qe (mg/g) and qt (mg/g) are the amounts of analyte adsorbed at equilibrium and time t (min), respectively; and k_1 (min^{-1}) is the rate constant of the Lagergren-first-order kinetics model. The k_1 and qe were calculated from the slope and intercept of the plot $\ln(q_e - q_t)$ versus t, respectively. Figures 4.53, 4.54 and table 4.10 outline the parameters of the first order kinetic parameters of AC/Ni and AC/CeO_2/Fe. The results were compared it with the second order model and the experimental q_e. It can be clearly seen that the correlation coefficients for the thiophene, BT and DBT in the first order kinetic model were lower than the second order model. In addition, the calculated q_e values are not in accordance with the experimental q_e. It can therefore be concluded that the adsorption process does not obey the pseudo first order kinetics.

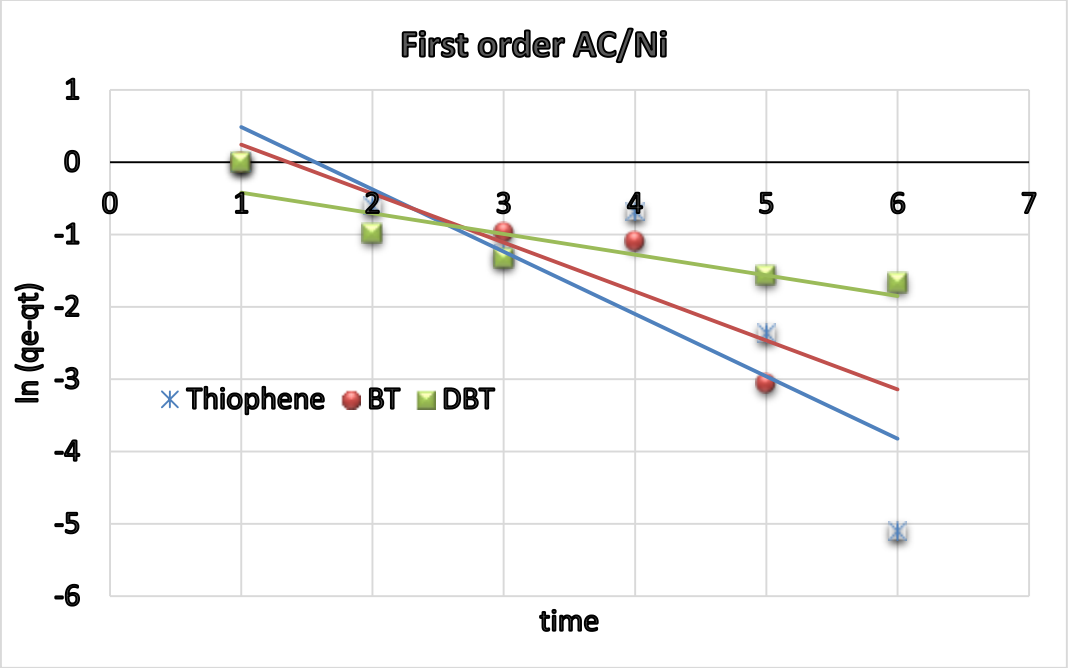

Figure 4.53: *First order pseudo kinetics for adsorption of thiophene, BT and DBT by AC/Ni*

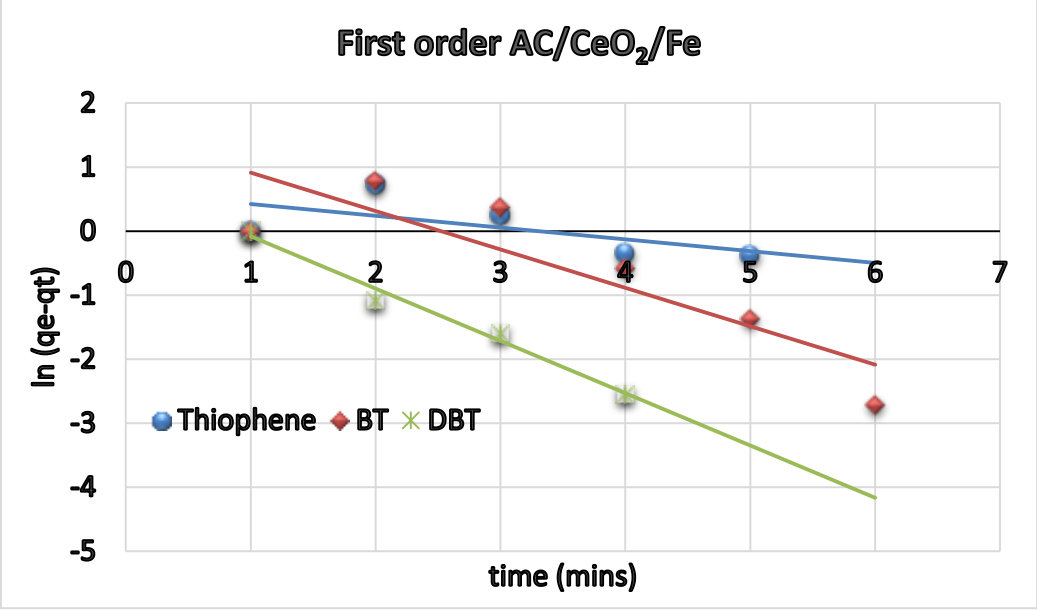

Figure 4.54: *First order pseudo kinetics for adsorption of thiophene, BT and DBT by AC/CeO_2/Fe*

Table 4.10: Pseudo first order, pseudo second order and intraparticle diffusion parameters for adsorption of thiophene, BT and DBT on AC-Nickel and AC/CeO2-Fe

			Pseudo first order			Pseudo second order			Intraparticle diffusion		
Adsorbent	Compound	Experimental q_e (mg/g)	K_1	Calculated q_e	R^2	K_2 (g/mg min)	Calculated q_e	R^2	$K_{i.d}$	C	R^2
AC-Nickel	Thiophene	6.8	0.048	1.13	0.8477	0.168	6.34	0.9948	0.0131	6.37	0.0305
	BT	6.45	0.0436	1.28	0.8767	0.124	5.711	0.9954	0.0379	6.26	0.1791
	DBT	18.51	0.0067	3.02	0.804	0.147	18.24	0.9999	0.03	18.67	0.4392
AC-CeO2-Fe	Thiophene	7.78	0.0353	2.48	0.922	0.061	7.58	0.9961	0.1948	5.5626	0.905
	BT	7.23	0.0389	2.26	0.9864	0.095	7.11	0.9984	0.2777	4.7965	0.9277
	DBT	16.63	0.0556	0.4	0.9748	0.394	16.52	0.9998	0.019	16.395	0.3935

The pseudo second order model is based on the assumption that the rate limiting step of a reaction may be chemisorption which involves valence forces by sharing or electron exchange between the adsorbent and the adsorbate (Wang *et al*., 2008). The pseudo second order kinetics can be expressed from the equation given by (McKay *et al*., 1999). The equation is given as:

$$\frac{t}{q_t} = \frac{1}{k_2 q_e^2} + \frac{t}{q_e}$$

Where q_t is the amount of adsorption thiophene, BT and DBT (mg/g) at time (min) and k_2 (g/ (mg min)) is the adsorption rate constant of pseudo-second-order adsorption. The slope and intercept of the linear plots of t/qt against t yield the values of 1/qe and $1/k_2 q_e^2$. The qe and k_2 can be obtained from the slope and intercept of figure 4.55 and 4.56 respectively for AC/Ni and AC/CeO_2/Fe. The values of the rate constants, maximum amount adsorbed and the correlation coefficients are given in table 4.10. It can be clearly seen that the R^2 and calculated q_e values of thiophene, BT and DBT agrees with the second order kinetic model.

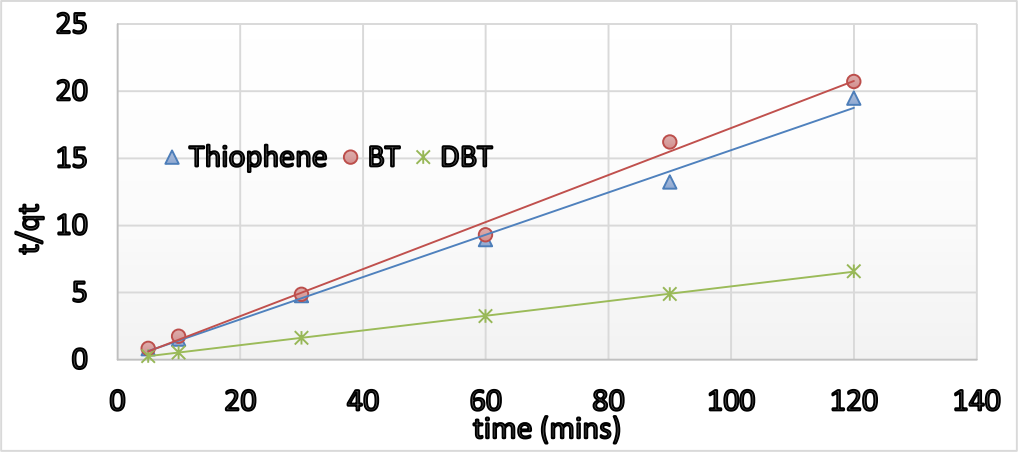

Figure 4.55*: second order pseudo kinetics for adsorption of thiophene, BT and DBT by AC/Ni*

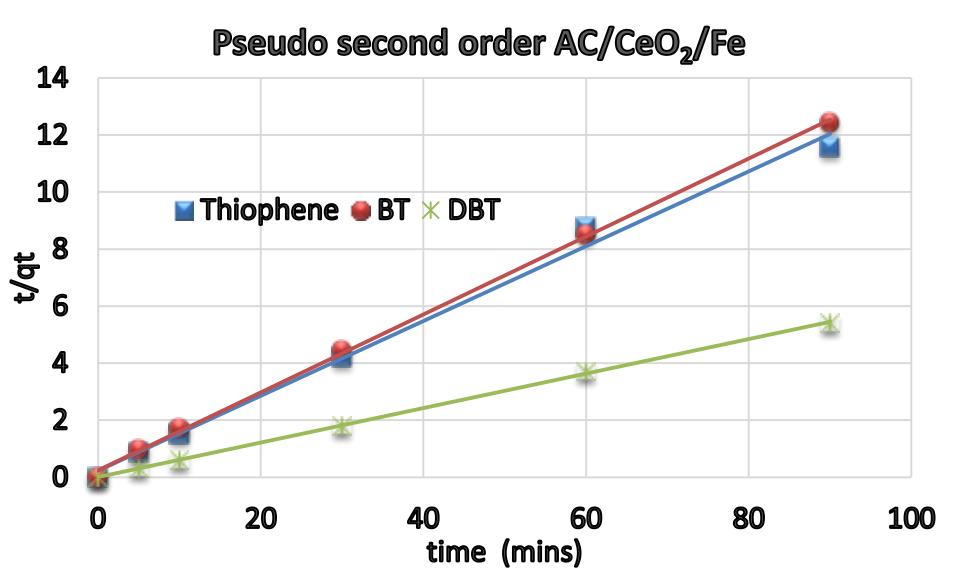

Figure 4.56*: second order pseudo kinetics for adsorption of thiophene, BT and DBT by AC/CeO₂/Fe*

The kinetic experimental results were also fitted to the Weber's intraparticle diffusion mechanism to gain insight understanding to the mechanisms and rate controlling steps affecting the adsorption kinetics (Weber *et al*., 1963). The kinetic results were analyzed by the intraparticle diffusion model to elucidate the diffusion mechanism. The following equation was applied:

$$q_t = k_{id} t^{1/2} + C$$

where C is the intercept (mg/g) which is related to the boundary layer thickness and k_{id} is the slope which represents the intraparticle diffusion rate constant (mg/g h1/2), which can be calculated from the slope of the linear plot of q_t versus $t^{1/2}$. The intraparticle diffusion plots of the adsorbents AC/Ni and AC/CeO_2/Fe are depicted in figure 4.57 and 4.58 respectively.

The results indicate that the adsorbents have higher adsorption efficiency toward DBT over the other two refractory sulfur compounds. This can be concluded from the intercept as

presented in (table 4.10). The correlation coefficient (R^2) and intercept of DBT are higher than that of thiophene and BT table (4.10) indicating greater contribution of the surface sorption is the rate controlling step in case of DBT adsorption. If the regression of qt versus $t^{1/2}$ is linear and passes through the origin, then intraparticle diffusion is the sole rate-limiting step. However, the linear plots at each dosage did not pass through the origin. This indicates that the intraparticle diffusion was not only rate controlling step (Hameed *et al*., 2008)

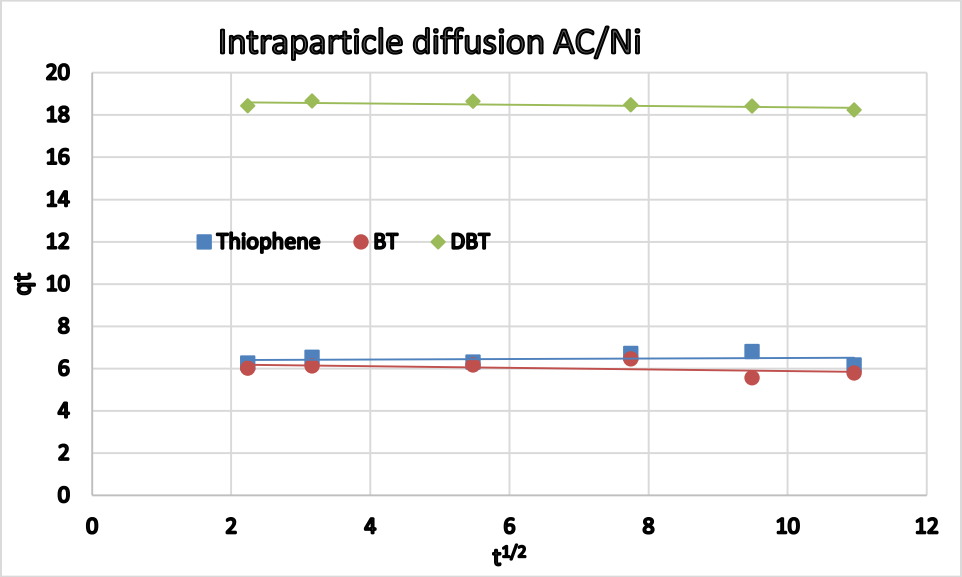

Figure 4.57*: Plots for evaluating intraparticle diffusion rate constant for sorption of Thiophene, BT and DBT onto AC/Ni*

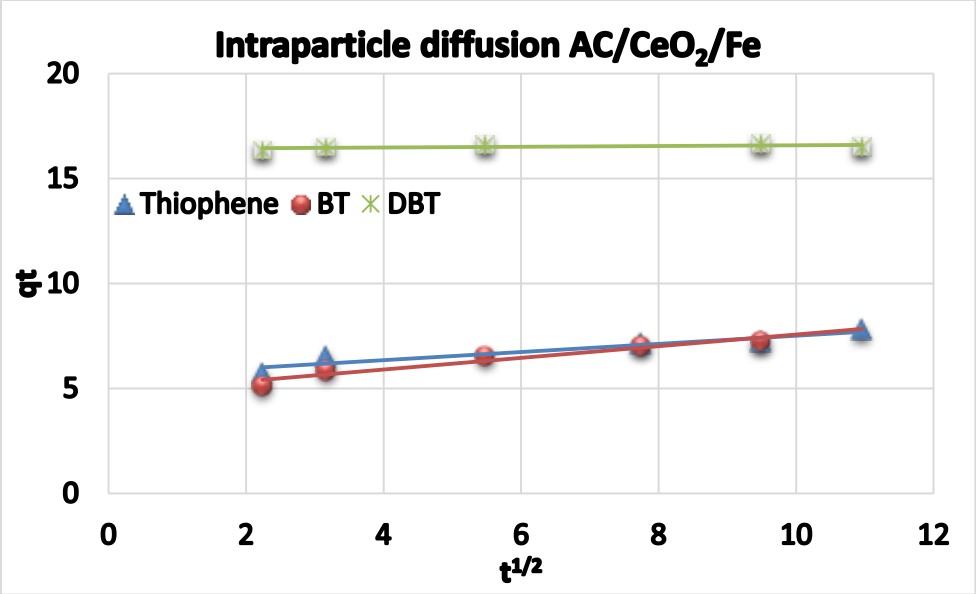

Figure 4.58: *Plots for evaluating intraparticle diffusion rate constant for sorption of Thiophene, BT and DBT onto AC/CeO_2/Fe*

4.18 Adsorption Isotherms

The purpose of adsorption isotherms is to relate the adsorbate concentration in the bulk and the adsorbed amount at the interface (Eastoe *e*t *a*l., 2000). Adsorption capacity is an important parameter in adsorption because it determines how much of an adsorbent is required for quantitative enrichment of adsorbates from given solutions. The adsorption of thiophene, BT and DBT in this study were analyzed by Langmuir and Freundlich isotherms.

4.18.1 Langmuir adsorption isotherm

The Langmuir adsorption model is based on the assumption that maximum adsorption corresponds to a saturated monolayer of solute molecules on the adsorbent surface, with no lateral interaction between the sorbed molecules.

The Langmuir equation that governs the adsorption of thiophene, BT and DBT is given as:

$$\frac{C_e}{q_e} = \frac{1}{K_L q_m} + \frac{C_e}{q_m}$$

Where q_e (mg g^{-1}) is the amount adsorbed at equilibrium concentration C_e (mg L^{-1}), q_m (mg g^{-1}) is the Langmuir constant representing maximum monolayer capacity and K_L is the Langmuir constant related to the energy of adsorption. The slope and intercept of linear plots of Ce/qe against Ce (Figures 4.59 and 4.60 respectively) yield the values of $1/q_m$ and $1/K_L q_m$

The adsorption capacity q_m for the refractory sulfur compounds on AC/Ni and AC/CeO_2/Fe followed the order thiophene < BT < DBT. The dimensionless constant separation factor R_L is considered an integral part of Langmuir isotherm. The equation is given below:

$$R_L = \frac{1}{1 + K_L C_0}$$

Where C_0 is the initial concentration of the analytes (mg/L), and K_L (L/mg) is Langmuir constant. The shape of the isotherm can better be represented by R_L value where $R_L > 1$ indicates an unfavorable process, $R_L = 1$ indicates linearity and $R_L < 1$ but > 0 indicates a favorable process. The results obtained from table 4.11 show that the adsorption of DBT on the adsorbent is a favorable process.

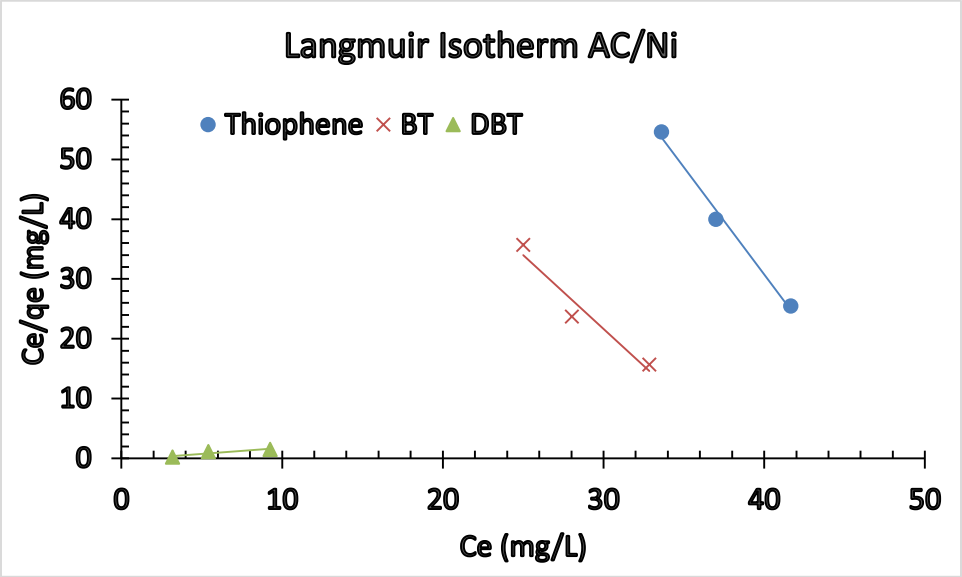

Figure 4.59: *plot of Langmuir isotherm for adsorption of thiophene, BT and DBT by AC/Ni*

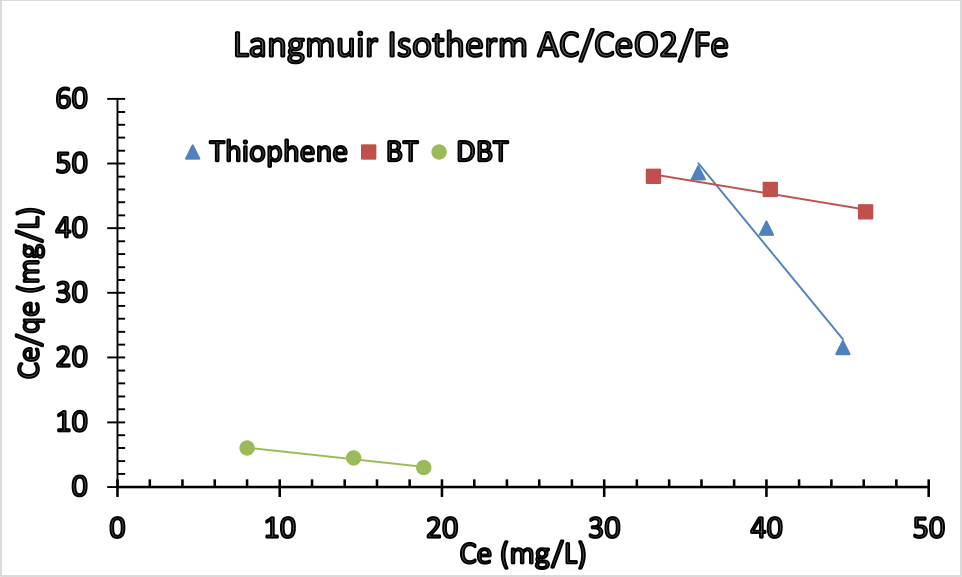

Figure 4.60: *plot of Langmuir isotherm for adsorption of thiophene, BT and DBT by AC/CeO_2/Fe*

Table 4.11: Langmuir and Freundlich Isotherms constant for AC/Ni and AC/CeO2/Fe

Adsorbents	Compounds	Langmuir Isotherm constant				Freundlich Isotherm constant			
		q_m (mg/g)	K_L (L/mg)	R^2	R_L	K_f	1/n	n	R^2
AC-Nickel	Thiophene	0.27816412	0.020597	0.917	0.4891	6.58E-08	4.5679	0.218919	0.9997
	BT	0.40650407	0.0257317	0.9414	0.4664	1.97E-06	3.982	0.25113	0.9954
	DBT	4.95049505	0.7534502	0.8707	0.0235	0.38736	1.3819	0.723641	0.998
AC-CeO2-Fe	Thiophene	0.32894737	0.0191111	0.969	0.483	6.35E-08	4.5446	0.220041	0.9993
	BT	2.47524752	0.0065121	0.9581	0.747	2.33E-05	2.9433	0.339755	1
	DBT	3.7037037	0.0326932	0.9851	0.3659	0.065599	1.5585	0.641643	0.9987

4.18.2 Freundlich adsorption isotherm

Freundlich isotherm is an empirical equation employed to describe heterogeneous systems or multilayer sorption (Freundlich *e*t *a*l., 1906). The Freundlich isotherm can be expressed in the following equation:

$$q_e = K_F C_e^{1/n} \rightarrow \ln q_e = \ln K_F + \frac{1}{n} lnC_e$$

Where q_e (mg.g-1) is amount of absorbed material in absorbent surface, K_F and n are Freundlich constants with K_F (mg/g) is the adsorption capacity of the sorbent and n giving an indication of how favorable the adsorption process. The magnitude of the exponent, 1/n (g/L), gives an indication of the favorability of adsorption. Values of n > 1 represent favorable adsorption condition (Poots *e*t *a*l., 1978). To determine the constants K_F and n, the linear form of the equation may be used to produce a graph of ln(q_e) against ln(C_e) Figures 4.61 a and 4.62 respectively. Values of K_F and n are calculated from the intercept and slope of the plot.

Results in (table 4.11) showed the values of n are more than one which means that it is a favorable adsorption process. As it is shown in (table 4.11), the adsorption capacity of the metal loaded adsorbent toward DBT is higher than that toward BT and thiophene. The comparison of the R^2 values from (table 4.11) indicates that Freundlich isotherm model yields a better fit to the experimental data than Langmuir isotherm.

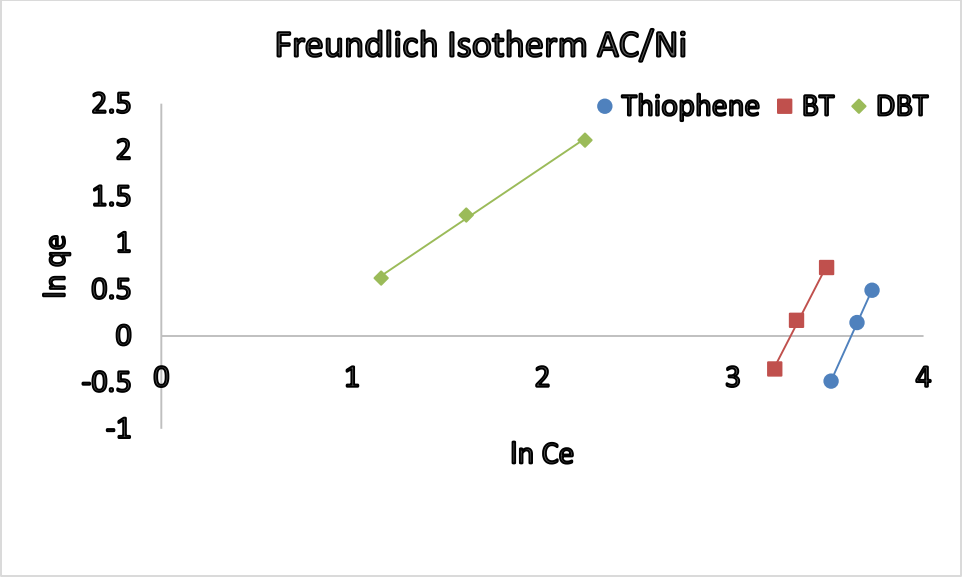

Figure 4.61: *plot of Freundlich isotherm for adsorption of thiophene, BT and DBT by AC/Ni*

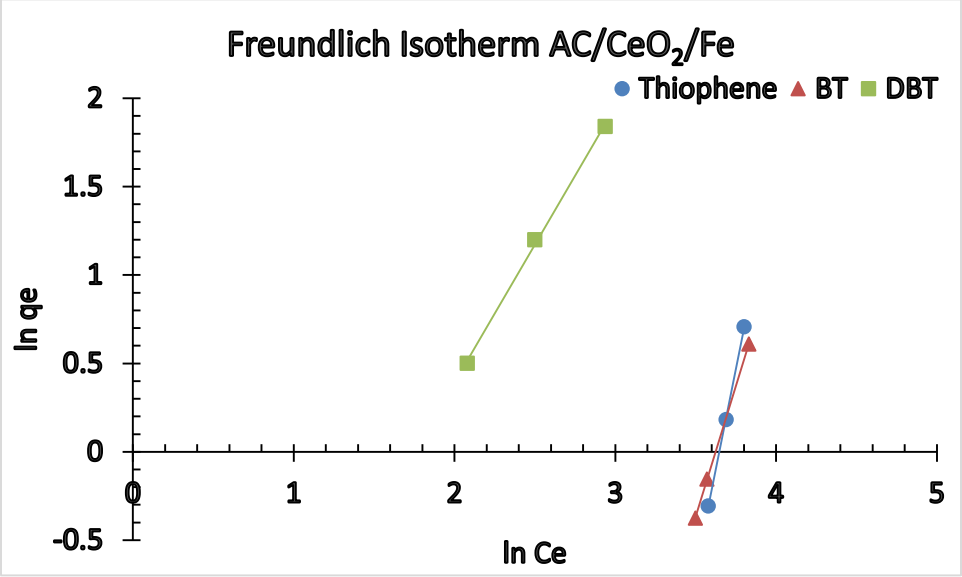

Figure 4.62: *plot of Freundlich isotherm for adsorption of thiophene, BT and DBT by AC/CeO_2/Fe*

4.19 Regeneration of AC/Ni and AC/CeO_2/Fe

The major concern about the use of adsorbent in ADS is the regeneration and disposal of the adsorbent. The regeneration methods to restore carbon adsorptive capacity of thiophenes are thermal, solvent and ultrasound approaches. Thermal regeneration method was employed in this work despite having some drawbacks of distorting the integrity of micropores and important surface functional groups to examine the level of damage temperature may have on the synthesized adsorbents and the level of efficiency the adsorbents may show. The regeneration was done by heating the adsorbent in air for 3 h at 350°C. The temperature which is believe to be the optimum for vaporizing all the sulfur compounds from the adsorbent (boiling point of thiophene, BT and DBT is 84°C, 221°C and 333°C respectively). The results are shown in figures (4.63 and 4.64 respectively). The percentage removal of the sulfur compounds showed continued decrease in the adsorptive capacity of the adsorbents however they still showed great promise in the removal DBT even after three cycles of regeneration. The order of desulfurization after three cycles of regeneration followed the sequence: DBT (47%) > BT (12.19%) > T (10%) in AC/Ni and DBT (47%) > T (13%) > BT (12%) in AC/CeO_2/Fe.

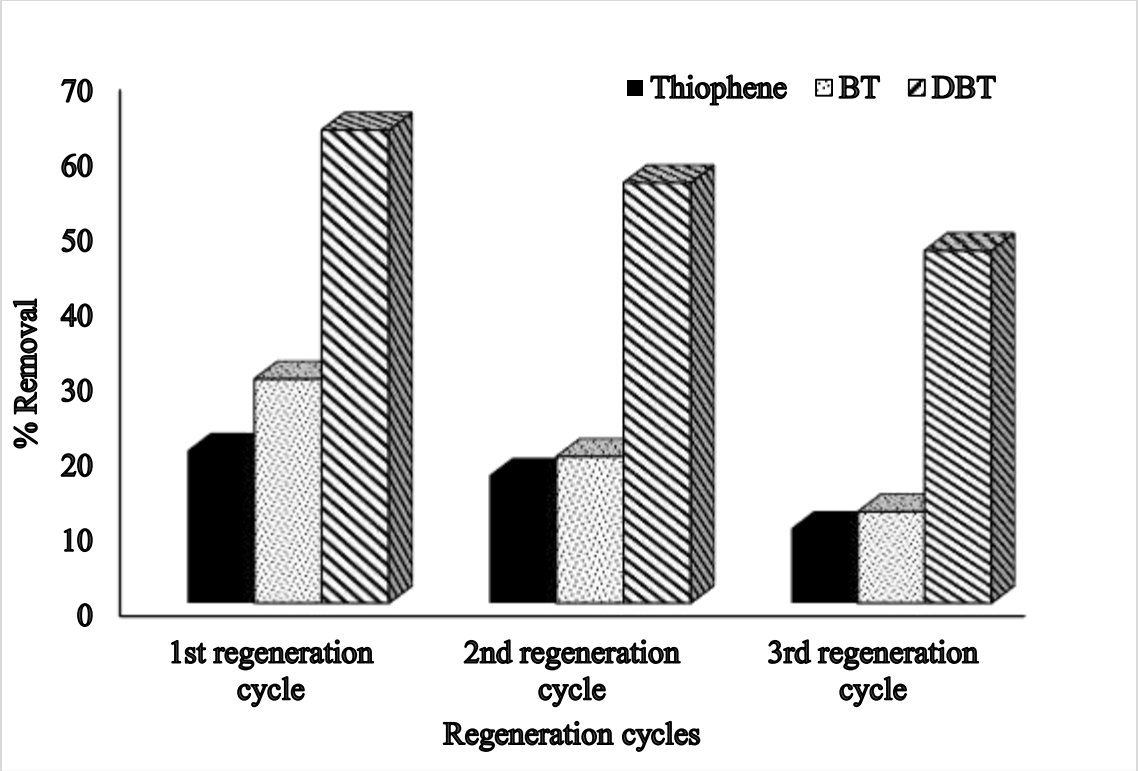

Figure 4.63*: Efficiency of AC/Ni after three regeneration cycles*

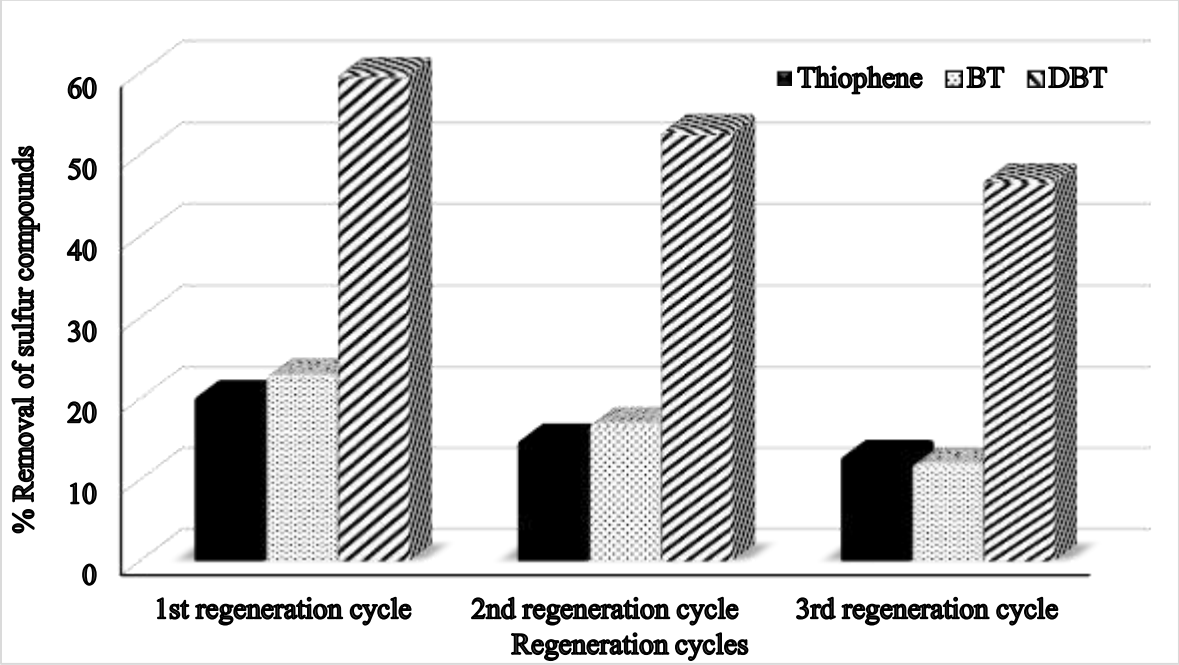

Figure 4.64*: Efficiency of AC/CeO_2/Fe after three regeneration cycles*

AC/CeO_2/Fe was selected for SEM image to confirm the efficiency of the regeneration process. The result from the SEM//EDX analysis is given in figure 4.65 and the image confirms the absence of elemental sulfur after the adsorption process. However, the % weight of the metals in the adsorbent increased showing the occurrence of calcination in the adsorbent. The weight percent of the elements found on the surface of the adsorbent is as follows: Carbon (54.89), oxygen (25.35), iron (13.87) and cerium (5.89).

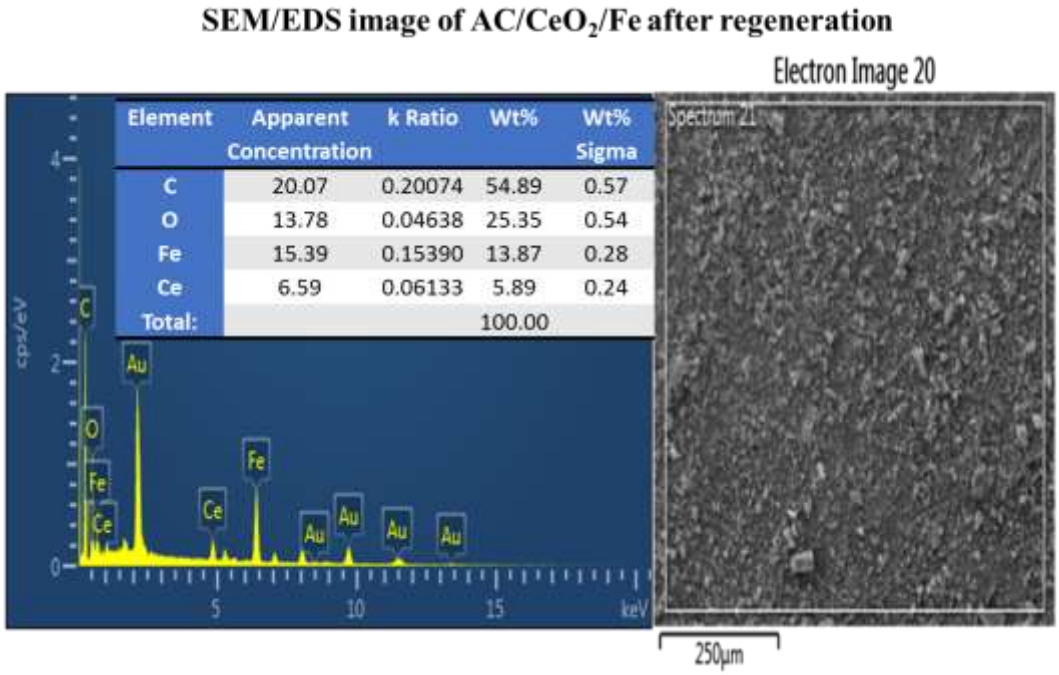

Figure 4.65*: SEM/EDX image of AC/CeO_2/Fe after regeneration*

CHAPTER FIVE

CONCLUSION AND RECOMMENDTION

This chapter summarizes the important findings encountered from this work and the major conclusions are also outlined. Recommendations for future research work to be conducted are also elucidated.

5.1 Conclusions

This thesis utilized WRTs for the synthesis of AC. Pyrolysis of the WRTs was conducted at different temperatures (250 to 550℃) and varying time conditions (0.5 to 5 h) to isolate carbon black from gasses and liquid fuels. The optimum pyrolysis temperature was found to be 500℃ for 5 h. Activation of the synthesized AC was also carried out at various temperatures (500 to 900℃) and 900℃ for 5 h was found to be the optimum. The AC produced was treated with NaOH and HNO_3 at various temperatures ranging from 30 to 90℃ for the enhancement of surface area and porosity. It was realized that AC treated with HNO_3 at 90℃ was the best in terms of surface area and surface acidic functional groups that are responsible for adsorption of so many compounds. The AC was characterize using Bohm's titration experiment, determination of surface pH, BET surface area, XRD, FTIR and SEM/EDX. Model fuel sample containing the refractory sulfur compounds T, BT and DBT was prepared. The adsorptive ability of the synthesized carbon was tested in both batch and fixed bed modes. The adsorbent performs extremely well in the removal of the larger sulfur molecule (DBT) in all the experiment conducted due to the presence of chemical interaction between the pi electrons of the refractory sulfur compound and the

synthesized AC. The adsorbent was also tested for its thermal regeneration ability and it showed great promise.

Nickel, cerium and iron were loaded on the AC alone or in combination. The synthesized materials were characterized by FTIR, SEM/EDX, XRD and BET surface area. The adsorbents were tested for their sorption abilities and AC/Nickel with AC/CeO_2/Fe showed great promise in the adsorption of refractory sulfur compounds, this is evident as most researchers reported the selectivity of nickel, cerium and iron to refractory sulfur compounds. This means that chemical interaction between the metals, the adsorbent and the sulfur plays a cardinal role in the adsorption process. Loading of metals on the synthesized AC improved the adsorption of the other refractory sulfur compounds (T and BT). The kinetics results indicates that the adsorption followed a second order reaction while the experimental results best fit Freundlich isotherm. Regeneration of the nanocomposite AC also showed a great promise.

5.2 Recommendations

The present research demonstrates the feasibility of using WRTs to synthesize AC for ADS. Future research work should focus on the treatment methods of enhancing the surface area and surface acidic functional groups on the surface of the adsorbent. Loading of metals on the adsorbent increased its adsorptive potential in view of this other metals and metal oxides such as cobalt, copper, and zinc, can be loaded and tested as well. The adsorbent should be tested on real crude oil samples to understand its suitability to replace the commercial AC that is widely used for adsorptive studies. Furthermore, the adsorbent can be tested on other pollutants since environmental pollutants are numerous.

References

Abdulaziz A. Al-Saadi, Tawfik A. Saleha, Vinod Kumar Gupta "Spectroscopic and computational evaluation of cadmium adsorption using activated carbon produced from rubber tires" Journal of Molecular Liquids 188 (2013) 136–142

Ali Mansouri, Abbas Ali Khodadadi, Yadollah Mortazavi "Ultra-deep adsorptive desulfurization of a model diesel fuel on regenerable Ni–Cu/-Al2O3 at low temperatures in absence of hydrogen" Journal of Hazardous Materials 271 (2014) 120–130

Alicia M. Oickle, Sarah L. Goertzen, Katelyn R. Hopper, Yasmin O. Abdalla, Heather A. Andreas "Standardization of the Boehm titration: Part II. Method of agitation, effect of filtering and dilute titrant" carbon 48 (2010) 3313 –3322

Anbia M., Z. Parvin, "Desulfurization of fuels by means of a nanoporous carbon adsorbent", chemical engineering research and design, 89, 641-647, 2011

Ankur Srivastav, Vinal Chandra Srivastava "Adsorptive desulfurization by activated alumina" Journal of Haz. Materials 170 (2009) 1133-1140.

Ansari, A.A., P.R. Solanki and B.D. Malhotra, 2009. Hydrogen peroxide sensor based on horse radish peroxidase immobilized nanostructured cerium oxide film. J. Biotechnol., 142: 179-184.

Antoniou N., G.Stavropoulos, A.Zabaniotou, "Activation of end of life tyres pyrolytic char for enhancing viability of pyrolysis – Critical review, analysis and recommendations for a hybrid dual system" Renewable and Sustainable Energy Reviews 39 (2014) 1053–1073

Aranda A, MurilloR, GarcíaT, MastralAM. "Simulation and optimization of tyre-based steam activated carbons production for gas-phase polycyclic aromatic hydrocarbons abatement. ChemEngJ2012; 187:123–32.

Ariyadejwanich P, Tanthapanichakoon W, Nakagawa K , Mukai S R, Tamon H. "Preparation and characterization of mesoporous activated carbon from waste tires". Carbon 2003; 41:157–64

Arturo J. Herna´ndez-Maldonado and Ralph T. Yang: "New Sorbents for Desulfurization of Diesel Fuels via π-Complexation" AIChE Journal 2004 Vol. 50, No. 4

Asadullah M, Anisur Rahman M, Abdul Motin M and Borhanus Sultan M (2007), "Adsorption studies on activated carbon derived from steam activation of jute stick char", J Surf Sci Technol., Vol. 23, No. 1-2, pp. 73-80

Babich I. V., J. A. Moulijin "Science and technology of novel processes for deep desulfurization of oil refinery streams: A review" Fuel 82 (2003) 607-631

Bej Shyamal K "Revamping of diesel hydro-desulfurizers: Options available and future research needs" Fuel Process. Technol Vol (85), Is (13), (2004), pp1503–1517.

Ben Li, Wanpeng Liu, Hong Wu, Shengnan Yu, Ruijian Cao, Zhongyi Jiang "Desulfurization of model gasoline by bioinspired oleophilic nanocomposite membranes" Journal of Membrane Science 415–416 (2012) 278–287

Beom K. Jung, Sung Hwa Jhung "Adsorptive removal of benzothiophene from model fuel, using modified activated carbons, in presence of diethylether" Fuel 145 (2015) 249–255

Bezeverkhyy I, Ryzhikov A, Gadacz G and Bellat J P, "Kinetics of thiophene reactive adsorption on Ni/SiO2 and Ni/ZnO", Catalysis Today130 (2008) 199–205

Billy T H Guan, Puziah Abdul Latif and Taufiq Y H Yap, "Physical preparation of activated carbon from sugarcane bagasse and corn Husk and its physical and chemical Characteristics Int. J. Engg. Res. & Sci. & Tech. Vol. 2, No. 3, 2013

Boehm H. P. "Surface oxides on carbon and their analysis: a critical assessment" Carbon 40 (2002) 145–149

Boehm H.P., Adv. Catal. 16, 179 (1966)

Borja Rodríguez-Cabo, Héctor Rodríguez, Eva Rodil, Alberto Arce, Ana Soto: "Extractive and oxidative-extractive desulfurization of fuels with ionic liquids" Fuel 117A (2014), pp 882–889

Bösmann A., L. Datsevich, A. Jess, A. Lauter, C. Schmitz, P. Wasserscheid: "Deep desulfurization of diesel fuel by extraction with ionic liquids" Chem Commun, 23 (2001), pp. 2494–2495

Bouchelta C, Salah Medjram M, Bertrand O and Bellat J P (2008), "Preparation and characterization of activated carbon from date stones by physical activation with steam", J Anal Appl Pyrol., Vol. 82, No. 1, pp. 70-77

Brunauer S., Emmett P. H., Teller E. Adsorption of gasses in multimolecular layer J. Am. Chem. Soc. 1938, 60, 309-319

Brunauer S., L.S. Deming, W.E. Demomg, E. Teller, "On a theory of the van der Waals adsorption of gases" J. Am. Chem. Soc. 62 (1940) 1723–1732

Celia Marı´n-Rosas, Luis F. Ramı´rez-Verduzco, Florentino R. Murrieta-Guevara, Gonzalo Herna´ndez-Tapia, and Luis M. Rodrı´guez-Otal "Desulfurization of Low Sulfur Diesel by Adsorption Using Activated Carbon: Adsorption Isotherms" Ind. Eng. Chem. Res. 2010, 49, 4372–4376

Chang Yu, Xiaoming Fan, Limei Yu, Teresa J. Bandosz, Zongbin Zhao, and Jieshan Qiu "Adsorptive Removal of Thiophenic Compounds from Oils by Activated Carbon Modified with Concentrated Nitric Acid" *Energy Fuels* 2013, 27, 1499−1505

Chang Yu.; Qiu, J. S.; Sun, Y. F.; Li, X. H.; Chen, G.; Zhao, Z. B. "Adsorption removal of thiophene and dibenzothiophene from oils with activated carbon as adsorbent: effect of surface chemistry" J. Porous Mater. 2008, 15, 151−157.

Cheruku S.K., T. Banerjee: "Liquid–liquid equilibrium data for 1-ethyl-3-methylimidazolium acetate–thiophene–diesel compound: experiments and correlations" J Solution Chem, 41 (2012), pp. 898–913

Chiang, H. L.; Huang, C. P.; Chiang, P. C.; You, J. H. "Effect of metal additives on the physico-chemical characteristics of activated carbon exemplified by benzene and acetic acid adsorption" Carbon 1999, 37, 1919

Choi G-G, Jung S-H, Oh S-J, Kim J-S. "Total utilization of waste tire rubber through pyrolysis to obtain oils and CO_2 activation of pyrolysis char" Fuel Process Technol 2014; 123:57–64.

Chunshan Song. An overview of new approaches to deep desulfurization for ultra-clean gasoline, diesel fuel and jet fuel. Catalysis Today 86 (2003) 211–263.

Costas Pelekani, Vernon L. Snoeyink. "A kinetic and equilibrium study of competitive adsorption between atrazine and Congo red dye on activated carbon: the importance of pore size distribution" Carbon 39 (2001) 25–37

Dasgupta S, Gupta P, Nanoti A, Goswami A. N, Garg M. O., Tangstad E, Stocker M. "Adsorptive desulfurization of diesel by regenerable nickel based adsorbents" Fuel, 108 (2013) 184-189.

De S. K., A. I. Isayev and K. Khait, Eds, Rubber Recycling, Taylor and Francis, Boca Raton, FL (2005).

Demiral H, Demiral Ý, Karabacakoðlu B and Tümsek F (2011), "Production of activated carbon from olive bagasse by physical activation", Chem Eng Res Des., Vol. 89, No. 2, pp. 206-213

Deng, H.; Yang, L.; Tao, G.; Dai, J. (2009) Preparation and characterization of activated carbon from cotton stalk by microwave assisted chemical activation: Application in methylene blue adsorption from aqueous solution. J. Hazard. Mater., 166 (2–3): 1514.

Duan Aijun, Zheng Peng, Zhao Liang, Ji Jingjing, Zhao Zhen "Computational simulation application in the research of desulfurization mechanism. The 9th International conference on computer science & education (ICCSE 2014) August 22-24, 2014. Vancouver, Canada.

Eastoe J., J.S. Dalton Dynamic surface tension and adsorption mechanisms of surfactants at the air water interface Adv. J. Colloid Interface Sci., 85 (2000), pp. 103–144

Eber J., P. Wasserscheid, A. Jess: "Deep desulfurization of oil refinery streams by extraction with ionic liquids" Green Chem, 6 (2004), pp. 316–322

Edward L.K. Mui , W.H. Cheung , Gordon McKay "Tyre char preparation from waste tyre rubber for dye removal from effluents" Journal of Hazardous Materials 175 (2010) 151–158

Estrella Escalona Platero, Domenica Scarano, Adriano Zecchina, Giancarlo Meneghini, Roberto De Franceschi "Highly sintered nickel oxide: surface morphology and FTIR investigation of CO adsorbed at low temperature" Surface Science 350 (1996) 113–122.

Faghihian, Hossein, Naeemi, Shakiba "Application of a Novel Nanocomposite for Desulfurization of a Typical Organo Sulfur Compound" Iran. J. Chem. Chem. Eng. Vol. 32, No. 3, (2013)

Farhat Ali Mohammad, Abdullah Al-Malki, Bassam El-Ali, Gary Martinie, Mohammad N. Siddiqui "Deep desulphurization of gasoline and diesel fuels using non-hydrogen consuming techniques" Fuel 85 (2006) 1354–1363

Fengkui Yin, Jianglong Yu, Sushil Gupta, Shaoyan Wang, Dongmei Wang, Li Yang, Arash Tahmasebi "Sulfidation of a Novel Iron Sorbent Supported on Lignite Chars during Hot Coal Gas Desulfurization" Physics Procedia 24 (2012) 290 – 296

Foo, K.Y.; Hameed, B.H. (2010). "Insights into the modeling of adsorption isotherm systems". Chemical Engineering Journal 156 (1): 2–10

Freundlich H. Über die adsorption in lösungen (adsorption in solution) Z. Phys. Chem., 57 (1906), pp. 384–470

Fukunaga T., H. Katsuno, H. Matsumoto, O. Takahashi, Y. Akai, "Development of kerosene fuel processing system for PEFC" Catalysis Today 84 (2003) 197-200.

Garcia T., R. Murillo, D. Cazorla-Amoros, A.M. Mastral, A. Linares-Solano, "Role of the activated carbon surface chemistry in the adsorption of phenanthrene" Carbon 42 (2004) 1683 1689.

Georgii H. W. (1970). Contribution to the atmospheric sulfur budget. J. Geophys. Res, 75(2), 2365-2371.

Gil A., G. de la Puente, P. Grange, "Evidence of textural modifications of an activated carbon on liquid-phase oxidation treatments" Microporous Materials 12 (1997) 51-61

Girija D., Halehatty S. Bhojya Naik, C. N. Sudhamani and B. Vinay Kumar "Cerium oxide nanoparticles - a green, reusable, and highly efficient heterogeneous" Archives of Applied Science Research, 2011, 3 (3):373-382

Gonzalez JF, EncinarJM, González-GarcíaCM, SabioE, RamiroA, CanitoJL, Preparation of activated carbons from used tyres by gasification with steam and carbondioxide. Appl Surf Sci 2006; 252:5999–6004

Guoxian Yu, Shanxiang Lu, Hui Chen, and Zhongnan Zhu: "Oxidative Desulfurization of Diesel Fuels with Hydrogen Peroxide in the Presence of Activated Carbon and Formic Acid" Energy & Fuels 2005, 19, 447-452

Gupta V K, Gupta B, Rastogi A, Agarwal S, Nayak A. "Pesticides removal from wastewater by activated carbon prepared from waste rubber tire. WaterRes 2011; 45:4047–55.

Gupta VK, Nayak A, Agarwal S. "Performance evaluation and application of Oxygen enriched waste rubber tire adsorbent for the removal of hazardous aniline derivatives from wastewater. ChemEngJ 2012; 203:447–57.

Hameed B.H. D.K. Mahmoud, A.L. Ahmad "Equilibrium modeling and kinetic studies on the adsorption of basic dye by a low-cost adsorbent: Coconut (Cocos nucifera) bunch waste", Hazardous Materials, 158, 65–72, 2008.

Hernandez S. P., D. Fino, N. Russo "High performance sorbents for diesel oil desulfurization" Chemical Engineering Science 65 (2010) 603-609

Hideo Orita, Kunio Uchida and Naotsugu Itoh, "A volcano-type relationship between the adsorption energy of thiophene on promoted MoS2 cluster-model catalysts and the experimental HDS activity: ab initio density functional study", Applied Catalysis A: General 258 (2004) 115–120.

Holbrey J.D., I. López-Martín, G. Rothenberg, K.R. Seddon, G. Silveiro, X. Zheng: "Desulfurisation of oils using ionic liquids: selection of cationic and anionic components to enhance extraction efficiency" Green Chem, 10 (2008), pp. 87–92

Isam A. H. Al Zubaidy, Fatma Bin Tarsh, Noora Naif Darwish, Balsam Sweidan Sana Abdul Majeed, Aysha Al Sharafi, and Lamis Abu Chacra "Adsorption Process of Sulfur Removal from Diesel Oil Using Sorbent Materials" (2013) Vol.1(1): 66-68

Jae Hyung Kim, Xiaoliang Ma, Anning Zhou, Chunshan Song "Ultra-deep desulfurization and denitrogenation of diesel fuel by selective adsorption over three different adsorbents: A study on adsorptive selectivity and mechanism" Catalysis Today 111 (2006) 74-83.

Jasmin Shah, M. Rasul Jan, Fazal Mabood and M. Shahid "Conversion of Waste Tyres into Carbon Black and their Utilization as Adsorbent" Journal of the Chinese Chemical Society, 2006, 53, 1085-1089

Jianglong Yu, Fengkui Yin, Shaoyan Wang, Liping Chang, Sushil Gupta, "Sulfur removal property of activated-char-supported Fe–Mo sorbents for integrated cleaning of hot coal gases" Fuel 108 (2013) 91–98

Jia-Xiu Guo, Xiao-Li Liu, De-Ming Luo, Hua-Qiang Yin, Jian-Jun Li and Ying-Hao Chu "Influence of Calcination Temperatures on the Desulfurization Performance of Fe Supported Activated Carbons Treated by HNO_3" Ind. Eng. Chem. Res. 2015, 54, 1261−1270

Jia-xiu Guoa, Juan Lianga, Ying-Hao Chua, Ming-Chao Suna, Hua-Qiang Yina, Jian-Jun Li "Desulfurization activity of nickel supported on acid-treated activated carbons" Applied Catalysis A: General 421– 422 (2012) 142– 147

Jie Bu, Gabriel Loh, Chuandayani Gunawan Gwie, Silvia Dewiyanti, Michael Tasrif, Armando Borgna "Desulfurization of diesel fuels by selective adsorption on activated carbons: Competitive adsorption of polycyclic aromatic sulfur heterocycles and polycyclic aromatic hydrocarbons" Chemical Engineering Journal 166 (2011) 207–217

Jing Xiao, Chunshan Song, Xiaoliang Ma, and Zhong Li "Effects of Aromatics, Diesel Additives, Nitrogen Compounds, and Moisture on Adsorptive Desulfurization of Diesel Fuel over Activated Carbon" Ind. Eng. Chem. Res. 2012, 51, 3436−3443

Jintawat Chaichanawong, Takuji Yamamoto, Takao Ohmori, Akira Endo "Adsorptive desulfurization of bioethanol using activated carbon loaded with zinc oxide" Chemical Engineering Journal 165 (2010) 218–224

Kaminsky W. and H. Sinn, in "Book Recycling and Recovery of Plastics," J. Brandrup, M. Bittner, W. Michaeli, and G. Menges (Eds.), Hanser Publishers, Munich, 1995.

Kappe C. Oliver "Controlled Microwave Heating in Modern Organic Synthesis" Angew. Chem. Int. Ed. (2004), 43, 6250 –6284Khan A. "The theory of adsorption equilibria analysis based on general equilibrium constant expression. Turkish Journal of Chemistry, 36 (2012) 219-231.

Khezami L, Ould-Dris A and Capart R (2007), "Activated carbon from thermocompressed wood and other lignocellulosic precursors", Bio Res., Vol. 2, No. 2, pp. 193–209

Kostas S. Triantafyllidis, Eleni A. Deliyanni "Desulfurization of diesel fuels: Adsorption of 4, 6-DMDBT on different origin and surface chemistry nanoporous activated carbons" Chemical Engineering Journal 236 (2014) 406–414

Ku Bon Jun.; Joong Kee Lee, Dalkeun Park, Hyun-Ku Rheet. "Treatment of Activated Carbon To Enhance Catalytic Activity for Reduction of Nitric Oxide with Ammonia" Ind. Eng. Chem. Res. 1994,33, 2868-2874

Lagergren S., "About the theory of so-called adsorption of soluble substances", Kungliga Svenska Vetenskapsakademiens Handlingar, 24, 1–39, 1898

Langmuir, I. The adsorption of gases on plane surfaces of glass, mica and platinum J. Am. Chem. Soc. 1918, 40, 1361-1403.

Leh F., K. M. Chan (1973). Sulfur compounds: Pollution, health effects and biological function. J. Chem. edu, 50(4), p246.

Liang Zhao, Yan Chen, Jinsen GAO, Yu Chen "Desulfurization mechanism of FCC gasoline: A review" Chem. Eng. China 2010, 4(3): 314–321

Lichun Huang, Guofu Wang, Zhangfeng Qin, Mei Dong, Mingxian Du, Hui Ge, Xuekuan Li, Yidong Zhao, Jing Zhang, Tiandou Hu, Jianguo Wang. In situ XAS study on the mechanism of reactive adsorption desulfurization of oil product over Ni/ZnO. Applied Catalysis B: Environmental 106 (2011) 26–38.

Lu Fan, Jie Chen, Jiaxiu Guo, Xia Jiang, Wenju Jiang "Influence of manganese, iron and pyrolusite blending on the physiochemical properties and desulfurization activities of activated carbons from walnut shell" Journal of Analytical and Applied Pyrolysis 104 (2013) 353–360

Ma, X . & Velu, V.& Sun, L.& Song, C., "Adsorptive desulfurization of diesel fuel over a metal sulfide-based adsorbent", Prepr. Pap.-Am. Chem. Soc., Div. Pet. Chem., vol. 48, 2, (2003), p.522-523

Mahadevan S., S.P. Behera, G. Gnanaprakash, T. Jayakumar, J. Philip, B.P.C. Rao "Size distribution of magnetic iron oxide nanoparticles using Warren–Averbach XRD analysis" Journal of Physics and Chemistry of Solids 73 (2012) 867–872

Manchon-Vizuete, E.,Macias-Garcia, A., Gisbert, A.N., Fernandez-Gonzalez, C., Gomez-Serrano, "Adsorption of mercury by carbonaceous adsorbents prepared from rubber of tyre wastes" Journal of Hazardous Materials B119 (2005) 231–238

Marijan Gotic, Svetozar Music, "Mo¨ssbauer, FT-IR and FE SEM investigation of iron oxides precipitated from FeSO4 solutions" Journal of Molecular Structure 834–836 (2007) 445–453

Marko Muzic, Katica Sertic-Bionda, Zoran Gomzi, Stefica Podolski, Sanda Telen "Study of diesel fuel desulfurization by adsorption" Chemical Engineering Research and Design 8 8 (2010) 487–495

Martinez J D, Puy N ,Murillo R ,García T ,Navarro M V ,Mastral A M."Waste tyre pyrolysis – a review. Renew Sustain Energy Rev 2013; 23:179–213.

Mathieu Y, Soulard M, Patarin J & Moliere M. Mesopourous materials for the removal of SO2 from gas streams. Fuel Processing Technology, 99 (2012) 35-42.

McKay G., Y.S. Ho, "Pseudo-second order model for sorption processes", Process Biochem, 34, 451–465, 1999

Min A, Harris AT. "Influence of carbon di oxide partial pressure and fluidization velocity on activated carbons prepared from scrap car tyre in a fluidized bed. ChemEngSci 2006; 61:8050–9.

Mochizuki Y., K. Sugawara Removal of organic sulfur from hydrocarbon resources using ionic liquids" Energy Fuel, 22 (2008), pp. 3303–3307

Moosavi E. S., S. A. Dastgheib and R. Karimzadeh, "Adsorption of Thiophenic Compounds from Model Diesel Fuel Using Copper and Nickel Impregnated Activated Carbons", Energies, 5, 4233-4250, 2012

Moreno-Castilla, C.; Lo´pez-Ramo´n, M. V.; Carrasco-Marin, F. "Changes in surface chemistry of activated carbons by wet Oxidation" Carbon 2000, 38, 1995-2001.

Morlanes N "Reaction mechanism of naphtha steam reforming on nickel-based catalysts, and FTIR spectroscopy with CO adsorption to elucidate real active sites" *Inter. Journal of Hydrogen Energy 38 (2013) 3588-3596*

Munawar Khalil, Robert L. Lee, Ning Liu "Hematite nanoparticles in aquathermolysis: A desulfurization study of thiophene" Fuel 145 (2015) 214–220

Mykola Seredych, Jakub Lison, Urs Jans, Teresa J. Bandosz "Textural and chemical factors affecting adsorption capacity of activated carbon in highly efficient desulfurization of diesel fuel" Carbon 47 (2009) 2491 – 2500

Nan Wang, Hai Fan, Shiyun Ai "Lignin templated synthesis of porous carbon–CeO_2 composites and their application for the photocatalytic desulphuration" Chemical Engineering Journal 260 (2015) 785–790

Nunes, M.R., Perez, G.M., Loguercio, L.F., Alves, E.W., Carreno, N.L.V., Martins, J.L., Garcia, I.T.S., 2011. J. Brazil Chem. Soc. 22, 2027.

Olivares-Marín M, Fernández-González C, Macías-García A and Gómez-Serrano V (2012), "Preparation of activated carbon from cherry stones by physical activation in air. Influence of the chemical carbonisation with HSO", J Anal Appl Pyrol., Vol. 94, pp. 131-137

Omer Refa Koseoglu, Adnan Al-Hajji, Jaffar H. Al-Nufaily, Dhiya Al Syed Ahmad, Qatif Hendrik Muller, "Process for Upgrading Whole Crude Oil to Remove Nitrogen and Sulfur" *Patent* US 2009/0120842 A1

Paul Chen J., and Shunnian Wu "Acid/Base-Treated Activated Carbons: Characterization of Functional Groups and Metal Adsorptive Properties" Langmuir 2004, 20, 2233-2242

Ping Cheng, Shengli Zhang, Peng Wang, Shiping Huang, Huiping Tian "First-principles investigation of thiophene adsorption on Ni13 and Zn@Ni12 nanoclusters", Computational and Theoretical Chemistry 1020 (2013) 136–142

Poots V.J.P., G. McKay, J.J. Healy Removal of basic dye from effluent using wood as an adsorbent J. Water Pollut. Contr. Fed., 50 (1978), pp. 926–935

Prashant S Kulkarni, Carlos A. M. Afonso "Deep desulfurization of diesel fuel using ionic liquids: current status and future challenges" 12 (2010) 1139-1149.

Quek, A., Balasubramanian, R., "Low-energy and chemical-free activation of pyrolytic tire char and its adsorption characteristics" 2009. J. Air Waste Manag. Assoc. 59, 747.

Rachid B. Slimane , Javad Abbasian "Utilization of metal oxide-containing waste materials for hot coal gas desulfurization" Fuel Processing Technology 70 (2001). 97–113

Rahimeh Naviri Fallah, Saeid Azizian "Removal of thiophenic compounds from liquid fuel by different modified activated carbon cloths" Fuel Processing Technology 93 (2012) 45–52

Ramaswamy V., M. Bhagwat, D. Srinivas, A.V. Ramaswamy Structural and spectral features of nano-crystalline copper-stabilized zirconia. Catalysis Today, 97 (2004), pp. 63–70

Renu G., V. V. Divya Rani, S. V. Nair, K. R. V. Subramanian, and Vinoth-kumar Lakshmanan "Development of Cerium Oxide Nanoparticles and Its Cytotoxicity in Prostate Cancer Cells" Advanced Science Letters Vol. 5, 1–9, 2012

Roop Chand Bansel, Mecknashi Goyal (2005): "Activated Carbon Adsorption" Taylor and Francis Group. USA.

Rozanska X, van Santen R A, Hutschka F, Hafner J. A periodic density functional theory study of thiophenic derivative cracking catalyzed by mordenite. J Catal, 2003, 215: 20–29

Saha S.K., P. Pramanik. Aqueous sol-gel synthesis of cordierite and cordierite-zirconia composite powders. Journal of Materials Science, 30 (1995), pp. 2855–2858

Sarah L. Goertzen, Kim D. The´riault, Alicia M. Oickle, Anthony C. Tarasuk, Heather A. Andreas "Standardization of the Boehm titration. Part I. CO2 expulsion and endpoint determination" Carbon 48 (2010) 1252 – 1261

Sarda K. K., A. Bhandari, K.K. Pant, Sapna Jain "Deep desulfurization of diesel fuel by selective adsorption over Ni/Al2O3 and Ni/ZSM-5 extrudates" Fuel 93 (2012) 86–91

Selvavathi V, V. Chidambaram, A. Meenakshisundaram, B. Sairam, B. Sivasankar "Adsorptive desulfurization of diesel on activated carbon and nickel supported systems" Catalysis Today 141 (2009) 99–102

Shah J, Rasul J M, Mabood F, Shahid M. Conversion of waste tyres into carbon black and their utilization asadsorbent. JChinChemSoc 2006; 53:1085–9.

Shahadat Hussain A. M. H., & Bruce J. Tatarchuk "Adsorptive desulfurization of jet and diesel fuels using Ag/TiOx–Al2O3 and Ag/TiOx–SiO2 adsorbents" Fuel 107 (2013) 465–473.

Shengli Zhang, Yonghong Zhang, Shiping Huang, Peng Wang, Huiping Tian "Mechanistic investigations on the adsorption of thiophene over Zn3NiO4 bimetallic oxide cluster" Applied Surface Science 258 (2012) 10148– 10153

Sing K. S. W. "Reporting Physiosorption Data Gas/Solid systems" Pure and Applied Chemistry, Vol 54, No 11, pp 2201-2218, 1982.

Soleimani M., Bassi A., & Margaritis A. (2007) "Biodesulfurization of refractory organic sulfur compounds in fossil fuels" Biotechnology Advances 25 (6), 570-96.

Song C., X. Ma, New design approaches to ultra-clean diesel fuels by deep desulfurization and deep dearomatization, Appl. Catal. B 41 (2003) 207.

Song S. C. "An Overview of new approaches to deep desulfurization for ultra-clean gasoline, diesel fuel and jet fuel" Catal Today. 86 (2003) 211-263.

Soumen Dasgupta, Pushpa Gupta, Aarti, Anshu Nanoti, Amar N. Goswami, Madhukar O. Garg, Elisabeth Tangstad, Ørnulv B. Vistad, Arne Karlsson, Michael Stöcker "Adsorptive desulfurization of diesel by regenerable nickel based adsorbents" Fuel 108 (2013) 184–189

Stavropoulos G G. Precursor materials suitability for super activated carbons production. Fuel Process Technol 2005; 86:1165–73.

Sumathi S., S. Bhatia, K.T. Lee, A.R. Mohamed "Cerium impregnated palm shell activated carbon (Ce/PSAC) sorbent for simultaneous removal of SO_2 and NO—Process study" Chemical Engineering Journal 162 (2010) 51–57

Takahashi A., R. T. Yang, C. L. Munson and D. Chinn. Cu(I)−Y-Zeolite as a Superior Adsorbent for Diene/Olefin Separation. Langmuir, (2001), 17, 8405–8413.

Tawara K, Nishimura T, Iwanami H. Ultra-deep hydrodesulfurization of kerosene for fuel cell system (Part 2) regeneration of sulfurpoisoned nickel catalyst in hydrogen and finding of autoregenerative nickel catalyst. Sekiyu Gakkaishi (Journal of the Japan Petroleum Institute), 2000, 43: 114–120

Tawfik A. Saleh, Vinod K. Gupta, Abdulaziz A. Al-Saadi "Adsorption of lead ions from aqueous solution using porous carbon derived from rubber tires: Experimental and computational study" Journal of Colloid and Interface Science 396 (2013) 264–269

Tawfik A. Saleha, Abdulaziz A. Al-Saadi, Vinod Kumar Gupta "Carbonaceous adsorbent prepared from waste tires: Experimental and computational evaluations of organic dye methyl orange" Journal of Molecular Liquids 191 (2014) 85–91

Tazibet, S.; Boucheffa, Y.; Lodewyckx, P. Heat treatment effect on the textural, hydrophobic and adsorptive properties of activated carbons obtained from olive waste. Microporous Mesoporous Mater. 2013, 170, 293−298

Thitiwan Nunthaprechachan, Sitthiphong Pengpanich, Mali Hunsom "Adsorptive desulfurization of dibenzothiophene by sewage sludge-derived activated carbon" Chemical Engineering Journal 228 (2013) 263–271

Toles C A, Marshall W E, Johns M M, Wartelle L H and McAloon A (2000), "Acidactivated carbons from almond shells: physical, chemical and adsorptive properties and estimated cost of production", Bioresour Technol. Vol. 71, No. 1, pp. 87-92

Turk B. S., R.P. Gupta, RTI's TReND Process for deep desulfurization of naphtha, Am. Chem. Soc., Div. Fuel Chem. Prepr. 46 (2001) 392

United States Environmental Protection Agency (USEPA) 2000. Heavy duty Engine and vehicle standards and highway diesel fuel sulfur control requirements. EPA420-F-00-0057, www.epa.gov/otaq/regs/hd2007/frm/f00057.pdf

United States Environmental Protection Agency (USEPA) 2006. Introduction of cleaner-burning diesel fuel enables advanced pollution control for cars, trucks and busses. EPA420-F-06-064, www.epa.gov/otaq/highway-diesel/regs/420f06064.pdf

United States Environmental Protection Agency (USEPAb) 2014. EPA sets tier 3 motor vehicle emission and fuel standards, strengthens clean cars program. EPA-420-F-14-010. www.epa.gov/otaq/documents/tier3/420f14010.pdf

Unites States Environmental Protection Agency (USEPAa) 2014. EPA sets tier 3 motor vehicle emission and fuel standards. EPA-420-F-14-009. www.epa.gov/otaq/documents/tier3/420f14009.pdf

Vimal Chandra Srivastava "An evaluation of desulfurization technologies for sulfur removal from liquid fuels" RSC Advances, 2012, 2, 759–783

Vinay M. Bhandari1, , Chang Hyun Ko, Jung Geun Park, Sang-Sup Han, Soon-Haeng Cho, Jong-Nam Kim "Desulfurization of diesel using ion-exchanged zeolites" Chem Eng Sci 61 (2006) pp 2599–2608

Vinod K. Gupta, M.R. Ganjali, Arunima Nayak, B. Bhushan, Shilpi Agarwal "Enhanced heavy metals removal and recovery by mesoporous adsorbent prepared from waste rubber tire" Chemical Engineering Journal 197 (2012) 330–342

Vinod Kumar Gupta, Arunima Nayak, Shilpi Agarwal, Inderjeet Tyagi "Potential of activated carbon from waste rubber tire for the adsorption of phenolics: Effect of pre- treatment conditions" Journal of Colloid and Interface Science 417 (2014) 420–430

Wang L., A. Wang, "Adsorption properties of congo red from aqueous solution onto surfactant-modified montmorillonite", J. Hazard. Mater, 160, 173–180, 2008.

Weber W. J., J.C. Morris, "Kinetics of adsorption on carbon from solution", J. Sanit. Eng. Div. Proceed. Am. Soc. Civil Eng. 89, 31–59, 1963.

Wei Xie, Liping Chang, Dehai Wang, Kechang Xie , Terry Wall, Jianglong Yu "Removal of sulfur at high temperatures using iron-based sorbents supported on fine coal ash" Fuel 89 (2010) 868–873

Weitkamp J., M. Schwark and S. Ernst, J. "Removal of thiophene impurities from benzene by selective adsorption in zeolite ZSM-5" Chem. Soc., Chem. Commun., 1991 (16) 1133–1134.

Wen-Hang Tian, Lin-Bing Sun, Xue-Lin Song, Xiao-Qin Liu, Yu Yin, and Gu-Se He "Adsorptive Desulfurization by Copper Species within Confined Space" Langmuir (2010), 26(22), 17398–17404

World Business Council for sustainable development (WBCSD 2008): Managing End of Life Tires.

Wu, X. H.; Hong, X. T.; Luo, Z. P.; Hui, K. S.; Chen, H. Y.; Wu, J. W. The effects of surface modification on the super-capacitive behaviors of novel mesoporous carbon derived from rod-like hydroxyapatite template. Electrochim. Acta 2013, 89, 400−406

Xiang Gao, Shaojun Liu, Yang Zhang, Zhongyang Luo, Kefa Cen "Physicochemical properties of metal-doped activated carbons and relationship with their performance in the removal of SO2 and NO" Journal of Hazardous Materials 188 (2011) 58–66

Xiaojun Ma, Hongmei Yang, Lili Yu, Yin Chen and Ying Li "Preparation, Surface and Pore Structure of High Surface Area Activated Carbon Fibers from Bamboo by Steam Activation" Materials 2014, 7, 4431-4441

Xinhai Xu, Shuyang Zhang, Peiwen Li, Yuesong Shen "Adsorptive desulfurization of liquid Jet-A fuel at ambient conditions with an improved adsorbent for on-board fuel treatment for SOFC applications" Fuel Processing Technology 124 (2014) 140–146

Xuan Meng, Huan Huang, and Li Shi "Reactive Mechanism and Regeneration Performance of NiZnO/Al2O3-Diatomite Adsorbent by Reactive Adsorption Desulfurization" Ind. Eng. Chem. Res. 2013, 52, 6092−6100

Xue Han, Hongfei Lin, Ying Zheng "Regeneration methods to restore carbon adsorptive capacity of dibenzothiophene and neutral nitrogen heteroaromatic compounds" Chemical Engineering Journal 243 (2014) 315–325

Yang K, Peng J, Srinivasakannan C, Zhang L, Xia H and Duan X (2010), "Preparation of high surface area activated carbon from coconut shells using microwave heating", Bioresour Technol., Vol. 101, No. 15, pp. 6163-6169.

Yang T. Ralph, Akira Takahashi, and Frances H. Yang "New Sorbents for Desulfurization of Liquid Fuels by π –Complexation" Ind. Eng. Chem. Res. 2001, 40, 6236-6239

Yang, X., L.E. Erickson, K.L. Hohn, P. Jeevanandam, and K.J. Klabunde, "Sol-Gell Cu-Al2O3 Adsorbents for Selective Adsorption of Thiophene out of Hydro carbon," Ind. Eng. Chem. Res. 45, 6169-6174 (2006).

Yi, H. H.; He, D.; Tang, X. L.; Wang, H. Y.; Zhao, S. Z.; Li, K. Effects of preparation conditions for active carbon-based catalyst on catalytic hydrolysis of carbon disulfide. Fuel 2012, 97, 337−343

Yuesong Shen, Peiwen Li, Xinhai Xu and Hong Liu: "Selective adsorption for removing sulfur: a potential ultra-deep desulfurization approach of jet fuels" RSC Adv., 2012, 2, 1700–1711

Yujun Wang, Chunling Zhang, Siwei Bi, Guangsheng Luo "Preparation of ZnO nanoparticles using the direct precipitation method in a membrane dispersion micro-structured reactor" Powder Technology 202 (2010) 130–136

Zabaniotou A, Madau P, Oudenne P D, Jung C G, Delplancke M P , FontanaA. "Active carbon production from used tire in two-stage procedure:industrial pyrolysis and bench scale activation with H2O–CO2 mixture. JAnalAppl Pyrolysis 2004; 72:289–97.

Zabaniotou A.A., N. Antoniou, G. Stavropoulos "Novel sorbent materials for environmental remediation via depolymerization of used tyres" Desalination and Water Treatment (2014) 1–10

Zeki Berk (2013): "Food Process Engineering and Technology" Chapter 12: "Adsorption and Ion Exchange" 2nd edition Food science and technology pages 311-327.

Zeng Y., S. Kaytakoglu, D. P. Harrison "Reduced cerium oxide as an efficient and durable high temperature desulfurization sorbent" Chemical Engineering Science 55 (2000) 4893-4900

Zhang S., Q. Zhang, Z.C. Zhang: "Extractive desulfurization and denitrogenation of fuels using ionic liquids" Ind Eng Chem Res, 43 (2004), pp. 614–622

Zhifeng Jiang, Jimin Xie, Deli Jiang, Xiaojun Wei and Min Chen "Modifiers-assisted formation of nickel nanoparticles and their catalytic application to p-nitrophenol reduction" CrystEngComm, 2013, 15, 560-569

Zongxuan Jiang, Yan Liu, Xiuping Sun, Fuping Tian, Fuxia Sun, Changhai Liang, Wansheng You, Chongren Han, and Can Li "Activated Carbons Chemically Modified by Concentrated H_2SO_4 for the Adsorption of the Pollutants from Wastewater and the Dibenzothiophene from Fuel Oils" Langmuir 2003, 19, 731-736

Vitae

Name	**DANMALIKI GADDAFI IBRAHIM**
Nationality	NIGERIAN
Date of Birth	08/07/1989
Email	gaddafdmalik@gmail.com; gaddafdmalik@yahoo.com
Academic Rank	Graduate Assistant
Address	Biochemistry Department, Usmanu Danfodiyo University Sokoto, Sokoto State, Nigeria.
Academic Background	B. Sc. Biochemistry from Usmanu Danfodiyo University Sokoto 2011.

Book Chapters:

T.A. Saleh, T.D. Shuaib, **G.I. Danmaliki**, Mohammad A. Al Daous "Carbon based materials and Nanocomposites for Desulfurization: Preparation and Properties" in a book titled: "Applying Nanotechnology to the Desulfurization Process in Petroleum Engineering" IGI Global. Accepted

T.A. Saleh, **G.I. Danmaliki**, T.D. Shuaib., Auwal M. Musa "Nanomaterials and Nanocomposites for Adsorptive Desulfurization: from synthesis to application" Book Chapter in a book titled: "Applying Nanotechnology to the Desulfurization Process in Petroleum Engineering" IGI Global. Accepted

Refereed Journal Articles:

"Optimization of the conversion process of waste rubber tires to activated carbon toward adsorptive desulfurization of thiophenes, under submission Industrial & Engineering Chemistry Research"

"Effects of acidic and basic treatments of activated carbon derived from waste rubber tires on adsorptive desulfurization of thiophenes" Journal of the Taiwan Institute of Chemical Engineers, manuscript # JTICE-D-15-00533. Under Review

Conference and Presentations:

Tawfik. A. Saleh, **Danmaliki, Gaddafi I**., Screening the adsorptive effect of metal oxides nanoparticles loaded activated carbons for sulfur compounds, 249th ACS National Meeting & Exposition, Denver, CO, United States, March 22-26, 2015 (2015), ENFL-456.

Tawfik A. Saleh; **Ibrahim Danmaliki**, "Adsorptive Desulfurization of Thiophene, Benzothiophene and Dibenzothiophene from Model Fuel by Carbons Derived From Waste Rubber Tires" (ARC' 14) 2014 10.5339/qfarc.2014.EEPP1106

KAUST Research Conference: Applied Functional Material Chemistry 27-28 October 2014. Gave a poster presentation titled: From waste to valuable materials: adsorptive desulfurization on nanoparticles loaded carbon-derived from waste rubber tires"

Petro Environment 2014, 7th Symposium on Environmental Progress in the Petroleum & Petrochemical Industry 24-26 February 2014 Seef Center, Al Khobar, Kingdom of Saudi Arabia